Entanglement in critical quantum systems : New results with boundaries

Andrei Rotaru

SORBONNE UNIVERSITÉ

LPTHE
LABORATOIRE DE PHYSIQUE THEORIQUE ET HAUTES ENERGIES

Thèse de Doctorat

DE SORBONNE UNIVERSITE

réalisée au
Laboratoire de Physique Théorique et Hautes Énergies

Sujet de la thèse :

Entanglement in critical quantum systems: New results with boundaries

présentée par
Andrei ROTARU

Présentée et soutenue publiquement à Paris le 5 Octobre 2023

devant le jury composé de :

Rapporteur:	**M.**	**Pasquale Calabrese**
Rapporteur:	**M.**	**German Sierra**
Examinateur:	**M.**	**Jérôme Dubail**
Président:	**M.**	**Jesper Lykke Jacobsen**
Examinatrice:	**M^{me}**	**Didina Serban**
Invité:	**M.**	**Jean-Marie Stéphan**
Invité:	**M.**	**Vincent Pasquier**
Directeur de Thèse:	**M.**	**Yacine Ikhlef**
Directeur de Thèse:	**M.**	**Benoît Estienne**

Abstract

The investigation of quantum entanglement has emerged as a prominent area of study in theoretical high-energy and condensed-matter physics. Initially driven by motivations rooted in black hole physics and the holographic principle, entanglement has been revealed to be a powerful tool for probing quantum many-body physics. This thesis is primarily concerned with the investigation of entanglement in 1D critical systems with open boundaries via entanglement quantifiers such as the *Rényi Entanglement Entropy* (REE) and the *Von Neumann Entanglement Entropy* (EE). This is done by employing the replica trick and twist field formalism, which allows one to reduce the calculation of REE in critical systems with open boundaries to the determinations of correlators in a $1+1D$ *cyclic orbifold Boundary Conformal Field Theory* (BCFT). In this framework, we first establish an exact and general result for the second REE of an interval in the bulk of such a system. Then, we specialize to critical one-dimensional quantum models described by compact boson BCFTs with Dirichlet and Neumann BC, for which we are able to calculate the REE of an interval more generally. As a by-product, we also obtain results for the REE and EE of systems described by a non-compact boson BCFT. The thesis also explores the calculation of REE for mixed BCs, in which case one needs to use the *Boundary Condition Changing Operators* (BCCOs) formalism. The analytical results for these investigations are compared with appropriate lattice numerics, to good agreement. Additionally, an algebraic framework is presented for cyclic orbifold conformal field theories, offering insights into their operator content and fusion rules, which complements the more physical and geometrical approaches of the other investigations.

Contents

Acronyms

BCCOs *Boundary Condition Changing Operators*

BCFT *Boundary Conformal Field Theory*

CFT *Conformal Field Theory*

EE *Von Neumann Entanglement Entropy*

LOCC *Local Operation Classical Communication*

RDM *Reduced Density Matrix*

REE *Rényi Entanglement Entropy*

UHP *Upper Half Plane*

Introduction

The understanding of entanglement in quantum systems has emerged as a paramount research area across multiple scientific communities. The idea of persisting quantum correlations between particles separated by vast distances[1] was first proposed in the landmark paper by Einstein, Podolsky, and Rosen (EPR) [1], where they argued on the incompleteness of quantum mechanics in the Copenhagen interpretation, due to its allowing of this type of "spooky action at a distance"[2]. In the decades since the EPR paper, many of the problems raised by [1] have been addressed, but the core issue persists to this day: *entanglement is a deeply puzzling feature of quantum mechanics*.

Consequentially, it has inspired a great deal of research into the foundations of this subject [2–4] , *complemented* by experimental investigations [5][3] which have established it as a substantial research interest. However, it could be said that the study of entanglement truly came into its own at the end of the second millennium, when the potential of quantum computing became apparent to scientists and funding agencies alike, following a series of important theoretical breakthroughs.

These advancements consisted of algorithm proposals for quantum computations, that would surpass the limits of efficiency of classical programming methods for certain types of problems. We mention, non-exhaustively, the Deutch-Jozsa [6], Shor [7] and Grover algorithms [8], as well as the first quantum teleportation protocols [9]. All of these methods would be, of course, a purely theoretical achievement if not for the development of quantum error correction proposals [10] around the same period, which paved the way for their real-life implementation. A key element in the design of these types of proposals is the entanglement between the different *qubits* involved in the computation. For certain algorithms, working with highly entangled states for qubits can lead to important speed-ups [11], while in the domain of quantum cryptography, entanglement is essential for the secure distribution of encryption keys between remote participants [12].

A by-product of these developments was the understanding that entanglement is a very useful resource for the numerical and analytical characterization of many-body quantum systems. This lesson has been especially illuminating in the study of their *continuous phase transitions*, for which the quantification of entanglement offers new insights into their properties, as later paragraphs will show.

Consider then a critical quantum system in D' dimensions. In such systems, continuous phase transitions can occur at absolute zero temperature and are characterized by abrupt shifts in the system's ground state and collective properties due to quantum fluctuations. Standard techniques allow for the mapping of D'-dimensional quantum systems, at temperature T, to classical statistical models

[1] The term "Verschränkung"(entanglement) has first been used by Schrödinger in a reply to the EPR paper

[2] Einstein, private communication with Bohr

[3] *Complimented* with a Nobel Prize in 2022

in $D = D' + 1$ dimensions [13]. Through this mapping, the quantum imaginary time is traded for an additional spatial dimension in the statistical model, with a length proportional to $1/T$. Then, the Hamiltonian of the quantum system can be interpreted as the anisotropic limit of the transfer matrix of the classical statistical model [14]. Furthermore, a continuous phase transition occurring in the quantum system at $T = 0$ corresponds to the same type of critical phenomena observed in the higher-dimensional classical system, *infinite* in one of its dimensions.

Now, let's shift our focus to such a classical *critical* statistical model in D dimensions, which possesses a tunable parameter g, since this framework is more straightforward when it comes to making contact with field theoretical methods. What characterizes continuum phase transitions in such systems is the power-law divergence of the correlation length ξ with respect to g, as we tune it towards its critical value. At the critical point itself, the correlation length becomes infinite, which implies that microscopic degrees of freedom are strongly correlated on all distance scales. Close to criticality, power law divergences (with different *critical exponents*) also characterize physical quantities of the theory such as the susceptibility, and specific heat.

In these regimes, interesting conceptual consequences follow, from the *universality hypothesis*: there is a subset of properties of a system close to the critical point (such as critical exponents and shape of correlation functions) of a *continuous* phase transition that does not depend on the microscopic details of their interactions. In consequence, critical statistical models can then be organized into comparatively few *universality classes*, determined by their global features (dimensionality, global symmetries, etc.).

Early support for these ideas was provided by Landau's theory of continuous phase transitions, through which one presupposes an ansatz for the free energy of a system as a function of the order parameter of the system so that it satisfies some global symmetry. This hypothesis is then used to obtain results for the critical exponents. This approach is valid, as long as fluctuations of the order parameter around its extremal value can be safely neglected, as is the case for systems of dimensions $D \geq 4$. For low-dimensional systems, however, the wrong results (compared to experiment) are obtained, and one needs to employ a different framework.

This framework is the *renormalization group*, an approach with a tumultuous history that spans decades and has fundamentally changed the scientific paradigm on the formulation of physical models. The idea of *renormalization* first appeared in the first half of the 20th century, as an *ad-hoc* mathematical artifice one must employ in perturbative calculations of particle physics, to obtain a finite result. This procedure introduced the idea that each QFT has an energy scale of validity, as well as a general sense of dissatisfaction for generations of theoretical physicists between the 1950s and 1960s.

It was the pioneering work [15] of Kenneth Wilson that resolved this impasse and, as a by-product, modified how we conceive of physical models, to this day. The conceptual starting point of this approach, first implemented for the 2D Ising model [16], is to consider the transformation of a theory with couplings $\{g_k\}$ under some type of coarse-graining operation. In the case of [16], the operation consists of dividing the initial lattice of size $L = Na$, with lattice spacing a into blocks of size $a' = ba$ of adjacent spins, and assigning to each of them a new block spin variable. Then, one arrives at a model for the block spins, on a lattice of size L, with lattice spacing a', and possibly higher-point interactions. In consequence, this block RG

transformation has effectively mapped the initial theory to a new one.

In a generalization of this, Wilson proposed that such considerations extended to all physical models, including QFTs. In this general framework, any theory comes with a built-in energy scale and couplings that depend on it. Under RG transformations, the scale is changed, and, implicitly, the couplings, so that theories "flow" into other theories. This procedure can be iterated until one arrives at a fixed point of the RG transformation, where the model is scale-invariant. The theories corresponding to these fixed points, Wilson realized, are exactly the ones describing continuous phase transitions. This offers a general explanation for the universality hypothesis: theories in the same universality class are related by RG transformations to the same fixed point.

The fixed points of the RG flow correspond to scale-invariant QFT defined on a D dimensional Riemannian manifold. It is conjectured [17] that, for generic D, under reasonable assumptions[4], the symmetry of the theory is enhanced to *conformal invariance* - the set of transformations that preserve angles between curves. The conjecture is open, with a few notable exceptions. One of them is $D = 4$, for which this statement has been proven to all orders in perturbation theory [18], but a complete, non-perturbative proof only exists for the two-dimensional case [19, 20].

This is not the only way in which the $D = 2$ case is special. In two dimensions, the symmetry has an infinite number of generators. The consequences of this realization have been integrated into a unified theoretical framework for the treatment of 2D *Conformal Field Theory* (CFT) by Belavin, Polyakov, and Zamolodchikov in the seminal paper [21], published in 1984. This work has proven to be extremely influential, leading to progress in string theory, mathematics, and, most relevantly for this thesis, the study of critical phenomena. To do a just and complete presentation of this continuously growing body of work is beyond the scope of this thesis[5], as it would require compressing copious material from several textbooks and many more research articles [14, 23–25]

In the case of continuous phase transitions, the identification of the scaling limit of the critical 2D classical model (or 1D critical quantum chain) as a specific 2D CFT enables the exact calculation of critical exponents and correlators. This breakthrough has significantly contributed to the quantitative understanding and classification of numerous continuous phase transitions [21]. As the formalism of 2D CFT has evolved, it has been extended to accommodate more features of discrete systems, such as extended symmetries [26, 27], boundaries [28–33], and defects [34–36]. Finally, 2D CFT plays an essential role in the quantification of entanglement in 1D critical quantum systems, which we will now clarify.

Let us consider a quantum system, prepared in some pure state, and define a spatial bipartition on it, say $A|B$. One then constructs a function (*entanglement measure*), satisfying certain common-sense properties[6], that associates a real number to each pure state. This essentially quantifies how the entanglement between the subsystems changes depending on the choice of bipartition.

A very important such function[7] is the Von Neumann entanglement entropy S_A. Crucially, for the ground states of a large class of many-body systems with

[4] These include reflection positivity, invariance under isometries of the spacetime, and others. See [17] for a detailed discussion

[5] For a partial interdisciplinary summary of this material, we recommend the presentation [22]

[6] The meaning of common-sense will be explored in the next chapter

[7] Depending on one's definition, it can be considered the *unique* measure of entanglement for pure bipartite states as we explain in Section 1.2

local interactions, this function has been observed to satisfy the *area law* : *the entanglement entropy scales with the size of the boundary separating A|B*.

The first instances of this intriguing relation were discovered in old works on the thermodynamics of black holes [37] [38], where entanglement was proposed as an explanation for their entropy. Recent developments in the AdS/CFT research have identified an area law as being connected with the *holographic principle* in QFT which can be formulated in layman's terms as: *the information content of a region of spacetime should depend on its surface area rather than on its volume*. For a detailed presentation of these topics, we refer the reader to specialized reviews and textbooks [39, 40]

We *stress* that the "area law" only addresses the leading behaviour of S_A and there are situations in which the subleading terms also contain interesting information. This is the case, for example, in two-dimensional quantum systems exhibiting *topological order*, for which the subleading correction to the area law is a constant known as *topological entropy* γ [41, 42]. This quantity encodes information about the topological phase in the system and can be used to detect it.

For one-dimensional quantum systems, if the area law holds, the entanglement entropy will saturate, to a constant value, independent of the choice of bipartition. This is the case for the ground state of any *local*, *gapped* Hamiltonian of spins with *finite* couplings and system size, as proven rigorously by Hastings in [43]. For non-critical free bosons and fermions as well, the area law is known to hold, albeit there are no rigorous proofs for this yet [44]. However, the scaling of S_A becomes much more interesting when the area law does not hold, for instance when some assumptions of [43] are relaxed. An intriguing example can be found in [45], where a semi-infinite 1D quantum chain with nearest-neighbour interactions has been engineered such that the entanglement entropy in the ground state satisfies a *volume law* $S_A \sim \ell$ with respect to the interval size ℓ.

The area law can also be invalidated at criticality when the Hamiltonian becomes gapless. The behaviour depends on the properties of the system, such as boundary conditions, as well as the nature of the bipartition. In the seminal work of [46], a systematic approach to the calculation of the entanglement entropy using the methods of 2D CFT has been put forward. One of the most well-known results obtained in this framework [47, 48] is the leading contribution to the entanglement entropy of an interval of length ℓ in an infinite system, $S_A \sim c/3 \log \ell$ where c is the central charge of the CFT that gives the scaling limit of the studied discrete system. For more intricate setups, the infringements to the area law become more mathematically involved. We will relegate these details of the method to the next chapter, as they are too gruesome to include here. The main idea, however, is that one can obtain, using 2D CFT, analytic predictions for the entanglement entropy associated with a critical system — with good analytic control on both leading and subleading contributions to it.

Understanding the dependence of the entanglement entropy on the length scales of the system, through the area law or its replacements for critical systems, also plays a crucial role in numerical quantum many-body studies. The "brute force" simulation of a generic state in the Hilbert space of such systems is extremely challenging due to the exponential growth in the number of particles of the parameters necessary to store it. In consequence, the system sizes one can study with these methods are quite puny.

To circumvent these difficulties, methods for state approximation have been developed, such as the Matrix Product State (MPS) representations of elements

of the Hilbert space. These are used in conjunction with methods like the Density Matrix Renormalization Group (DMRG) [49] to study the energy spectrum and correlation function of the model. These numerical approaches are based on *sensibly* disregarding a subset of the Hilbert space of the system (and their contribution to the quantities of interest) to save on computational resources. The amount of entanglement in the state determines how much of the Hilbert space we can "safely" discard for a particular numerical evaluation.

As discussed previously, for states of 1D local, gapped systems that obey the area law, the entanglement entropy in the system saturates as we increase their size, which means one can get very precise numerical results through DMRG methods at a convenient computational cost (see [50] and references therein). We remark that these techniques do not generalize straightforwardly to higher dimensions, since, for $D \geq 2$, the entanglement entropy of states satisfying the area law scales with the perimeter of the subsystem [44], so that eventually limitations of digital storage are reached, for large enough subsystem sizes.

For 1D critical systems, additional challenges appear, as the entanglement entropy does not saturate but grows with respect to the size of the system. In consequence, constructing a faithful MPS representation of a state requires, in principle, progressively more computational resources as one considers bigger systems. To surmount these issues, modifications to the MPS approach can be implemented [51], but another approach is to approximate the state by using the Multi-scale Entanglement Renormalization Ansatz (MERA) [52]. This latter approach is more accurate in the calculation of correlators and more natural for the simulation of ground states of critical systems due to its scale-invariance, but can sometimes be less efficient than the MPS approach when it comes to computing ground state energies and other local observables [53].

Having given a modicum of context on the relevance of entanglement to different areas of physics research, let us now finish this introductory section with a brief teaser of the chapters to come. In Chapter 1, we present a few notions of quantum information to give a quantitative definition of what entanglement measures are and discuss the ones relevant for this work. We follow this with a review of the replica approach to the calculation of entanglement entropies in critical systems, from a lattice perspective, and how this reduces, essentially, to the evaluation of correlators in a *cyclic orbifold CFT*. The next four chapters are in correspondence with the different projects completed during this doctoral program, for which the overarching themes are the study of entanglement in systems with boundaries and a more formal understanding of the properties of cyclic orbifold CFTs. We will give a more detailed summary of their content at the end of the technical introduction of Chapter 1.

Chapter 1

Entanglement, conformal field theory and all that

This chapter aims to explore the intricacies of quantifying entanglement in quantum systems. We will commence by presenting a few notions of quantum information theory, allowing us to discern the characteristics of a reliable measure of entanglement for pure states in bipartite systems. Then, we will introduce the entanglement measures of relevance for the present work, the REE, and review the *replica trick* approach to their calculation in 1D critical systems, focusing on the lattice realization of this formalism. Consequently, we review the twist operator approach and assess the main achievements and difficulties of this method.

1.1 A general setup

We consider a quantum system $\mathcal{S}$, with Hilbert space $\mathcal{H}$, defined on some spatial domain C. The state of such a system is encoded in the *density matrix* ρ, which is a *hermitian* ($\rho = \rho^\dagger$) and *positive semi-definite* ($\rho \geq 0$) operator, normalized such that $\mathrm{Tr}\rho = 1$. From these properties, one infers that the eigenvalues of ρ are strictly non-negative and sum up to 1.

If the density matrix can be written as $\rho = |\Psi\rangle\langle\Psi|$, with $|\Psi\rangle \in \mathcal{H}$, we classify the state of our system as *pure*. If this is not the case, the system is in a *mixed* state. In practice, to distinguish between these two kinds of states, it is sufficient to calculate the *quantum purity* of ρ , defined as $\gamma \equiv \mathrm{Tr}\rho^2 = \sum_i \lambda_i^2$, where λ_i are the eigenvalues of ρ. We then have:

$$\mathrm{Tr}\rho^2 < 1 \text{ (mixed)} \qquad \mathrm{Tr}\rho^2 = 1 \text{ (pure)} \tag{1.1}$$

In all the physical setups presented in this thesis, the initial state of the system is pure, so we will focus our attention on states with $\mathrm{Tr}\rho^2 = 1$.

Let us now consider a bipartition of C into regions A and B, such that the Hilbert space $\mathcal{H}$ factorizes[1]

$$\mathcal{H} = \mathcal{H}_A \otimes \mathcal{H}_B \tag{1.2}$$

where $\mathcal{H}_A, \mathcal{H}_B$ encode the degrees of freedom in regions A and B respectively.

[1] In lattice gauge theories, for example, the Hilbert space of *physical* (gauge-invariant) states does not admit such a tensor product decomposition with respect to the Hilbert spaces of each subsystem and the quantification of entanglement becomes more subtle. Several proposals have been put forward to address this issue [54–56]

One of the central objects employed in the study of quantum entanglement is the *Reduced Density Matrix* (RDM):

$$\rho_A = \mathrm{Tr}_B \, |\Psi\rangle \langle\Psi| \tag{1.3}$$

defined as a partial trace over the Hilbert space of the subsystem B. It is important to note that the partial trace operation does not, in general, preserve the purity of the state, a fact that can be easily deduced from the *Schmidt decomposition* .

Schmidt decomposition

Let there be a quantum system, composed of two subsystems A and B with Hilbert space dimensions d_A, d_B respectively, and let $d = \min(d_A, d_B)$. Any pure state $|\Psi\rangle$ has a Schmidt decomposition

$$|\Psi\rangle = \sum_{i=1}^{d} \mu_i \, |i, A\rangle \, |i, B\rangle \,, \tag{1.4}$$

where $\mu_i \geq 0$ are known as **Schmidt coefficients** and $\{|i, A\rangle\}$, $\{|i, B\rangle\}$ are sets of orthonormal vectors in A and B respectively. The **Schmidt rank** r is defined as the total number of non-vanishing Schmidt coefficients.

Using the Schmidt decomposition for some generic pure state ρ, and taking the trace over $\mathcal{H}_B$, one now finds:

$$\rho_A = \sum_{i=1}^{d} \lambda_i \, |i, A\rangle \langle i, A| \tag{1.5}$$

where the eigenvalues $\lambda_i = \mu_i^2$ of the RDM, also referred to as the **entanglement spectrum**, are determined by the Schmidt coefficients. We can then conclude that the RDM is pure if and only if there is only one non-vanishing Schmidt coefficient μ_i equal to unity. This is equivalent to the **factorizability** of the initial state $|\Psi\rangle \langle\Psi|$ over the bipartition $A|B$, and thus, it implies there is no entanglement between A and B [57].

On the other hand, (1.4) also allows us to define a notion of **maximally entangled states** $|\Psi_{max}\rangle$[57] - states for which all Schmidt coefficients are identical and non-vanishing so that $\mu_i = 1/\sqrt{d}$.

The RDM is essential for constructing *entanglement measures* - scalar quantities that allow us to meaningfully characterize entanglement. To understand what a "good" entanglement measure is, we will introduce a few more concepts from quantum information theory, following standard references [57, 58].

1.1.1 What is a good entanglement measure?

It is pedagogical to frame our discussion in the foreground of an imaginary experimental setup: Alice and Bob are researchers, working together on a quantum system S, prepared in some initial *pure* state $|\Psi\rangle$. They implement a bipartition $A|B$ of the system, and each of them *carefully*(without changing $|\Psi\rangle$) transports the subsystem labelled by the initial of their name to their private workstations. There, they are allowed to perform operations on the partition in front of them.

Now, we should establish what kind of *operations* Alice and Bob are allowed to perform on their quantum subsystems - these are formalized by the notion of *quantum channel*.

Definition 1.1. ***Quantum channel/Proper quantum operation*** *A quantum channel is a linear map Φ between density matrices that acts as:*

$$\rho \to \rho' = \Phi(\rho) = \sum_i A_i \rho A_i^\dagger$$

where the matrices A_i are known as ***Kraus operators****, and are constrained to satisfy*

$$\sum_i A_i^\dagger A_i = \mathbf{1} \tag{1.6}$$

NB*: In general, the states ρ and ρ' can belong to different Hilbert spaces, so that the Kraus operators are not necessarily square matrices.*

The condition (1.6) ensures that the map Φ is *trace-preserving*, i.e. $\mathrm{Tr}\rho' = 1$. Now, with respect to the bipartition $A|B$ of our system, we can define the notion of *local operation*.

Definition 1.2. ***Local operation*** *Consider two quantum channels Φ_A, Φ_B, acting on a state ρ as:*

$$\rho \to \Phi_A(\rho) = \sum_i (A_i \otimes \mathbb{I}_B)\rho(A_i^\dagger \otimes \mathbb{I}_B)$$
$$\rho \to \Phi_B(\rho) = \sum_j (\mathbb{I}_A \otimes B_i)\rho(\mathbb{I}_A \otimes B_i^\dagger)$$

A ***local operation*** *is then defined as the quantum channel $\Phi_A \otimes \Phi_B$ acting on states ρ as:*

$$[\Phi_A \otimes \Phi_B](\rho) = \sum_i \sum_j \left(A_i \otimes B_j\right) \rho \left(A_i^\dagger \otimes B_j^\dagger\right)$$

where the condition:

$$\sum_{ij} \left(A_i^\dagger \otimes B_j^\dagger\right)\left(A_i \otimes B_j\right) = \mathbb{I}$$

follows trivially from the trace-preserving property of Φ_A and Φ_B.

We will also define here the slightly less restrictive *separable operations*:

Definition 1.3. ***(Separable operations)*** *A* ***separable operation*** *Φ_S is a* ***quantum channel*** *acting on a state ρ as:*

$$\rho \to \Phi_S(\rho) = \sum_i (A_i \otimes B_i)\, \rho \left(A_i^\dagger \otimes B_i^\dagger\right) \tag{1.7}$$

with A_i and B_i acting in $\mathcal{H}_A$ and $\mathcal{H}_B$, respectively.

Note that for a separable operation Φ_S one can have $\sum_i A_i^\dagger A_i \neq \mathbf{1}$, $\sum_i B_i^\dagger B_i \neq \mathbf{1}$. This means that the set of local operations **LO** is a subset of the set of separable operations **SO**[57].

Referring back to the experimental setup of Alice and Bob, their tinkering with the subsystems A and B can be understood as a *local operation* acting on the initial state of the system ρ . On top of this, the researchers are allowed to exchange

among themselves classical information, in the sense of Shannon information theory[59]. Combinations of local operations and transmission of classical information constitute a fundamental type of process in quantum information theory, known as *Local Operation Classical Communication* (LOCC). A simple example of LOCC would consist of Alice measuring an observable on the subsystem A, and communicating the results to Bob.

Although intuitively easy to understand, LOCC operations have technically involved formal descriptions. They have been rigorously defined, initially for protocols with a finite number of rounds of classical communication in [60], and generalized to an infinite number of rounds in [61]. In practice, however, these definitions are difficult to use and instead one takes advantage of the fundamental result of [62], which establishes that the LOCC protocols form a subset of **SO** so that any LOCC protocol can be written in the form (1.7).

Moving on, we can now establish what criteria define an entanglement measure for *pure* states. There is some uncertainty in the literature regarding the minimal set of properties such a quantity should satisfy, so we will differentiate between universally accepted axioms and additional constraints on entanglement measures, following [58].

Entanglement measures

Consider a quantum system $\mathcal{S}$ with Hilbert space $\mathcal{H}$ of finite dimension $d = \dim \mathcal{H}$, and a spatial bipartition of it $A|B$. Then, let there be a map $E : \mathcal{M} \to \mathbb{R}^+$ with $\mathcal{M}$, the set of *pure* density matrices of $\mathcal{S}$ (acting on $\mathcal{H}$) . We say $E(\rho)$ is an *entanglement measure* with respect to $A|B$, if it satisfies the **essential** properties[58, 63]

1. **Monotonicity (under LOCC)** Let Φ be a LOCC operation, such that $\Phi(\rho) \in \mathcal{M}$. Then we must have
$$E(\rho) \geq E(\Phi(\rho))$$
2. **Discriminance** $E(\rho) = 0$ if ρ is separable

Then, there are **additional properties** one can require, of which we mention [58]:

3. **Normalization** If $\rho \in \mathcal{M}$ is maximally entangled, then $E(\rho) = \log(d)$
4. **Asymptotic continuity** Let there be two *sequences* of Hilbert spaces $\{\mathcal{H}_A^{(n)}\}$ and $\{\mathcal{H}_B^{(n)}\}$, and define, for each n, the space $\mathcal{H}^{(n)} = \mathcal{H}_A^{(n)} \otimes \mathcal{H}_B^{(n)}$. Then, we say that $E(\rho)$ satisfies *asymptotic continuity* if, for **any** two sequences of *pure states* $\{\rho_n\}$ and $\{\sigma_n\}$, with ρ_n and σ_n acting on $\mathcal{H}_n$ one has
$$\|\rho_n - \sigma_n\| \to 0 \Rightarrow \frac{E(\rho_n) - E(\sigma_n)}{1 + \log \dim \mathcal{H}_n} \to 0 \text{ as } n \to \infty \tag{1.8}$$
Heuristically, this property ensures that the entanglement per qubit is continuous under "small" changes in the state - such as adding and removing a relatively small number of qubits to the system [60]. For measures that do not satisfy the above property, one can engineer setups exhibiting *entanglement locking* [64], for which removing (or measuring) even a single qubit from a state can dramatically change the value of the entanglement measured by $E(\rho)$.

We stress that the presentation above holds only for bipartite quantum systems prepared in *pure* states. For mixed ρ, the discussion of what properties a good entanglement measure should satisfy is much more sophisticated, and we refer the interested reader to [57, 58] for a detailed treatment.

1.1.2 Entanglement measures for pure states

Arguably the most important entanglement measure for pure states in bipartite systems is the *von Neumann entanglement entropy* (**EE**) which is defined as:

$$S(A) = -\mathrm{Tr}\rho_A \log \rho_A = -\sum_i \lambda_i \log \lambda_i \tag{1.9}$$

where $\{\lambda_i\}$ are the eigenvalues of ρ_A. The EE for pure states satisfies both the essential and additional properties associated with entanglement measures defined in the previous section [57, 63]. Furthermore, it satisfies a few more important properties that we will now outline [57]:

1. **Subadditivity**: Let A, B be subsystems of the quantum system $\mathcal{S}$. The following inequality holds:

$$S(A) + S(B) \geq S(A \cup B) \tag{1.10}$$

2. **Strong subadditivity** Let A, B, C be subsystems of A. The following inequality holds:

$$S(A \cup C) + S(B \cup C) \geq S(A \cup B \cup C) + S(C) \tag{1.11}$$

3. **Araki-Lieb inequality** Let A, B be generic subsystems of the quantum system $\mathcal{S}$. The following inequality holds:

$$|S(A) - S(B)| \leq S(A \cup B) \tag{1.12}$$

   Note that for complementary intervals, $S(A \cup B) = 0$ and we must have that:

$$S(A) = S(B) \tag{1.13}$$

Another important class of measures of bipartite entanglement and a natural generalization of the EE are the *Rényi entanglement entropies* (REE) defined as:

$$S_n(A) = \frac{1}{1-n} \log \mathrm{Tr}_A \rho_A^n \qquad n \in \mathbb{R}^+ \tag{1.14}$$

Crucially, the von Neumann entropy can be recovered as the $n \to 1$ limit of the REE:

$$S(A) = \lim_{n \to 1} S_n(A) \tag{1.15}$$

There are a few "standout" REE, which encode important properties about the state of the system:

- **The Hartley/Max entropy**

$$S_0(A) = \log r \tag{1.16}$$

  encodes the Schmidt rank r of the state of the system ρ

- **The second Rényi entropy**

$$S_2(A) = -\log \mathrm{Tr}_A \rho_A^2 \tag{1.17}$$

  encodes the purity of the RDM

- **Single-copy entanglement/Min entropy**

$$S_\infty(A) = \lim_{n\to\infty} S_n(A) = -\log \lambda_{max} \tag{1.18}$$

  allows us to recover $\mu_{\max}$, the largest eigenvalue in the spectrum of the RDM

We note that, for $n \neq 1$, the REE do not fulfil any of the properties (1.10)-(1.12). Furthermore, they do not satisfy the asymptotic continuity and normalization properties, so the REE do not qualify as entanglement measures if one includes these additional constraints in the definition. In fact, for the case of bipartite quantum systems prepared in pure states, the EE is the *unique* entanglement measure that satisfies these additional properties [58, 60].

Despite being less impressive quantifiers of entanglement, the REE do hold an important theoretical advantage over the EE: analytical tractability. The direct computation of $S(A)$ is difficult, as it requires either the diagonalization of ρ_A, or an advantageous analytic characterization of ρ_A. Such an approach can be followed, notably, for $1D$ *non-interacting* fermionic and bosonic many-body systems prepared in their ground state [65, 66].

For critical $1D$ models, a different strategy is pursued: one computes the REE for generic *integer* $n \geq 2$, and then *analytically continues* (if possible) the result to $n \to 1$ to recover the EE from (1.15). In the work of Cardy and Calabrese [46], the versatile *replica trick* approach to calculating REE has been introduced for this purpose, which we will now proceed to present.

1.2 Entanglement for 1D quantum systems - The replica trick

To illustrate the replica trick, we will consider a $1D$ quantum system of N sites (labelled $\{0, \ldots, N-1\}$), and lattice spacing ϵ with Hamiltonian H and periodic BC, at zero temperature. The system is prepared in its ground state $|\Psi_0\rangle$ Now, we introduce a spatial bipartition of the system into two subregions, namely the interval $A = [u, v]$ with $0 < u < v < L = N\epsilon$ and its complement B. The aim, then, is to calculate the n^{th} REE of $|\Psi_0\rangle$ with respect to this bipartition.

We will *assume* that the quantum Hamiltonian for the physical 1D system is obtained in the *anisotropic limit* [67] of the transfer matrix of a classical 2D statistical model, which we call $\widehat{\mathcal{M}}$. Let us now consider a pair of states $|\alpha\rangle, |\beta\rangle$ for the subsystem A. We can then express the elements of the RDM:

$$(\rho_A)_{\alpha\beta} \equiv \langle\alpha| \mathrm{Tr}_B(|\Psi_0\rangle\langle\Psi_0|) |\beta\rangle \tag{1.19}$$

in the path integral approach

$$(\rho_A)_{\alpha\beta} = \frac{Z_{\alpha\beta}}{Z_1}, \tag{1.20}$$

where Z_1 stands for the partition function of $\widehat{\mathcal{M}}$ on $\mathbb{C}_L$ (the infinite cylinder of width L), and $Z_{\alpha\beta}$ is the partition function on the infinite cylinder with a cut along

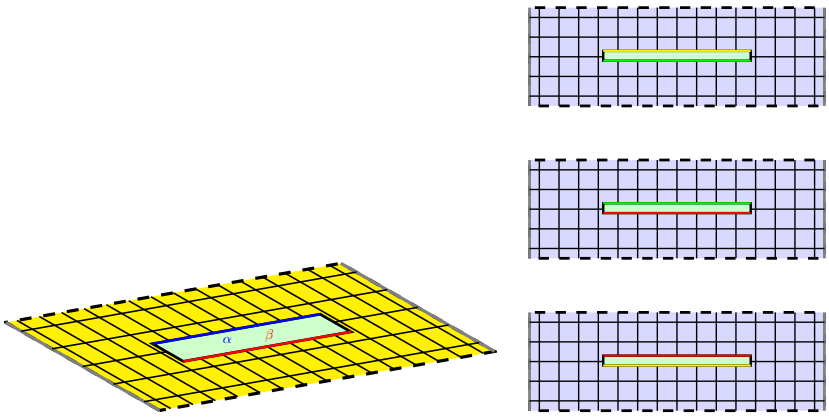

Figure 1.1: (a) The cylinder partition function associated to a matrix element $(\rho_A)_{\alpha\beta}$ of the ground-state density matrix ρ_A. The solid grey edges are identified. (b) The partition function associated to $\mathrm{Tr}_A(\rho_A^n)$ for $n = 3$. The solid grey edges are identified. The colours on the sides of the slits indicate the sewing order of the copies.

the segment $[u, v]$ of length $\ell = v - u$, and boundary conditions defined by the configurations α and β on both sides of the cut: see Fig. 1.1a. By construction, ρ_A has unit trace. If n is a positive integer, the quantity $\mathrm{Tr}_A(\rho_A^n)$ is obtained by stacking n copies of the cylinder, and connecting them cyclically along the cut, to form the replicated surface $\mathcal{R}_n$ depicted in Fig. 1.1.b. Thus, we have the relation

$$\mathrm{Tr}_A(\rho_A^n) = \frac{Z_n}{Z_1^n}\,, \tag{1.21}$$

where Z_n is the partition function of the model $\widehat{\mathcal{M}}$, supported on the replicated surface $\mathcal{R}_n$. This surface is a ramified covering of $\mathbb{C}_L$, with branch points located at the extremities of the interval A. Geometrically, these branch points are conical singularities with an excess angle $2\pi(n-1)$. Conical singularities are *not* singularities as far as the smooth (and even complex) structure is concerned[2]. But they are singularities in the sense of Riemannian geometry: while the metric is flat everywhere else on $\mathcal{R}_n$, there is a delta-function of negative curvature (proportional to the excess angle) localized at each branch point, following the Gauss-Bonnet theorem [68].

Instead of working with replicated surfaces, we can adopt a different perspective, and replicate the degrees of freedom. To establish this idea, let us consider in more detail the 2D statistical model $\widehat{\mathcal{M}}$, which we can take, for convenience, to be a classical spin model on the infinite cylinder, with nearest-neighbour interactions. The partition function on $\mathbb{C}_L$ is

$$Z_1 = \sum_{\{s(i)\}} \prod_{\langle i,j\rangle} W[s(i), s(j)]\,, \tag{1.22}$$

where $s(i)$ is the spin on site i, $\langle i, j\rangle$ denotes a pair of neighbouring sites, and W is the Boltzmann weight which defines the local interaction.

[2] in the sense that there exists a smooth (and in fact holomorphic) coordinate chart about any branch point.

For any positive integer n, we can define the discrete *cyclic orbifold* of $\widehat{\mathcal{M}}$. This model, which we denote $\widehat{\mathcal{M}}_n$, lives on the original surface $\mathbb{C}_L$, which we parametrize using discrete coordinates $m \in \{0, N-1\}$ and $t \in \mathbb{Z}$, so that $u = m_u\epsilon$ and $v = m_v\epsilon$. However, at each lattice site i, we have n independent spin variables $(s_1(i), \ldots, s_n(i))$, and the nearest-neighbour interactions are given by $\prod_{a=0}^{n-1} W[s_a(i), s_a(j)]$ – in other words, the copies $a = 0, \ldots, n-1$ are decoupled. The partition function for n decoupled copies thus reads

$$Z(\widehat{\mathcal{M}}_n) = \sum_{\{s_a(i)\}} \prod_{\langle i,j\rangle} \prod_{a=1}^{n} W[s_a(i), s_a(j)] = Z_1^n \,. \tag{1.23}$$

Local operators are n-tuples of $\widehat{\mathcal{M}}$-operators. Additionally, since the model has an internal $\mathbb{Z}_n$ symmetry generated by cyclic permutations of the copies, we can have topological defects, which are oriented lines across which the local interaction is modified as $W[s_a(i), s_a(j)] \mapsto W[s_a(i), s_{a+1}(j)]$. We thus introduce the *lattice twist operators* $\widehat{\sigma}$ and $\widehat{\sigma}^\dagger$, which insert the endpoints of a topological defect of this type.

We note that the construction of such defect operators is pretty standard in statistical models enjoying a discrete or continuous symmetry - this includes for instance $\mathbb{Z}_2$ disorder operators in the Ising model [69], and "electric" defects in the six-vertex model [33]. In consequence, one can establish the relation:

$$\langle \hat{\sigma}_{m_u,0} \hat{\sigma}^\dagger_{m_v,0} \rangle = \frac{Z_n}{Z_1^n} \,, \tag{1.24}$$

where we have employed the translational invariance of the model to set the "time" coordinate of the twist operators to $t = 0$. The left-hand side is a correlator of the orbifold model $\widehat{\mathcal{M}}_n$ on the infinite cylinder, and the numerator Z_n on the right-hand side is, as above, the partition function of the original model $\widehat{\mathcal{M}}$ on the ramified covering $\mathcal{R}_n$ of $\mathbb{C}_L$.

By generalizing the above construction, one can establish that correlation functions of twist operators on a generic Riemann surface Σ exactly correspond to partition functions of $\widehat{\mathcal{M}}$, supported on ramified coverings Σ_n of Σ with branch points at the position of the twists. In this way, the Rényi entropy of an interval $A = [u, v]$, for positive integer, $n \geq 2$ is related to a correlation function of twist operators in the cyclic orbifold of $\widehat{\mathcal{M}}$:

$$\boxed{S_n(A) = \frac{1}{1-n} \log \langle \widehat{\sigma}_{m_u,0} \widehat{\sigma}^\dagger_{m_v,0} \rangle \,.} \tag{1.25}$$

where m_u and m_v once again denote the discrete coordinates of the extremal sites in the interval.

1.3 The twist field formalism at criticality

While the *replica trick* approach presented in Section 1.2 is valid for generic $1D$ quantum systems, it leads to particularly impressive results when the models are tuned to criticality.

The scaling limit $N \to \infty$, $\epsilon \to 0$, and $L = N\epsilon = const.$ of the lattice model $\widehat{\mathcal{M}}$, with *lattice spacing* ϵ supported on the cylinder, $\mathbb{C}_L$ is the 2D CFT $\mathcal{M}$ with

Euclidean spacetime $\mathbb{C}_L$. In the context of our discussion, $\mathcal{M}$ is referred to as the *mother* or *seed* CFT and has a central charge c.

Similarly, the scaling limit of the lattice theory $\widehat{\mathcal{M}}_n$ living on $\mathbb{C}_L$ corresponds to the *cyclic orbifold* CFT $\mathcal{M}_n$, which is defined on the infinite cylinder of circumference L and has a central charge of nc. To construct a cyclic orbifold CFT, one replicates n times the theory $\mathcal{M}$, resulting in $\mathcal{M}^{\otimes n}$, the tensor product of n copies of $\mathcal{M}$. This replicated theory possesses a global discrete symmetry, namely, invariance under permutations of the n copies.

Next, one needs to gauge the Abelian $\mathbb{Z}_n$ subgroup of cyclic permutations. This process involves enlarging the space of configurations to include oriented defect lines that implement a $\mathbb{Z}_n$ domain wall. This means that the new theory includes configurations that are related by cyclic permutations of the n copies, as well as configurations that differ by the insertion of a $\mathbb{Z}_n$ domain wall.

In consequence, the spectrum of $\mathcal{M}_n$ consists of two types of operators. On one hand, the theory contains untwisted fields $\phi_1 \otimes \dots \phi_n$, which are simply n-tuples of operators in the *seed* CFT $\mathcal{M}$. Additionally, the theory contains *twisted operators* $\mathcal{O}^{[k]}$ with an associated $\mathbb{Z}_n$ *charge* $[k]$ which insert defect lines in the CFT. To understand their effect, let us consider untwisted operators of the type:

$$\phi_{(a)} \equiv \mathbf{1} \otimes \cdots \otimes \mathbf{1} \otimes \underset{(a)}{\phi} \otimes \mathbf{1} \otimes \cdots \otimes \mathbf{1} \,. \tag{1.26}$$

where $\mathbf{1}$ is the identity operator in the *mother* CFT $\mathcal{M}$, and ϕ acts on copy (a). The monodromy of a twisted field $\mathcal{O}^{[k]}$ relative to $\phi_{(a)}$ is:

$$\phi_{(a)}(e^{2i\pi}z, e^{-2i\pi}\bar{z}) \cdot \mathcal{O}^{[k]}(0) = \phi_{(a-k)}(z,\bar{z}) \cdot \mathcal{O}^{[k]}(0) \,. \tag{1.27}$$

meaning the $\mathcal{O}^{[k]}$ implement the cyclic permutation symmetry on the $\phi_{(a)}$.

Of key importance are the *bare twist fields* $\sigma^{[1]}, \sigma^{[-1]}$, which we often denote, for convenience $\sigma, \sigma^\dagger$. They are primary operators, with conformal dimensions [70]

$$h_\sigma = \bar{h}_\sigma = c/24(n - 1/n) \tag{1.28}$$

and are the most *relevant* twist operators with charges ± 1. Under the state-operator correspondence, they are associated with the lowest energy states in the twisted sectors ± 1.

In this framework, one can recover, following [46, 71], the CFT counterpart to the relation (1.24):

$$\frac{\mathcal{Z}(\Sigma_n)}{\mathcal{Z}(\Sigma)^n} = \langle \sigma(w_1,\bar{w}_1)\sigma^\dagger(w_2,\bar{w}_2)\rangle_\Sigma \,, \tag{1.29}$$

where $\mathcal{Z}(\Sigma_n)$ is the partition function of the mother CFT $\mathcal{M}$ on the surface Σ_n, and $(w_i, \bar{w}_i)$ are coordinates on the surface Σ.

Similar relations to (1.29) can be inferred for orbifold correlators with both twisted and untwisted field insertions:

$$\langle (\phi_1 \otimes \dots \phi_n)(w,\bar{w})\sigma(w_1,\bar{w}_1)\sigma^\dagger(w_2,\bar{w}_2)\rangle_\Sigma = \langle \sigma(w_1,\bar{w}_1)\sigma^\dagger(w_2,\bar{w}_2)\rangle_\Sigma \langle \prod_{j=1}^{n} \phi_j(we^{2\pi i a}, \bar{w}e^{-2\pi i a})\rangle_{\Sigma_n} \tag{1.30}$$

To illustrate how the notions presented in this section allow us to calculate REE and find the EE, we will re-derive, in the framework and conventions of this thesis, a standard result of [46].

Example 1: EE in a periodic system

We consider the same setup as in Section 1.2, tuned to criticality. We want to calculate, for generic $n \geq 2$, the REE of an interval $A = [u, v]$ of size $\ell = v - u$:

$$S_n(A) = \frac{1}{1-n} \log \langle \widehat{\sigma}_{m_u,0} \widehat{\sigma}^{\dagger}_{m_v,0} \rangle \tag{1.31}$$

In the continuum limit $\epsilon \to 0$, lattice operators can be expressed as a *local* combination of CFT scaling fields [14]. For the lattice twist operator $\widehat{\sigma}$, we should then have [72–74]:

$$\widehat{\sigma}_{m,t} = c_n \, \epsilon^{2h_\sigma} \sigma(w, \bar{w}) + \dots \tag{1.32}$$

where $w = \epsilon m + it\epsilon$ is the continuum coordinate on the infinite cylinder $\mathbb{C}_L$, c_n is a non-universal amplitude, and the dots correspond to less relevant operators of twist charge +1. Note that a similar expansion holds for $\widehat{\sigma}^{\dagger}$, but containing twist fields with $[k] = [-1]$. We stress that since these expansions are local, they do not depend on the particular choice of surface the lattice model is supported on, or the BC imposed on it.

Plugging (1.32) in (1.31), we find:

$$S_n(A) = \frac{1}{1-n} \log \epsilon^{4h_\sigma} \langle \sigma(u,u) \sigma^{\dagger}(v,v) \rangle_{\mathbb{C}_L} + \frac{2 \log c_n}{1-n} + \dots \tag{1.33}$$

where $u = m_u \epsilon, v = m_v \epsilon$, with $0 < u < v < L$. Thus, to leading order, $S_n(A)$ is determined by a two-point function of *bare* twist fields on $\mathbb{C}_L$

We now remind a standard CFT result for the 2-point function of primary operators on the infinite cylinder [23]:

$$\langle \sigma(u,u) \sigma^{\dagger}(v,v) \rangle_{\mathbb{C}_L} = \left(\frac{L}{\pi} \sin \frac{\pi \ell}{L} \right)^{-4h_\sigma} \tag{1.34}$$

Putting everything together, we recover the result of [46] for the REE :

$$S_n(A) = \frac{c(n+1)}{6n} \log \left(\frac{L}{\pi \epsilon} \sin \frac{\pi \ell}{L} \right) + \frac{2 \log c_n}{1-n} + \dots \tag{1.35}$$

By analytically continuing to $n \to 1$, one finds:

$$S(A) = \frac{c}{3} \log \left(\frac{L}{\pi \epsilon} \sin \frac{\pi \ell}{L} \right) + 2c_1' + \dots \tag{1.36}$$

where $c_1' = \lim_{n \to 1} \frac{\log c_n}{1-n}$.

Note that by taking the $L \to \infty$ limit, one recovers the famous result of [47] for an interval of length ℓ in an infinite system:

$$S(A) = \frac{c}{3} \log \frac{\ell}{\epsilon} + 2c_1' + \dots \tag{1.37}$$

In the above example, we have considered one of the simplest applications of the twist field formalism for the calculation of the REE and the determination of the EE. However, this can be extended to more generic bipartitions and setups.

Example 2: Disjoint intervals in a periodic system

For example, one can consider the entanglement between a union of $M \geq 2$ disjoint intervals $A = [u_1, v_1] \cup \cdots \cup [u_M, v_M]$, with $u_i, v_i \in [0, L]$ and the rest of the system with *periodic* BC. In this case, obtaining REE rests on the evaluation of a $2N$ point correlator of twist fields on the *closed* surface Σ[3] :

$$\left\langle \prod_{i=1}^{M} \sigma(w_i, \bar{w}_i)\sigma^{\dagger}(w_i, \bar{w}_i) \right\rangle_{\Sigma} \tag{1.38}$$

which are difficult to evaluate, for generic CFTS. Alternatively, by (1.29), one can try to compute the partition function $\mathcal{Z}(\Sigma_n)$ of $\mathcal{M}$ on the branched covering Σ_n. We now remind the Riemann-Hurwitz formula:

$$\chi(\Sigma_n) = n\chi(\Sigma) + \sum_{i=1}^{2M}(k_i - 1)\,, \tag{1.39}$$

which relates the Euler characteristic $\chi(\Sigma) = 2-2h$ of a Riemann surface Σ of genus h to that of its n-sheeted cover $\chi(\Sigma_n)$, for which the covering map $\pi : \Sigma_n \to \Sigma$ has $2M$ branch points with ramification index $k_i = n$. This implies that the genus g of Σ_n is:

$$\boxed{g = (n-1)(M-1) + nh} \tag{1.40}$$

Let us now review the current status of the computation of such partition function for generic CFTs. At $g = 1$, one is essentially dealing with a *torus* partition function $\mathcal{Z}(\tau, \bar{\tau})$ which is invariant under the $PSL(2, \mathbb{Z})$ (modular) group:

$$\mathcal{Z}(\tau) = \mathcal{Z}\left(\frac{a\tau + b}{c\tau + d}\right), \quad \text{for all} \quad \begin{pmatrix} a & b \\ c & d \end{pmatrix} \in \mathrm{SL}(2, \mathbb{Z}) \tag{1.41}$$

The $\mathcal{Z}(\tau, \bar{\tau})$ have been calculated exactly for a variety of CFTs such as Virasoro minimal models [75, 76], WZW models and free bosonic and fermionic CFTs [23]. If a CFT is consistently defined at $g = 0$ and $g = 1$, in the sense of [77], then it will be consistently defined on all surfaces with $g \geq 2$. The results of [77] guarantee then that the partition functions at $g \geq 2$ are well-defined mathematical objects, but their calculation is still an open problem for most CFTs. Relevant exceptions to this status are partition functions for free bosonic and fermionic CFTs on closed surfaces, which have been computed in a series of seminal works in the 80's [70, 78], in which cyclic orbifold CFTs were studied for string theoretical reasons. Beyond these, however, higher genus partition functions are only understood for a few theories [79, 80]. We note, for completeness, that there are also impressive formal results for the partition functions of Virasoro *minimal models* through the Coulomb gas approach [81] on surfaces of genus $g > 1$ [82, 83], but a glance at their expressions should convince the reader of their manifest impracticability for the calculation of the REE .

With these considerations in mind, it is now clear why *exact* calculations of the REE for disjoint intervals are difficult, for most CFTs. Despite this, important results for the REE in these setups have been obtained for arbitrary $M \geq 2$, for the Dirac fermion and Ising CFTs [84–86], as well as for the compactified boson of radius R [87, 88]

[3] At zero temperature $\Sigma \equiv \mathbb{C}_L$ while at finite $T > 0$, the surface Σ is a torus

In this latter case, let us review the results for the REE $S_n(A)$ for two disjoint intervals $A = [u_1, v_1] \cup [u_2, v_2]$ in a periodic system of length L. For a generic CFT, the moments of the RDM are related to a 4-point correlator of twist fields:

$$\mathrm{Tr}\rho_A^n = c_n^4 \langle \sigma(u_1)\sigma^\dagger(v_1)\sigma(u_2)\sigma^\dagger(v_2)\rangle \tag{1.42}$$

so that by global conformal invariance the REE have the form

$$\begin{aligned} S_n(A) =& \frac{c(n+1)}{6n} \log\left(\frac{s_L(u_1-u_2)s_L(v_1-v_2)}{s_L(u_1-v_1)s_L(u_2-v_2)s_L(u_1-v_2)s_L(u_2-v_1)}\right) \\ &+ \frac{1}{1-n}\log \mathcal{F}_n(r) + \frac{4\log c_n}{1-n} \end{aligned} \tag{1.43}$$

where

$$r = \frac{s_L(u_1-v_1)s_L(u_2-v_2)}{s_L(u_1-u_2)s_L(v_1-v_2)}, \qquad s_L(u) = \frac{L}{\pi}\sin\left(\frac{\pi u}{L}\right) \tag{1.44}$$

and $\mathcal{F}_n(r)$ is a universal function chosen so that $\mathcal{F}_n(r) \to 1$ as $r \to 0$ or $r \to 1$.

In the work of [87], which focuses on the case $M = 2$, for critical systems described by the CFT of a compact boson of radius R, the function $\mathcal{F}_n(r)$ was found to be

$$\mathcal{F}_n(r) = \frac{\Theta(0 \mid R^2\boldsymbol{\tau}/2)\Theta(0 \mid 2\boldsymbol{\tau}/R^2)}{[\Theta(0 \mid \boldsymbol{\tau})]^2}, \tag{1.45}$$

where $\boldsymbol{\tau}$ is an $(n-1)\times(n-1)$ matrix with elements

$$\tau_{ij}(r) \equiv \mathrm{i}\frac{2}{n}\sum_{k=1}^{n-1} \sin(\pi k/n)\frac{F_{k/n}(1-r)}{F_{k/n}(r)}\cos[2\pi k(i-j)/n] \tag{1.46}$$

where $F_{k/n}(y) \equiv {}_2F_1(k/n, 1-k/n; 1; y)$ is the Gauss hypergeometric function In this setup, sending $n \to 1$ in the first term of (1.43) is straightforward, while the analytic continuation of $\mathcal{F}_n(r)$ is still an open problem. Progress has been made in this direction, however, through the numerical extrapolation methods introduced in [89] and employed in works such as [90].

This example highlights one important limitation of the twist field approach for the determination of the EE. To obtain it, one needs to be able to solve what are essentially two distinct problems. The first one is the CFT calculation of the REE for a generic integer n using the twist field approach. The second difficulty is purely mathematical: analytically continuing the $S_n(A)$ to $n = 1$. In the "success story" of (1.36), both problems are tractable. In most cases, however, even when the REE have been calculated for generic n, the analytic continuation remains elusive [88].

Let us now explore another setup, which has been the main subject of this thesis: the quantification of entanglement in critical quantum systems with open BC. The characteristics of entanglement are significantly influenced by the presence of such physical boundaries, which has been extensively studied in various contexts [46, 91–96]. These studies have yielded valuable insights into the subject. Notably, in the case of holographic entanglement entropy [97, 98], examining the effects of boundaries [99–102] has offered a fresh perspective on the information paradox [103–107].

For such setups as well, the twist field formalism can be employed, but there are several supplementary technicalities which we will now review.

1.4 REE in systems with open BC

We will consider a $1D$ quantum system with identical open BCs with both its bulk and boundary tuned to criticality, at zero temperature.

The scaling limit of such a system will be given by a BCFT $\mathcal{M}$ with conformal BC α defined on an infinite strip $\mathbb{S}_L$ of width $L = N\epsilon$. Such theories have been intensely studied since their elaboration in Cardy's works [28, 29, 108], and we refer the reader to [24] for a recent and thorough presentation.

In this case, the simplest setup to consider is that of an interval $A = [0, \ell]$, with $\ell = m\epsilon$, starting at one of the boundaries of the system. The constructions of Sections 1.2 and 1.3 can now be generalized to this setup. In the replica trick approach, one has to evaluate a partition function on the n-sheeted strip $\mathbb{S}_{L,n}$ with a *single* branch point corresponding to the bulk end of the interval A [71]. In the twist field approach, on the other hand, the moments of the RDM are given by the lattice correlator:

$$\mathrm{Tr}_A \rho_A^n = \langle \widehat{\sigma}_{m,0} \rangle_{\mathbb{S}_L}^{(\alpha,\alpha)} \tag{1.47}$$

The leading BCFT contribution to this quantity is given by the *one-point twist correlator*:

$$\langle \sigma(\ell) \rangle_{\mathbb{S}_L}^{(\alpha)} \tag{1.48}$$

By simple arguments of conformal invariance [28], it should have the form [46]:

$$\langle \sigma(\ell) \rangle_{\mathbb{S}_L}^{\alpha} = \mathcal{A}_\sigma^{(\alpha)} \left[\frac{2L}{\pi} \sin\left(\frac{\pi \ell}{L} \right) \right]^{-\Delta_n} \tag{1.49}$$

where the *one-point structure constant* $\mathcal{A}_\sigma^{(\alpha)}$ can also be fixed by BCFT arguments [109, 110] to be

$$\mathcal{A}_\sigma^{(\alpha)} = g_\alpha^{1-n} \tag{1.50}$$

where g_α is the Ludwig-Affleck ground state degeneracy [32] in the mother BCFT, defined as the overlap between its ground state and the conformal boundary state $|\alpha\rangle$. In consequence, one arrives at:

$$\langle \sigma(\ell) \rangle_{\mathbb{S}_L}^{\alpha} = g_A^{1-n} \left[\frac{2L}{\pi} \sin\left(\frac{\pi \ell}{L} \right) \right] \tag{1.51}$$

and finds the leading contribution to the REE to be:

$$S_n([0, \ell]) \sim \frac{c(n+1)}{12n} \log\left(\frac{2L}{\pi\epsilon} \sin \frac{\pi \ell}{L} \right) + \log g_\alpha + \frac{\log c_n}{1-n} \tag{1.52}$$

It is important to note that the same non-universal amplitude c_n appears in both (1.52) and (1.35) and originates from the *locality* of the expansion in (1.32). This provides an alternative and more general explanation for the relation observed in [71, 111] between the non-universal terms in the REE (1.52) and (1.35).

Another remarkable fact about the result (1.52) is that all the information about the particularities of the conformal BC α is encoded in the *boundary entropy* $\log g_\alpha$. This boundary entropy allows exploring the boundary renormalization group (RG) flows induced by the change of boundary conditions [112, 113]. For all other setups, the dependence on the conformal BC becomes more complicated, as we shall see in later chapters of this thesis.

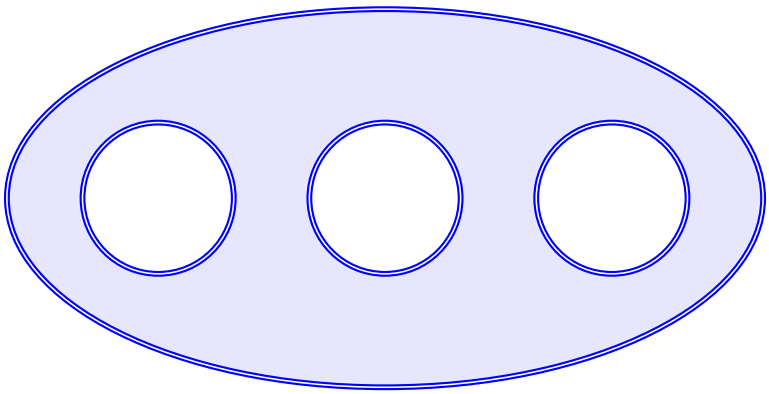

Figure 1.2: A Riemann surface with $\chi = -2$

Moving on, the result in (1.52) can be continued to $n \to 1$ to recover another celebrated result for the EE [46]:

$$S(A) = \frac{c}{6} \log\left(\frac{2L}{\pi\epsilon} \sin\frac{\pi\ell}{L}\right) + \log g_\alpha + c_1' \tag{1.53}$$

When dealing with more general bipartitions, it is expected that the analytic continuation may pose some challenges. In the case of open BC, it should be noted that even determining the REE is more difficult.

Consider, for example, a bipartition such that $A = [u, v]$ is strictly in the bulk of the system so that $0 < u < v < L$. To find the BCFT prediction for $S_n(A)$ in this case, one needs to calculate the twist 2-point function on the infinite strip $\mathbb{S}_L$ with conformal BC α [71] :

$$\langle \sigma(u)\sigma^\dagger(v)\rangle^{(\alpha)}_{\mathbb{S}_L} \tag{1.54}$$

Such correlators are difficult to solve for generic *seed* BCFTs and arbitrary n, since they require more in-depth knowledge of the cyclic orbifold BCFT.

From the replicated surface point of view, the problem of determining the REE in this setup is even more difficult to address, compared to the periodic case. The replicated surface $\mathcal{S}_{L,n}$ has genus 0 and n disconnected boundaries, so that its Euler characteristic is:

$$\chi_{open} = 2 - n \tag{1.55}$$

Such a surface is conformally equivalent to a disk from which one has cut $n-1$ additional holes, as shown in Figure 1.2. For $n = 2$, this is of course an annulus, for which the partition function is well understood for a variety of BCFTs [25, 36, 114]. This observation is the cornerstone for the calculation of the second REE , presented in Chapter 2.

For $n > 2$, however, few results are known. The difficulty stems from the fact that objects of interest in a BCFT $\mathcal{M}$ defined on some open surface Σ are computed or constructed by some implementation of a *doubling trick*. Qualitatively, this means relating correlators in $\mathcal{M}$ to *chiral* CFT amplitudes on the *double* $D(\Sigma)$ - the surface obtained by duplicating all the points in the bulk of Σ [115]. The most well-known example of such a procedure is *Cardy's doubling trick* [28, 29] whose general statement is that n-point functions of bulk primary operators on the *Upper Half Plane* (UHP) satisfy the same *Ward identities* as $2n$-point correlators of *chiral* primary fields on $\mathbb{C}$.

In a generalization of this, to calculate the BCFT partition function on an open surface Σ_n^{open} of Euler characteristic $\chi_{open} = 2 - n$ one can relate it to a CFT partition

function on a closed Riemann surface Σ_n^{closed} with $\chi_{closed} = 4 - 2n$. In consequence, one needs to both calculate this latter quantity and "reverse" the doubling trick to recover the zero-point function on Σ_n^{open}. This is a difficult task for most BCFTs.

One should observe, however, that Σ_n^{closed} is the *same* Riemann surface (up to conformal mapping) that is involved in the determination of the REE for two disjoint intervals, so these two problems are closely related. As we will show in Chapter 3, one can make this connection explicit.

Generalizing to the case of M disjoint intervals at zero temperature (even for the compact boson) adds an extra layer of challenge. In this case, the open replicated surface $\Sigma_{n,M}^{open}$ has $g = (n-1)(M-1)$ and $\chi_{open} = 1 - (n-1)(2M-1)$, and the known results [88] for the partition function on the double of $D(\Sigma_{n,M}^{open})$ are more difficult to manipulate.

While the discussion so far has focused on quantifying entanglement in the ground state of a critical quantum system, we remark that one can also use these types of CFT methods to obtain results for the REE for excited states. Notably, such investigations were done in [116, 117] for critical systems with a free CFT description and in [118] for those described by minimal models. We anticipate here that the work in [118], based on finding ODEs satisfied by the twist field correlators that describe the *REE* of an interval for excited states, is deeply connected to the investigations in 4, for the *REE* of an interval in the ground state of a system with *different* open BC.

1.5 Outline

We will present, then, in the following chapters of this thesis, our contribution to the understanding of entanglement in systems with identical open BC. Firstly, in Chapter 2, we reveal the calculation of the 2nd REE for a subsystem A in a generic $1D$ critical system described by a BCFT $\mathcal{M}$ with conformal BC α and show how the dependence of $S_2(A)$ on α is encoded in the annulus partition function $\mathcal{Z}_{\alpha|\alpha}$ of $\mathcal{M}$. This arises due to the conformal equivalence between a two-sheeted infinite strip, with branch points at the ends of the interval A and an annulus of suitably chosen aspect ratio, which we establish quantitatively by building suitable conformal maps. We verify our findings with numerical checks on the Ising model, based on *Peschel's trick*[65].

Then, in Chapter 3, we focus our attention on 1D quantum systems described by the BCFT of a compact boson with compactification radius R for both Dirichlet and Neumann BC. For this computation, we have adapted the path integral and SET methods of [70], also employed in [87], to account for the presence of a conformal boundary. We were able to derive an *exact* result for the REE $S_n(A)$ for an interval in the bulk of the system, and all integer $n \geq 2$. For finite R, we were not able to find the analytic continuation to $n \to 1$. However, in the decompactification limit $R \to \infty$, we've managed, by employing some convenient identities [87], to obtain analytic expressions for $S(A)$, for both Dirichlet and Neumann BC. Beyond various analytical checks, we've checked our $R \to \infty$ results with lattice predictions for the harmonic chain.

In Chapter 4, we consider yet another generalization of the setup of (1.52): the implementation of *mixed* BC $\alpha \neq \beta$, i.e. tuning the boundaries of the $1D$ system to different critical points. At the level of the CFT this requires the introduction of *Boundary Condition Changing Operators*(BCCOs), that implement the change in

BCs. For an interval A starting at one of the boundaries of the system, the BCFT contributions to the REE are calculated as 3-point functions of one (bulk) twist field and two BCCOs. We introduce a general procedure for deriving differential equations for these correlators and show how, for small n, they can be solved by conformal bootstrap methods. To this end, we exploit the null vector conditions on the orbifold primary states, inherited from the ones of the mother BCFT by the *induction procedure* [119] as well as various orbifold Ward identities. This method also allows a good handle of finite-size corrections, which we analyse for both the critical Ising chain and the three-state Potts model.

In Chapter 5, we will present a more formal algebraic construction of the cyclic orbifold CFT $\mathcal{M}_n$ of diagonal and rational mother CFTs. After identifying the maximal symmetry subalgebra of $\mathcal{M}_n$, we classify the operator content with respect to it and obtain the fusion rules and fusion numbers for all prime n. It is an almost self-contained presentation and acts as a complement to the geometrical approach of Chapters 2 and 4, and as a helpful toolbox for the calculations of Chapter 4.

Chapter 2

Second Rényi entropy and annulus partition function for one-dimensional quantum critical systems with boundaries

2.1 Summary

In this chapter, heavily based on [120], we present new results pertaining to the calculation of the second REE $S_2(A)$ of an interval A in the bulk of a one-dimensional critical system with *identical* open boundaries. In this section, we will present the results, as well as outline the methods and ideas involved in their derivation.

We are considering systems whose scaling limit is given by a generic BCFT $\mathcal{M}$ with central charge c and conformal BC α. We take the length of the system to be $L = N\epsilon$, where N is the number of sites and ϵ is the lattice spacing. Hence, we consider bipartitions $A = [u, v]$ with $0 < u < v < L$ as in Figure 2.1.

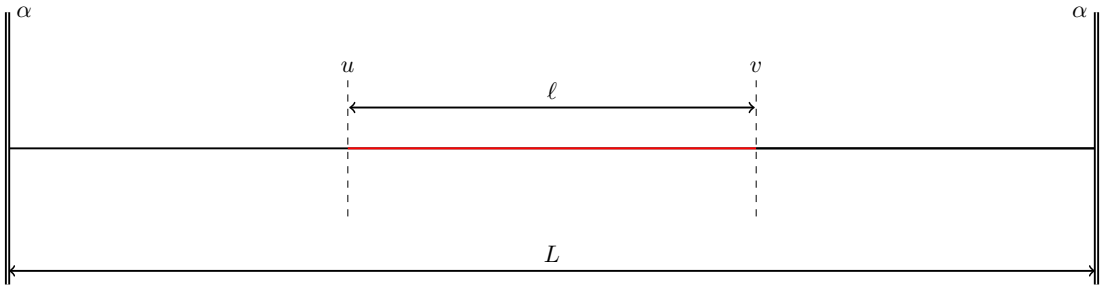

Figure 2.1: Interval in the bulk of a system with open BC

In comparison with the well-known result of [46] for an interval containing one of the boundaries of the system (which we have rederived in Section 1.4) there is an extra complication: the BCFT contribution to the REE is now determined by a *two-point function* of twist fields on $\mathbb{S}_L$ the infinite strip of width L

$$\langle \sigma(u)\sigma(v)\rangle^{(\alpha)}_{\mathbb{S}_L} \tag{2.1}$$

where σ denotes the bare twist operator in the $\mathbb{Z}_2$ orbifold BCFT. We can, alternatively, write the above correlator in terms of the partition function of the seed

BCFT $\mathcal{M}$ on a replicated surface:

$$\langle\sigma(u)\sigma(v)\rangle^{(\alpha)}_{\mathbb{S}_L} = \frac{\mathcal{Z}(\mathbb{S}_{L,2})}{\mathcal{Z}(\mathbb{S}_L)^2} \tag{2.2}$$

where $\mathbb{S}_{L,2}$ is a two-sheeted cover of the strip with branch points at u and v.

One can now map the twist field correlator in (2.2) to the unit disk $\mathbb{D}$ using:

$$w \mapsto z = \frac{s_L(w-u)}{s_L(w+u)}, \qquad s_L(w) = \frac{2L}{\pi}\sin\frac{\pi w}{2L}\,. \tag{2.3}$$

We now write the twist field correlator on $\mathbb{D}$ as:

$$\langle\sigma(0,0)\sigma(x,\bar{x})\rangle^{(\alpha)}_{\mathbb{D}} = \left[|x|^2(1-|x|^2)\right]^{-\frac{c}{8}} \mathcal{F}_2^{(\alpha)}(x) \tag{2.4}$$

where x is the cross ratio on the unit disk $\mathbb{D}$, given by:

$$x = \frac{s_L(v-u)}{s_L(v+u)} \tag{2.5}$$

and $\mathcal{F}_2^{(\alpha)}(x)$, is a universal function of the cross-ratio x that also depends on the conformal BC α. We have defined $\mathcal{F}_2^{(\alpha)}(x)$, so that that $\mathcal{F}_2^{(\alpha)}(x) \to 1$ as $x \to 0$ and $\mathcal{F}_2^{(\alpha)}(x) \to g_\alpha^{-2}$ as $x \to 1$ for generic BCFTs [1]. This is consistent with the notation of Chapter 3 and other results in the literature [121].

Hence, the main analytical achievement we present in this chapter is the computation of $\mathcal{F}_2^{(\alpha)}(x)$ in terms of the annulus partition function of the mother CFT:

$$\boxed{\mathcal{F}_2^{(\alpha)}(x) = g_\alpha^{-2}\, 2^{-\frac{c}{3}} \left[|x|^2(1-|x|^2)\right]^{\frac{c}{12}} Z_{\alpha|\alpha}(\tau)\,,} \tag{2.6}$$

where $Z_{\alpha|\alpha}(\tau)$ is the partition function on the annulus $\mathbb{A}_\tau$ of unit circumference, width $\mathrm{Im}\,\tau/2$, and boundary condition α on both edges, and g_α is the groundstate degeneracy [32]. The parameter τ (which is pure imaginary) is related to x via:

$$\left[\frac{\theta_2(\tau)}{\theta_3(\tau)}\right]^2 = |x|\,, \quad \text{or equivalently} \quad \tau(x,\bar{x}) = i\,\frac{{}_2\mathrm{F}_1\left(\frac{1}{2},\frac{1}{2},1;1-|x|^2\right)}{{}_2\mathrm{F}_1\left(\frac{1}{2},\frac{1}{2},1;|x|^2\right)}\,, \tag{2.7}$$

where the $\theta_j(\tau)$'s are the Jacobi elliptic functions (see appendix A.1.1).

These results are completely general and apply to any mother BCFT. This includes, of course, CFTs built from minimal models and Wess-Zumino-Witten models (for which the annulus partition functions have been determined in [36, 114]), free and compactified bosonic CFTs [23] to name a few. This result is reminiscent of the well-known relation between the twist four-point function on the sphere and the torus partition function $Z(\tau,\bar{\tau})$ [70, 122, 123]

$$\langle\sigma(0)\sigma(\eta,\bar{\eta})\sigma(1)\sigma(\infty)\rangle_{\mathbb{C}} = 4^{-\frac{c}{3}}\left|\eta(1-\eta)\right|^{-\frac{c}{12}} Z(\tau,\bar{\tau})\,, \qquad \eta = \left[\frac{\theta_2(\tau)}{\theta_3(\tau)}\right]^4. \tag{2.8}$$

The final result for the S_2 entropy of an interval $A = [u,v]$ in a system of length L is, up to an additive non-universal constant coming from the normalization of the lattice twist operator :

[1] There are cases in which the asymptotic behaviour of $\mathcal{F}_2^{(\alpha)}(x)$ is more subtle, see Appendix B.5.1

Second Rényi entropy of an interval in the bulk

$$S_2^{\alpha}([u,v]) = \frac{c}{24}\log\left[s_L(2u)s_L(2v)s_L^2(v+u)s_L^2(v-u)\right] + 2\log g_\alpha - \log Z_{\alpha|\alpha}(\tau)$$

To derive this result for generic BCFTs, two ingredients are essential. The first one is the observation that $\mathbb{D}_{2,x}$, the two-sheeted cover of the unit disk, with branch points at 0 and x is conformally equivalent to the annulus $\mathbb{A}_\tau$, through the map:

$$t \mapsto z = g(t) = \left(\frac{\theta_4(t|\tau)}{\theta_1(t|\tau)}\right)^2 \tag{2.9}$$

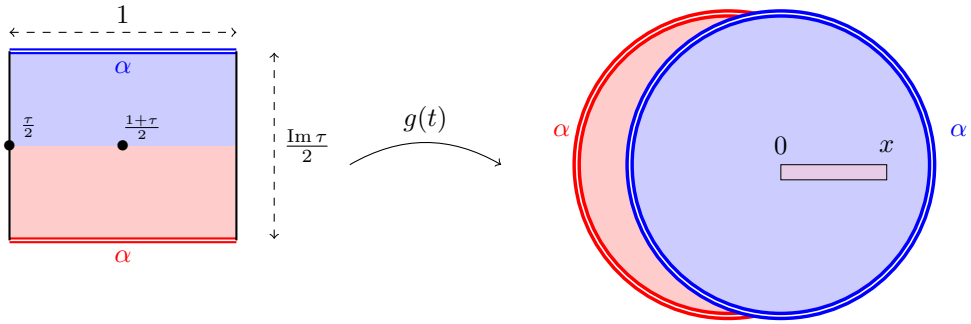

Figure 2.2: The annulus $\mathbb{A}_\tau$ – *fundamental domain pictured here* – is mapped through g to the two-sheeted disk $\mathbb{D}_{2,x}$. The black edges are identified.

The second ingredient is a variation of the **SET method**, a well-established technique for the calculation of CFT correlators [70]. One considers the following combination of orbifold correlators

$$\frac{\langle T_{\text{orb}}(z)\sigma(0,0)\sigma(x,\bar{x})\rangle_{\mathbb{D}}^{(\alpha)}}{\langle\sigma(0,0)\sigma(x,\bar{x})\rangle_{\mathbb{D}}^{(\alpha)}} \tag{2.10}$$

where $T_{\text{orb}}(z) = T(z)\otimes\mathbf{1} + \mathbf{1}\otimes T(z)$ is the SET of the $\mathbb{Z}_2$ orbifold of $\mathcal{M}$. In the replicated surface picture, one finds, using (1.30):

$$\frac{\langle T_{\text{orb}}(z)\sigma(0,0)\sigma(x,\bar{x})\rangle_{\mathbb{D}}^{(\alpha)}}{\langle\sigma(0,0)\sigma(x,\bar{x})\rangle_{\mathbb{D}}^{(\alpha)}} = 2\langle T(z)\rangle_{\mathbb{D}_{2,x}}^{\alpha} \tag{2.11}$$

By taking advantage of the operator product expansion (OPE) between $T_{\text{orb}}(z)$ and the bare twist fields, and utilizing the mapping given by Equation (2.9) to connect the right-hand side of Equation (2.11) with the annulus partition function $\mathbb{Z}_{\alpha|\alpha}(\tau)$, one can ultimately derive (2.6).

While the above procedure is general, we were able to produce an *alternative* derivation of (2.4) for A-series minimal model seed BCFTs. The main idea was to employ Cardy's mirror trick[28, 124], to write the disk correlator (2.4) as a linear expansion of conformal blocks on the sphere. The details of the calculation are relegated to Appendix A.2.

Numerical checks

To check the theoretical prediction obtained in Section 2.2 with numerical determinations of the Rényi entropy in a critical lattice model, we have considered the

critical Ising chain with free BC, with Hamiltonian

$$H_{\text{free}} = -\sum_{j=1}^{N-1} s_j^x s_{j+1}^x - \sum_{j=1}^{N} s_j^z \,, \tag{2.12}$$

where the s_j^a act as Pauli matrices σ^a at site j and trivially on the other sites of the system. We stress that both the *bulk* and the *boundary* of the chain are critical at this point in the parameter space of the model. The scaling limit of this model is the $\mathcal{M}(4,3)$ A-series minimal model CFT of central charge $c = 1/2$, with free (f) conformal BC. The annulus partition function $Z_{f|f}(\tau)$ is given by:

$$Z_{f|f}(\tau) = \sqrt{\frac{\theta_3(\tau)}{\eta(\tau)}} = 2^{1/6}\left(x\sqrt{1-x^2}\right)^{-\frac{1}{12}} \tag{2.13}$$

This model can be mapped to a fermionic chain through a Jordan-Wigner (JW) transformation

$$c_k^\dagger = \prod_{j=0}^{k-1} s_j^z s_k^+ \,, \qquad s_k^\pm \equiv \frac{1}{2}(s_k^x \pm i\, s_k^y) \,. \tag{2.14}$$

Using *Peschel's trick* [125, 126] one can recover the entanglement spectrum from the eigenvalues of the $N \times N$ *correlation matrix* of this fermionic model. In consequence, one can recover the Rényi entropies for large sizes with an advantageous computational cost that scales as $O(N)$ with the number N of spins in the system, instead of the $O(2^N)$ cost associated with directly determining the entanglement spectrum in the spin chain.

For numerics, it will be useful to consider the *shifted* second Renyi entropy in the lattice, which we define as:

$$\mathcal{G}_2^\alpha([m_u, m_v]) \equiv \widehat{S}_2^\alpha([m_u, m_v]) - \frac{1}{8}\log\left(\frac{2N}{\pi}\right) = -\log\langle\widehat{\sigma}_{m_u,0}\widehat{\sigma}_{m_v,0}\rangle_{\mathrm{S}_L}^{(\alpha)} - \frac{1}{8}\log\left(\frac{2N}{\pi}\right) , \tag{2.15}$$

so that, in the scaling limit, the leading BCFT contribution to (2.15) is

$$\mathcal{G}_2^\alpha([m_u, m_v]) \sim -\log\langle\sigma(u,\bar{u})\sigma(v,\bar{v})\rangle_{\mathrm{S}_L}^{(\alpha)} - \frac{1}{8}\log\left(\frac{2L}{\pi}\right) \tag{2.16}$$

where $u = m_u\epsilon$ and $v = m_v\epsilon$, and $\ell = v - u \equiv m\epsilon$

To investigate the agreement between the lattice data and the CFT result, we have considered two ways of "growing" the interval length ℓ and depicted the results in Figure 2.3. For the right side of Figure 2.3, we have considered an interval that starts in the middle of the chain and grows towards one end. This corresponds on the lattice to applying the first twist operator to the middle of the chain, and the second one progressively closer to the right boundary. In the left side of Figure 2.6, we consider the S_2 entropy as the interval length ℓ is grown equidistantly from the middle of the chain towards the boundaries. We see, in both cases, that the agreement with the CFT prediction is very good, although, as we will detail later in this chapter, one needs to consider unusually large system sizes to reach it, due to severe finite-size effects.

We now give here the organization of this chapter. Section 2.2 provides a detailed derivation of the main result (2.1) and a non-trivial check that our calculation does recover the result of [46, 94, 126] for the second Rényi entropy of an

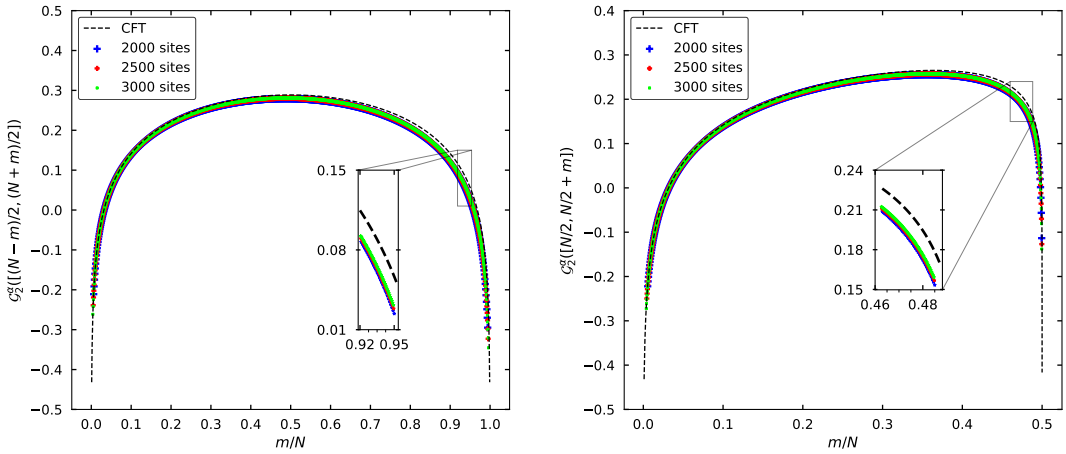

Figure 2.3: Plots of shifted Rényi entropy $\mathcal{G}_2^f([m_u, m_v])$ for the Ising chain with free BC, against the scaled interval size m/N. The deviations from the theoretical predictions are stronger as the interval is grown towards the boundaries

interval A touching the boundary. We also recover the known results for the Dirac fermion [127–129] and more generally the compact scalar field of [121]. Lastly, we extend our results to exact expressions for the mutual information and the entropy distance in specific situations. In Section 2.3, we compare our numerical results with the BCFT prediction (2.1) for the critical Ising spin chain, based on *Peschel's trick*. We also carry out a careful analysis of the finite-size effects. In Section 2.4, we conclude with a recapitulation of our results and comment on future directions for exploration. The Appendices A.1, A.2 and A.3 contain respectively our notations and conventions for elliptic functions, the alternate derivation of the main result based on boundary CFT techniques applied to the $\mathbb{Z}_2$ orbifold, and the computation of the bosonic annulus partition function.

2.2 Exact calculation of the second Rényi entropy

We consider a one-dimensional quantum critical system of finite length L, with open boundary conditions, and at zero temperature. We are interested in the second Rényi entropy of an interval $[u, v]$. The critical point is assumed to be described by a CFT. For a large enough system, the boundary flows to a renormalisation-group fixed point. We will therefore assume that the boundary condition is scale invariant. For a given bulk universality class, there is a set of possible such conformal boundary conditions $\{B_\alpha\}$ [108],[30],[124],[130]. We restrict to the case where the same boundary conditions are applied at the two ends of the system, and we assume that there is a non-degenerate ground state $|\psi_0\rangle$.

Evaluating the second Rényi entropy $S_2^\alpha([u, v])$ boils down to the computation of the following correlator in the $\mathbb{Z}_2$ orbifold of the original CFT [87], [46], [110],[96]:

$$\langle \sigma(u, \bar{u})\sigma(v, \bar{v})\rangle_{\mathbb{S}_L}^{(\alpha)} = \exp[-S_2^\alpha([u, v])]\,, \tag{2.17}$$

where σ denotes the twist operator[2]. This correlator is evaluated on the infinite

[2]Here, even though u and v are real, and hence $u = \bar{u}$ and $v = \bar{v}$, we use the standard notations

strip (with imaginary time running along the imaginary axis) $\mathbb{S}_L = \{w \in \mathbb{C},\, 0 < \mathrm{Re}(w) < L\}$ of width L with boundary condition (α) on both sides of the strip. Alternatively, this two-point function is equal to the following ratio of partition functions [46, 47]:

$$\langle \sigma(u,\bar{u})\sigma(v,\bar{v})\rangle^{(\alpha)}_{\mathbb{S}_L} = Z_2(u,v)/Z_1^2\,, \tag{2.18}$$

where Z_1 stands for the strip partition function, and $Z_2(u,v)$ stands for the partition function on a two-sheeted covering of the infinite strip with branch points at u and v, being understood that all edges have the same conformal boundary condition α. The main result of this paper rests on the fact that this Riemann surface (once compactified) is conformally equivalent to an annulus, as was observed in [110]. It is therefore not surprising that the two-twist correlation function is equal, up to some universal prefactors, to the annulus partition function. We present two different ways to derive this result. The first method, which we now detail, is more geometric in nature: we unfold the two-sheeted Riemann surface into an annulus via an explicit conformal mapping. The second method, which is more algebraic, is based on Cardy's mirror trick [108, 130] applied to the $\mathbb{Z}_2$ orbifold. This second approach, which employs a larger set of BCFT and orbifold concepts, has been relegated to Appendix A.2 to avoid congesting the logical flow of the chapter.

2.2.1 Conformal equivalence to the annulus

To construct an explicit conformal map between the two-sheeted strip and the annulus, it is convenient to first map the strip to the unit disk via

$$w \mapsto z = \frac{s_L(w-u)}{s_L(w+u)}, \qquad s_L(w) = \frac{2L}{\pi}\sin\frac{\pi w}{2L}\,. \tag{2.19}$$

The above conformal map also sends the two-sheeted strip (with branch points at $w = u$ and $w = v$) to the two-sheeted unit disk $\mathbb{D}_{2,x}$ with branch points at $z = 0$ and $z = x$, with

$$x = \frac{s_L(v-u)}{s_L(v+u)} = \frac{\sin\frac{\pi}{2L}(v-u)}{\sin\frac{\pi}{2L}(v+u)}\,. \tag{2.20}$$

Note that x is real, and $0 < x < 1$. Let us now describe the conformal mapping sending $\mathbb{D}_{2,x}$ to an annulus. First, for any complex number τ with $\mathrm{Im}\,\tau > 0$, the function

$$t \mapsto z = g(t) = \left(\frac{\theta_4(t|\tau)}{\theta_1(t|\tau)}\right)^2 \tag{2.21}$$

is a biholomorphic map from the torus of modular parameter τ to the double-sheeted cover of the Riemann sphere with four branch points at positions

$$g(0) = \infty\,, \quad g\left(\frac{1+\tau}{2}\right) = x\,, \quad g\left(\frac{\tau}{2}\right) = 0\,, \quad g\left(\frac{1}{2}\right) = \frac{1}{x}\,, \tag{2.22}$$

with

$$x = \left(\frac{\theta_2(\tau)}{\theta_3(\tau)}\right)^2, \qquad \tau = \mathrm{i}\,\frac{{}_2\mathrm{F}_1\left(\frac{1}{2},\frac{1}{2},1;1-x^2\right)}{{}_2\mathrm{F}_1\left(\frac{1}{2},\frac{1}{2},1;x^2\right)}\,, \tag{2.23}$$

$\sigma(u,\bar{u})$ and $\sigma(v,\bar{v})$ for bulk operators, which emphasizes the fact that the correlation function is not a holomorphic function of u and v.

and where the $\theta_j(t,q)$'s are Jacobi theta functions (see Appendix A.1.1 for definitions and conventions). Using the properties (A.3) of these functions, we readily see that the function g satisfies the identity:

$$g(t+\tau/2) = g(t)^{-1}\,, \tag{2.24}$$

for any t on the torus. In the present situation, since $0 < x < 1$, the modular parameter τ is pure imaginary, with $\mathrm{Im}\,\tau > 0$. Then, from the above relation we get

$$g\left(\frac{\tau}{2}+\bar{t}\right) = \overline{g(t)^{-1}}\,. \tag{2.25}$$

Now notice that identifying t and $\tau/2+\bar{t}$ amounts to folding the torus into an annulus of unit width, and height $\mathrm{Im}\,\tau/2$

$$\mathbb{A}_\tau = \left\{ t \in \mathbb{C}/\mathbb{Z}, \qquad \frac{\mathrm{Im}\,\tau}{4} \le \mathrm{Im}\,t \le \frac{3\,\mathrm{Im}\,\tau}{4} \right\}, \tag{2.26}$$

while identifying z and $1/\bar{z}$ on the two-sheeted Riemann sphere yields the two-sheeted unit disk $\mathbb{D}_{2,x}$. In essence, these foldings are the reverse of Cardy's mirror trick [30]. The relation (2.25) ensures that the map g descends to the quotient, yielding a biholomorphic map from the annulus $\mathbb{A}_\tau$ to the two-sheeted unit disk $\mathbb{D}_{2,x}$, as shown in Figure 2.

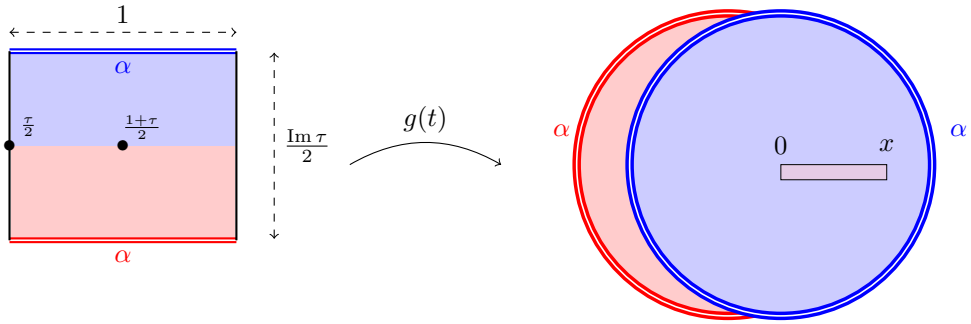

Figure 2.4: The annulus $\mathbb{A}_\tau$ – *fundamental domain pictured here* – is mapped through g to the two-sheeted disk $\mathbb{D}_{2,x}$. The black edges are identified.

2.2.2 Rényi entropy of an interval in the bulk

Recall that the twist σ is a primary operator of conformal dimensions $h_\sigma = \bar{h}_\sigma = c/16$ in the $\mathbb{Z}_2$ orbifold CFT. Using conformal covariance under the map (2.19), we can relate the twist correlation functions on the strip and the unit disk:

$$\langle \sigma(u,\bar{u})\sigma(v,\bar{v})\rangle^{(\alpha)}_{\mathbb{S}_L} = (s_L(u+v))^{-c/4}\,\langle \sigma(0,0)\sigma(x,\bar{x})\rangle^{(\alpha)}_{\mathbb{D}}\,, \tag{2.27}$$

where

$$x = \bar{x} = \frac{s_L(v-u)}{s_L(u+v)} \ge 0\,. \tag{2.28}$$

The strategy (adapted from [70]) to compute $\langle \sigma(0,0)\sigma(x,\bar{x})\rangle^{(\alpha)}_{\mathbb{D}}$ in terms of an annulus partition function is the following. We insert the stress-energy tensor T_{orb} into the twist correlation function on the unit disk and study the behaviour of the

function $\langle T_{\rm orb}(z)\sigma(0,0)\sigma(x,\bar{x})\rangle_{\mathbb{D}}^{(\alpha)}$ as $z \to x$. Since σ is a primary operator, we have the OPE

$$T_{\rm orb}(z)\sigma(x,\bar{x}) = \frac{h_\sigma \sigma(x,\bar{x})}{(z-x)^2} + \frac{\partial_x \sigma(x,\bar{x})}{z-x} + \text{regular terms}, \tag{2.29}$$

and thus

$$\partial_x \log\langle\sigma(0,0)\sigma(x,\bar{x})\rangle_{\mathbb{D}}^{(\alpha)} = \frac{1}{2\pi i}\oint_{C_x} \frac{\langle T_{\rm orb}(z)\sigma(0,0)\sigma(x,\bar{x})\rangle_{\mathbb{D}}^{(\alpha)}}{\langle\sigma(0,0)\sigma(x,\bar{x})\rangle_{\mathbb{D}}^{(\alpha)}}\, dz\,, \tag{2.30}$$

where the integration contour C_x encloses the point x and goes anti-clockwise. However, in (2.29) and (2.30) the parameter x stands for a complex variable (independent of $\bar{x}$). Setting $x = \bar{x}$ thus yields

$$\partial_x \left(\log\langle\sigma(0,0)\sigma(x,\bar{x})\rangle_{\mathbb{D}}^{(\alpha)}\big|_{x=\bar{x}} \right) = 2 \times \frac{1}{2\pi i}\oint_{C_x} \frac{\langle T_{\rm orb}(z)\sigma(0,0)\sigma(x,\bar{x})\rangle_{\mathbb{D}}^{(\alpha)}}{\langle\sigma(0,0)\sigma(x,\bar{x})\rangle_{\mathbb{D}}^{(\alpha)}}\, dz\,. \tag{2.31}$$

We will drop the $|_{x=\bar{x}}$, but from now on x is assumed – without loss of generality – to be real positive, with $0 < x < 1$.

In terms of the mother theory, $\langle T_{\rm orb}(z)\sigma(0,0)\sigma(x,\bar{x})\rangle_{\mathbb{D}}^{(\alpha)}$ is the one-point function of the stress-energy tensor on the two-sheeted surface $\mathbb{D}_{2,x}$. Since $T_{\rm orb}(z) = T(z)\otimes\mathbb{I} + \mathbb{I}\otimes T(z)$, we can write

$$\frac{\langle T_{\rm orb}(z)\sigma(0,0)\sigma(x,\bar{x})\rangle_{\mathbb{D}}^{(\alpha)}}{\langle\sigma(0,0)\sigma(x,\bar{x})\rangle_{\mathbb{D}}^{(\alpha)}} = 2\langle T(z)\rangle_{\mathbb{D}_{2,x}}^{\alpha}\,, \tag{2.32}$$

where the last equality comes from the symmetry under the exchange of the two copies of the unit disk. The last step is to compute $\langle T(z)\rangle_{\mathbb{D}_{2,x}}^{\alpha}$ by exploiting the conformal equivalence between the two-sheeted cover of the disk $\mathbb{D}_{2,x}$ and the annulus $\mathbb{A}_\tau$ via the map $z = g(t)$ described in (2.21):

$$\langle T(z)\rangle_{\mathbb{D}_{2,x}}^{\alpha} = \left(\frac{dt}{dz}\right)^2 \langle T(t)\rangle_{\mathbb{A}_\tau}^{\alpha} + \frac{c}{12}\{t,z\}\,, \tag{2.33}$$

where $\{t,z\}$ denotes the Schwarzian derivative of the map g. First, the one-point function of $T(z)$ on the annulus is

$$\langle T(t)\rangle_{\mathbb{A}_\tau}^{\alpha} = 2i\pi\partial_\tau \log Z_{\alpha|\alpha}(\tau)\,, \tag{2.34}$$

where $Z_{\alpha|\alpha}(\tau)$ denotes the partition function on the annulus $\mathbb{A}_\tau$ (with boundary condition α on both edges). Let $|\alpha\rangle$ be the boundary state associated to the boundary condition α. Since $\mathbb{A}_\tau$ has unit width, and height $\beta/2 = -i\tau/2$, we have

$$Z_{\alpha|\alpha}(\tau) = \langle\alpha|e^{i\pi\tau(L_0+\bar{L}_0-c/12)}|\alpha\rangle\,. \tag{2.35}$$

We can exploit the differential equation (A.17) obeyed by the map $z = g(t)$, namely

$$\left(\frac{dt}{dz}\right)^2 = -\frac{1}{4\pi^2\theta_3^4(\tau)z(z-x)(1-xz)}\,, \tag{2.36}$$

to derive

$$\langle T(z)\rangle_{\mathbb{D}_{2,x}}^{\alpha} = \frac{x(1-x^2)}{4z(z-x)(1-zx)}\partial_x \log Z_{\alpha|\alpha}(\tau) + \frac{c}{12}\{t,z\}\,, \tag{2.37}$$

where we have also used the relation (A.11). The Schwarzian derivative can be easily evaluated using (2.36), yielding

$$\{t,z\} = \frac{3x^2(1+z^4) - 4\,(x+x^3)\,(z+z^3) + 2\left(2x^4+x^2+2\right)z^2}{8z^2(z-x)^2(1-xz)^2}\,, \tag{2.38}$$

and in particular, the residue at $z \to x$ is

$$\frac{1}{2\pi i}\oint_{C_x} \{t,z\}\,dz = -\frac{1-2x^2}{4x\,(1-x^2)} = -\frac{1}{8}\partial_x \log x^2(1-x^2)\,. \tag{2.39}$$

Finally plugging the above in (2.31) we get

$$\partial_x \log\langle\sigma(0,0)\sigma(x,\bar{x})\rangle_{\mathbb{D}}^{(\alpha)} = \partial_x \log Z_{\alpha|\alpha}(\tau) - \frac{c}{24}\partial_x \log x^2(1-x^2)\,. \tag{2.40}$$

Upon integration, we obtain

$$\langle\sigma(0,0)\sigma(x,\bar{x})\rangle_{\mathbb{D}}^{(\alpha)} = \text{const} \times \left[x^2(1-x^2)\right]^{-\frac{c}{24}} Z_{\alpha|\alpha}(\tau)\,. \tag{2.41}$$

To fix the multiplicative constant in the above relation, we consider the leading behaviour as x tends to zero. In this limit, we have $\mathrm{Im}\,\tau \to +\infty$ and $q \to 0$, with the relation $q = e^{2i\pi\tau} \sim (x/4)^4$. Thus

$$Z_{\alpha|\alpha}(\tau) = \langle\alpha|e^{i\pi\tau(L_0+\bar{L}_0-c/12)}|\alpha\rangle \underset{\mathrm{Im}\,\tau\to\infty}{\sim} q^{-c/24}\,g_\alpha^2\,, \qquad g_\alpha = |\langle\alpha|0\rangle|\,, \tag{2.42}$$

where $|0\rangle$ is the normalized ground state wavefunction of the Hamiltonian with periodic boundary conditions. The twist operator σ is normalized so that

$$\langle\sigma(0,0)\sigma(x,\bar{x})\rangle_{\mathbb{D}}^{(\alpha)} \underset{x\to 0}{\sim} x^{-c/4}\,, \tag{2.43}$$

and hence the fully explicit relation (2.41) is

$$\boxed{\langle\sigma(0,0)\sigma(x,\bar{x})\rangle_{\mathbb{D}}^{(\alpha)} = g_\alpha^{-2}\,2^{-\frac{c}{3}}\left[x^2(1-x^2)\right]^{-\frac{c}{24}} Z_{\alpha|\alpha}(\tau)\,.} \tag{2.44}$$

Note that in the above equation we have assumed $x = \bar{x}$, with $0 < x < 1$. For a generic complex x on the unit disk, the result still holds up to replacing x by $|x|$ in the *r.h.s.* as well as in (2.23). Back to the original problem on the strip, we obtain

$$\langle\sigma(u,\bar{u})\sigma(v,\bar{v})\rangle_{\mathbb{S}_L}^{(\alpha)} = g_\alpha^{-2}2^{-\frac{c}{3}}\left[s_L(v+u)^2 s_L(v-u)^2 s_L(2u) s_L(2v)\right]^{-\frac{c}{24}} Z_{\alpha|\alpha}(\tau)\,, \tag{2.45}$$

and we get the announced result (2.1) for the second Rényi entropy.

2.2.3 Rényi Entropy of an interval touching the boundary

As a check for the formula (2.45), we want to recover the expression for the Rényi entropy S_2 of an interval $A = [0,\ell]$ touching the boundary of the chain [46, 94, 96, 111, 131]:

$$S_2^\alpha([0,\ell]) = \frac{c}{8}\log\left[\frac{2L}{\pi}\sin\left(\frac{\pi\ell}{L}\right)\right] + \log g_\alpha\,. \tag{2.46}$$

Let us consider the two-point function $\langle\sigma(u,\bar{u})\sigma(v,\bar{v})\rangle^{(\alpha)}_{\mathbb{S}_L}$ in the limit $u \to 0$. On the left-hand side of (2.45), we can use the bulk-boundary OPE:

$$\sigma(u,\bar{u}) \underset{u\to 0}{\sim} A^{\alpha}_{\sigma}\,(u+\bar{u})^{-c/8}\,\mathbb{I}\,, \tag{2.47}$$

where $A^{\alpha}_{\sigma} = (g_\alpha)^{-1}$ is the OPE coefficient for the bulk operator σ approaching a boundary with boundary condition α, and giving rise to the boundary identity operator $\mathbb{I}$. Hence, for u real:

$$\langle\sigma(u,\bar{u})\sigma(\ell)\rangle^{(\alpha)}_{\mathbb{S}_L} \underset{u\to 0}{\sim} (g_\alpha)^{-1}\,(2u)^{-c/8}\,\langle\sigma(\ell)\rangle^{(\alpha)}_{\mathbb{S}_L}\,. \tag{2.48}$$

On the right-hand side of (2.45), the limit $u \to 0$ corresponds to $x \to 1$ and $\tau \to 0$, with

$$\widetilde{q} = e^{-2i\pi/\tau} \sim \left(\frac{1-x^2}{16}\right)^2 \to 0\,. \tag{2.49}$$

In a rational CFT, the annulus partition function decomposes on the characters of primary representations V_k as

$$Z_{\alpha|\alpha}(\tau) = \sum_k n^k_{\alpha\alpha}\,\chi_k(-1/\tau)\,, \qquad \chi_k(\tau) = \mathrm{Tr}_{V_k}\left(q^{L_0-c/24}\right)\,. \tag{2.50}$$

In the limit $\widetilde{q} \to 0$, we get $Z_{\alpha|\alpha}(\tau) \sim n^0_{\alpha\alpha}\widetilde{q}^{-c/24}$, where $k = 0$ stands for the identity operator, and $n^0_{\alpha\alpha} = 1$, since we assumed a non-degenerate ground state $|\psi_0\rangle$. Thus

$$Z_{\alpha|\alpha}(\tau) \sim \left(\frac{1-x^2}{16}\right)^{-c/12} \sim 2^{\frac{c}{4}}\left(\frac{s_L^2(v)}{u\,s_L(2v)}\right)^{\frac{c}{12}}\,, \tag{2.51}$$

where we have used (2.20) to obtain the second relation. After some simple algebra, one gets for the right-hand side of (2.45):

$$\langle\sigma(u)\sigma(v)\rangle^{(\alpha)}_{\mathbb{S}_L} \underset{u\to 0}{\sim} g_\alpha^{-2}\left(\frac{1}{\frac{2L}{\pi}\sin\frac{\pi\ell}{L}}\right)^{c/8}(2u)^{-c/8}\,. \tag{2.52}$$

Hence, comparing (2.48) and (2.52), we recover the well known one-point function

$$\langle\sigma(\ell)\rangle^{(\alpha)}_{\mathbb{S}_L} = g_\alpha^{-1}\left(\frac{1}{\frac{2L}{\pi}\sin\frac{\pi\ell}{L}}\right)^{c/8}\,, \tag{2.53}$$

which indeed yields (2.46).

2.2.4 Compact boson

We can further apply our main formula (2.1) by recovering the known results for the Dirac fermion [127–129] and more generally the compact boson [121]. We consider a compact scalar field $\phi \equiv \phi + 2\pi R$ with action

$$S[\phi] = \frac{1}{8\pi}\int d^2r\,\partial_\mu\phi\,\partial^\mu\phi\,, \tag{2.54}$$

and Dirichlet boundary conditions. The relevant annulus partition function is (see Appendix A.3)

$$Z(\tau) = \frac{\theta_3(-R^2/\tau)}{\eta(-1/\tau)}\,. \tag{2.55}$$

Before plugging this partition function into our main formula (2.1), let us write it as

$$Z(\tau) = \frac{\theta_3(-1/\tau)}{\eta(-1/\tau)} \times \frac{\theta_3(-R^2/\tau)}{\theta_3(-1/\tau)} = \frac{\theta_3(\tau)}{\eta(\tau)} \times \frac{\theta_3(-R^2/\tau)}{\theta_3(-1/\tau)} \,. \tag{2.56}$$

Now using

$$\frac{\theta_3(\tau)}{\eta(\tau)} = 2^{1/3}\left[x^2(1-x^2)\right]^{-\frac{1}{12}} = 2^{\frac{1}{3}}\left(\frac{s_L^2(v-u)s_L(2u)s_L(2v)}{s_L^4(v+u)}\right)^{-\frac{1}{12}} \,. \tag{2.57}$$

we find (up to an additive constant)

$$\mathrm{S}_2^a([u,v]) = \frac{1}{8}\log\frac{s_L(2u)s_L(2v)s_L^2(v-u)}{s_L^2(v+u)} - \log\mathcal{F}_2(\tau)\,, \tag{2.58}$$

where the function $\mathcal{F}_2(\tau)$ is given by

$$\mathcal{F}_2(\tau) = \frac{\theta_3(-R^2/\tau)}{\theta_3(-1/\tau)} = \frac{\sum_{m\in\mathbb{Z}} \exp\left(-i\pi m^2R^2/\tau\right)}{\sum_{m\in\mathbb{Z}} \exp\left(-i\pi m^2/\tau\right)} \,. \tag{2.59}$$

This is equivalent to the formulae (13) and (18) of [121] provided $\bar{\mathcal{M}} = i\pi/4\tau$ in (18) [although we note a typo in the first term of (13)], and the result for the Dirac fermion [namely $\mathcal{F}_2(\tau) = 1$ for $R = 1$] follows.

2.2.5 Other entanglement measures

In this section, we present two other entanglement measures related to the second Rényi entropy: mutual information and entropy distance. Here they are defined in the same context as considered above, namely in a critical 1d quantum system of finite size L, with open boundaries, and the same conformal boundary condition on both sides.

When considering two disjoint subsystems A and B, a standard measure of the information "shared" by A and B is given by the *mutual information* $I_{A:B}$, defined as (see [132] and references therein)

$$I_{A:B} = S_A + S_B - S_{A\cup B}\,, \tag{2.60}$$

where S stands for a given measure of entanglement for a single subsystem. Using our result (2.1), we can express the mutual information (associated with the second Rényi entropy) of two intervals each touching a different boundary of the system, namely $A = [0,u]$ and $B = [v,L]$. After some straightforward algebra on (2.1) and (2.46), we get

$$I_{[0,u]:[v,L]} = \frac{c}{12}\log\left[\frac{s(2u)s(2v)}{s(v+u)s(v-u)}\right] + \log Z_{\alpha|\alpha}(\tau)\,. \tag{2.61}$$

Back to the situation of a subsystem A consisting of a single interval $[u,v]$ inside the bulk of the system, we turn to the question of quantifying how much

the whole spectrum of the density matrix ρ_A depends on the choice of external parameters (see [133] and references therein) – in the present case, the external parameter is the boundary condition. Here, we shall use the n-norm of an operator Λ, defined as

$$\|\Lambda\|_n = \left\{\mathrm{Tr}\left[(\Lambda^\dagger\Lambda)^{n/2}\right]\right\}^{1/n}, \tag{2.62}$$

and the associated Schatten distance[3]

$$D_n(\rho,\rho') = \|\rho-\rho'\|_n\,. \tag{2.63}$$

To be specific, we denote by $\rho_{A,\alpha}$ the reduced density matrix associated with the ground state of our finite critical systems with boundary conditions α on both sides of the system. Then we consider the Schatten distance $D_n(\rho_{A,\alpha},\rho_{A,\beta})$, where α and β are two distinct conformal BCs. We restrict to the value $n=2$, and we have

$$D_2(\rho_{A,\alpha},\rho_{A,\beta}) = \left[\frac{1}{2}\mathrm{Tr}\,\rho_{A,\alpha}^2 + \frac{1}{2}\mathrm{Tr}\,\rho_{A,\beta}^2 - \mathrm{Tr}(\rho_{A,\alpha}\rho_{A,\beta})\right]^{1/2}. \tag{2.64}$$

The first two terms in (2.64) are given by (2.1), whereas the third term is obtained by a slight generalization of the previous discussion. Indeed, we can write this term as the two-twist correlation function

$$\mathrm{Tr}(\rho_{A,\alpha}\rho_{A,\beta}) \sim \langle\sigma(u,\bar u)\sigma(v,\bar v)\rangle^{(\alpha\beta)}_{\mathbb{S}_L} \tag{2.65}$$

on the infinite strip with BC α (resp. β) on both sides, for the first (resp. second) copy of the mother CFT in the $\mathbb{Z}_2$ orbifold. Through the same line of argument as in Section 2.2.2, we obtain

$$\langle\sigma(u,\bar u)\sigma(v,\bar v)\rangle^{(\alpha\beta)}_{\mathbb{S}_L} = (g_\alpha g_\beta)^{-1}2^{-\frac{c}{3}}\left[s_L(v+u)^2 s_L(v-u)^2 s_L(2u)s_L(2v)\right]^{-\frac{c}{24}} Z_{\alpha|\beta}(\tau)\,. \tag{2.66}$$

As a result, we get

$$D_2(\rho_{A,\alpha},\rho_{A,\beta}) = 2^{-\frac{c}{6}}\left[s_L(v+u)^2 s_L(v-u)^2 s_L(2u)s_L(2v)\right]^{-\frac{c}{48}} K_{\alpha\beta}(\tau)\,, \tag{2.67}$$

where

$$K_{\alpha\beta}(\tau) = \left[\frac{Z_{\alpha|\alpha}(\tau)}{2g_\alpha^2} + \frac{Z_{\beta|\beta}(\tau)}{2g_\beta^2} - \frac{Z_{\alpha|\beta}(\tau)}{g_\alpha g_\beta}\right]^{1/2}. \tag{2.68}$$

Plugging in the expression of the annulus partition function in terms of Ishibashi states (A.26)

$$Z_{\alpha|\beta}(\tau) = \langle\alpha|e^{i\pi\tau(L_0+\bar L_0-c/12)}|\beta\rangle = \sum_j (\Psi_j^\alpha)^*\Psi_j^\beta\chi_j(\tau) \tag{2.69}$$

yields

$$K_{\alpha\beta}(\tau) = \left[\frac{1}{2}\sum_j \left|A_j^\alpha - A_j^\beta\right|^2\chi_j(\tau)\right]^{1/2}. \tag{2.70}$$

Interestingly the term $j=0$ cancels out, as follows from $A_0^\alpha = A_0^\beta = 1$. This means that the vacuum sector does not contribute to the Schatten distance. Furthermore,

[3] While the most interesting distance is D_1, it can be extremely difficult to evaluate directly. One can instead exploit a replica trick developed in [134, 135]: one first computes the distance D_n for all even n, followed by an analytic continuation to $n=1$.

this last expression is rather suggestive: it is the distance associated with the following L^2 norm (weighted by the positive coefficients $\chi_j(\tau)/2$) on the A_j space

$$\|A\| = \left[\frac{1}{2}\sum_j \left|A_j\right|^2 \chi_j(\tau)\right]^{1/2} . \tag{2.71}$$

We shall now consider some limiting cases of the Schatten distance (2.67).

Small interval in the bulk

The limit of a very small interval in the bulk is recovered for $u \to v$, which corresponds to $q = e^{2i\pi\tau} \to 0$. In this regime we have

$$\chi_j(\tau) \sim q^{h_j - c/24} \tag{2.72}$$

As mentioned above the term $j = 0$ does not contribute, so the L^2 norm (2.71) is dominated by the term j_0 corresponding to the most relevant state such that

$$A^\alpha_{j_0} \neq A^\beta_{j_0} . \tag{2.73}$$

Then

$$K_{\alpha\beta}(\tau) \sim \frac{1}{\sqrt{2}}\left|A^\alpha_{j_0} - A^\beta_{j_0}\right| q^{h_{j_0}/2 - c/48} . \tag{2.74}$$

and in the limit of a small interval in the bulk ($\ell \to 0$) the Schatten distance behaves, up to a constant prefactor, as

$$D_2(\rho_{A,\alpha}, \rho_{A,\beta}) \underset{\ell\to 0}{\sim} \ell^{2h_{j_0} - c/8} \frac{\left|A^\alpha_{j_0} - A^\beta_{j_0}\right|}{s_L (2v)^{2h_{j_0}}} . \tag{2.75}$$

Interval touching the boundary

In the limit $u \to 0$ (v fixed), the parameter q goes to 1 so it is more convenient to work with $\tilde{q} = e^{-2i\pi/\tau}$. Thus we use expression (2.68) together with

$$Z_{\alpha|\beta}(\tau) = \sum_k n^k_{\alpha\beta}\, \chi_k(-1/\tau) , \qquad \chi_k(-1/\tau) = \mathrm{Tr}_{V_k}\left(\tilde{q}^{L_0 - c/24}\right) \underset{\tilde{q}\to 0}{\sim} \tilde{q}^{h_k - c/24} , \tag{2.76}$$

For the vacuum sector to propagate, the left and right conformal boundary conditions must be the same [114] :

$$n^0_{\alpha\beta} = \delta_{\alpha\beta} \tag{2.77}$$

This implies that the identity character χ_0 does not appear in the expansion of $Z_{\alpha|\beta}(\tau)$ for $\alpha \neq \beta$. Thus, the leading order behaviour of the annulus partition function is:

$$Z_{\alpha|\beta}(\tau) \sim \tilde{q}^{-c/24 + h_{k_0}} \tag{2.78}$$

where k_0 corresponds to the most relevant state that can propagate with boundary conditions α on one side and β on the other. Equivalently, h_{k_0} is the lowest allowed conformal dimension in the spectrum of boundary changing operators between

α and β. This implies that for an interval strictly touching the boundary the states $\rho_{A,\alpha}$ and $\rho_{A,\beta}$ simply become orthogonal

$$D_2(\rho_{A,\alpha},\rho_{A,\beta}) \underset{u\to 0}{\to} \sqrt{\|\rho_{A,\alpha}\|^2+\|\rho_{A,\beta}\|^2}\,. \tag{2.79}$$

Furthermore the vanishing of the scalar product between $\rho_{A,\alpha}$ and $\rho_{A,\beta}$ as $u \to 0$ is controlled by h_{k_0} :

$$\frac{\mathrm{Tr}(\rho_{A,\alpha}\rho_{A,\beta})}{\|\rho_{A,\alpha}\|\|\rho_{A,\beta}\|} = \frac{Z_{\alpha|\beta}(\tau)}{\sqrt{Z_{\alpha|\alpha}(\tau)Z_{\beta|\beta}(\tau)}} \underset{u\to 0}{\sim} u^{2h_{k_0}} \left(\frac{s_L(2v)}{8s_L^2(v)}\right)^{2h_{k_0}}. \tag{2.80}$$

2.3 Comparison with numerics and finite-size scaling

2.3.1 Rényi entropy in a quantum Ising chain

To compare the theoretical prediction obtained in Section 2.2 with numerical determinations of the Rényi entropy in a critical lattice model, we have focused on the model that was the most numerically accessible, *i.e.* the Ising spin chain with *free boundary conditions*, with Hamiltonian:

$$H_{\text{free}} = -\sum_{j=1}^{N-1} s_j^x s_{j+1}^x - h\sum_{j=1}^{N} s_j^z\,, \tag{2.81}$$

where the s_j^a have their usual definition – they act as Pauli matrices σ^a at site j and trivially on the other sites of the system. The chain is taken to have length $L = N\epsilon$, where ϵ is the lattice spacing, and N is the number of spins. The *scaling limit* of this system corresponds to taking $N \to \infty$ and $\epsilon \to 0$ while keeping the chain length L fixed. Finally, to achieve criticality, the external field h should be set to $h = 1$. We stress that both the *bulk* and the *boundary* of the chain are critical at this point in the parameter space of the model.

A convenient feature of this model is that it can be mapped to a fermionic chain through a Jordan-Wigner (JW) transformation

$$a_k^\dagger = \prod_{j=0}^{k-1} s_j^z s_k^+\,, \qquad s_k^\pm \equiv \frac{1}{2}(s_k^x \pm i\, s_k^y)\,. \tag{2.82}$$

Once the Hamiltonian of the fermionic chain has been obtained, one proceeds to find a basis of fermionic operators $\eta_i, \eta_i^\dagger$ that diagonalizes it – and still satisfies the standard anti-commutation relations $\{\eta_i, \eta_j^\dagger\} = \delta_{ij}$, *etc.* For free or periodic boundary conditions, the procedure is standard, and we refer the reader to the excellent review [136]. Having found the diagonal fermionic basis $\eta_i, \eta_i^\dagger$ one proceeds to build the correlation matrix $\mathbf{M} \equiv \langle \boldsymbol{\eta}\cdot\boldsymbol{\eta}^\dagger\rangle$ with $\boldsymbol{\eta} \equiv (\eta_1,\dots,\eta_N,\eta_1^\dagger,\dots,\eta_N^\dagger)^T$. The eigenvalues of $\mathbf{M}$ are simply related to the values of the entanglement spectrum, and thus one can calculate Rényi entropies for large sizes with an advantageous computational cost that scales as $O(N)$ with the number N of spins in the system. This method, known in the literature as *Peschel's trick* [65, 137], has been employed in several works [125, 126] for both free and periodic boundary conditions, and we refer to them for detailed explanations of the implementation.

Due to the JW "strings" of s^z operators in (2.82), the relation between the fermionic and spin reduced density matrices of a given subsystem may be non-trivial [125, 138]. For free and periodic BC though, the ground-state wavefunction has a well-defined *parity* of the fermion number, and, as a consequence, the fermionic and spin reduced density matrices of a single interval can be shown to coincide. The Peschel trick fails, however, for the case of fixed BC, where the above feature of the wavefunction no longer holds, as pointed out in [125]. There has been progress, however, in adapting the trick to fixed BC, for the case of an interval touching the boundary [125, 126, 139]. Extending the technique to efficiently find the entanglement spectrum for an interval A that does not touch the boundary is still an open problem.

To give concrete expressions to compare with the numerical data, we will quickly review some basic aspects of the CFT description of the critical Ising chain. It is well known that in the critical regime, the scaling limit of the infinite and periodic Ising chains is the Ising CFT, namely the CFT with central charge $c = 1/2$ and an operator spectrum consisting of three primary operators – the identity $\mathbb{I}$, energy ε and spin operators σ – and their descendants [23]. The case of open boundaries is also well understood from the CFT perspective. There are three conformal boundary conditions for the Ising BCFT, which, in the framework of radial quantization on the annulus, allow the construction of the following physical boundary states [23, 30]:

$$|f\rangle = |\mathbf{1}\rangle\!\rangle - |\varepsilon\rangle\!\rangle \quad \textit{(free BC)}\,, \tag{2.83}$$

$$|\pm\rangle = \frac{1}{\sqrt{2}}|\mathbf{1}\rangle\!\rangle + \frac{1}{\sqrt{2}}|\varepsilon\rangle\!\rangle \pm \frac{1}{2^{1/4}}|\sigma\rangle\!\rangle \quad \textit{(fixed BC)}\,, \tag{2.84}$$

where $|i\rangle\!\rangle$ denotes the Ishibashi state [30, 140] corresponding to the primary operator i. The physical boundary states $|\alpha\rangle$ are in one-to-one correspondence with the primary fields of the bulk CFT[4]: $|f\rangle \leftrightarrow \sigma$ and $|\pm\rangle \leftrightarrow \mathbb{I}/\varepsilon$. The annulus partition function for the Ising BCFT is compactly written in terms of Jacobi theta functions for all diagonal choices of BCs $(\alpha|\alpha)$ and, in consequence, in terms of the parameter x defined in Section 2.2

$$Z_{f|f}(\tau) = \sqrt{\frac{\theta_3(\tau)}{\eta(\tau)}} = 2^{1/6}\left(x\sqrt{1-x^2}\right)^{-\frac{1}{12}}\,. \tag{2.85}$$

and

$$Z_{+|+}(\tau) = Z_{-|-}(\tau) = \frac{\sqrt{\theta_3(\tau)} + \sqrt{\theta_4(\tau)}}{2\sqrt{\eta(\tau)}} = 2^{1/6}\frac{1+x^{\frac{1}{4}}}{2}\left(x\sqrt{1-x^2}\right)^{-\frac{1}{12}}\,. \tag{2.86}$$

These relations allow us to express the orbifold two-point correlator on the disk in an elementary way:

$$\langle\sigma(0,0)\sigma(x,\bar{x})\rangle_{\mathbb{D}}^{(f,f)} = \left[|x|^2(1-|x|^2)\right]^{-\frac{1}{8}}\,, \tag{2.87}$$

$$\langle\sigma(0,0)\sigma(x,\bar{x})\rangle_{\mathbb{D}}^{(+,+)} = \frac{1+|x|^{\frac{1}{4}}}{2}\left[|x|^2(1-|x|^2)\right]^{-\frac{1}{8}}\,, \tag{2.88}$$

which is, of course, very convenient for numerical checks. Note that the $\mathbb{Z}_2$ orbifold of the Ising model is equivalent to a special case of the critical Ashkin-Teller model [142]. Therefore, the CFT we are considering here is nothing but the

[4]This statement is strictly true if the bulk CFT is diagonal, see [141] for a detailed discussion.

$\mathbb{Z}_2$ orbifold of a free boson. This might explain why the above two-point functions end up being so simple.

Recall that the lattice operator $\widehat{\sigma}_{m,t}$ labelled by discrete indices is described in the scaling limit by $\widehat{\sigma}_{m,t} \sim c_2\, \epsilon^{2h_\sigma}\, \sigma(w,\bar{w})$, where $w = \epsilon m + i\epsilon t$, and c_2 is a non-universal amplitude. Hence, to obtain collapsed data for various chain lengths, it will be convenient to introduce

$$\mathcal{G}_2^{\alpha}([m_u,m_v]) \equiv \widehat{S}_2^{\alpha}([m_u,m_v]) - \frac{1}{8}\log\left(\frac{2N}{\pi}\right) = -\log\langle \widehat{\sigma}_{m_u,0}\widehat{\sigma}_{m_v,0}\rangle_{\mathbb{S}_L}^{(\alpha)} - \frac{1}{8}\log\left(\frac{2N}{\pi}\right), \quad (2.89)$$

so that, in the scaling limit, one expects from (2.27)

$$\mathcal{G}_2^{\alpha}([m_u,m_v]) \sim -\log\langle\sigma(u,\bar{u})\sigma(v,\bar{v})\rangle_{\mathbb{S}_L}^{(\alpha)} - \frac{1}{8}\log\left(\frac{2L}{\pi}\right) \quad (2.90)$$

$$\sim -\log\langle\sigma(0,0)\sigma(x,\bar{x})\rangle_{\mathbb{D}}^{(\alpha)} + \frac{1}{8}\log\left[\sin\frac{\pi(u+v)}{2L}\right], \quad (2.91)$$

where $u = \epsilon m_u$ and $v = \epsilon m_v$. We remind that the length of the interval is given by $\ell = v - u = \epsilon m$ with $m = m_v - m_u$, and emphasize that the entanglement is considered as the *ground state* of the free BC Ising chain.

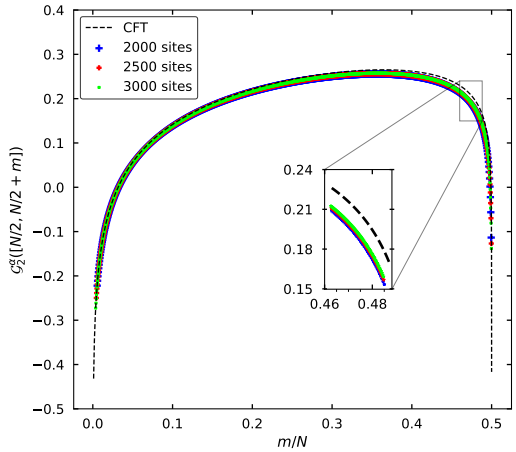

Figure 2.5: Plot of shifted Rényi entropy $\mathcal{G}_2^f([N/2, N/2+m])$ for the Ising chain with free BC, against the scaled interval size m/N. The deviations from the theoretical predictions are stronger as the interval grows closer to the boundary.

To graphically emphasize the agreement between the fermionic chain data and the theoretical prediction, we have looked at two ways of "growing" the interval length ℓ. In Figure 2.5, we have considered an interval that starts in the middle of the chain and grows towards one end. This corresponds on the lattice to applying the first twist operator to the middle of the chain, and the second one progressively closer to the right boundary. Since twist operators are placed *between lattice sites*, one should consider even system sizes. The curves of Figure 2.6, follow the dependence of the S_2 entropy as the interval length ℓ is grown equidistantly from the middle of the chain towards the boundaries. We see, in both cases, that the agreement with the CFT prediction is very good, although, as we will detail below, one needs to consider unusually large system sizes to reach it.

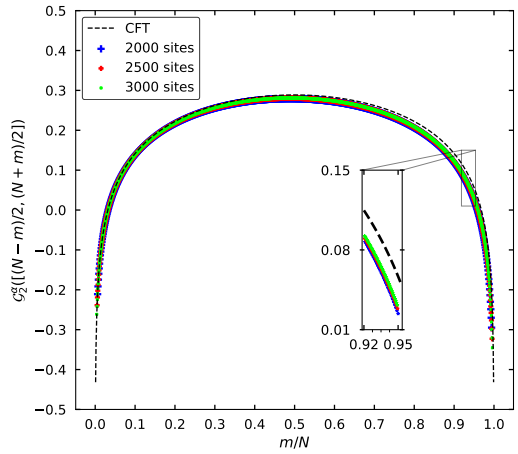

Figure 2.6: Plot of shifted Rényi entropy $\mathcal{G}_2^f([N-m)/2,(N+m)/2])$ for the Ising chain with free BC, against the scaled interval size m/N. The deviations from the theoretical predictions are stronger as the interval is grown towards the boundaries.

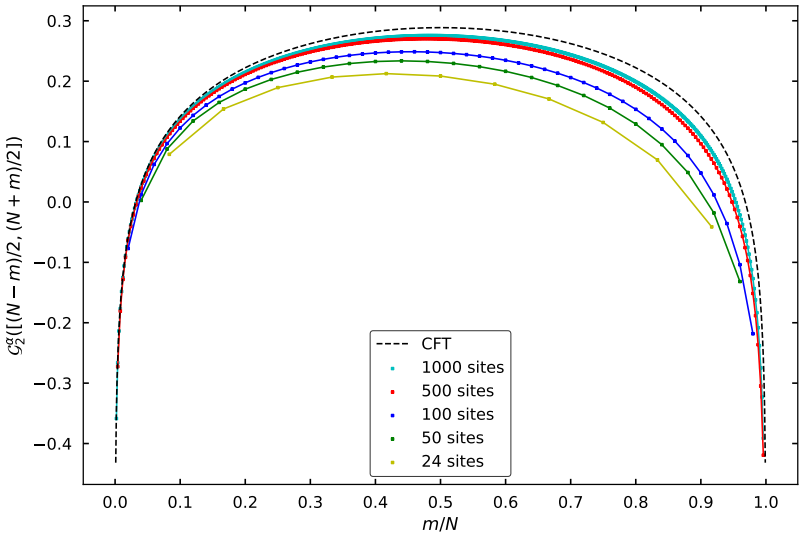

Figure 2.7: Plot of shifted Rényi entropy $\mathcal{G}_2^f([(N-m)/2,(N+m)/2])$ for a wide range of system sizes. The sizes typically accessible to exact diagonalization ($N \sim 10$) or DMRG methods ($N \sim 10^3$) suffer from large finite-size effects.

2.3.2 Finite-size effects

There is a plethora of sources of finite-size corrections to the orbifold CFT result calculated in Section 2.2. One should be aware of corrections from irrelevant *bulk* and *boundary* deformations of the Hamiltonian [143], as well as unusual corrections to scaling as analysed in [144, 145]. Finally, one should generically worry about parity effects [146] but, in agreement with [147], we have found no such corrections in the numerical results.

The strongest corrections, however, come from the subleading scaling of the

lattice twist operators [118]. We remind that the lattice twist operator $\widehat{\sigma}$ can be expressed, in the continuum limit $\epsilon \to 0$ as a *local* combination of scaling operators [67]:

$$\widehat{\sigma}_{m,t} = c_2\, \epsilon^{2h_\sigma} \sigma(w,\bar{w}) + c_2^\varepsilon\, \epsilon^{2h_{\sigma_\varepsilon}} \sigma_\varepsilon(w,\bar{w}) + \dots \tag{2.92}$$

where the integers (m,t) give the lattice position of the operator as $w = \epsilon(m+it)$, and the dots in (2.92) denote the contribution from descendant operators. The amplitudes c_2 and c_2^ε of the scaling fields are non-universal, and thus cannot be inferred from CFT methods. However, since the expansion (2.92) does not depend on the global properties of the system, it is independent of the choice of BC. Using the exact results for the correlation matrix $\mathbf{M}$ of the fermionic system associated with an infinite Ising chain [148], and the well-known result for the Rényi entropies of an interval of length ℓ in an infinite system [46, 47], one can find a fit for the values of c_2 and c_2^ε.

Moving on, the *excited twist operator* σ_ε can be defined through point-splitting as [118],[149]:

$$\sigma_\varepsilon(w,\bar{w}) := \lim_{\eta\to w} \Big[(2|\eta - w|)^{2h_\varepsilon}\, \sigma(w,\bar{w}) (\varepsilon(\eta,\bar{\eta}) \otimes \mathbb{I}) \Big] . \tag{2.93}$$

This operator has conformal dimensions $h_{\sigma_\varepsilon} = \bar{h}_{\sigma_\varepsilon} = h_\sigma + h_\varepsilon/2$. The expansion (2.92) implies that in our case, the correlator of twist operators on the Ising spin chain with free boundary conditions can be expressed in terms of CFT correlators as:

$$\begin{aligned} \langle \widehat{\sigma}_{m_u,0}\, \widehat{\sigma}_{m_v,0} \rangle_N^{(f,f)} &= (c_2)^2\, \epsilon^{4h_\sigma}\, \langle \sigma(u,\bar{u})\sigma(v,\bar{v}) \rangle_{\mathbb{S}_L}^{(f,f)} \\ &\quad + (c_2 c_2^\varepsilon)\, \epsilon^{4h_\sigma + h_\varepsilon} \Big[\langle \sigma_\varepsilon(u,\bar{u})\sigma(v,\bar{v}) \rangle_{\mathbb{S}_L}^{(f,f)} + \langle \sigma(u,\bar{u})\sigma_\varepsilon(v,\bar{v}) \rangle_{\mathbb{S}_L}^{(f,f)} \Big] \\ &\quad + \dots \end{aligned} \tag{2.94}$$

Using the map (2.19), and recalling that $L = Na$, we get

$$\langle \widehat{\sigma}_{m_u,0}\, \widehat{\sigma}_{m_v,0} \rangle_N^{(f,f)} = (c_2)^2 \left(\frac{\pi}{2N}\right)^{c/4} \frac{\langle \sigma(0,0)\sigma(x,\bar{x}) \rangle_{\mathbb{D}}^{(f,f)}}{\left[\sin \frac{\pi(u+v)}{2L}\right]^{c/4}} + (c_2 c_2^\varepsilon) \left(\frac{\pi}{2N}\right)^{c/4+h_\varepsilon} G_L(u,v) + \dots \tag{2.95}$$

where $u = m_u\epsilon$ and $v = m_v\epsilon$ are the physical positions of the twist operators, and x is given by (2.20). The first term in the right-hand side of (2.95) corresponds to the two-point function (2.45), whereas the function $G_L(u,v)$ in the second term is defined as

$$G_L(u,v) = \frac{y^{-h_\varepsilon} \langle \sigma_\varepsilon(0,0)\sigma(x,\bar{x}) \rangle_{\mathbb{D}}^{(f,f)} + y^{h_\varepsilon} \langle \sigma(0,0)\sigma_\varepsilon(x,\bar{x}) \rangle_{\mathbb{D}}^{(f,f)}}{\left[\sin \frac{\pi(u+v)}{2L}\right]^{c/4+h_\varepsilon}} , \tag{2.96}$$

with $y = \sin\frac{\pi u}{L} / \sin\frac{\pi(u+v)}{2L}$. The exact determination of the function $G_L(u,v)$ is beyond the scope of the present work – for instance, through a conformal mapping, it would imply the calculation of the one-point function of the energy operator on the annulus. Since, in the Ising CFT, we have $h_\varepsilon = 1/2$, this second term gives a correction of order $1/\sqrt{N}$ to the Rényi entropy predicted by (2.1), which is in agreement with the results of [96, 127, 144]. This is a very significant correction, and it shows why the system sizes accessible through exact diagonalization (limited to $N < 30$) are not sufficient to separate the leading contribution from its subleading corrections.

To show the dramatic effect of this term, Figure 2.7 contains a comparison of the collapse for diverse system sizes. As noticed in other works [94], where DMRG methods were used, system sizes of $N \sim 100$ are not enough to satisfyingly collapse the data.

Furthermore, the module organization of the fields in the orbifold CFT implies that the scaling exponents of finite-size corrections are half-integer spaced: there will be contributions both at relative order $O(N^{-1})$, and $O(N^{-3/2})$, and so on. This increases the difficulty of a finite-size analysis since there are more terms with significant contributions for the system sizes that are numerically accessible. To illustrate this, we give in Figure 2.8 a plot of the subleading contributions to the lattice twist correlator

$$F_{\text{subleading}}(j,k) = \langle \widehat{\sigma}_{m_u,0}\, \widehat{\sigma}_{m_v,0} \rangle_N^{(f,f)} - (c_2)^2 \left(\frac{\pi}{2N}\right)^{c/4} \frac{\langle \sigma(0,0)\sigma(x,\bar{x})\rangle_{\mathbb{D}}^{(f,f)}}{\left[\sin\frac{\pi(u+v)}{2L}\right]^{c/4}}\,. \tag{2.97}$$

The plot shows that even at $N \sim 10^3$ the collapse is not perfect.

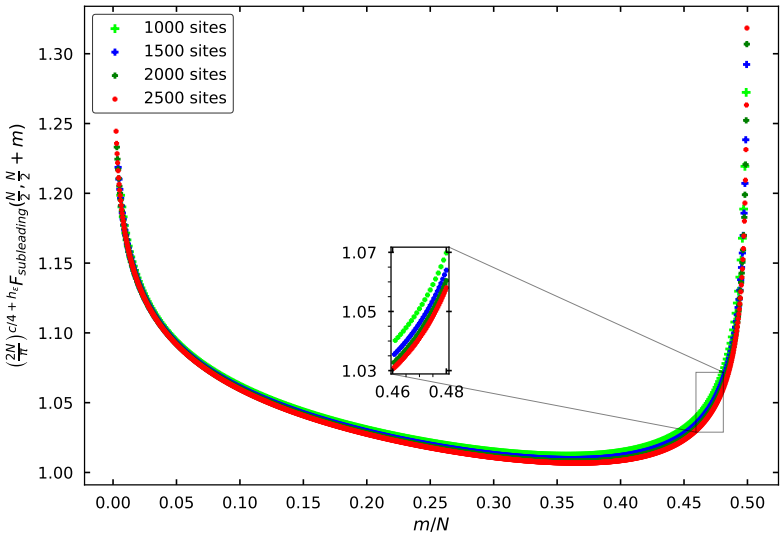

Figure 2.8: The rescaled subleading contribution $(2N/\pi)^{c/4+h_\varepsilon} F_{\text{subleading}}$ to the lattice two-point function of twist fields, for an interval starting in the middle of the chain and growing towards one boundary. The plot shows that even at large system sizes, the finite-size corrections are significant.

2.4 Conclusion

In this chapter, we have reported exact results for the Rényi entropy S_2 of a single interval in the ground state of a 1D critical system with open boundaries, assuming the same boundary conditions on both sides. This amounts to computing the two-point function of twist operators in the unit disk with diagonal BCs (α) in the $\mathbb{Z}_2$ orbifold framework.

By constructing a biholomorphic mapping from the annulus to the two-sheeted disk, we have managed to express the orbifold two-point correlator of twist fields in terms of the annulus partition function of the mother CFT. We have also detailed in the Appendix an alternative derivation of the result for minimal CFTs in the A-series.

We have numerically checked the CFT result and found good agreement with Ising spin chain data, for free BC. It was, however, necessary to achieve large system sizes for this purpose, as the finite-size corrections decayed slowly ($\sim N^{-h_\varepsilon}$ relatively to the dominant term) with the number of sites, as opposed to the case of an interval in a periodic chain, where this decay is of order N^{-2h_ε} (see [118] for instance). Checking the result for other models and BCs could be achieved through more sophisticated numerical techniques, like (adaptations of) the DMRG approach (see [94, 150]).

To generalize the method of this section to Rényi entropies S_n^α with $n \geq 2$, one would need, essentially, good analytic control of the partition function of the mother BCFT on surfaces with n boundary components, which are not known for generic BCFTs. In Chapter 3, we manage to perform such a calculation, for the BCFT of a compact boson of radius R, with either Neumann or Dirichlet BC.

A natural extension would be to consider the second Rényi entropy for a system with different conformal BCs on each side of the strip. However, this situation adds the extra complication of insertions of boundary condition changing operators into the correlator of twist operators [130], thus requiring a calculation of the four-point function of boundary operators on the two-sheeted disk. The simpler setup of an interval containing one of the boundaries can, however, be addressed, as we shall show in Chapter 4.

Chapter 3

Entanglement entropies of an interval for the massless scalar field in the presence of a boundary

3.1 Summary

In this chapter, based on [151], we present new results for the calculation of the REE $S_n(A)$ for the compact and non-compact massless scalar BCFT either on the half line or on the segment, when the same boundary condition is imposed at both endpoints in the latter case. Both Dirichlet BC and Neumann BC are investigated.

These results give the leading contribution to the REE of an interval in the ground state of a one-dimensional quantum critical system with open boundaries, whose scaling limit is realized by one of the aforementioned BCFTs. In consequence, for the compact case, our analysis applies to a gapless one-dimensional quantum system belonging to the Luttinger liquid universality class, whose low energy behaviour is captured by the massless compact real boson, which is a CFT with $c = 1$. A prototypical example is the spin-$\frac{1}{2}$ XXZ spin chain (see Appendix B.1).

Our results are valid when such a system is defined on a segment of finite length L or the half line - the latter case can be easily obtained from the former by taking the limit $L \to \infty$.

Figure 3.1: Spatial bipartitions considered in this chapter: the interval A (red segment) is either on the half line (left panel) or on the segment of finite length L (right panel), and the boundary condition is labelled by α. In the right panel, the same boundary condition is imposed at both endpoints of the segment.

We consider the spatial bipartition of the system given by an interval $A = (u, v)$ and its complement when A is not adjacent to the boundary, namely $0 < u < v < L$, as shown in Figure 3.1. The moments of the reduced density matrix ρ_A read

$$M_n^\alpha(A) \equiv \operatorname{Tr} \rho_A^n = \langle \hat{\sigma}_{m_u,0}\, \hat{\sigma}^\dagger_{m_v,0} \rangle \tag{3.1}$$

where $\hat{\sigma}$ and $\hat{\sigma}^\dagger$ are the lattice twist operators discussed in Section 1.2 and m_u, m_v are lattice coordinates such that $u = m_u\epsilon$, $v = m_v\epsilon$. We remind that in the scaling

limit, the lattice operator σ can be expanded into a linear combination of scaling fields in the corresponding conformal field theory model, and the most relevant among these primaries is the bare twist operator σ, with scaling dimension [46]

$$\Delta_n = \frac{c}{12}\left(n - \frac{1}{n}\right) \tag{3.2}$$

Hence [72, 73, 152]

$$\hat{\sigma} = c_n \, \epsilon^{\Delta_n} \, \sigma + \dots \tag{3.3}$$

where dots correspond to less relevant fields whose contribution to $\mathrm{Tr}\,\rho_A^n$ matters when finite size corrections are taken into account. The prefactor c_n is a non-universal constant coming from the normalization of the microscopic operator $\hat{\sigma}$ and ϵ is a UV cut-off, like e.g. the lattice spacing. Thus, the moments of the reduced density matrix $M_n^\alpha(A)$ in (3.1) can be written as

$$M_n^\alpha(A) = \; c_n^2 \, \epsilon^{2\Delta_n} \, \langle \sigma(u)\, \sigma^\dagger(v) \rangle_{\mathbb{S}_L} \tag{3.4}$$

where $\mathbb{S}_L = \{w \in \mathbb{C},\, 0 < \mathrm{Re}(w) < L\}$ is the infinite strip (with imaginary time running along the imaginary axis) of width L with boundary condition α on both sides of the strip. The moments $\mathrm{Tr}\rho_A^n$ for the interval on the half line with either Dirichlet and Neumann BC are obtained by taking the $L \to \infty$ in (3.4).

The CFT quantities that we are considering are related to the two-point functions of twist fields $\langle \sigma(u)\, \sigma^\dagger(v) \rangle_{\mathbb{S}_L}$ on the strip $\mathbb{S}_L \equiv \{w \in \mathbb{C},\, 0 < \mathrm{Re}(w) < L\}$. Since the strip is conformally equivalent to the unit disk $\mathbb{D} \equiv \left\{z \in \mathbb{C}\,, |z| \leqslant 1\right\}$ via the map:

$$w \mapsto z = \frac{s(w-u)}{s(w+u)} \qquad s(w) \equiv \frac{2L}{\pi} \sin\!\left(\frac{\pi w}{2L}\right) \tag{3.5}$$

we have

$$\langle \sigma(u)\, \sigma^\dagger(v) \rangle_{\mathbb{S}_L} = \; \frac{\langle \sigma(0)\, \sigma^\dagger(x) \rangle_{\mathbb{D}}}{s(u+v)^{2\Delta_n}} \qquad x = \frac{s(v-u)}{s(u+v)}, \tag{3.6}$$

where the same boundary condition is imposed on both the boundaries of $\mathbb{S}_L$ holds on the boundary of $\mathbb{D}$. In the case of the BCFT on the half line, it is convenient to consider the right half plane geometry $RHP \equiv \left\{z \in \mathbb{C}\,, \mathrm{Re}(z) \geqslant 0\right\}$, which can be studied by taking $L \to \infty$ in (3.6), finding

$$\langle \sigma(u)\, \sigma^\dagger(v) \rangle_{RHP} = \; \frac{\langle \sigma(0)\, \sigma^\dagger(x) \rangle_{\mathbb{D}}}{(u+v)^{2\Delta_n}} \qquad x = \frac{v-u}{v+u} \tag{3.7}$$

Thus, the computation of Rényi entropies we are interested in boils down to evaluating the two-point function of twist fields $\langle \sigma(0)\, \sigma^\dagger(x) \rangle_{\mathbb{D}}$ on the unit disk, when $0 < x < 1$, which can be written as:

$$\langle \sigma(0)\, \sigma^\dagger(x) \rangle_{\mathbb{D}}^{(\alpha)} = [r(1-r)]^{-\Delta_n} \, \mathcal{F}_n^{(\alpha)}(r) \qquad r = x^2 \tag{3.8}$$

where $\mathcal{F}_n^{(\alpha)}(r)$ is a universal function, conventionally chosen so that $\mathcal{F}_n^{(\alpha)}(r) \to 1$ as $r \to 0$.

In consequence, the moments of the RDM take the following form

$$M_n^\alpha(A) \equiv n \mathrm{Tr}\, \rho_A^n = \; c_n^2 \, \frac{\mathcal{F}_n^{(\alpha)}(r)}{\mathcal{P}(u,v)^{\Delta_n}} \tag{3.9}$$

where

$$\mathcal{P}(u,v) \equiv \frac{s(2u)\, s(2v)\, s(v-u)^2}{\epsilon^2\, s(v+u)^2} \qquad r \equiv \left(\frac{s(v-u)}{s(v+u)}\right)^2 \tag{3.10}$$

and $\mathcal{F}_n^{(\alpha)}$ depends on the specific BCFT model, which is characterized also by the boundary conditions labelled by α, and is related to partition functions on the Riemann sphere with n boundary components. In particular, $\mathcal{F}_2^{(\alpha)}$ is essentially the annulus partition function, which is consistent with [120] and the results of Chapter 3.

The moments (3.9) straightforwardly provide the REE of an interval A for a BCFT on the strip

$$S_n^{\alpha}(A) = \frac{\Delta_n}{n-1} \log\Big[\mathcal{P}(u,v)\Big] + \frac{\log\Big[c_n^2\, \mathcal{F}_n^{(\alpha)}(r)\Big]}{1-n} \tag{3.11}$$

which lead to the corresponding single copy entanglement (1.18) given by

$$S_{\infty}^{\alpha}(A) = \frac{c}{12} \log\Big[\mathcal{P}(u,v)\Big] + \lim_{n\to\infty} \frac{\log\Big[c_n^2\, \mathcal{F}_n^{(\alpha)}(r)\Big]}{1-n} \tag{3.12}$$

The expressions (3.4) and (3.9) for the moments of the reduced density matrix naturally lead to the introduction of two kinds of ratios that are UV finite. A first type of ratio can be defined for an assigned boundary condition α as follows

$$R_n^{(\alpha)}(A) \equiv \frac{M^{\alpha}(A)}{M^{\alpha}(A_u)\, M^{\alpha}(A_v)} \tag{3.13}$$

where $A_u \equiv [0,u]$ and $A_v \equiv [0,v]$ (see Figure 3.1). In the BCFT we are considering, by using the expressions in (3.9)-(3.10), this ratio becomes

$$R_n^{(\alpha)}(A) = g_{\alpha}^{2(n-1)}\, \frac{\mathcal{F}_n^{(\alpha)}(r)}{r^{\Delta_n}} \tag{3.14}$$

From (3.13) and (1.14), the following UV finite combination of entanglement entropies is obtained

$$\mathcal{I}_n(A) \equiv S_n(A_u) + S_n(A_v) - S_n(A) \tag{3.15}$$

For a BCFT on a segment, by using (3.11), one finds that this UV finite combination becomes

$$\mathcal{I}_n(A) = -\frac{c}{12}\left(1+\frac{1}{n}\right)\log(r) + \frac{\log\Big[\mathcal{F}_n^{(\alpha)}(r)\Big]}{n-1} + 2\log g_{\alpha} \tag{3.16}$$

which is a function of the harmonic ratio r in (3.10).

Another type of UV finite ratio can be introduced only through the interval A, without using the entanglement entropies of intervals adjacent to the boundary. Instead, two different conformally invariant boundary conditions α_1 and α_2 must be considered. From (3.4) and (3.9), these ratios are defined as

$$\frac{M_n^{(\alpha_1)}(A)}{M_n^{(\alpha_2)}(A)} = \frac{\mathcal{F}_n^{(\alpha_1)}(r)}{\mathcal{F}_n^{(\alpha_2)}(r)} \tag{3.17}$$

which leads to the following difference of Rényi entropies

$$S_n^{\alpha_1}(A) - S_n^{\alpha_2}(A) = \frac{1}{1-n} \log\left(\frac{\mathcal{F}_n^{(\alpha_1)}(r)}{\mathcal{F}_n^{(\alpha_2)}(r)}\right) \tag{3.18}$$

where we have denoted by $S_n^\alpha(A)$ the Rényi entropies (1.14), to highlight its dependence on the boundary condition α. We remark that the above expressions hold for a BCFT on a segment and that the corresponding expressions for the BCFT on the half-line are obtained by taking $L \to \infty$.

We remind that the disk two-point function (3.63) can be equivalently evaluated as the following ratio of partition functions [46]

$$\langle \sigma(0)\, \sigma^\dagger(x) \rangle_{\mathbb{D}} = \mathcal{Z}_n(x)/\mathcal{Z}_1^n \tag{3.19}$$

where $\mathcal{Z}_n(x)$ stands for the BCFT partition function on the n-sheeted covering of the unit disk $\mathbb{D}_n$ with branch points at 0 and x, while $\mathcal{Z}_1$ is simply the BCFT partition function on the unit disk.

Strategy for BCFT computation

The goal, then, is to evaluate the partition function $\mathcal{Z}_n(x)$ or, equivalently, the two-point correlators on the disk in (3.19). This is presented in detail in Section 3.2, but we will summarize here the main ideas involved. The crucial insight is that this problem is conceptually related, through the "generalized" mirror trick in [115], to the calculation of the REE of two disjoint intervals on the infinite line for the compact boson CFT in [71].

In this case, the moments $\mathrm{Tr}\,\rho_A^n$ are obtained as the partition function of the model on a specific n-sheeted Riemann surface $\mathcal{M} = \mathscr{M}_n$ which is a Riemann surface obtained through the replica construction, with genus $g = n - 1$ (see the Appendix A of [85]). For a CFT, this special Riemann surface is characterized by the harmonic ratio of the endpoints of the two intervals, which is a real parameter in $(0, 1)$. For instance, $\mathscr{M}_4$ has genus $g = 3$ and it is shown in the left panel of Figure 3.2 for the special case of two equal intervals. Further analyses and generalisations of $\mathscr{M}_n$ have been discussed e.g. in [85, 88, 153].

The method of the images allows one to find the n-sheeted Riemann surface $\mathcal{M} = \mathscr{S}_n$ for a BCFT on the half line and in its ground state as follows. Consider $\mathscr{M}_n$ for two intervals of equal length (when $n = 4$, see the left panel of Figure 3.2), which exhibits a $\mathbb{Z}_2$ symmetry (a reflection) with respect to a plane (see the black plane in the middle panel of Figure 3.2). The n-sheeted Riemann surface $\mathscr{S}_n$ corresponds to one of the two halves identified by this reflection plane, whose union gives $\mathscr{M}_n$. Thus, $\mathscr{S}_n$ has the topology of a sphere with n boundaries, which has genus $g = 0$ and Euler characteristic $\chi = 2 - n$ (for $n = 4$, see the right panel of Figure 3.2). Such a surface, is of course, conformally equivalent to the n-sheeted disk $\mathbb{D}_n$.

Let us now sketch our computational strategy, based on adapting the methods of [70] (which were also employed in [71]) to account for the conformal BC. Following [70], in the path integral on $\mathbb{D}_n$ for the partition function, we decompose the field $\phi = \phi_{\rm cl} + \phi_{\rm qu}$ into the classical field $\phi_{\rm cl}$ and a quantum part $\phi_{\rm qu}$. The Euclidean action of the massless compact real boson on a generic Riemann surface $\mathcal{M}$ equipped with metric $g_{\mu\nu}$ and whose target space is a circle of radius R reads

$$S[\phi] = \frac{1}{8\pi} \int_{\mathcal{M}} g^{\mu\nu}\, \partial_\mu \phi\, \partial_\nu \phi\, \sqrt{|g|}\, d^2x \qquad \phi \sim \phi + 2\pi R \tag{3.20}$$

Since the action $S[\phi]$ is quadratic and $\phi_{\rm cl}$ satisfies the equation of motion, (3.20) admits the decomposition $S[\phi] = S[\phi_{\rm cl}] + S[\phi_{\rm qu}]$.

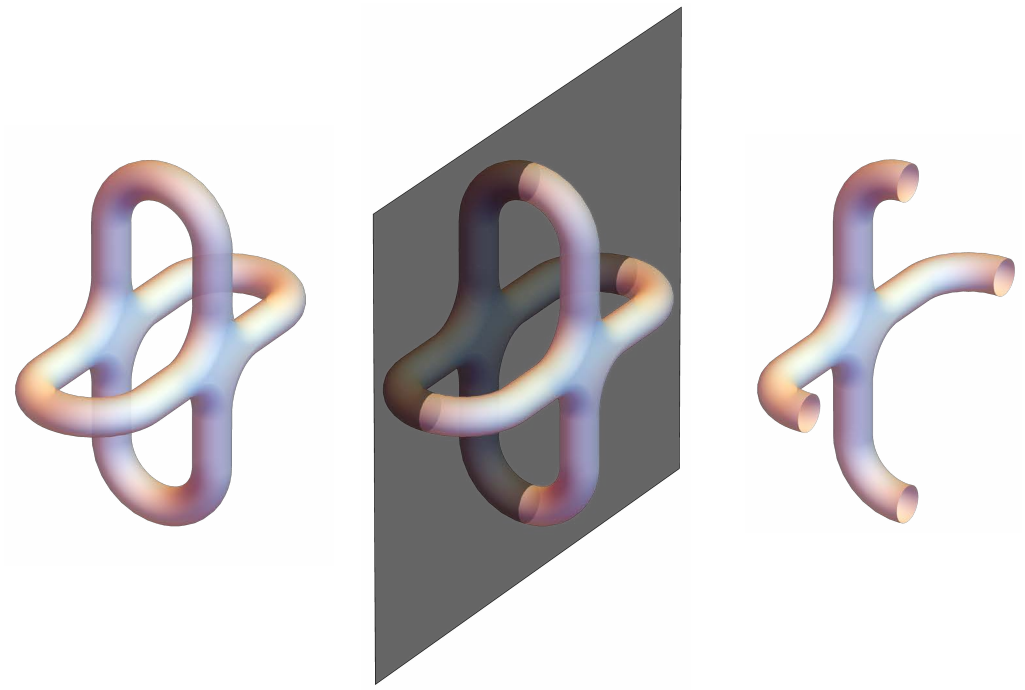

Figure 3.2: The Riemann surface $\mathscr{S}_4$ (right panel) is topologically a sphere with four boundaries. It is obtained by exploiting the reflection symmetry of $\mathscr{M}_4$ for two equal intervals (left panel) with respect to a plane (the black plane in the middle panel).

This implies that the partition function on the Riemann surface $\mathcal{M}$ factorizes as follows

$$\mathcal{Z}(\mathbb{D}_n) = \mathcal{Z}_{\rm cl}(\mathbb{D}_n; R)\, \mathcal{Z}_{\rm qu}(\mathbb{D}_n) \tag{3.21}$$

where the classical and the quantum terms are defined respectively as

$$\mathcal{Z}_{\rm cl}(\mathbb{D}_n; R) \equiv \sum_{\boldsymbol{m}} e^{-S[\phi_{\rm cl}^{(m)}]} \qquad \mathcal{Z}_{\rm qu}(\mathbb{D}_n) \equiv \int [D\phi_{\rm qu}]\, e^{-S[\phi_{\rm qu}]} \tag{3.22}$$

where $\phi_{\rm cl}^{(m)}$ is the classical solution with winding m and the sum in $\boldsymbol{m}$ is over all possible windings of the classical solutions. Note that while the classical part depends on the compactification radius R, due to configurations of ϕ_{cl} with non-trivial winding, the quantum term $\mathcal{Z}_{\rm qu}(\mathcal{M})$ is independent of the compactification radius R.

To calculate $\mathcal{Z}_{\rm cl}(\mathbb{D}_n; R)$, one first finds the classical solutions on the double $D(\mathbb{D}_n)$ in the standard way [70]. Following this, the effect of imposing the Dirichlet or Neumann BC is to select a subset of these classical solutions which contribute to the partition function on $\mathbb{D}_n$.

For the quantum part, it is simpler to calculate $\mathcal{Z}_{\rm qu}(\mathbb{D}_n)$ as the square root of the partition function of a *complex* boson Φ. Then, one can use the methods of [70, 71, 154], together with the gluing conditions of the U(1) currents at the boundary, to calculate the result.

For convenience, we give here a dictionary between the notation of [71] and the conventions of this chapter. In our calculations, we have set $g = 1/2$, $\eta = R^2$ and, in consequence, the Luttinger parameter and the compactification radius are related as $K = R^{-2}$. We will relegate to Section 3 a detailed comparison of our result in (3.23) with the universal function $\mathcal{F}_n$ of [71].

Few explicit analytic expressions for $\mathcal{F}_n^{(\alpha)}$ in (3.9) are available in the literature: for the massless Dirac field, where $\mathcal{F}_n^{(\alpha)} = 1$ identically for any value of n and independently of the (conformally invariant) boundary conditions [129], and for the massless compactified scalar for $n = 2$ and a generic conformally invariant boundary condition, in terms of the annulus partition function [120]. In this chapter, we extend the latter result for the massless compactified scalar to a generic value of the Rényi index n, focussing on Dirichlet BC and Neumann BC .

Let us collect here the results for the universal functions $\mathcal{F}_n^{(\alpha)}$ derived in this chapter. At *finite* compactification radius R we have:

Main results at finite R

The universal functions $\mathcal{F}_n^{(\alpha)}$ for Dirichlet (D) and Neumann (N) boundary conditions to be:

$$\mathcal{F}_n^{(\mathrm{D})}(r) = \frac{\Theta\Big(\boldsymbol{\tau}(r)/R^2\Big)}{\Theta\Big(\boldsymbol{\tau}(r)\Big)} \qquad \mathcal{F}_n^{(\mathrm{N})}(r) = \frac{\Theta\Big(R^2\,\boldsymbol{\tau}(r)/4\Big)}{\Theta\Big(\boldsymbol{\tau}(r)\Big)} \tag{3.23}$$

where

$$\Theta(\boldsymbol{h}) \equiv \sum_{\boldsymbol{m}\in\mathbb{Z}^{n-1}} \mathrm{e}^{\mathrm{i}\pi\,\boldsymbol{m}^{\mathrm{t}}\cdot\boldsymbol{h}\cdot\boldsymbol{m}} \tag{3.24}$$

is the *Siegel theta function* and $\boldsymbol{\tau}$ the *period matrix* of [71]

$$\boldsymbol{\tau}_{ij}(r) \equiv \mathrm{i}\,\frac{2}{n}\sum_{k=1}^{n-1} \sin(\pi k/n)\,\frac{F_{k/n}(1-r)}{F_{k/n}(r)}\,\cos\Big[2\pi k(i-j)/n\Big] \tag{3.25}$$

where $1 \leqslant i, j \leqslant n-1$ and $F_{k/n}(r) =_2 F_1(k/n, 1-k/n; 1; r)$.

From the results (3.23) and equations (3.8) and (3.19) , we observe that the following relation occurs between the partition functions corresponding to Dirichlet and Neumann BC

$$\mathcal{Z}_n^{(\mathrm{N})}(R) = \mathcal{Z}_n^{(\mathrm{D})}(2/R) \tag{3.26}$$

This provides a non-trivial consistency check of the dependence on the compactification radius R in (3.23); indeed, for the compact massless boson this *T-duality* relation is expected to hold, as discussed in [25] for the annulus (i.e. the $n = 2$ case) and in [155] for a generic Riemann surfaces with boundaries.

The limit of large compactification radius $R \to \infty$ corresponds to the case where the target space is the infinite line. In this regime, we find that the moments $\mathrm{Tr}\rho_A^n$ of the interval $A = [u, v]$ on the strip of length L for Dirichlet and Neumann BC become respectively

$$M_n^{(\mathrm{D})}(A) = \frac{c_n^2}{\mathcal{P}(u,v)^{\Delta_n}}\,\widetilde{\mathcal{F}}_n^{(\mathrm{D})}(r) \qquad M_n^{(\mathrm{N})}(A) = \frac{c_n^2}{\mathcal{P}(u,v)^{\Delta_n}}\,\widetilde{\mathcal{F}}_n^{(\mathrm{N})}(r) \tag{3.27}$$

where c_n are non-universal constants as in (3.3) and we have denoted the universal functions by $\widetilde{\mathcal{F}}_n^{(\mathrm{D})}$ to distinguish them from the *finite* R case.

We note that here the c_n is assumed to relate twist fields in the $\mathbb{Z}_n$ orbifold of the non-compact boson BCFT and lattice twist operators in a harmonic chain model that is properly regularized in the UV and IR. In the case of Dirichlet boundary conditions, the constant c_n has the same UV origin as in Eq. (3.3). The case of

Neumann boundary conditions is more subtle, as the lattice model requires an IR regularization due to the presence of a zero mode.

We now report our results in this regime:

Main results in the decompactification limit

- For $n \geq 2$ the result is:

$$\widetilde{\mathcal{F}}_n^{(\mathrm{D})}(r) \equiv \frac{1}{\sqrt{\prod_{k=1}^{n-1} F_{k/n}(1-r)}} \qquad \widetilde{\mathcal{F}}_n^{(\mathrm{N})}(r) \equiv \frac{1}{\sqrt{\prod_{k=1}^{n-1} F_{k/n}(r)}} \tag{3.28}$$

- By using (3.27), we can also obtain the UV finite combination (3.18) in this regime, which reads

$$S_n^{(\mathrm{D})}(A) - S_n^{(\mathrm{N})}(A) = \frac{1}{2(n-1)} \sum_{k=1}^{n-1} \log\left(\frac{F_{k/n}(1-r)}{F_{k/n}(r)}\right) \tag{3.29}$$

- In the limit $n \to \infty$, we have found:

$$\lim_{n\to\infty} \frac{1}{n-1} \log \widetilde{\mathcal{F}}_n^{(\mathrm{D})}(r) = \int_0^1 \log\Big[F_\kappa(1-r)\Big] d\kappa \tag{3.30}$$

and

$$\lim_{n\to\infty} \frac{1}{n-1} \log \widetilde{\mathcal{F}}_n^{(\mathrm{N})}(r) = \int_0^1 \log\Big[F_\kappa(r)\Big] d\kappa \tag{3.31}$$

which allow for the swift numerical evaluation of the single copy entanglement defined in (3.12).

- Using the results of [71], one finds:

$$\lim_{n\to 1} \frac{1}{1-n} \log \widetilde{\mathcal{F}}_n^{(\mathrm{D})}(r) = \frac{\mathrm{i}}{2} \int_{-\mathrm{i}\infty}^{\mathrm{i}\infty} \frac{\pi z \, \log[F_z(1-r)]}{[\sin(\pi z)]^2} \, dz \tag{3.32}$$

and

$$\lim_{n\to 1} \frac{1}{1-n} \log \widetilde{\mathcal{F}}_n^{(\mathrm{N})}(r) = \frac{\mathrm{i}}{2} \int_{-\mathrm{i}\infty}^{\mathrm{i}\infty} \frac{\pi z \, \log[F_z(r)]}{[\sin(\pi z)]^2} \, dz \tag{3.33}$$

so that the EE can be evaluated numerically .

Comparison with numerical results in the decompactification limit

In Sec. 3.3 we check the validity of the analytic expressions in (3.27) and (3.29) against numerical results for the entanglement entropies of a block of consecutive sites in the spatial bipartitions shown in Figure 3.1 for harmonic chains defined either on the semi-infinite line or on the segment, when either Dirichlet BC or Neumann BC are imposed.

The Hamiltonian of a finite harmonic chain with nearest neighbour spring-like interactions made by $N-1$ sites in the interior and two sites at its endpoints reads

$$\widehat{H} = \sum_{i=0}^{N} \left(\frac{1}{2m}\hat{p}_i^2 + \frac{m\omega^2}{2}\hat{q}_i^2\right) + \sum_{i=0}^{N-1} \frac{\kappa}{2}(\hat{q}_{i+1} - \hat{q}_i)^2 \tag{3.34}$$

in terms of the position and the momentum operators $\hat{q}_i$ and $\hat{p}_i$, that are hermitian operators satisfying the canonical commutation relations $[\hat{q}_i, \hat{q}_j] = [\hat{p}_i, \hat{p}_j] = 0$ and $[\hat{q}_i, \hat{p}_j] = \mathrm{i}\delta_{i,j}$ (we set $\hbar = 1$). At the endpoints of the harmonic chain we impose the same boundary condition, which is either Dirichlet BC

$$\hat{q}_0 = \hat{q}_N = 0 \tag{3.35}$$

or Neumann BC

$$\hat{q}_1 - \hat{q}_0 = 0 \qquad\qquad \hat{q}_N - \hat{q}_{N-1} = 0 \tag{3.36}$$

The entanglement entropies $S_A^{(n)}$ for a spatial interval $A = [u, v]$, with $u = m_u\epsilon, v = m_v\epsilon$, containing $m_A = m_v - m_u$ consecutive sites can be computed through the method developed in [44, 65, 66, 156–161]. The first step consists in constructing the *reduced* correlation matrices Q_A and P_A, whose generic elements are respectively $\langle \hat{q}_i \hat{q}_j \rangle$ and $\langle \hat{p}_i \hat{p}_j \rangle$, with $i, j \in A$. In both cases of interest (finite N and $N \to \infty$), their analytical expressions are known [157, 162, 163] or can be found (3.97) for Dirichlet and Neumann BC.

The next step is to diagonalize, for each choice of bipartition $A|B$, the matrix $Q_A \cdot P_A$. Similarly to Peschel's trick, the eigenvalues of this matrix determine the entanglement spectrum of the harmonic chain for that particular bipartition from which the entanglement entropies are readily obtained.

We've considered four setups in the harmonic chain. For each boundary condition (Neumann or Dirichlet) we've analyzed both the infinite chain on the semi-infinite line and the finite chain made by N consecutive sites on the segment. The continuum limit of the lattice results was compared against the corresponding noncompact boson BCFT predictions on the right half plane RHP (for $N \to \infty$) and the strip $\mathbb{S}_L$ (finite N).

In the case of Dirichlet b.c., our lattice data are taken by setting $\omega = 0$ in the analytic expressions for $\langle \hat{q}_i \hat{q}_j \rangle$ and $\langle \hat{p}_i \hat{p}_j \rangle$, given in (3.84) and (3.87), since they remain well-defined in this limit. Instead, when Neumann b.c. are imposed, the $\langle \hat{q}_i \hat{q}_j \rangle$ correlator in (3.89) diverges in the massless limit $\omega \to 0$ because of the occurrence of a zero mode. This forces us to set a small but non-vanishing mass: in our analysis we have chosen $\omega m_A \sim 10^{-10}$ for the semi-infinite chains and $\omega N \sim 10^{-10}$ for the finite chains, which are much smaller than the other scales.

With these specifications, we have performed numerical comparisons for a variety of entanglement quantifiers and bipartitions, copiously detailed in Section 3.3. Of this, we will only reproduce here our numerical results for the EE and the EE difference between Dirichlet and Neumann BC, since the EE is an entanglement measure by all definitions [1]. In the case of the massless scalar field in the decompactification regime that we are exploring, we consider (3.29) and its analytic continuation $n \to 1$, which can be easily obtained from (3.32) and(3.33). The results of our analyses for this UV finite quantity are shown in Figure 3.3.

The collection of the lattice data has been performed by setting m_v to a constant value in both setups: we have chosen $\in \{100, 200, 400\}$ for the semi-infinite chains, while we took $= N/2$ with $N \in \{100, 200, 400\}$ for the finite chains. Then, we varied $m_u \in \{1, \ldots, m_v - 1\}$ and plotted the entanglement entropy in terms of m_A/m_v and the entropy difference in terms of the corresponding cross ratio r in each case. For Neumann BC, we have set $\omega m_v \sim 10^{-10}$ in both the semi-infinite and finite chains. The agreement between the lattice data points and the corresponding BCFT predictions is excellent in all these cases. In the insets of Figure 3.3 we have

[1] See Section 1.1.1

reported $S_{A;\alpha}$ − const, where the constant value that has been subtracted is given by $\frac{1}{6}\log(2m_v)$ for the semi-infinite chains (left panel) and $\frac{1}{3}\log(2N/\pi)$ for finite chains (right panel).

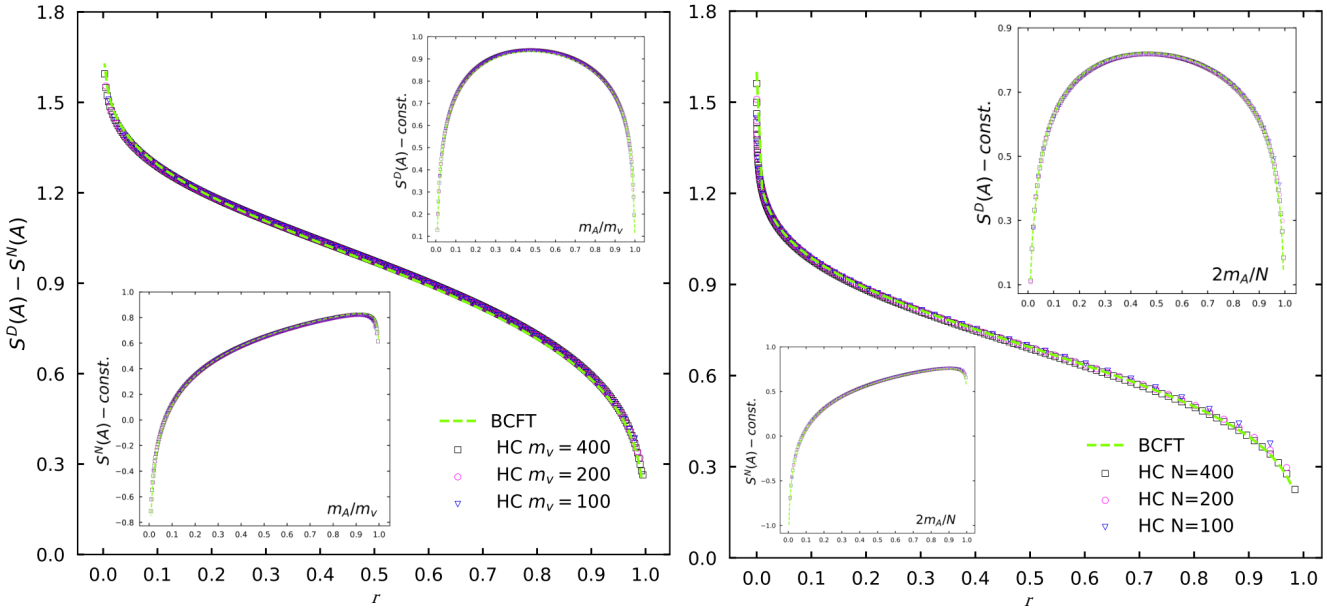

Figure 3.3: The difference between the entanglement entropy for Dirichlet BC and Neumann BC for the bipartitions of Figure 3.1, either in the semi-infinite chains (left panel) or in the finite chains (right panel). The insets show the entanglement entropy for the two different boundary conditions.

Let us now summarize the outline of this chapter. We shall first present in Section 3.2 the calculation of the twist 2-point function on the disk at finite R, and in the decompactification limit $R \to \infty$. In Section 3.3, we check the results in the decompactified limit against numerics in the harmonic chain, in a variety of setups. For Dirichlet BC, the agreement is excellent for all the quantities considered, while for Neumann BC, at larger values of the Rényi index n, the numerical results deviate from the BCFT prediction - we presume this disagreement might be due to the introduction of a zero mode regulator in the harmonic chain with Neumann BC. We then conclude this chapter with Section 3.4, in which we discuss possible extensions of this setup. Finally, in the appendix associated with this chapter, we have relegated the more technical derivations of this work.

3.2 Entanglement entropies in the unit disk

In this section, we discuss the main BCFT calculation of this chapter. As anticipated in Sec. 3.1, we employ the mirror trick to evaluate the partition function $\mathcal{Z}(\mathscr{S}_n)$ for the compact boson on the specific surface $\mathscr{S}_n$ occurring in our problem because of the replica construction. Since the action is quadratic, the partition function factorizes into a classical part and a quantum part, which are evaluated separately.

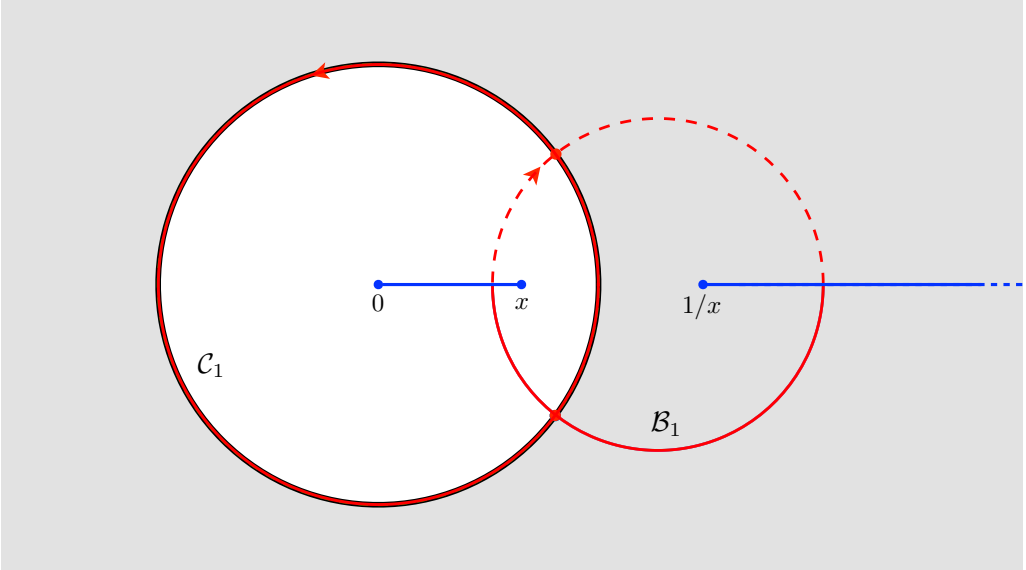

Figure 3.4: The cycles (red curves) employed in Sec. 3.2.1. Solid curves lie in the first sheet, while dashed lines stand for curves on the second sheet. The unit disk $\mathbb{D}$ corresponds to the white region. The twist fields are located at the origin and x.

3.2.1 Partition function

Mirror trick

In Sec. 3.1 we have qualitatively discussed that evaluating the Rényi entropies for the bipartitions in Figure 3.1 corresponds to computing a partition function on a surface $\mathcal{M} = \mathscr{S}_n$ with boundary which is topologically equivalent to a sphere with n equal disks removed (for $n = 4$, see the right panel of Figure 3.2). In a BCFT, this partition function can be obtained also as the two-point function $\langle \sigma(0)\, \sigma^{\dagger}(x) \rangle_{\mathbb{D}}$ of twist-fields on the unit disk $\mathbb{D}$, placed at the origin and at x, with $0 < x < 1$.

The replica construction introduces the branched covering $\mathcal{M} = \mathscr{D}_n$, which is obtained by joining cyclically n copies of $\mathbb{D}$ through the cut along the interval $(0, x)$. A standard approach to investigate partition functions on a Riemann surface $\mathcal{M}$ with boundaries is to introduce the so-called *double* of $\mathcal{M}$, that we denote by $D(\mathcal{M})$ [115]. The double of $\mathcal{M}$ is a compact Riemann surface endowed with an anti-holomorphic involutive map ζ (called a real structure) such that $\mathcal{M} = D(\mathcal{M})/\zeta$ and the boundary $\partial\mathcal{M}$ corresponds to the fixed points of ζ. For instance, the double of the upper half plane is the whole plane with $\zeta(z) = \bar{z}$ and the double of the right half plane is the entire plane with real structure given by the reflection w.r.t. the vertical axis. The double of the unit disk $\mathbb{D}$ is the Riemann sphere $\mathbb{CP}^1$ with real structure $\zeta(z) = 1/\bar{z}$. This construction is allowed when $\partial\mathcal{M}$ is analytic w.r.t. the complex structure induced by the metric and this condition is verified for $\mathscr{D}_n$. Thus, $D(\mathscr{D}_n)$ is simply the n-sheeted covering of the Riemann sphere $\mathbb{CP}^1$ with branch points at $0, x, 1/x$ and ∞ and the anti-holomorphic involution is (a lift of) $\zeta(z) = 1/\bar{z}$. The case of the interval in the right half plane is considered in Figure 3.2.

The first step of our analysis consists of constructing a canonical homology basis for the genus $n-1$ surface $D(\mathscr{D}_n)$ that is compatible with the involution ζ. Consider the cycles $\mathcal{C}_1$ and $\mathcal{B}_1$ shown in Figure 3.4. The contour $\mathcal{C}_1$ is any cycle in the same homology class as the unit circle. In particular, its homology class

is invariant (even) under ζ. On the other hand, the homology class of $\mathcal{B}_1$ is odd under ζ; indeed $\mathcal{B}_1$ can be chosen so that $\zeta(\mathcal{B}_1)$ is the same loop as $\mathcal{B}_1$, but with the opposite orientation. These contours can be replicated on each sheet through the deck transformation f sending sheet j to $j+1$, i.e. $\mathcal{C}_{j+1} = f(\mathcal{C}_j)$ and $\mathcal{B}_{j+1} = f(\mathcal{B}_j)$, for $1 \leqslant j \leqslant n-1$. Since the deck transformation commutes with the real structure ζ, the (homology class of the) cycles $\mathcal{B}_j$ and $\mathcal{C}_j$ are respectively odd and even under ζ. Although the contours $\mathcal{C}_j$ and $\mathcal{B}_j$ for $1 \leqslant j \leqslant n-1$ generate the whole homology group, they do not form a canonical basis because $\mathcal{B}_j$ intersects both $\mathcal{C}_j$ and $\mathcal{C}_{j+1}$. More precisely, their intersection numbers are $\sharp(\mathcal{C}_i, \mathcal{B}_j) = \delta_{i,j} - \delta_{i,j+1}$. However, the cycles $\mathcal{A}_j = \mathcal{C}_1 + \cdots + \mathcal{C}_j$ are such that $\sharp(\mathcal{A}_i, \mathcal{B}_j) = \delta_{i,j}$ (and $\sharp(\mathcal{A}_i, \mathcal{A}_j) = 0$) and therefore $(\mathcal{A}_j, \mathcal{B}_j)$ is a canonical homology basis. Furthermore, this basis satisfies $\zeta(\mathcal{A}_j) = \mathcal{A}_j$ and $\zeta(\mathcal{B}_j) = -\mathcal{B}_j$ (up to smooth deformations). Thus, under ζ, each $\mathcal{A}_j$ is invariant, while each $\mathcal{B}_j$ just changes its orientation. The period matrix corresponding to this canonical homology basis is (3.25) and its derivation is discussed in Appendix B.2.

We are interested in the partition function of the compact real massless boson $\phi \sim \phi + 2\pi R$ on a compact Riemann surface $\mathcal{M}$ with boundaries. The action (3.20) for this BCFT can be written also as follows

$$S[\phi] = \frac{1}{8\pi}\int_{\mathcal{M}} g(d\phi, d\phi)d\mu = \frac{1}{8\pi}\int_{\mathcal{M}} d\phi \wedge \star\, d\phi = \frac{\mathrm{i}}{4\pi}\int \partial\phi \wedge \bar{\partial}\phi \tag{3.37}$$

where g is the metric tensor on $\mathcal{M}$, whose volume form is $d\mu = \sqrt{|g|}\, d^2x$, and $\star$ is the Hodge star operator. In the last equality we introduced the Dolbeault operators $\partial = \frac{1}{2}(d + i \star d)$ and $\bar{\partial} = \frac{1}{2}(d - i \star d)$. The same boundary conditions are imposed on all the boundary components of $\partial\mathcal{M}$ and in our case, they are either Dirichlet BC or Neumann BC . The action (3.37) is invariant under Weyl rescaling $g \to e^{\varphi} g$. Such invariance can be made more manifest by introducing the decomposition $d\phi = \partial\phi + \bar{\partial}\phi$ and using that $\star\, dz = -\mathrm{i}dz$, $\star\, d\bar{z} = \mathrm{i}d\bar{z}$, which imply $\star\, d\phi = -\mathrm{i}\partial\phi + \mathrm{i}\bar{\partial}\phi$. This leads to the last expression in (3.37), which is manifestly independent of the metric (in a given conformal class). The partition function $\mathcal{Z} = \int [D\phi]\, \mathrm{e}^{-S[\phi]}$ is obtained by performing the path integration over all field configurations that satisfy the appropriate boundary conditions in $\partial\mathcal{M}$, which are Neumann BC or Dirichlet BC in our analysis. A non-compact real boson ϕ takes values in $\mathbb{R}$, while in the compact case that we are considering the real field ϕ takes values in the circle of radius R, i.e. in $\mathbb{R}/(2\pi R\,\mathbb{Z})$. Thus, in the latter case, the field configurations can be classified through their windings (or instanton sectors). This means that

$$\int_{\mathcal{P}_j} d\phi = 2\pi n_j R \qquad\qquad n_j \in \mathbb{Z} \tag{3.38}$$

where the integer n_j determines the winding number corresponding to the path $\mathcal{P}_j$, which can be either a non-contractible cycle on the Riemann surface or an open path connecting two of its boundary components.

Following the standard procedure to deal with these windings discussed in [70], in the path integral for the partition function we decompose the field $\phi = \phi_{\text{cl}} + \phi_{\text{qu}}$ into the classical field ϕ_{cl} and a quantum part ϕ_{qu}. The classical solution ϕ_{cl} is a harmonic function $\phi_{\text{cl}} : \mathcal{M} \to \mathbb{R}/(2\pi R\,\mathbb{Z})$ satisfying (3.38) (hence it depends on the winding vector $\boldsymbol{n}$, having n_j as j-th element), while the quantum field ϕ_{qu} does not have windings.

The quadratic form of the action (3.37) combined with the fact that $\phi_{\rm cl}$ is a solution of the equation of motion lead to decomposition $S[\phi] = S[\phi_{\rm cl}] + S[\phi_{\rm cl}]$, where only the classical term $S[\phi_{\rm cl}]$ depends on the winding vector. This implies that the partition function on the Riemann surface $\mathcal{M}$ factorises as follows

$$\mathcal{Z}(\mathcal{M}) = \mathcal{Z}_{\rm cl}(\mathcal{M}; R)\, \mathcal{Z}_{\rm qu}(\mathcal{M}) \tag{3.39}$$

where the classical and the quantum terms are defined respectively as

$$\mathcal{Z}_{\rm cl}(\mathcal{M}; R) \equiv \sum_{\boldsymbol{n}} e^{-S[\phi_{\rm cl}]} \qquad \mathcal{Z}_{\rm qu}(\mathcal{M}) \equiv \int [D\phi_{\rm qu}]\, e^{-S[\phi_{\rm qu}]} \tag{3.40}$$

We remark that the quantum term $\mathcal{Z}_{\rm qu}(\mathcal{M})$ is independent of the compactification radius R.

Classical term

We consider first the classical part $\mathcal{Z}_{\rm cl}(\mathcal{M}; R)$ of the partition function in (3.21) in the case of *same* Dirichlet BC $\phi = \phi_0$, where ϕ_0 is a constant in $\mathbb{R}/(2\pi R\,\mathbb{Z})$. Crucially we impose the *same* constant ϕ_0 on on all the components of $\partial\mathcal{M}$ (see Appendix B.1). Exploiting the $U(1)$ invariance of the theory, we assume $\phi_0 = 0$ without loss of generality. Classical solutions of this Dirichlet problem are thus harmonic functions $\phi_{\rm cl}$ that vanish on the boundary. Combining the vanishing (mod $2\pi R$) of $\phi_{\rm cl}$ on $\partial\mathcal{M}$ with the fact that any harmonic function is (locally) the real part of an analytic function, $\phi_{\rm cl}$ can be extended to the double $D(\mathcal{M})$ through the Schwarz reflection principle via the condition $\phi_{\rm cl}(\zeta(p)) = -\phi_{\rm cl}(p)$. This means that classical solutions $\phi_{\rm cl}$ on $\mathcal{M}$ satisfying vanishing Dirichlet BC are in one-to-one correspondence with classical solutions on the double $D(\mathcal{M})$ that are odd under ζ. Hence, $d\phi_{\rm cl}$ is a harmonic form on $D(\mathcal{M})$ satisfying $\zeta^* d\phi_{\rm cl} = -d\phi_{\rm cl}$, where ζ^* denote the pullback by ζ.
On the other hand, the even harmonic forms on $D(\mathcal{M})$ are such that $\zeta^* d\phi_{\rm cl} = d\phi_{\rm cl}$ and their restriction to $\mathcal{M}$ provides the classical solutions satisfying Neumann BC for all the components of $\partial\mathcal{M}$. In this case $\phi_{\rm cl}$ can be extended to $D(\mathcal{M})$ via $\phi_{\rm cl}(\zeta(p)) = \phi_{\rm cl}(p)$. Alternatively, we can consider the dual field $\theta_{\rm cl}$, which is defined by $d\theta_{\rm cl} = \star\, d\phi_{\rm cl}$. When $\phi_{\rm cl}$ satisfies Neumann BC, the dual field $\theta_{\rm cl}$ obeys Dirichlet BC; hence $\zeta^* d\theta_{\rm cl} = -d\theta_{\rm cl}$. Since $\zeta_{\rm cl}$ is an orientation reversing isometry, it anticommutes with the Hodge star operator and therefore $\zeta^* d\phi_{\rm cl} = d\phi_{\rm cl}$.

In the computation of the moments $\operatorname{Tr}\rho_A^n$ for the bipartitions shown in Figure 3.1, the Riemann surface $\mathcal{M} = \mathscr{D}_n$ is topologically equivalent to a sphere with n disks removed (for $n = 4$, see the right panel of Figure 3.2). Its double $D(\mathscr{D}_n)$ is the compact Riemann sphere of genus $g = n - 1$ described in Sec. 3.2.1. When $n = 4$, the double $D(\mathscr{D}_n)$ is topologically equivalent to the Riemann surface shown in the left panel of Figure 3.2. Consider the canonical homology basis $(\mathcal{A}_j, \mathcal{B}_j)$ discussed in Sec. 3.2.1. It is a standard result of Hodge theory [164] that there exists a unique dual basis (α_j, β_j) of real harmonic one-forms such that

$$\oint_{\mathcal{A}_i} \alpha_j = \delta_{ij} \qquad \oint_{\mathcal{B}_i} \alpha_j = 0 \qquad \text{and} \qquad \oint_{\mathcal{A}_i} \beta_j = 0 \qquad \oint_{\mathcal{B}_i} \beta_j = \delta_{ij}\,. \tag{3.41}$$

Because the homology class of $\mathcal{A}_i$ and $\mathcal{B}_i$ are respectively even and odd under sigma, the relations (3.41) are also satisfied by $\zeta^*\alpha_j$ and $-\zeta^*\beta_j$. Hence, it follows

from uniqueness that $\zeta^* \alpha_j = \alpha_j$ and $\zeta^* \beta_j = -\beta_j$, meaning that, under ζ, the one-forms α_j are even, while β_j are odd. For Dirichlet BC such that ϕ takes the same value (modulo $2\pi R$) on each boundary component of $\partial \mathscr{D}_n$, we have that

$$\int_{\mathcal{B}_j^+} d\phi_{\rm cl} = 2\pi R\, m_j \qquad\qquad m_j \in \mathbb{Z} \tag{3.42}$$

where $j \in \{1, \dots, n-1\}$; being $\mathcal{B}_j^+$ defined as the part of $\mathcal{B}_j$ that lies inside $\mathscr{D}_n$, hence $\mathcal{B}_j^+$ is a path connecting the j-th component to the $(j+1)$-th component of of $\partial \mathscr{D}_n$ (see Figure 3.4). On $D(\mathscr{D}_n)$, we thus have that:

$$\oint_{\mathcal{B}_j} d\phi_{\rm cl} = 4\pi R\, m_j \qquad\qquad m_j \in \mathbb{Z} \tag{3.43}$$

Moreover, since ϕ is constant on each boundary component, we have $\oint_{\mathcal{A}_j} d\phi_{\rm cl} = 0$ for all the allowed values of j. The analytic continuation of $d\phi_{\rm cl}$ to $D(\mathscr{D}_n)$ only involves the odd harmonic forms β_j as follows

$$d\phi_{\rm cl} = 4\pi R \sum_j m_j \beta_j \tag{3.44}$$

The Riemann bilinear relation [164] provides the value of the action (3.37) for this classical solution. It reads

$$S[\phi_{\rm cl}] = \frac{1}{8\pi} \int_{\mathscr{D}_n} d\phi_{\rm cl} \wedge \star\, d\phi_{\rm cl} \;=\; \frac{1}{16\pi} \int_{D(\mathscr{D}_n)} d\phi_{\rm cl} \wedge \star\, d\phi_{\rm cl} \;=\; \pi R^2\, \mathbf{m}^{\rm t} \cdot \boldsymbol{\tau}_2^{-1} \cdot \boldsymbol{m} \tag{3.45}$$

where $\boldsymbol{\tau}_2 \equiv \mathrm{Im}(\boldsymbol{\tau})$ is the imaginary part of the $(n-1) \times (n-1)$ period matrix $\boldsymbol{\tau}$ of $D(\mathscr{D}_n)$ in the canonical homology basis $(\mathcal{A}_j, \mathcal{B}_j)$. In our case, the period matrix is purely imaginary. Indeed, given a basis of the holomorphic one-forms ω_k such that $\oint_{\mathcal{A}_j} \omega_k = \delta_{j,k}$, we have $\zeta^* \omega_k = \overline{\omega}_k$ and therefore

$$\overline{\boldsymbol{\tau}}_{i,j} = \int_{\mathcal{B}_i} \bar{\omega}_j = \int_{\zeta(\mathcal{B}_i)} \omega_j = -\,\boldsymbol{\tau}_{i,j} \tag{3.46}$$

From (3.45) and the first expression in (3.40), for vanishing Dirichlet BC one obtains

$$\mathcal{Z}^{(\rm D)}_{n,\,\rm cl} \;=\; \Theta\Big(-R^2\, \boldsymbol{\tau}^{-1}\Big) \tag{3.47}$$

in terms of the Siegel theta function (3.24) and of the period matrix defined by (3.25), whose derivation is discussed in the Appendix B.2.

The case where Neumann BC are imposed on all the n boundary components of $\mathscr{D}_n$ can be addressed by adapting the steps described above for Dirichlet boundary conditions. For Neumann BC, the classical solutions can be extended to $D(\mathscr{D}_n)$ through the requirement $\phi_{\rm cl} \circ \zeta = \phi_{\rm cl}$, as already mentioned. Given the canonical homology base introduced above (see Sec. 3.2.1 and (3.41)), these classical solutions correspond to harmonic forms $d\phi_{\rm cl}$ satisfying

$$\int_{\mathcal{A}_j} d\phi_{\rm cl} = 2\pi n_j R \qquad\qquad \int_{\mathcal{B}_j} d\phi_{\rm cl} = 0 \qquad\qquad n_j \in \mathbb{Z} \tag{3.48}$$

where $j \in \{1, \dots, n-1\}$ and the absence of winding over $\mathcal{B}_j$ follows from the fact that $d\phi_{\rm cl}$ is even under ζ. Thus we have

$$d\phi_{\rm cl} = 2\pi R \sum_j n_j \alpha_j \tag{3.49}$$

Again, the Riemann bilinear relation allows us to compute the action (3.37) for these classical solutions and the result is

$$S[\phi_{\rm cl}] = \frac{\pi R^2}{4}\, \mathbf{n}^{\rm t} \cdot \boldsymbol{\tau} \cdot \boldsymbol{\tau}_2^{-1} \cdot \bar{\boldsymbol{\tau}} \cdot \mathbf{n} = -\,\mathrm{i}\, \frac{\pi R^2}{4}\, \mathbf{n}^{\rm t} \cdot \boldsymbol{\tau} \cdot \mathbf{n} \tag{3.50}$$

where the last step has been obtained by using that $\boldsymbol{\tau}$ is pure imaginary, i.e. $\boldsymbol{\tau} = \mathrm{i}\, \boldsymbol{\tau}_2$. Finally, we obtain

$$\mathcal{Z}^{(\rm N)}_{n,\,\rm cl} = \Theta\big(R^2\, \boldsymbol{\tau}/4\big) \tag{3.51}$$

in terms of the Siegel theta function (3.24).

Quantum term

The quantum part of the partition function in (3.21) and (3.40) for $\mathcal{M} = \mathscr{D}_n$ is independent of the compactification radius R. Rather than determining the quantum determinant of the Green function of the Laplacian on $\mathscr{D}_n$, we find it more convenient to adapt the analysis discussed in [71], which is heavily based on the method introduced in [70]. In Sec. 3.2.1 the field ϕ has been decomposed into the sum $\phi = \phi_{\rm cl} + \phi_{\rm qu}$. In the following analysis of the quantum term $\phi_{\rm qu}$ is denoted just by ϕ to enlighten the expressions. Since $\mathcal{M} = \mathscr{D}_n$ is made by n copies of the unit disk joined cyclically along the cut $(0, x)$, the path integral in (3.40) can be rewritten by introducing a field ϕ_j on the j-th copy, for $1 \leqslant j \leqslant n$. The total action reads $S[\phi] = \sum_j S[\phi_j]$ and the fields on the consecutive copies are coupled through their boundary condition along the cut.

Following [165], it is useful to perform a discrete Fourier transform for the n bosonic fields in the different replicas and introduce

$$\tilde{\phi}_k = \frac{1}{\sqrt{n}} \sum_{j=1}^{n} \mathrm{e}^{-2\pi \mathrm{i}\, k\, j/n}\, \phi_j \qquad\qquad 1 \leqslant k \leqslant n \tag{3.52}$$

which is a complex combination of fields; hence it is more convenient to replace the real bosons ϕ_j with the complex bosons Φ_j throughout the computation. The result for the real field is obtained by taking the square root of the final expression. The fields introduced through the transformation (3.52) are decoupled. However, the coupling of the original fields ϕ_j through the cut imposes the following twist condition around the origin

$$\tilde{\phi}_k(e^{2i\pi} z, e^{-2i\pi} \bar{z}) = \mathrm{e}^{2\pi \mathrm{i}\, k/n}\, \tilde{\phi}_k(z, \bar{z}) \tag{3.53}$$

and a similar one around the branch point at x, with the phase factor $\mathrm{e}^{2\pi \mathrm{i}\, k/n}$ in the r.h.s. replaced by its complex conjugate.

The partition function of a complex scalar on the Riemann sphere satisfying the above twisted boundary conditions around four branch points for an assigned value of k/n has been studied in [70]. In the case of the unit disk $\mathbb{D}$ and of two branch points we are dealing with, this analysis tells us that the corresponding

partition function can be written as the two-point function of particular twist fields $\sigma_{k/n}$ and $\sigma^\dagger_{k/n}$ placed at the endpoints of the branch cut. This leads us to write the quantum part of the partition function as the following product (up to normalization)

$$\mathcal{Z}^2_{n,\,\mathrm{qu}} = \prod_{k=1}^{n-1} \langle \sigma_{k/n}(0)\, \sigma^\dagger_{k/n}(x) \rangle_{\mathbb{D}} \tag{3.54}$$

where the mode corresponding to $k = n$ does not contribute because the corresponding twist field is the identity operator.

A method to determine $\langle \sigma_{k/n}(0)\, \sigma^\dagger_{k/n}(x) \rangle_{\mathbb{D}}$ was developed in [70] and it is based on the expectation value of the stress-energy tensor $T(z)$ in the presence of the twist fields. In Appendix B.3 the analysis of [70] has been adapted to the specific cases under investigation and the main results are presented below. We find that

$$\partial_x \log \langle \sigma_{k/n}(0)\, \sigma^\dagger_{k/n}(x) \rangle_{\mathbb{D}} = \mathrm{Res}_{z\to x} \frac{\langle T(z)\, \sigma_{k/n}(0)\, \sigma^\dagger_{k/n}(x) \rangle_{\mathbb{D}}}{\langle \sigma_{k/n}(0)\, \sigma^\dagger_{k/n}(x) \rangle_{\mathbb{D}}} \tag{3.55}$$

$$= -2h_{k/n} \left(\frac{1}{x} + \frac{1}{x - 1/\bar{x}} \right) - \partial_x \log \left[E^{(\alpha)}_{k/n}(x) \right] \tag{3.56}$$

where

$$h_{k/n} \equiv \frac{1}{2}\, \frac{k}{n} \left(1 - \frac{k}{n} \right) \qquad E^{(\alpha)}_{k/n}(x) \equiv \begin{cases} F_{k/n}\big(1 - |x|^2\big) & \text{Dirichlet BC} \\ F_{k/n}\big(|x|^2\big) & \text{Neumann BC} \end{cases} \tag{3.57}$$

(we remind that $F_{k/n}(y) \equiv {}_2F_1(k/n, 1 - k/n; 1; y)$). As for the quantum part of the partition function (3.54), this leads to

$$\partial_x \log \mathcal{Z}_{n,\,\mathrm{qu}} = -\Delta_n \left(\frac{1}{x} + \frac{1}{x - 1/\bar{x}} \right) - \partial_x \log E^{(\alpha)}_n(x) \tag{3.58}$$

where we used that $\sum_{k=1}^{n-1} h_{k/n} = \Delta_n = \frac{1}{12}(n - 1/n)$ (see (3.2) with $c = 1$), and we introduced

$$E^{(\alpha)}_n(x) \equiv \sqrt{\prod_{k=1}^{n-1} E^{(\alpha)}_{k/n}(x)} \tag{3.59}$$

From the relations reported in Appendix C of [71], the function $E^{(\alpha)}_n(x)$ in (3.57) can be expressed as a Siegel theta function as follows

$$\sqrt{\prod_{k=1}^{n-1} F_{k/n}(|x|^2)} = \Theta\Big(\boldsymbol{\tau}(|x|)\Big) \qquad \sqrt{\prod_{k=1}^{n-1} F_{k/n}(1 - |x|^2)} = \Theta\Big(-\boldsymbol{\tau}(|x|)^{-1}\Big) \tag{3.60}$$

in terms of the Siegel theta (3.24) and of the period matrix $\boldsymbol{\tau}(x)$ defined in (3.25). Then, integrating (3.58), for the quantum part of the partition function we get

$$\mathcal{Z}_{n,\,\mathrm{qu}}(x) \propto \frac{1}{\mathcal{P}(x)^{\Delta_n}\, E^{(\alpha)}_n(x)} \qquad \mathcal{P}(x) \equiv |x|^2 \big(1 - |x|^2\big) \tag{3.61}$$

where

$$E^{(\alpha)}_n(x) \equiv \begin{cases} \Theta\Big(\boldsymbol{\tau}(|x|)\Big) & \text{Dirichlet BC} \\ \Theta\Big(-\boldsymbol{\tau}(|x|)^{-1}\Big) & \text{Neumann BC} \end{cases} \tag{3.62}$$

and the overall constant, which can depend both on n and the BC, will be fixed later.

Two point functions of twist fields

Combining the classical part and the quantum part of the partition function, given by (3.47)-(3.51) and (3.61)-(3.62) respectively, we find that the two-point functions of the twist fields on the unit disk $\mathbb{D}$ for the compactified massless scalar field with either Dirichlet BC or Neumann BC read respectively

$$\langle \sigma_n(0)\, \sigma_n^\dagger(x)\rangle_{\mathbb{D}}^{(\mathrm{D})} \propto \frac{1}{\mathcal{P}(x)^{\Delta_n}} \frac{\Theta\big(-R^2\,\boldsymbol{\tau}(x)^{-1}\big)}{\Theta\big(-\boldsymbol{\tau}(x)^{-1}\big)} = \frac{1}{R^{n-1}\,\mathcal{P}(x)^{\Delta_n}} \frac{\Theta\big(\boldsymbol{\tau}(x)/R^2\big)}{\Theta\big(\boldsymbol{\tau}(x)\big)} \tag{3.63}$$

$$\langle \sigma_n(0)\, \sigma_n^\dagger(x)\rangle_{\mathbb{D}}^{(\mathrm{N})} \propto \frac{1}{\mathcal{P}(x)^{\Delta_n}} \frac{\Theta\big(R^2\,\boldsymbol{\tau}(x)/4\big)}{\Theta\big(\boldsymbol{\tau}(x)\big)} \tag{3.64}$$

where $\mathcal{P}(x)$ has been defined in (3.61) and the last expression of (3.63) has been obtained by employing the following identity

$$\Theta\big(-\boldsymbol{\tau}(x)^{-1}\big) = \sqrt{\det\big(-\mathrm{i}\boldsymbol{\tau}(x)\big)}\,\Theta\big(\boldsymbol{\tau}(x)\big) \tag{3.65}$$

which involves the Siegel theta function (3.24) and the period matrix (3.25).

In the limit $x \to 0$, for the generic element (3.25) of the period matrix we have that $\boldsymbol{\tau}(x)_{i,j} \to +\mathrm{i}\infty$; therefore $\Theta(\eta\boldsymbol{\tau}(x)) \to 1$ for any constant $\eta > 0$, which implies that $\mathcal{F}_n^{(\alpha)}(x) \to 1$ as $x \to 0$ for any finite value of R. By applying this observation to (3.63) and (3.64), at the leading order we find that

$$\langle \sigma_n(0)\, \sigma_n^\dagger(x)\rangle_{\mathbb{D}}^{(\alpha)} \sim \frac{1}{|x|^{2\Delta_n}} \qquad x \to 0 \qquad \alpha \in \big\{\mathrm{D},\mathrm{N}\big\} \tag{3.66}$$

which fixes the overall normalizations in (3.63) and (3.64). Thus, we find the final result for the twist correlator on the unit disk:

$$\langle \sigma_n(0)\, \sigma_n^\dagger(x)\rangle_{\mathbb{D}}^{(\mathrm{D})} = \mathcal{P}(x)^{-\Delta_n} \frac{\Theta\big(\boldsymbol{\tau}(x)/R^2\big)}{\Theta\big(\boldsymbol{\tau}(x)\big)} \quad \langle \sigma_n(0)\, \sigma_n^\dagger(x)\rangle_{\mathbb{D}}^{(\mathrm{N})}, = \mathcal{P}(x)^{-\Delta_n} \frac{\Theta\big(R^2\,\boldsymbol{\tau}(x)/4\big)}{\Theta\big(\boldsymbol{\tau}(x)\big)} \tag{3.67}$$

Finally, the two-point twist correlators on the unit disk in (3.67) provide the expressions for the two-point twist correlator on the infinite strip and right half plane geometries, which are given by (3.6) and (3.7) respectively, as discussed in Sec 3.1.From this, one readily recovers all the sought-after entanglement measures.

The Rényi entropies for the massless scalar field in the case of Dirichlet BC and the spatial bipartition in the right panel of Figure 3.1 have been already studied in [166], where implicit results have been found. This analysis has been developed further in [121] for inhomogeneous systems. To apply the results of these works, linear integral equations must be solved and, since analytic solutions have not been found, approximate results can be obtained numerically by discretising the interval A, as discussed in [166]. This provides an important benchmark for our analytic results corresponding to Dirichlet BC; and we checked[2] that our BCFT expression is compatible with the one obtained numerically in [166]. In particular, for $n \leqslant 5$ and various sizes for the interval, we have found numerical agreement between the period matrix $\boldsymbol{\tau}$ in (3.25) and the matrix $\mathcal{M}$ of [166], once the difference

[2]We are grateful to Alvise Bastianello for having shared with us his notebook for the numerical evaluation of the expression obtained in [166].

in the notations has been taken into account. Also the compatibility for the Rényi entropies when $n \leqslant 5$ and for various values for the compactification radius $R \in (0.5, 3)$ has been checked. As n increases, higher accuracy in the discretization procedure is needed to find agreement with our BCFT results in the continuum.

It is now interesting to make a more careful comparison with the results of [71], which used similar techniques to calculate Rényi entropies for two disjoint intervals in the infinite line. As already mentioned in Section 3.1, their calculation is centred around the evaluation of the partition function of the compact boson of radius R, on an n-sheeted Riemann surface $\mathcal{M}_n$, which is characterized by the same period matrix τ as the *double* $D(\mathcal{D}_n)$ of the n-sheeted disk of our setup.

Based on this geometrical connection, it is interesting to compare the universal function $\mathcal{F}_n^{[CCT'09]}$ of [71] , which we reproduce below in our conventions

$$\mathcal{F}_n^{[CCT'09]}(r) = \frac{\Theta\Big(R^2\tau(r)/2\Big)\Theta\Big(2\tau(r)/R^2\Big)}{[\Theta\Big(\tau(r)\Big)]^2} \tag{3.68}$$

with the results for Neumann and Dirichlet BC in (3.23).

We note that the multiplicative factors of the period matrices in the Riemann-Siegel functions in the numerator of (3.68) are not the same as the ones in the numerators of (3.23). This difference arises in the calculation for the classical part, from two sources: the winding condition around the cycle B_j for the Dirichlet BC (3.43), and the fact that for classical action (3.45) the spacetime is $\mathcal{D}_n$, and not $D(\mathcal{D}_n)$, as it would be in the bulk case.

Thus, we found no obvious correspondence between the results for two disjoint intervals on $\mathcal{M}_n$ and the results for Neumann and Dirichlet BC for a compact boson with the *same* compactification radius R. However, we notice the relation:

$$\mathcal{F}_n^{[CCT'09],R}(r) = \mathcal{F}_n^{(\mathrm{D}),R/\sqrt{2}}(r)\mathcal{F}_n^{(\mathrm{N}),R\sqrt{2}}(r) \tag{3.69}$$

between the universal function $\mathcal{F}_n^{[CCT'09],R}$ for a compact boson CFT of radius R, in the two disjoint interval setup, and the functions $\mathcal{F}_n^{(\mathrm{D}),R/\sqrt{2}}(r)$, $\mathcal{F}_n^{(\mathrm{N}),R\sqrt{2}}(r)$ for one interval in the bulk, for compact boson BCFTs with Dirichlet and Neumann BC and *different* compactification radii $R/\sqrt{2}$ and $R\sqrt{2}$, respectively.

Beyond purely analytical considerations, such a relation between the bulk and boundary entanglement properties of compact boson CFTs could be of interest for numerical investigations of entanglement in the critical XXZ chain.

3.2.2 Decompactification regime

An important regime to explore is given by the decompactification regime $R \to \infty$.

Taking this limit in (3.23) does not provide well-defined finite expressions. A similar problem already arises for the conformal boundary states of the compact boson BCFT. Indeed, the boundary states corresponding to Dirichlet and Neumann BC can be constructed through the $|(m,n)\rangle\rangle$ Ishibashi states as follows [142]

$$|\mathrm{N}\rangle_R = \sqrt{\frac{R}{2}} \sum_{n\in\mathbb{Z}} |(0,n)\rangle\rangle \qquad\qquad |\mathrm{D}\rangle_R = \sqrt{\frac{1}{R}} \sum_{m\in\mathbb{Z}} |(m,0)\rangle\rangle \tag{3.70}$$

and do not have a well-defined behaviour as $R \to \infty$. For these boundary states, a formal regularization scheme for the compact boson BCFT data (spectrum of

primary fields, boundary states, structure constants) has been implemented [167, 168] to construct a well-defined decompactification limit. However, extending this procedure to the $\mathbb{Z}_N$ orbifold of the compact boson BCFT is beyond the scope of this work.

Well-defined expressions in the decompactification limit can be obtained as follows. Since $\Theta\Big(R^2\,\tau(x)/4\Big) \to 1$ and $\Theta\Big(-R^2\,\tau(x)^{-1}\Big) \to 1$ in this limit, and disregarding proportionality constants for the moment, it is straightforward to find that the two-point functions of twist fields in (3.63) and (3.64) become respectively

$$\langle \sigma_n(0)\,\sigma_n^\dagger(x)\rangle_{\mathbb{D}}^{(\mathrm{D})} \propto \frac{1}{\mathcal{P}(x)^{\Delta_n}}\,\widetilde{\mathcal{F}}_n^{(\mathrm{D})}\Big(x^2\Big) \qquad \langle \sigma_n(0)\,\sigma_n^\dagger(x)\rangle_{\mathbb{D}}^{(\mathrm{N})} \propto \frac{1}{\mathcal{P}(x)^{\Delta_n}}\,\widetilde{\mathcal{F}}_n^{(\mathrm{N})}\Big(x^2\Big) \tag{3.71}$$

where we have employed the identities (3.60) and the functions (3.28). To fix the CFT normalization in the above expressions, a careful, and slightly technical consideration of the $x \to 0$ limit of (3.71) is necessary. We relegate it to Appendix B.5.1 and give here the final results for the two-point functions on the unit disk in the decompactification regime:

$$\langle \sigma_n(0)\,\sigma_n^\dagger(x)\rangle_{\mathbb{D}}^{(\mathrm{D})} = \frac{1}{\mathcal{P}(x)^{\Delta_n}}\,\widetilde{\mathcal{F}}_n^{(\mathrm{D})}\Big(x^2\Big) \qquad \langle \sigma_n(0)\,\sigma_n^\dagger(x)\rangle_{\mathbb{D}}^{(\mathrm{N})} = \frac{1}{\mathcal{P}(x)^{\Delta_n}}\,\widetilde{\mathcal{F}}_n^{(\mathrm{N})}\Big(x^2\Big) \tag{3.72}$$

From (3.72) we arrive at the results reported in Section 1.14

As for the Rényi entropies of an interval in the segment, from (3.11) we have

$$S_n^\alpha(A) = \frac{\Delta_n}{n-1}\,\log\Big[\mathcal{P}(u,v)\Big] + 2\frac{\log\Big(c_n\Big)}{1-n} + \frac{1}{2(n-1)}\sum_{k=1}^{n-1}\log\Big[F_{k/n}(y_\alpha)\Big] \tag{3.73}$$

where $y_{\mathrm{D}} \equiv 1-r$ and $y_{\mathrm{N}} \equiv r$ (we remind that $F_{k/n}(y)$ has been introduced in the text below (3.25)). The corresponding result for the interval on the half line is obtained by taking the limit $L \to \infty$ in (3.73).

Finally, by using (3.16) and (3.73), we find the following UV finite quantity

$$\mathcal{I}_A^{(n)} = \frac{\Delta_n}{1-n}\,\log(r) + \frac{1}{2(1-n)}\sum_{k=1}^{n-1}\log\Big[F_{k/n}(y_\alpha)\Big] \tag{3.74}$$

where we have also employed that $g_D = g_N = 1$ in our conventions, as shown in B.5.1, and compatible with existing results in the literature [24]. As for the entanglement entropy, the analytic continuation $n \to 1$ of (3.73) can be studied by employing the following result [71]

$$\lim_{n\to 1}\partial_n\Bigg(\sum_{k=1}^{n-1}\log\Big[F_{k/n}(y)\Big]\Bigg) = \int_{-\mathrm{i}\infty}^{\mathrm{i}\infty}\frac{\pi z\,\log[F_z(y)]}{[\sin(\pi z)]^2}\,\frac{dz}{\mathrm{i}} \equiv -\,\mathcal{D}_1'(y) \tag{3.75}$$

where the integral along the imaginary axis defining $\mathcal{D}_1'(y)$ is evaluated numerically. This leads to the following result for the entanglement entropy of the interval in the segment

$$S^\alpha(A) = \frac{1}{6}\,\log\Big[\mathcal{P}(u,v)\Big] - \frac{\mathcal{D}_1'(y_\alpha)}{2} + 2c_1' \tag{3.76}$$

where the constant non-universal shift is given by $c_1' \equiv \lim_{n\to 1}\frac{\log c_n}{1-n}$. The entanglement entropy of an interval on the half line is obtained by taking the $L \to \infty$ limit of (3.76).

From the UV finite quantity (3.74), we find it worth introducing

$$\widehat{\mathcal{I}}^{(n)}_{A;\alpha} \equiv \mathcal{I}^{(n)}_{A} - \frac{\Delta_n}{1-n}\log(r) \tag{3.77}$$

Its analytic continuation $n \to 1$ reads

$$\widehat{\mathcal{I}}^{(1)}_{A;\alpha} = \frac{\mathcal{D}'_1(y_\alpha)}{2} \tag{3.78}$$

in terms of (3.75), where the constant shifts depend on the boundary conditions.

The limit $n \to \infty$ of (3.73) provides the single copy entanglement entropy in the decompactification regime. By introducing

$$\lim_{n\to\infty} \frac{1}{n-1}\sum_{k=1}^{n-1} \log\Big[F_{k/n}(y)\Big] = \int_0^1 \log\Big[F_\kappa(y)\Big] d\kappa \equiv \mathcal{S}(y) \tag{3.79}$$

where the integral defining $\mathcal{S}(y)$ can be evaluated numerically. For the single copy entanglement entropy of the interval in the segment, one finds

$$S^\alpha_\infty([u,v]) = \frac{1}{12}\log\Big[\mathcal{P}(u,v)\Big] + \frac{\mathcal{S}(y_\alpha)}{2} + 2c'_\infty \tag{3.80}$$

where $c'_\infty \equiv \lim_{n\to\infty} \frac{\log c_n}{1-n}$. The limit $L \to \infty$ of (3.80) provides the single copy entanglement entropy of the interval in the half-line in the decompactification regime.

3.3 Numerical results from harmonic chains

In this section, we compare the BCFT results reported in Sec 3.1 and Sec. 3.2.2 for the decompactification regime with the entanglement entropies of a block of consecutive sites in the spatial bipartitions shown in Figure 3.1 for harmonic chains defined either on the semi-infinite line or on the segment, when either Dirichlet BC or Neumann BC are imposed.

The Hamiltonian of a finite harmonic chain with nearest neighbour spring-like interactions made by $N-1$ sites in the interior and two sites at its endpoints reads

$$\widehat{H} = \sum_{i=0}^{N}\left(\frac{1}{2m}\hat{p}_i^2 + \frac{m\omega^2}{2}\hat{q}_i^2\right) + \sum_{i=0}^{N-1}\frac{\kappa}{2}(\hat{q}_{i+1}-\hat{q}_i)^2 \tag{3.81}$$

in terms of the position and the momentum operators $\hat{q}_i$ and $\hat{p}_i$, that are hermitian operators satisfying the canonical commutation relations $[\hat{q}_i,\hat{q}_j] = [\hat{p}_i,\hat{p}_j] = 0$ and $[\hat{q}_i,\hat{p}_j] = \mathrm{i}\delta_{i,j}$ (we set $\hbar = 1$). At the endpoints of the harmonic chain we impose the same boundary condition, which is either Dirichlet BC

$$\hat{q}_0 = \hat{q}_N = 0 \tag{3.82}$$

or Neumann BC

$$\hat{q}_1 - \hat{q}_0 = 0 \qquad \hat{q}_N - \hat{q}_{N-1} = 0 \tag{3.83}$$

We consider these quadratic systems in their ground state, that is a Gaussian state. Since these are free systems, the crucial objects to perform our numerical

analysis are the correlation matrices Q and P, whose generic elements are the two-point correlators in the ground state, i.e. $\langle \hat{q}_i \hat{q}_j \rangle$ and $\langle \hat{p}_i \hat{p}_j \rangle$ respectively [44, 65, 66, 156–161].

For the Dirichlet BC (3.82), the generic elements of the correlation matrices Q and P are given respectively by [169]

$$\langle \hat{q}_i \hat{q}_j \rangle = \frac{1}{N} \sum_{k=1}^{N-1} \frac{1}{m\omega_k} \sin(\pi k\, i/N) \, \sin(\pi k\, j/N) \tag{3.84}$$

$$\langle \hat{p}_i \hat{p}_j \rangle = \frac{1}{N} \sum_{k=1}^{N-1} m\omega_k \, \sin(\pi k\, i/N) \, \sin(\pi k\, j/N) \tag{3.85}$$

where the dispersion relation reads

$$\omega_k \equiv \sqrt{\omega^2 + \frac{4\kappa}{m} \Big[\sin(\pi k/(2N)) \Big]^2} \, > \, \omega \qquad\qquad 1 \leqslant k \leqslant N-1 \tag{3.86}$$

In the massless regime (i.e. when $\omega = 0$) and in the thermodynamic limit $N \to \infty$, these correlators simplify respectively to [163]

$$\langle \hat{q}_i \hat{q}_j \rangle = \frac{1}{2\pi \sqrt{\kappa m}} \Big(\psi(1/2 + i + j) - \psi(1/2 + i - j) \Big) \tag{3.87}$$

$$\langle \hat{p}_i \hat{p}_j \rangle = \frac{2\sqrt{\kappa m}}{\pi} \left(\frac{1}{4(i+j)^2 - 1} - \frac{1}{4(i-j)^2 - 1} \right) \tag{3.88}$$

where $\psi(z)$ is the digamma function. These correlators can be employed to investigate the semi-infinite massless harmonic chain with Dirichlet BC at its origin.

When the Neumann BC (3.83) are imposed, the generic elements of the correlation matrices Q and P read respectively [162, 170]

$$\langle \hat{q}_i \hat{q}_j \rangle = \frac{1}{2} \sum_{k=1}^{N-1} \frac{1}{m\omega_k} V_{i,k} \, V_{j,k} \qquad\qquad \langle \hat{p}_i \hat{p}_j \rangle = \frac{1}{2} \sum_{k=1}^{N-1} m\omega_k \, V_{i,k} \, V_{j,k} \tag{3.89}$$

where

$$\omega_k \equiv \sqrt{\omega^2 + \frac{4\kappa}{m} \Big[\sin(\theta_k/2) \Big]^2} \qquad\qquad \theta_k \equiv \frac{\pi(k-1)}{N-1} \tag{3.90}$$

and

$$V_{i,k} = \sqrt{\frac{2 - \delta_{k,1}}{N-1}} \, \cos\Big(\theta_k (i - 1/2) \Big) \tag{3.91}$$

The correlators in (3.89) can be written as $\langle \hat{q}_i \hat{q}_j \rangle = \frac{1}{2} M^{(1)}_{i,j}$ and $\langle \hat{p}_i \hat{p}_j \rangle = \frac{1}{2} M^{(-1)}_{i,j}$, where $M^{(\eta)}_{i,j}$ is defined as follows

$$M^{(\eta)}_{i,j} \equiv \frac{1}{(N-1)\,(m\omega)^\eta} + \frac{2}{N-1} \sum_{k=2}^{N-1} \frac{\cos[\theta_k (i - 1/2)] \, \cos[\theta_k (j - 1/2)]}{\Big(2\sqrt{\kappa m} \Big)^\eta \Big\{ m\omega^2/(4\kappa) + [\sin(\theta_k/2)]^2 \Big\}^{\eta/2}} \tag{3.92}$$

In the thermodynamic limit $N \to \infty$, this expression becomes

$$\mathcal{I}^{(\eta)}_{i,j} \equiv \frac{2}{\pi \Big(2\sqrt{\kappa m} \Big)^\eta} \int_0^\pi \frac{\cos[\theta (i - 1/2)] \, \cos[\theta (j - 1/2)]}{\Big\{ m\omega^2/(4\kappa) + [\sin(\theta/2)]^2 \Big\}^{\eta/2}} \, d\theta \tag{3.93}$$

$$= \frac{1}{\pi \Big(\sqrt{2\kappa m} \Big)^\eta \Big[m\omega^2/(2\kappa) + 1 \Big]^{\eta/2}} \int_0^\pi \frac{\cos[\theta(i+j-1)] + \cos[\theta(i-j)]}{\Big\{ 1 - \Big[m\omega^2/(2\kappa) + 1 \Big]^{-1} \cos(\theta) \Big\}^{\eta/2}} \, d\theta$$

By employing the following formula [171]

$$F(a,b;n,\tilde{a}^2) \equiv \frac{1}{\pi}\int_0^\pi \frac{\cos(n\theta)}{(1-a\cos\theta)^b}\,d\theta = \frac{2^b\,\Gamma(n+b)}{a^b\,\Gamma(n+1)\Gamma(b)}\,\tilde{a}^{n+b}\;{}_2F_1\Big(b,n+b\,;n+1\,;\tilde{a}^2\Big) \tag{3.94}$$

with $\tilde{a} \equiv \big(1-\sqrt{1-a^2}\big)/a$, the integral in the last step of (3.93) can be performed, finding

$$\mathcal{I}^{(\eta)}_{i,j} = \frac{1}{\big(\sqrt{2\kappa m}\,\tilde{\omega}\big)^\eta}\Big[\,F\Big(1/\tilde{\omega}^2,\eta/2\,;i+j-1,\tilde{a}^2\Big)+F\Big(1/\tilde{\omega}^2,\eta/2\,;i-j,\tilde{a}^2\Big)\,\Big] \tag{3.95}$$

where $\tilde{\omega}^2 \equiv m\omega^2/(2\kappa)+1$. This observation allows us to write the analytic expressions of the correlators in (3.89) in the thermodynamic limit in terms of (3.95) as follows

$$\langle\hat{q}_i\hat{q}_j\rangle = \frac{1}{2}\,\mathcal{I}^{(1)}_{i,j} \qquad\qquad \langle\hat{p}_i\hat{p}_j\rangle = \frac{1}{2}\,\mathcal{I}^{(-1)}_{i,j} \tag{3.96}$$

In the massless limit $\omega \to 0$, these expressions become respectively

$$\langle\hat{q}_i\hat{q}_j\rangle = -\frac{1}{2\pi\sqrt{\kappa m}}\Big(\psi\Big(|i-j|+\tfrac{1}{2}\Big)+\psi\Big(i+j+\tfrac{1}{2}\Big)+\log(m\omega^2/\kappa)+4\gamma+\log(4)+2\,\psi\Big(\tfrac{1}{2}\Big)\Big) \tag{3.97}$$

$$\langle\hat{p}_i\hat{p}_j\rangle = -\frac{\sqrt{\kappa m}}{2\pi}\left(\frac{1}{(i-j)^2-1/4}+\frac{1}{(i+j-1)^2-1/4}\right) \tag{3.98}$$

where $\gamma = -\psi(1) \simeq 0.5772$ is the Euler-Mascheroni constant. In all our numerical analyses we have set $\kappa = m = 1$.

We remark that all the finite correlation matrices Q and P introduced above are symmetric matrices satisfying $\mathsf{Q}\,\mathsf{P} = \frac{1}{4}\mathbf{1}$, where $\mathbf{1}$ is the identity matrix, as expected for the ground state.

Another important feature to highlight is the occurrence of the zero mode: while it is forbidden by the Dirichlet BC (3.82), it is allowed by the Neumann BC (3.83). The occurrence of the zero mode heavily influences the massless limit $\omega \to 0$ of the corresponding correlators. Indeed, while for Dirichlet BC (see (3.84) and (3.85)) finite results are obtained in this limit, for Neumann BC (see (3.89)) the term corresponding to $k = 1$ in $\langle\hat{q}_i\hat{q}_j\rangle$ is divergent as $\omega \to 0$. Hence, exploring the massless regime is more delicate when Neumann BC are imposed because the zero mode could lead to effects that are difficult to quantify through analytic methods.

The entanglement entropies $S^{(n)}_A$ of a block A made by m_A consecutive sites can be computed through a well-established method [44, 65, 66, 156–161]. The first step consists of introducing the reduced correlation matrices Q_A and P_A, whose generic elements are respectively $\langle\hat{q}_i\hat{q}_j\rangle$ and $\langle\hat{p}_i\hat{p}_j\rangle$, with $i,j \in A$. Then, the Rényi entropies $S^{(n)}_A$ are obtained as follows

$$S_n(A) = \frac{1}{n-1}\sum_{j=1}^{m_A}\log\left[\left(\mu_j+\frac{1}{2}\right)^n-\left(\mu_j-\frac{1}{2}\right)^n\right] \tag{3.99}$$

where $\{\mu_1^2,\dots,\mu_{m_A}^2\}$ is the spectrum of the $m_A \times m_A$ matrix $\mathsf{Q}_A\,\mathsf{P}_A$ and provide the symplectic eigenvalues $\{\mu_1,\dots,\mu_{m_A}\}$ of the covariance matrix $\mathsf{Q}_A \oplus \mathsf{P}_A$. The limits

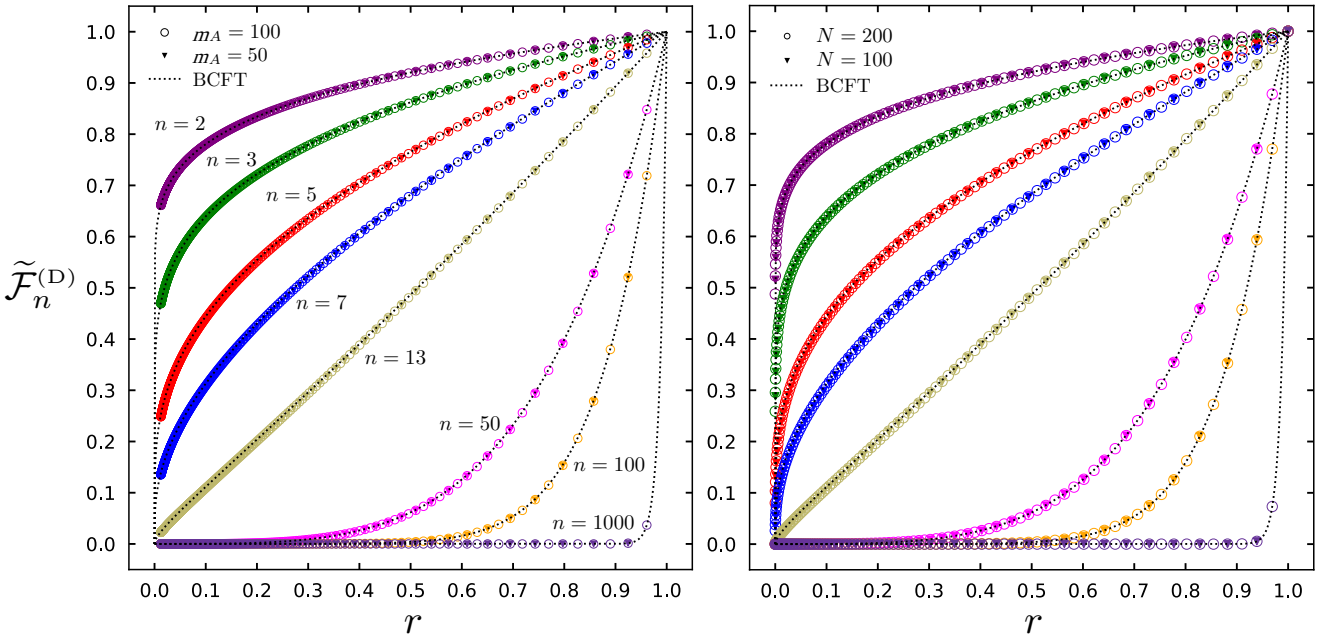

Figure 3.5: The function $\widetilde{\mathcal{F}}_n^{(\mathrm{D})}$ for the bipartitions in Figure 3.1 with Dirichlet boundary conditions. The black dotted lines correspond to the BCFT result given by the first expression in (3.28). The data points have been obtained for the block of m_A consecutive sites either in the semi-infinite chain (left panel) or on the finite chain made by N sites (right panel) with Dirichlet BC (see Sec. 3.3).

$n \to 1$ and $n \to \infty$ of (3.99) give respectively the entanglement entropy

$$S(A) = \sum_{j=1}^{m_A} \log\left[\left(\mu_j + \frac{1}{2}\right)\log\left(\mu_j + \frac{1}{2}\right) - \left(\mu_j - \frac{1}{2}\right)\log\left(\mu_j - \frac{1}{2}\right)\right] \tag{3.100}$$

and the single-copy entanglement

$$S_\infty(A) = \sum_{j=1}^{m_A} \log\left(\mu_j + \frac{1}{2}\right) \tag{3.101}$$

In the following, we report some numerical results for the entanglement entropies of a block A made by m_A consecutive sites providing the bipartitions shown in Figure 3.1, when either Dirichlet BC or Neumann BC are imposed and the whole harmonic chain is in its ground state. This leads to four possible setups for the harmonic chain: either an infinite chain on the semi-infinite line or a finite chain made by N consecutive sites on the segment, and either Dirichlet BC or Neumann BC (we remind that, in the case of the segment, the same BC is chosen at both its boundaries). The continuum limit of the lattice results for the semi-infinite chain and for the segment are compared against the corresponding BCFT expressions for the massless scalar field in the decompactification regime, either on the right half plane RHP or on the strip $\mathbb{S}_L$ respectively.

Unless stated otherwise, for the semi-infinite chains the interval size m_A is kept fixed while its distance from the boundary is varied in such a way that r covers the whole range $r \in (0, 1)$. Instead, in the finite chains of even size N, the whole range $r \in (0, 1)$ is spanned by keeping one endpoint of A fixed in the middle of the chain (this is not ambiguous for even values of N) while the interval grows towards one of the boundaries of the finite chain.

In the case of Dirichlet BC, our lattice data are taken by setting $\omega = 0$ in the correlators (3.84) and (3.87), which are still well-defined in this limit. Instead, when Neumann BC are imposed, the first correlator in (3.89) diverges in the massless limit $\omega \to 0$ because of the occurrence of the zero mode corresponding to $k = 1$. This forces us to set a small but non-vanishing mass: in our analysis we have chosen $\omega m_A \sim 10^{-10}$ for the semi-infinite chains and $\omega N \sim 10^{-10}$ for the finite chains, which are much smaller than the other scales in each setup. This procedure is the standard one in the case of periodic BC (or infinite chain), where the zero mode occurs as well.

For the harmonic chains on the semi-infinite line, when Dirichlet BC are observed, we have observed that block sizes $m_A \in \{50, 100\}$ are large enough to obtain a nice agreement with the BCFT predictions. Instead, for Neumann BC large sizes for the blocks are typically needed: we used $m_A \in \{200, 400\}$ for the semi-infinite chains and $N \in \{100, 200\}$ for the finite chains.

We find it worth remarking that, in all the figures of this chapter, the lattice data corresponding to Dirichlet BC have not been shifted to be compared with the BCFT curves for all the UV finite quantities considered. On the other hand, for the ones corresponding to Neumann BC, we have to introduce a constant shift depending on the Rényi index and the lattice zero-mode regulator, that we are not able to characterize analytically. It would be interesting to establish a quantitative relation between this shift and ω, if it exists (see e.g. [170, 172] for some results in this direction).

When the block A is not adjacent to the boundary, one can consider also the blocks A_u and A_v, starting from the boundary, and made by m_u and m_v consecutive sites as shown in Figure 3.6. The subsystems A, A_u and A_v lead to construct the ratios (3.13), which provide the combination of entanglement entropies in (3.15). The BCFT expressions for the UV finite ratios (3.13) are obtained by combining (3.14) and (3.28), which tell us also that it is worth considering $r^{\Delta_n} R_A^{(n)}$, for both the finite and semi-infinite chains. From (3.10), we have that the ratio r is given by $r = [s(m_v - m_u)/s(m_v + m_u)]^2$ for the finite chains and $r = [(m_v - m_u)/(m_v + m_u)]^2$ for the semi-infinite chains.

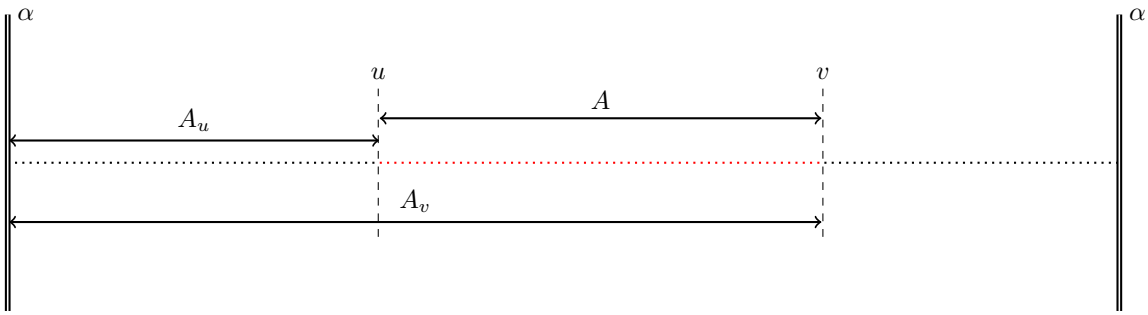

Figure 3.6: The three intervals relevant for constructing UV finite ratios (3.13). For the semi-infinite chain, the α boundary on the right is sent to infinity

The numerical data for these quantities and the corresponding BCFT expressions are shown in Figure 3.5 for Dirichlet BC and in Figure 3.7 and Figure 3.8 for Neumann BC. A remarkable agreement between the lattice data points in the scaling limit and the BCFT predictions are observed for Dirichlet BC, for any value of r considered and even for very large values of the Rényi index n. Instead, when Neumann BC are imposed, we obtain a nice agreement for $n \leqslant 7$ and $r \in (0.5, 1)$. To understand these discrepancies, for Neumann BC we have

reported also the UV finite ratio (3.13) in the cases of $n = 3$, $n = 13$ and $n = 50$ (see Figure 3.8), according to the colour code adopted in Figure 3.7. To enhance the visibility of the data, the curves for various values of n have been deliberately shifted vertically. The relation between the BCFT expressions of the quantities considered in Figure 3.7 and Figure 3.8 is given in (3.14). The nice behaviour of the lattice data points w.r.t. the BCFT curves in Figure 3.8 suggests that, in Figure 3.7, larger blocks and system sizes are needed to obtain a better match with the BCFT predictions.

Another possible reason for this discrepancy in Figure 3.7 could be related to the occurrence of the zero mode. We have noticed that as n is increased to larger values, at fixed N or m_A, one needs smaller regulating ω for the HC data to converge (up to shift). Thus, for the regulators ω and system sizes considered in (3.7) the hypothesis that the HC data and the CFT results differ only by a shift might not hold over the full range $r \in (0, 1)$.

However, as mentioned earlier in this section, to probe beyond this assumption one needs to analytically characterize the dependence of $\mathcal{F}_n^{(\mathrm{N})}$ on ω in the harmonic chain, as well as the finite-size corrections to the CFT result we've found. From the point of view of numerics, it seems that to find good agreement between the HC data and the CFT prediction at large n one needs to simultaneously work with larger system sizes and smaller regulators ωN, to the effect of greatly increased computational time.

Finally, it seems that the data for $\mathcal{F}_n^{(\mathrm{N})}(r)$ is particularly sensitive to these effects, as opposed to the quantities plotted in Figures 3.8 and 3.13. The deviation from the CFT prediction in the $r \to 0$ case is less evident compared to Figure 5, which could simply be an artefact of plotting on a logarithmic scale. In any case, a quantitative understanding of these effects is beyond the analytical and numerical goals of this project.

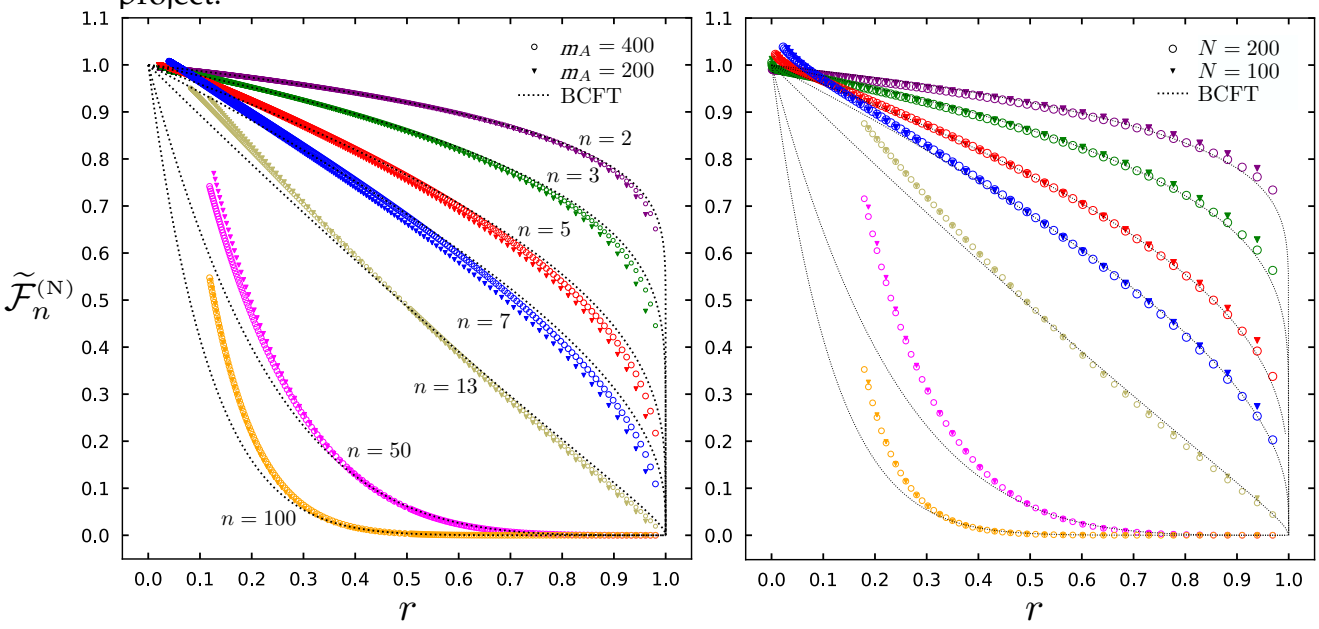

Figure 3.7: The function $\widetilde{\mathcal{F}}_n^{(\mathrm{N})}$ for the bipartitions in Figure 3.1 with Neumann boundary conditions. The black dotted lines correspond to the BCFT result given by the second expression in (3.28). The data points have been obtained for the block of m_A consecutive sites either in the semi-infinite chain (left panel) or on the finite chain made by N sites (right panel) with Neumann BC, as discussed in Sec. 3.3.

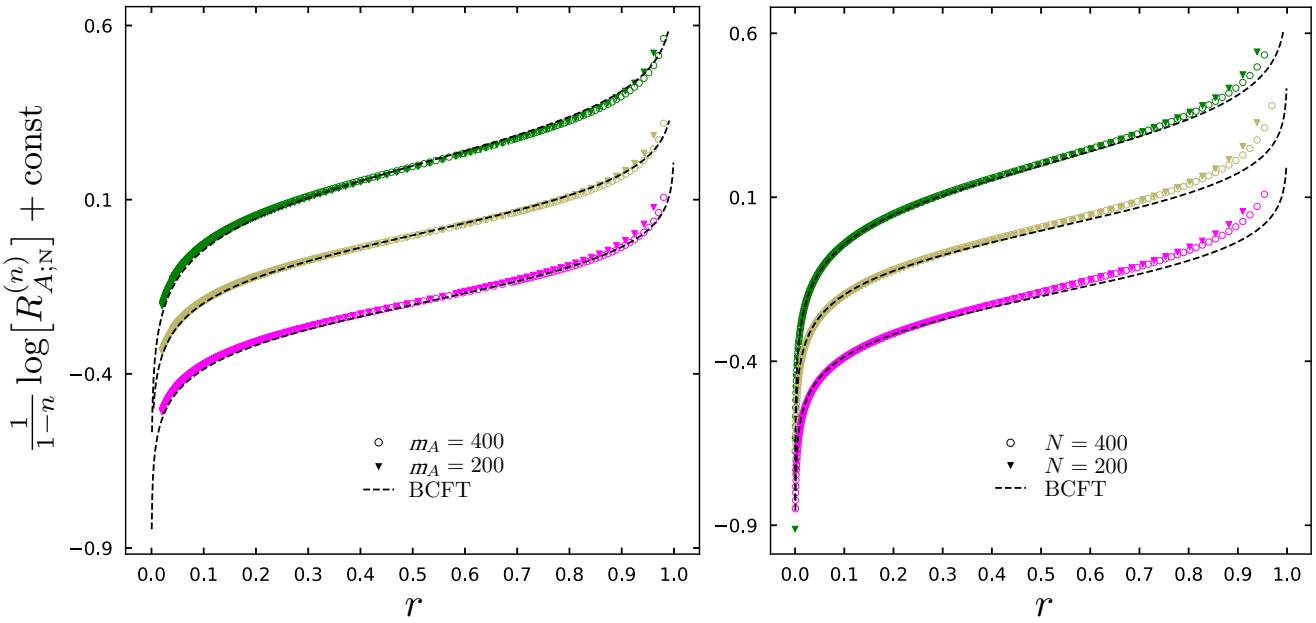

Figure 3.8: The UV finite ratio (3.13) for the bipartitions shown in Figure 3.1 with Neumann BC and $n \in \{3, 13, 50\}$, with the same colour code of Figure 3.7. We have introduced artificial vertical shifts of the curves for different values of n to enhance the distinguishability of the data.

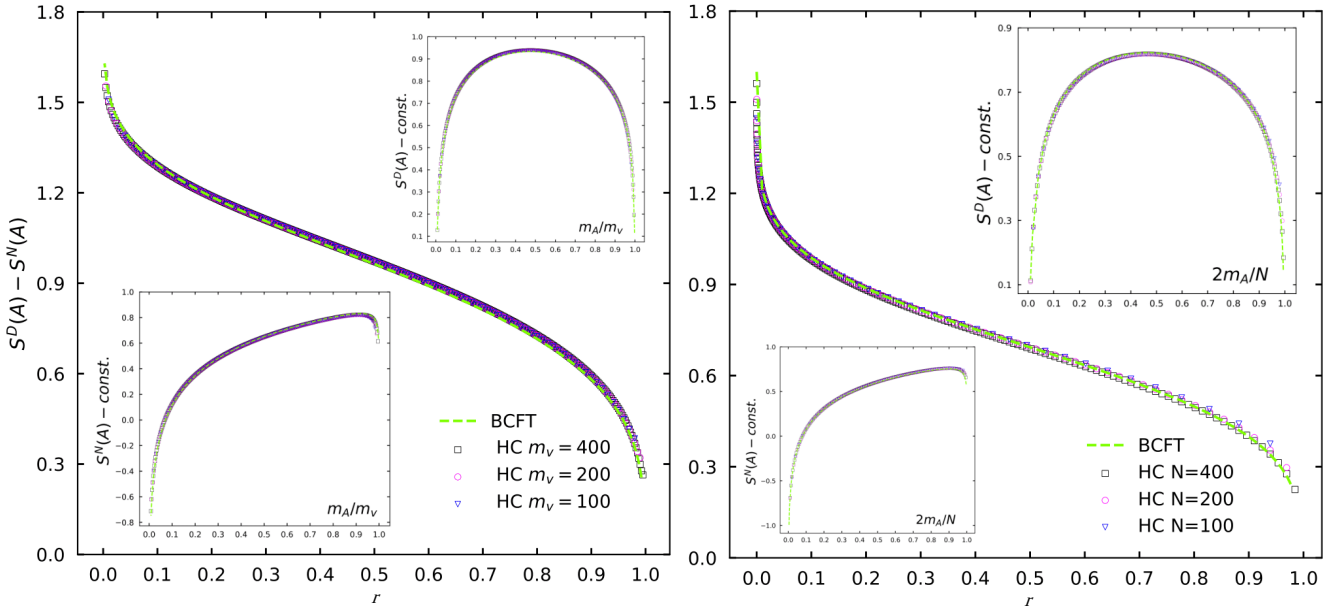

Figure 3.9: The difference between the entanglement entropy for Dirichlet BC and Neumann BC for the bipartitions of Figure 3.1, either in the semi-infinite chains (left panel) or in the finite chains (right panel). The insets show the entanglement entropy for the two different boundary conditions. The BCFT curves have been obtained from (3.76).

In Sec. 3.1 we have observed that the difference (3.18) between the entanglement entropies corresponding to two different conformally invariant boundary conditions is another interesting UV finite quantity to investigate and it is a function of the harmonic ratio r. In the case of the massless scalar field in the decompactification regime that we are exploring, we consider (3.29) and its analytic continuation $n \to 1$, which can be easily written by using (3.76). The results of our analyses for this UV finite quantity are shown in Figure 3.9.

The collection of the lattice data has been performed by setting m_v to a constant value in both setups: we have chosen $m_v \in \{100, 200, 400\}$ for the semi-infinite chains, while we took $m_v = N/2$ with $N \in \{100, 200, 400\}$ for the finite chains. Then, we varied $m_u \in \{1, \dots, m_v - 1\}$ and plotted the entanglement entropy in terms of m_A/m_v and the entropy difference in terms of the corresponding cross ratio r in each case. For Neumann BC, we have set $\omega m_v \sim 10^{-10}$ in both the semi-infinite and finite chains. In the case of Dirichlet BC, we have considered $\omega = 0$, but we checked that introducing a small non-vanishing ω, such that $\omega m_v \sim 10^{-10}$, does not lead to changes that can be observed. The agreement between the lattice data points and the corresponding BCFT predictions is excellent. In the insets of Figure 3.9 we have reported $S_{A;\alpha} - \text{const}$, where the constant value that has been subtracted is given by $\frac{1}{6}\log(2m_v)$ for the semi-infinite chains (left panel) and $\frac{1}{3}\log(2N/\pi)$ for finite chains (right panel).

In Sec. 3.2.2 we have introduced the UV finite quantity (3.77), obtained from (3.15) and (3.14), which depends on the cross-ratio r. Its limit $n \to 1$ is given by the following combination

$$\widehat{\mathcal{I}}^{(1)}_{A;\alpha} = \lim_{n\to 1} \frac{\log\left(r^{\Delta_n} R^{(n)}_A\right)}{1-n} = S^\alpha(A_u) + S^\alpha(A_v) - S^\alpha(A) + \frac{1}{6}\log r \tag{3.102}$$

Our results for this UV finite quantity are reported in Figure 3.10 and Figure 3.11

for Dirichlet BC and Neumann BC respectively. The corresponding BCFT expressions are given by (3.78), which correspond to the dashed lines in these figures. When imposing Dirichlet boundary conditions, we observe a remarkable consistency between the lattice data points and the BCFT prediction, indicating an excellent agreement for this quantity. Instead, a slight discrepancy is found in the case of Neumann BC, which might be due to the zero mode, whose effect we are not able to quantify.

The numerical analysis discussed above allows to evaluate also the corresponding single copy entanglement (1.18) by applying (3.101). The resulting numerical data in the thermodynamic limit can be compared with the BCFT predictions given by (3.80) and (3.79). These comparisons are shown in Figure 3.12 and Figure 3.13 for Dirichlet and Neumann BC respectively (semi-infinite chains and finite chains made by N sites have been considered in the left and right panels respectively). In these figures, the harmonic chain data for $n \to \infty$ have been obtained through (3.101). In particular, by using (3.14), one obtains

$$\lim_{n\to\infty} \frac{\log\left(r^{\Delta_n} R_A^{(n)}\right)}{1-n} = S_\infty^\alpha(A) - S_\infty^\alpha(A_u) - S_\infty^\alpha(A_v) - \frac{1}{12}\log r \tag{3.103}$$

Also in this analysis, we observe an excellent agreement between the lattice data points in the scaling limit and the corresponding BCFT predictions for Dirichlet BC; while in the case of Neumann BC, some discrepancy occurs (see the right panel of Figure 3.13, for small values of r)

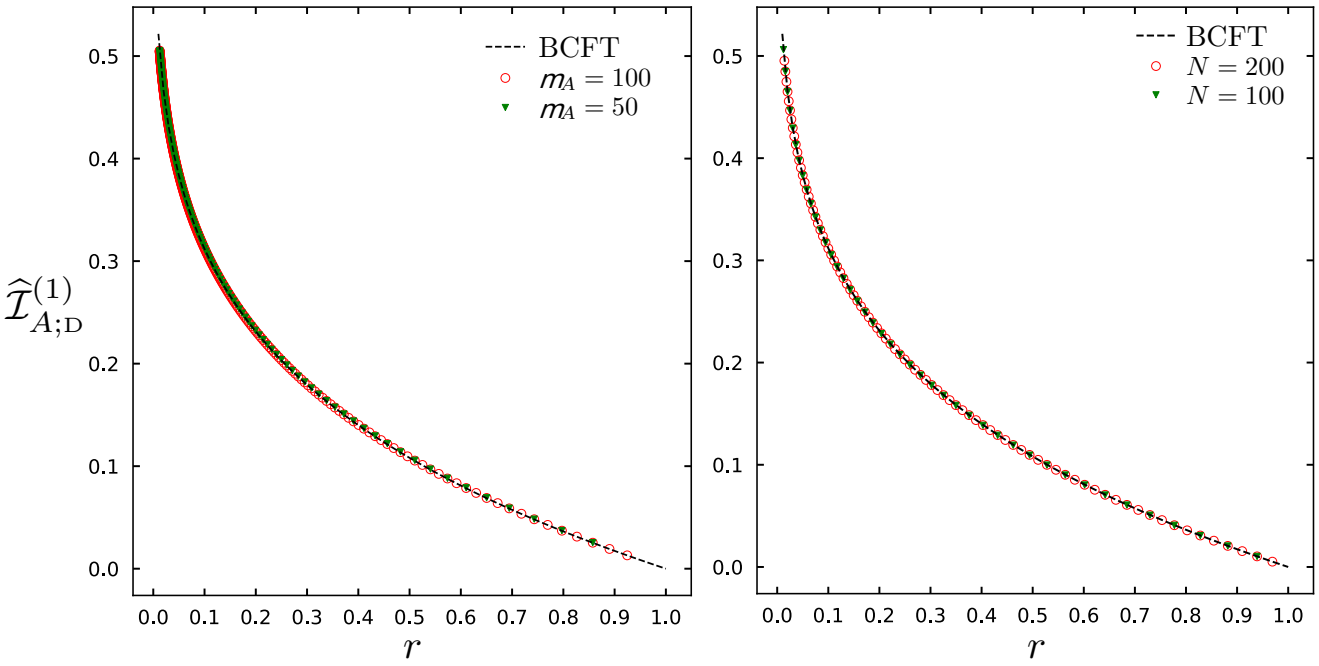

Figure 3.10: The UV finite quantity (3.102) for Dirichlet BC. The dashed curves correspond to the BCFT prediction (3.78). The results for the semi-infinite chains and the finite chains made by N sites are reported in the left and right panels respectively.

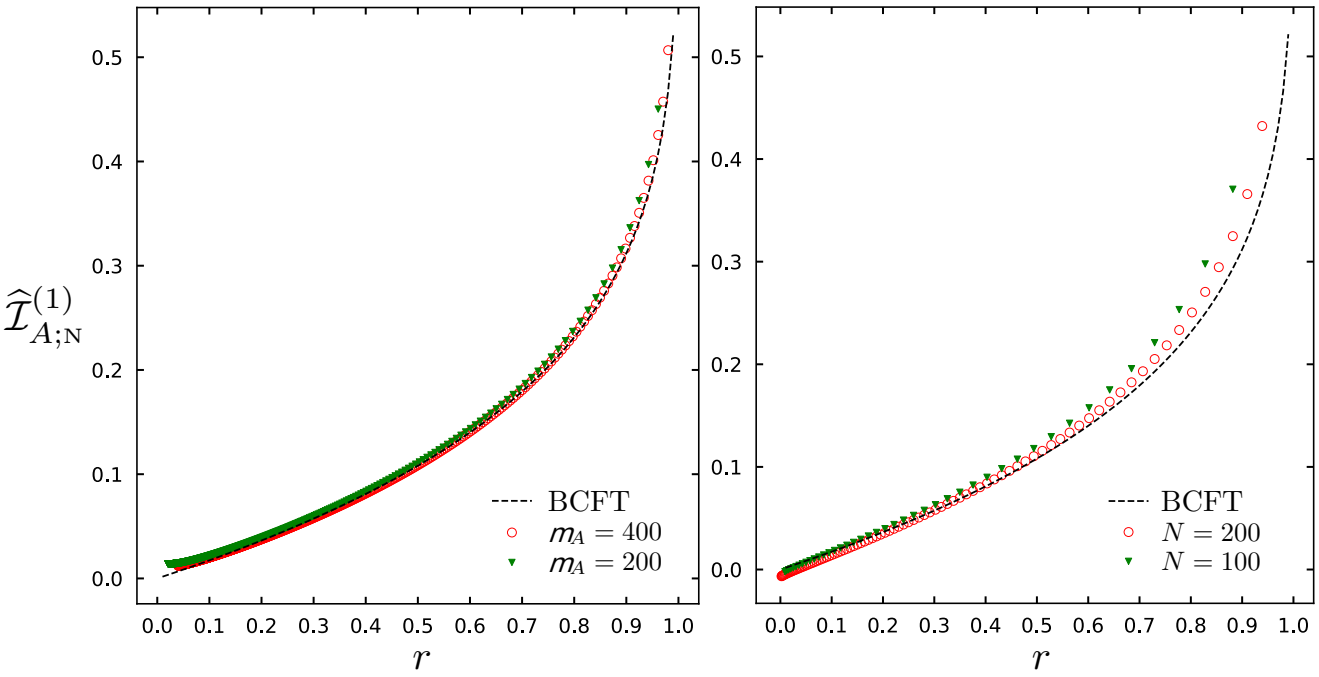

Figure 3.11: The UV finite quantity (3.102) for Neumann BC, with the same notation described in the caption of Figure 3.10.

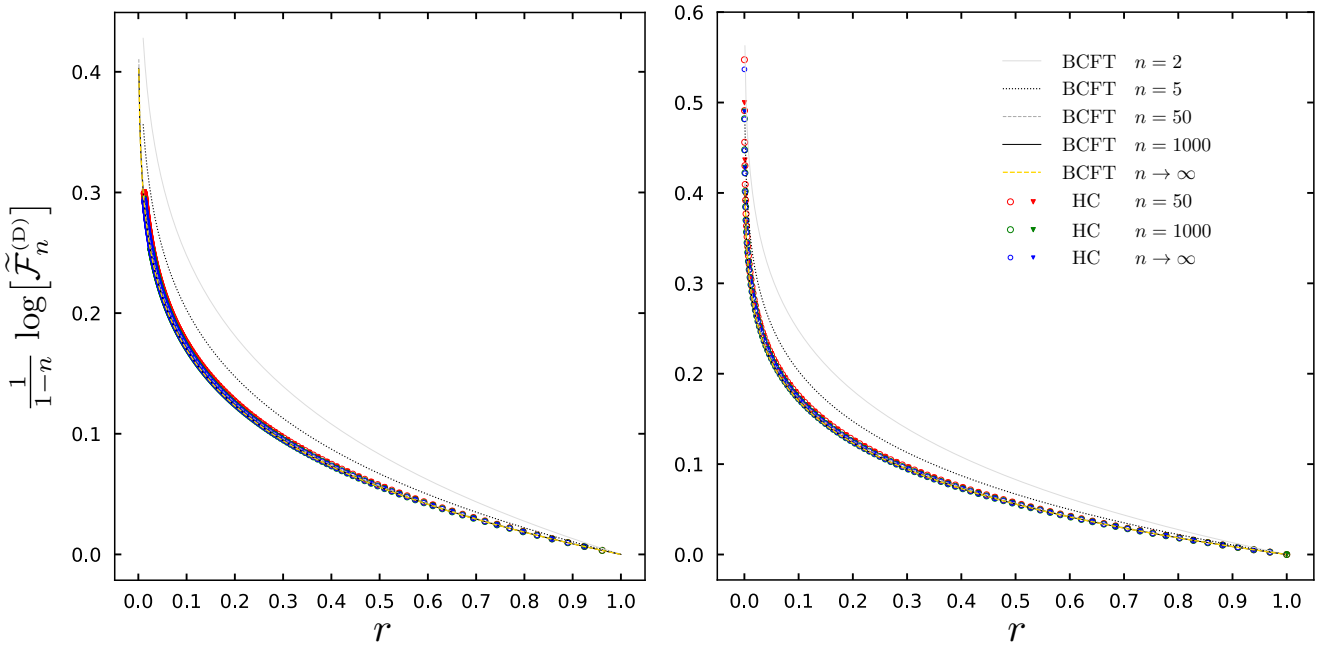

Figure 3.12: Single copy entanglement entropy for the bipartitions in Figure 3.1 (see (3.103)) when Dirichlet BC are imposed. The same harmonic chains of Figure 3.5 have been employed.

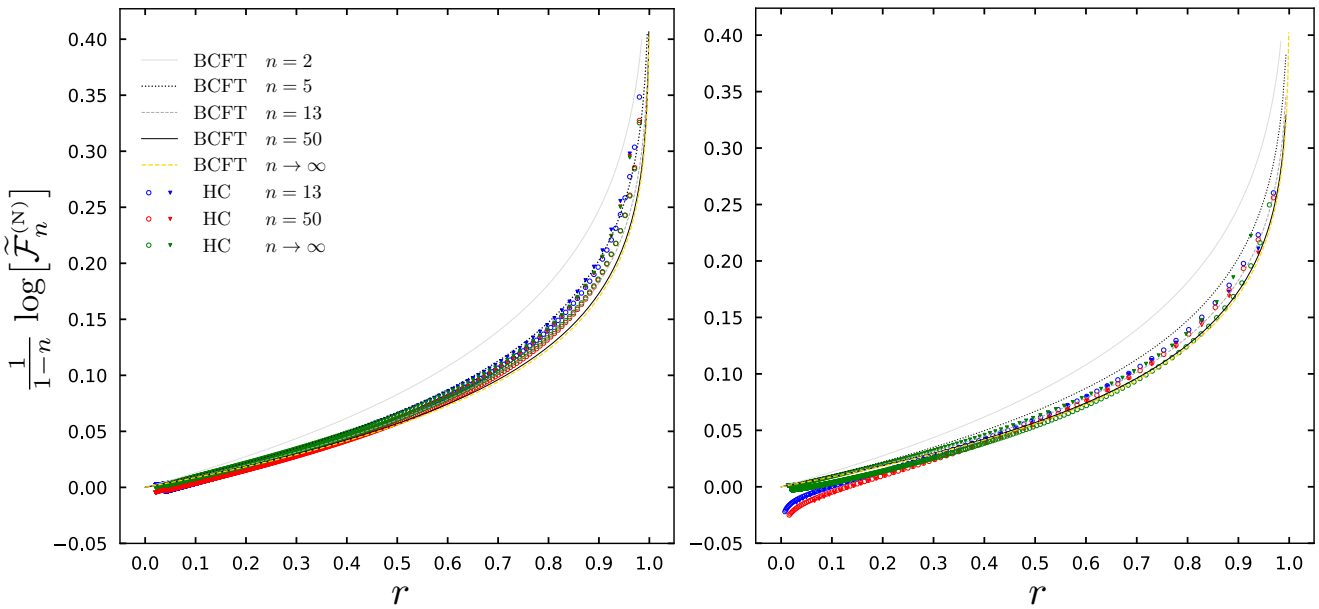

Figure 3.13: Single copy entanglement entropy for the bipartitions in Figure 3.1 (see (3.103)) when Neumann BC are imposed. The same harmonic chains of Figure 3.7 have been employed.

3.4 Conclusions

In this chapter, we have employed CFT techniques to calculate the leading behaviour of entanglement entropies in a critical one-dimensional system belonging to the Luttinger liquid universality class. Specifically, we have examined the scenarios where region A is an interval located on the half line or within a segment that is not adjacent to the system boundary, as depicted in Figure 3.1.

In the case of the segment, the same boundary condition has been imposed at both endpoints. Both Dirichlet and Neumann boundary conditions have been considered. Our main results for the interval in the half line and in the segment are given in (3.11), with the functions $\mathcal{F}_n^{(\alpha)}(r)$ given in (3.23), written in terms of the Siegel theta function and of the period matrix (3.25), which occurs also for the entanglement entropies of two disjoint intervals on the line [71]. Our analysis extends the one performed in [120], whose results are recovered when $n = 2$. Furthermore, we have checked numerically that our analytical expressions are compatible with the implicit results of [166] for the compact boson with Dirichlet boundary conditions.

In the decompactification regime, the analytic expressions found through the BCFT approach of the twist fields method (see Sec. 3.2.2) have been compared with the corresponding numerical results obtained in harmonic chains (see Sec. 3.3) for the bipartitions shown in Figure 3.1. In the case of Dirichlet BC excellent agreement has been found (see Figure 3.5, Figure 3.10 and Figure 3.12), while for Neumann BC some discrepancies occurs (see Figure 3.7, Figure 3.8, Figure 3.11 and Figure 3.13). It is important to note that both the non-compact massless scalar field and the harmonic chain exhibit a zero mode when Neumann boundary conditions are applied. Consequently, they lack a normalizable ground state, requiring the introduction of an infrared cut-off. The discrepancy observed may originate from the method employed to regulate these models. In the case of the harmonic chain, the zero mode was regulated by introducing a small mass, while for the non-compact boson, the zero mode was regulated by compactifying the target space. Finite size corrections in particular are expected to be sensitive to the IR regulator [172]. Also, the UV finite quantity is given by the difference between the entanglement entropy corresponding to different BC has been studied, finding excellent agreement with the numerical lattice data (see Figure 3.9).

Natural extensions of our analysis involving the compact scalar could be performed by considering mixed boundary conditions [173], or non-vanishing temperature for the entire system, or a non vanishing mass [174], or a subsystem made by the union of a generic number of disjoint intervals [88, 175, 176], or spatially inhomogeneous backgrounds [121, 128, 166], or defects [150, 177–180].

Our results can be developed further in various directions. As for the lattice calculations in the harmonic chains discussed in Sec. 3.3, a general issue to address is to find a way to control analytically the effects of the zero mode. In our analysis, this could help to understand the above-mentioned discrepancies between our BCFT expressions and the lattice results when Neumann BC are imposed. We find it worth investigating the spatial bipartitions in Figure 3.1 also in other interesting 1+1 dimensional models like the Ising BCFT [29], interacting BCFT models (see e.g. the Liouville field theory [181, 182]). It may also be interesting to explore further the effect of physical boundaries for other related entanglement quantifiers like the entanglement Hamiltonians and their spectra [109, 183–196] or the logarithmic negativity [163, 197–206].

Chapter 4

Renyi entropies for one-dimensional quantum systems with mixed boundary conditions

4.1 Introduction

In this chapter, we consider the Rényi entanglement entropy in an open system with *mixed boundary conditions*, when the subregion A is a single interval *touching the boundary* – we take the boundary condition (BC) at one end of the chain to be different from the BC at the other end (see Figure 4.1). In the scaling limit, such an open critical system is described by a Boundary Conformal Field Theory (BCFT), with a well-understood [30, 31, 108, 124] correspondence between the chiral Virasoro representations and the *conformal boundary conditions* allowed by the theory, and an algebra of boundary operators that interpolate between them.

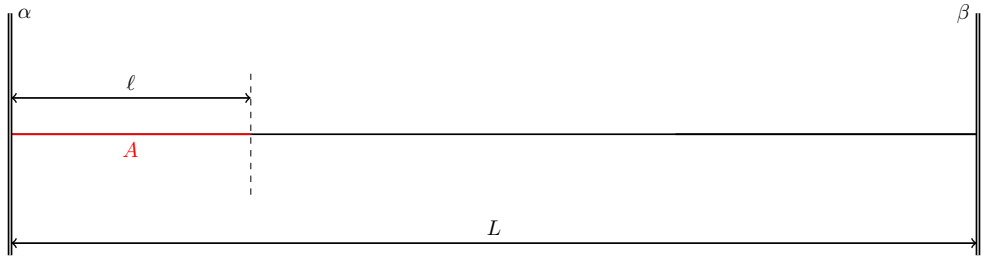

Figure 4.1: An interval of length ℓ in a 1d critical chain with mixed BC ($\alpha\beta$) and length L.

The more accessible setup of an interval touching one of two *identical* boundaries has been thoroughly analysed using either conformal field theory methods [46, 87, 94, 120, 207] or exact free fermion techniques [125, 126, 139]. These analytical studies have been complemented with numerical implementations based on density-matrix renormalization group (DMRG) techniques [96, 111, 208, 209] and other methods [210]. In that setup, the subsystem A is at the end of a finite system with the same boundary condition α on both sides. The computation of the Rényi entanglement entropies rests on the evaluation of a twist one-point function on the upper half-plane. Such a correlation function is straightforwardly fixed by conformal invariance, and as a consequence, the entanglement entropy exhibits a simple dependence on the interval and system sizes. Explicitly, in the case of an interval of length ℓ at the end of a system of size L, one finds the leading universal

behaviour (1.52), derived in [46] . When one studies systems with mixed BC, at the level of the BCFT one has to introduce BCCOs, and thus the corresponding correlators are more complicated. The core idea of this framework is that the singular behaviour associated with the change in boundary conditions can be encoded in the form of operators placed on the boundary, that interpolate between regions of different BC $\alpha \neq \beta$. Thus, to compute the Rényi entropy S_n in this setup, we will evaluate *three-point functions* with one twist operator and two BCCO insertions. Such setups have already been studied for the Ising and XX chains in [94], at the level of the CFT on the replicated surface, and rely on the knowledge of relatively simple closed-form expressions for the $2n$-point correlator of BCCOs on the unit disk for their calculations. However, such knowledge is the exception, rather than the norm, for generic BCFTs.

In this chapter, we present an alternative method to compute such twist correlation functions with mixed BCs, based on the null-vectors of the BCCOs. The most technically demanding part of this framework is finding Ordinary Differential Equations (ODEs) that the correlators satisfy. According to Cardy's doubling trick [108], in the half-plane geometry, the three-point functions of interest obey the same Ward identities as a four-point conformal block with the corresponding operators, where the bulk twist operator $\sigma(z, \bar{z})$ is replaced by the insertion of $\sigma(z)\sigma^{\dagger}(\bar{z})$. Thus, in an adaptation of the method of [118], we can derive a differential equation by combining knowledge of the null-vector conditions obeyed by the twisted and untwisted fields under the symmetry algebra of the cyclic orbifold [119] with the derivation of well-chosen Ward identities obtained from current insertions in the correlators of interest. The final ingredient is the determination of a subset of the (bulk and boundary) structure constants of the cyclic orbifold BCFT, which fix the specific linear combination of solutions of the differential equation that gives the sought correlator.

We have illustrated this approach with a variety of BCFT setups, that share a common assumption: in the mother CFT, the mixed boundary conditions $(\alpha\beta)$ are implemented by a BCCO which is degenerate at level two under the Virasoro algebra.

We provide here the outline of the chapter. In Section 4.2, we give a more concrete description of our setup and a summary of the analytical results obtained in this work. Section 4.3 contains a comparison of our BCFT results with lattice data, for both the Ising and three-state Potts critical chains. In Section 4.4 we review some elements of the cyclic orbifold construction, with a focus on its implementation on the upper-half plane. We discuss in this section the bulk and boundary operator algebra and show how some orbifold bulk and boundary structure constants can be expressed in terms of mother BCFT quantities by unfolding and factorizing arguments. We dedicate Section 4.5 to the derivation of ODEs for the different setups described above. On top of the announced derivations involving orbifold Ward identities, we also use the results on the fusion rules of the $\mathbb{Z}_n$ cyclic orbifold of [211] and some mathematical facts about the hypergeometric differential equation, to derive low-order differential equations for the Ising case. Finally, we have relegated the more technical derivations to the Appendix, to avoid congesting the logical flow of the paper.

4.2 Setup and summary of analytic results

We consider a quantum system at criticality on an open chain of size L, whose universal properties are captured by a two-dimensional boundary conformal field theory (BCFT). The left and right sides of the system are governed by conformal boundary conditions denoted as α and β respectively. Our objective is to evaluate the entanglement entropy of the ground state between the interval $A = [0, \ell]$ and the remaining part of the system $B = [\ell, L]$, as depicted in Figure 4.1.

In the thermodynamic limit[1] the n^{th} Rényi entropy $S_n(\ell)$ is given (up to a non-universal additive constant), by a correlation function of twist fields σ[46] :

$$S_n(l) = \frac{1}{1-n} \log\langle\sigma(w,\bar{w})\rangle^{(\alpha\beta)}_{\mathbb{S}_L}, \qquad w = \bar{w} = \ell \tag{4.1}$$

where $\mathbb{S}_L$ denote the infinite strip (with imaginary time running along the imaginary axis)

$$\mathbb{S}_L = \{w \in \mathbb{C},\ 0 < \mathrm{Re}(w) < L\} \tag{4.2}$$

with boundary condition (α, β) on both sides of the strip. When $\alpha = \beta$, the result is well known [46] and is given by (1.52). At the CFT level, having the same boundary condition $\alpha = \beta$ at both ends of the chain implies that the ground state is conformally trivial, in the sense that its image under the state-operator correspondence is the boundary identity operator. That is to say, the ground state is the highest weight state $|\psi_{11}\rangle$ with conformal dimension $h_{11} = 0$. Upon mapping to the upper half plane $\mathbb{H}$ via the map $z : \mathbb{S}_L \to \mathbb{H}$

$$z(w) = -e^{-\frac{i\pi w}{L}} = e^{\frac{i\pi(L-w)}{L}} \tag{4.3}$$

computing the entanglement entropy boils down to the evaluation of a one-point function

$$\langle\sigma(w,\bar{w})\rangle^{(\alpha\alpha)}_{\mathbb{S}_L} = \langle\Psi_{11}|\,\sigma(\ell)\,|\Psi_{11}\rangle^{(\alpha\alpha)}_{\mathbb{S}_L} = \left|\frac{\pi}{L}z\right|^{2h_\sigma} \langle\sigma\,(z,\bar{z})\rangle^{\alpha}_{\mathbb{H}} \tag{4.4}$$

from which one easily recovers (1.52). However, when distinct boundary conditions are employed, the ground state is no longer trivial. In this case, it is mapped, under the state-operator correspondence, to a BCCO $\Psi^{\alpha\beta}$ that interpolates between these distinct boundary conditions. Consequently, one has to evaluate a three-point function instead

$$\langle\sigma(w,\bar{w})\rangle^{(\alpha\beta)}_{\mathbb{S}_L} = \langle\Psi^{(\alpha\beta)}|\,\sigma(w,\bar{w})\,|\Psi^{(\alpha\beta)}\rangle_{\mathbb{S}_L} = \left|\frac{\pi}{L}z\right|^{2h_\sigma} \left\langle\Psi^{(\beta\alpha)}(\infty)\sigma\,(z,\bar{z})\,\Psi^{(\alpha\beta)}(0)\right\rangle_{\mathbb{H}} \tag{4.5}$$

Furthermore the CFT correlation function $\langle\sigma(w,\bar{w})\rangle^{(\alpha\beta)}_{\mathbb{S}_L}$ captures only the leading asymptotic behaviour of the entanglement entropy as the system size tends to infinity [118]. When comparing with a finite-size system, one needs to consider various sources of corrections originating from irrelevant deformations of the Hamiltonian in both the bulk and the boundary [144, 145]. Additionally, one should generally be concerned about parity effects [146]. The most significant corrections arise from the subleading scaling of the lattice twist operators [118].

[1] meaning $L, \ell \gg 1$, keeping $0 < \ell/L < 1$.

Similar to any other lattice operator, the lattice twist operator $\hat{\sigma}$ can be expressed, in the continuum limit, as a local combination of scaling operators [73, 74]

$$\hat{\sigma} \sim \sum_j c_n^j \epsilon^{2h_{\sigma_j}} \sigma_j \tag{4.6}$$

where $\epsilon \to 0$ is an ultraviolet cut-off such as *e.g.* the lattice spacing. The constants c_n^j are non-universal, dimensionful amplitudes, and the sum contains an infinite series of contributions from increasingly irrelevant operators. The leading operator is the bare twist field σ, which is primary with respect to the orbifold symmetry algebra $OVir \otimes O\bar{V}ir$. We shall denote its corresponding non-universal amplitude $c_n^{\mathbf{1}} \equiv c_n$ for brevity. The subleading contributions consist of its descendants with respect to this algebra, as well as the *composite* or excited twist fields σ_j [118, 149] and their descendants.

It is well known [94, 212] that for open systems, the finite-size corrections to the leading CFT prediction for the entanglement entropy are much more severe than for a periodic chain. To reproduce numerical data, it is crucial to identify and compute the leading finite-size correction, that is correlation functions involving excited twist fields

$$\langle \sigma_j(w,\bar{w}) \rangle_{S_L}^{(\alpha\beta)} = \left|\frac{\pi}{L} z\right|^{2h_{\sigma_j}} \left\langle \Psi^{(\beta\alpha)}(\infty) \sigma_j(z,\bar{z})\, \Psi^{(\alpha\beta)}(0) \right\rangle_{\mathbb{H}} \tag{4.7}$$

Let us now present a summary of the results obtained in this approach.

Summary of results

The main results of this chapter pertain to the second and third Rényi entropies, under a specific scenario where the boundary conditions (α, β) are chosen in such a way that the ground state of the mother BCFT of central charge:

$$c = 1 - \frac{6(1-g)^2}{g} \tag{4.8}$$

corresponds to $|\psi_{12}\rangle$, characterized by a conformal dimension $h_{12} = (3g-2)/4$. As a consequence, $|\psi_{12}\rangle$ possesses a null-vector at level 2, enabling us to establish an ordinary differential equation that governs the *orbifold* correlation function

$$\left\langle \Psi_{12}^{(\beta\alpha)}(\infty) \sigma_j(z,\bar{z})\, \Psi_{12}^{(\alpha\beta)}(0) \right\rangle_{\mathbb{H}} \tag{4.9}$$

for a primary excited twist field σ_j. Such differential equations can be solved analytically in some cases (see Section 4.5), but if closed-form solutions are not available one can always employ series methods (as explained in Appendix C.7). The solutions can then be used to determine (4.9) as detailed in Section 4.5.

In the $\mathbb{Z}_2$ orbifold of a generic BCFT, we have derived a second-order and a fourth-order ODE, respectively for the *bare* and *composite*[2] twist correlator. In the $\mathbb{Z}_3$ orbifold of a generic BCFT, we have determined a third-order ODE for the bare twist correlator. We have also worked out, for the case of the $\mathbb{Z}_2$ and $\mathbb{Z}_3$ cyclic orbifolds of the Ising BCFT, a variety of lower-order ODEs. All these ODEs are presented and derived in Section 5.

[2] obtained by fusing the bare twist operator with an untwisted operator ϕ.

Exact results for the $\mathbb{Z}_2$ orbifold

We have obtained an exact result[3] for the leading BCFT contribution to the *second* Rényi entropy, which applies to any critical system described by a BCFT based on a minimal model $\mathcal{M}(p,p')$ with mixed conformal BC (α,β) chosen such that the most relevant BCCO interpolating between them is $\psi_{12}^{(\alpha\beta)}$:

$$\boxed{S_2^{\alpha\beta}([0,\ell]) = \frac{c}{8}\log\frac{2L}{\pi\epsilon}\sin\left(\frac{\pi\ell}{L}\right) - \log F_2^{(\alpha\beta)}(\ell/L)} \tag{4.10}$$

where

$$F_2^{(\alpha\beta)}(\ell/L) = \frac{1}{g_\alpha}G_g(\ell/L) + \frac{1}{g_\beta}G_g((L-\ell)/L) \tag{4.11}$$

and G_g does not depend on the boundary conditions and is given by

$$G_g(\ell/L) = \frac{\sin 2\pi g}{\sin 3\pi g}\left(I_g\left(-\cos\frac{\pi\ell}{L}\right) + 2\cos\pi g\, I_g\left(\cos\frac{\pi\ell}{L}\right)\right) \tag{4.12}$$

with

$$I_g(x) = \left(\frac{1+x}{2}\right)^{2g-1} {}_2\mathrm{F}_1\left(g, 1-g; 2-2g\middle|\frac{1-x}{2}\right) \tag{4.13}$$

is essentially a Legendre function of the first kind. This expression depends in a very simple way on the boundary conditions α and β via the terms g_α and g_β, and is manifestly invariant under exchanging $\alpha \leftrightarrow \beta$ and $\ell \to L-\ell$. For $g \geq 1/2$, the function G_g interpolates smoothly between $G_g(0) = 1$ and $G_g(1) = 0$, making manifest that the first term in (4.11) dominates the small ℓ behaviour, while the second term controls the $\ell \to L$ asymptotic. To put it differently, $F_2^{(\alpha\beta)}(\ell/L)$ interpolates between its extremal values

$$F_2^{(\alpha\beta)}(0) = \frac{1}{g_\alpha}, \qquad \text{and} \qquad F_2^{(\alpha\beta)}(1) = \frac{1}{g_\beta}\,. \tag{4.14}$$

It is interesting to check that the theoretical prediction for this kind of mixed BC has the expected behaviour as the twist operator approaches the α and β boundaries. We remind that the second Rényi entropy of an interval ℓ touching one of the *identical* boundaries of a finite system of size L is given by:

$$S_2^{\gamma}([0,\ell]) = \frac{c}{8}\log\left[\frac{2L}{\pi\epsilon}\sin\left(\frac{\pi\ell}{L}\right)\right] + \log g_\gamma \tag{4.15}$$

In the limits $\ell \to 0$ and $\ell \to L$ the effect of the boundary β and respectively, α is suppressed. In consequence, we expect that this asymptotic behaviour is captured by (4.15) with $\gamma = \alpha$ and $\gamma = \beta$, correspondingly.

To illustrate this result, we have plotted in Figure 4.2 the Rényi entropy $S_2^{\alpha\beta}$ shifted by $\frac{c}{8}\log L$ for different choices of mixed *BC* in the *A*-series minimal model $\mathcal{M}(10,9)$. We remind that in such BCFTs, the conformal BC are in one-to-one correspondence with the primary fields ϕ_{rs} of the theory, and thus it is convenient to label them as $\alpha \equiv (r,s)$

[3] up to the usual non-universal additive constant

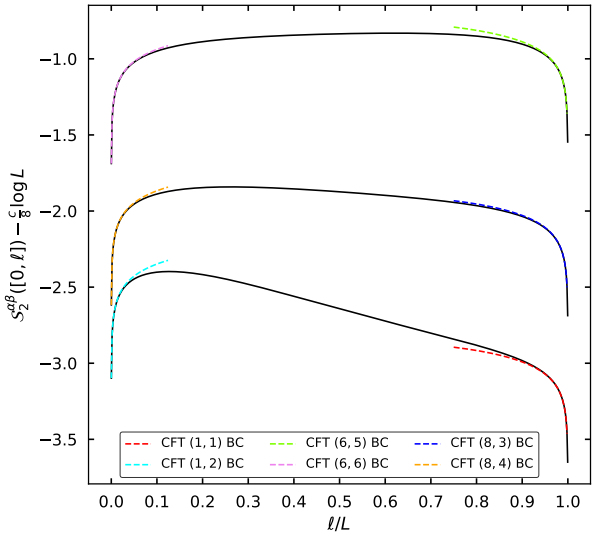

Figure 4.2: Shifted second Rényi entropies for the mixed BC setups $((1,2),(1,1))$, $((6,6),(6,5))$ and $((8,4),(8,3))$ for the BCFTs based on $\mathcal{M}(10,9)$. The black curves denote the mixed BC prediction interpolating between the identical BC results in each case.

Furthermore, we've found that for a subset of these pairs of conformal BCs (α,β) in a generic minimal model $\mathcal{M}(p,p')$, the expressions in (4.10) gains interesting features. At the level of the mother BCFT, this is the case whenever the operator $\psi_{13}^{(\beta\beta)}$ is not allowed in the theory. For BCFTs based on A-series minimal models $\mathcal{M}(p,p')$, this holds for any pair of mixed conformal BCs $(\alpha,\beta) \equiv ((r,2),(r,1))$, labelled by bulk primary fields with $1 \leq r < p$. In this case, the following relation holds for their corresponding ground state degeneracies

$$1 + 2\cos(\pi g)\frac{g_{(r,2)}}{g_{(r,1)}} = 0 \tag{4.16}$$

and the function $F_2^{(\alpha\beta)}$ simplifies into

$$F_2^{((r,2)(r,1))}\left(\frac{\ell}{L}\right) = \frac{1}{g_{(r,2)}}(-2\cos\pi g)\, I_g\left(\cos\frac{\pi l}{L}\right) \tag{4.17}$$

Consider now the *difference* in second Rényi entropies between two mixed BC setups $((r,2),(r,1))$ and $((r',2),(r',1))$ for the *same* bulk CFT. We then find the following universal result:

$$\boxed{\Delta S_2 = S_2^{((r',2),(r',1))} - S_2^{((r,2),(r,1))} = \log\frac{g_{(r,2)}}{g_{(r',2)}} = \log\frac{g_{(r,1)}}{g_{(r',1)}}} \tag{4.18}$$

where the latter equation follows from the expression of $g_{(r,s)} = S_{(r,s),(r_0,s_0)}/\sqrt{S_{(1,1),(r_0,s_0)}}$ [32] in terms of S-matrix elements of minimal models [23] - here (r_0,s_0) denote the Kac label of the field with the lowest conformal dimension of the *diagonal* bulk CFT. In particular, for unitary minimal models $(r_0,s_0) = (1,1)$.

We illustrate these ideas graphically for the A-series minimal model $\mathcal{M}(6,5)$ in Figure 4.3, by plotting the second Rényi entropies shifted by $\frac{c}{8}\log L$ for two mixed BC setups $((1,2),(1,1))$ and $((3,2),(3,1))$, together with the relevant identical BC setups for each case.

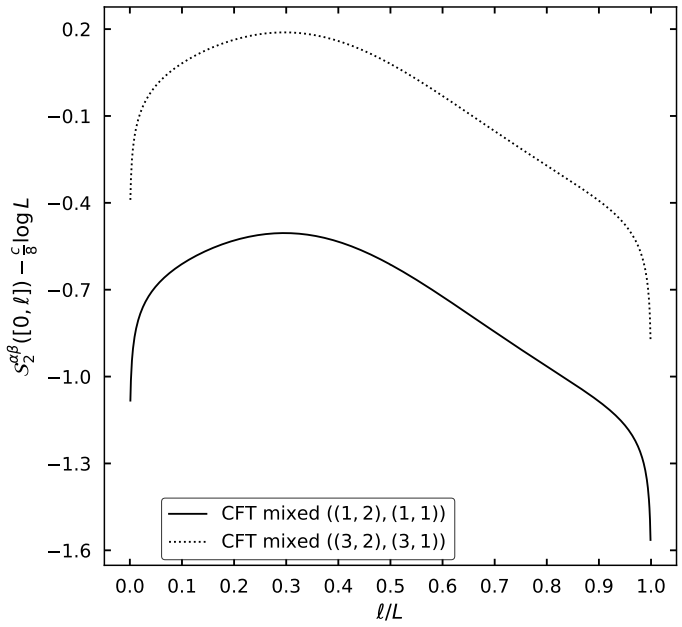

Figure 4.3: Shifted second Rényi entropies for the mixed BC setups $((1,2),(1,1))$ and $((3,2),(3,1))$ for the BCFTs based on $\mathcal{M}(6,5)$. The difference between the two curves is constant with respect to the interval size, and thus fixed by their respective asymptotic behaviours around $\ell \to 0$ and $\ell \to L$

4.3 Numerical results and finite-size corrections in quantum chains

To provide an independent appraisal of the validity of our CFT results, we have performed a numerical analysis on the Ising and three-state Potts open quantum chains for different settings of mixed BC. Once finite-size effects are properly accounted for, the validity of the CFT results becomes apparent.

We should note that the Rényi entropies in the Ising case have already been obtained, for generic n in the work of [94], through a different approach. We found that our analytical calculations (for $n = 2, 3$) are compatible with their results.

Furthermore, by studying the finite-size corrections to their result, we manage to quantitatively understand the deviation of the chain data from the leading CFT prediction in the DMRG numerical analysis of [94], even for relatively large system sizes $M \sim 10^2$ sites. Thus, when the subleading CFT contribution to the Rényi entropy is taken into account, as our analysis shall show, the agreement with the lattice data is excellent, even for the small system sizes $M \sim 26$ sites accessible to exact diagonalization.

4.3.1 The Ising quantum chain with mixed BC

The Hamiltonian of the Ising quantum chain with open BC, describing M spins with generic BC at the boundary, is given by:

$$H_{\alpha\beta} = -\sum_{j=1}^{M-1} s_j^z s_{j+1}^z - h \sum_{j=1}^{M} s_j^x - h_\alpha s_1^z - h_\beta s_M^z \,, \tag{4.19}$$

where $s_j^{x,y,z}$ denote Pauli spin operators acting non-trivially at site j, and as identity at all the other sites. We denote the lattice spacing by ϵ, so that the length of the chain is $L = M\epsilon$. The parameters h_α, h_β denote external fields (in the z direction) acting at the boundary sites $j = 1$ and $j = M$. The ground state of this Hamiltonian is then found by *exact diagonalization* (ED) for system sizes $M \leq 26$ sites, and from it, the Rényi entropies are extracted.

To take the *scaling limit* of the critical chain, we send $M \to \infty, \epsilon \to 0$ while keeping L fixed. In this limit, criticality is achieved in the bulk for $h = 1$, while each boundary admits three *critical points* $h_\alpha, h_\beta \in \{0, \pm\infty\}$.

From a CFT perspective, the scaling limit of the critical Ising chain with open boundaries is very well understood. It is described by the BCFT with central charge $c = 1/2$ and a bulk operator spectrum consisting of three primary operators – the identity $\mathbf{1}$ ($h_{\mathbf{1}} = 0$), energy ε ($h_\varepsilon = 0$) and spin operators s ($h_s = 1/16$)– and their descendants [23]. The three boundary critical points correspond to the three conformal boundary conditions for the Ising BCFT, which, in the framework of radial quantization on the annulus, allow the construction of the following physical boundary states [23, 108]:

$$|f\rangle = |\mathbf{1}\rangle\!\rangle - |\epsilon\rangle\!\rangle \qquad \textit{(free BC)}\,, \tag{4.20}$$

$$|\pm\rangle = \frac{1}{\sqrt{2}}|\mathbf{1}\rangle\!\rangle + \frac{1}{\sqrt{2}}|\epsilon\rangle\!\rangle \pm \frac{1}{2^{1/4}}|s\rangle\!\rangle \qquad \textit{(fixed BC)}\,, \tag{4.21}$$

where $|i\rangle\!\rangle$ denotes the Ishibashi state [108][140] corresponding to the primary operator i. The physical boundary states $|\alpha\rangle$ are in one-to-one correspondence with the primary fields of the bulk CFT [4]: $|f\rangle \leftrightarrow s$ and $|\pm\rangle \leftrightarrow \mathbf{1}/\varepsilon$. The boundary fields that interpolate between two conformal BCs can be inferred from this correspondence, as shown in [108],[130]. Thus, the spectrum of primary boundary fields $\psi_i^{(\alpha\beta)}$ of the Ising BCFT is the one of Table 4.1.

$(\alpha\beta)$	$+$	$-$	f
$+$	$\psi_{\mathbf{1}}$	ψ_ε	ψ_s
$-$	ψ_ε	$\psi_{\mathbf{1}}$	ψ_s
f	ψ_s	ψ_s	$\psi_{\mathbf{1}}, \psi_\varepsilon$

Table 4.1: Boundary operator spectrum of the Ising BCFT

On the discrete side, we are calculating the one-point correlator of the *lattice twist operator* $\hat{\sigma}(m,t)$, where (m,t) are square-lattice coordinates. In the scaling limit with $\epsilon \to 0$, $\hat{\sigma}(m,t)$ admits a *local* expansion into scaling operators of the corresponding orbifold CFT. The two most *relevant* terms in this expansion are:

$$\hat{\sigma}(m,t) = c_n\, \epsilon^{2h_\sigma} \sigma_{\mathbf{1}}(w,\bar{w}) + c_n^\varepsilon\, \epsilon^{2h_{\sigma_\varepsilon}} \sigma_\varepsilon(w,\bar{w}) + \text{less relevant terms}\,, \tag{4.22}$$

[4] This statement is strictly true if the bulk CFT is diagonal, see [213] for a detailed discussion.

with the composite twist operator σ_ε defined in (4.49) and $h_{\sigma_\varepsilon} = h_\sigma + h_\varepsilon/n$. The integers (m, t) parametrize the lattice, and they are related to the continuum coordinate on the strip as $w = (m + it)\epsilon$, $\bar{w} = (m - it)\epsilon$. We can take advantage of the translation invariance in the t direction to fix the "time" coordinate of the lattice twist operators to be $t = 0$. We will then denote their continuum coordinate by $\ell = m\epsilon$.

The amplitudes c_n and c_n^ε in (4.22) are not universal quantities, so we cannot determine them by CFT techniques. However, they are also independent of the global properties of the system (e.g. choice of BC) so they can be found from a numerical analysis of the infinite Ising chain. Here one can employ the free fermion techniques of [148] and the well-known analytical results for the Rényi entropy of an interval in an infinite system [46, 214] to fit for the values[5]

We can now express the lattice one-point twist correlator with generic mixed BC as an expansion of CFT correlators:

$$\langle \hat{\sigma}(m,0)\rangle^{\alpha\beta} = c_n \epsilon^{2h_\sigma} \langle \sigma(\ell,\ell)\rangle^{\alpha\beta}_{\mathbb{S}_L} + c_n^\varepsilon \epsilon^{2h_{\sigma_\varepsilon}} \langle \sigma_\varepsilon(\ell,\ell)\rangle^{\alpha\beta}_{\mathbb{S}_L} + \dots \tag{4.23}$$

Using the map (4.3), we can make the dependence on system size in (4.23) explicit:

$$\langle \hat{\sigma}(m,0)\rangle^{\alpha\beta} = c_n \left(\frac{M}{\pi}\right)^{-2h_\sigma} \langle \sigma(z,\bar{z})\rangle^{\alpha\beta}_{\mathbb{H}} + c_n^\varepsilon \left(\frac{M}{\pi}\right)^{-2h_{\sigma_\varepsilon}} \langle \sigma_\varepsilon(z,\bar{z})\rangle^{\alpha\beta}_{\mathbb{H}} + \dots \tag{4.24}$$

where $z = \exp(i\pi(L-\ell)/L), \bar{z} = \exp(-i\pi(L-\ell)/L)$. In our computational setup, the system sizes accessible through exact diagonalization are limited to $M \leq 26$ and, since twist operators are placed *between lattice sites*, we have only considered even system sizes.

With system sizes of this order of magnitude, finite-size corrections are quite strong. The most relevant corrections we have found arise from the subleading scaling of the lattice twist operator, given in equation (4.24). The relative scaling of the subleading term with respect to the leading one is $O\left(M^{-2h_\epsilon/n}\right)$. Finite-size corrections of this magnitude can be suppressed only with much larger system sizes $M \sim 10^3$ sites, as shown in [120] . Since we do not have access, numerically, to system sizes large enough to suppress these corrections, we had to take into account the first two terms in the expansion of (4.24) to find a good agreement with the lattice data. Furthermore, as the work of [94] suggests, the finite-size effects are still important, even at the much larger system sizes $M \sim 100$ sites accessible through DMRG methods. We mention that such subleading contributions to the lattice twist operator, which have been identified here from the operator spectrum of the $\mathbb{Z}_2$ cyclic orbifold, have previously been understood, through the path integral formalism on the corresponding replicated surface, under the name of "unusual corrections" [144, 145].

We give now the results in the $\mathbb{Z}_2$ orbifold for the correlators appearing in the expansion (4.23), for *mixed fixed* BC with $\alpha = +$, $\beta = -$ (calculated in Appendix

[5] Alternately, one could have used the exact result of [215] for c_n in the periodic Ising chain, to fit only for the non-universal constant c_n^ε

C.4) and mixed free-fixed BC with $\alpha = +$ and $\beta = f$:

$$\begin{aligned}
\langle\sigma_1(\ell,\ell)\rangle^{+-}_{\mathbb{S}_L} &= 2^{-5/2}\left(\frac{2L}{\pi}\right)^{-1/16}\frac{7+\cos\frac{2\pi\ell}{L}}{\left(\sin\frac{\pi\ell}{L}\right)^{1/16}}\,,\\
\langle\sigma_\varepsilon(\ell,\ell)\rangle^{+-}_{\mathbb{S}_L} &= 2^{-5/2}\left(\frac{2L}{\pi}\right)^{-9/16}\frac{1-9\cos\frac{2\pi\ell}{L}}{\left(\sin\frac{\pi\ell}{L}\right)^{9/16}}\,,\\
\langle\sigma_1(\ell,\ell)\rangle^{+f}_{\mathbb{S}_L} &= 2^{1/2}\left(\frac{2L}{\pi}\right)^{-1/16}\frac{\cos\frac{\pi\ell}{4L}}{\left(\sin\frac{\pi\ell}{L}\right)^{1/16}}\,,\\
\langle\sigma_\varepsilon(\ell,\ell)\rangle^{+f}_{\mathbb{S}_L} &= -2^{1/2}\left(\frac{2L}{\pi}\right)^{-9/16}\frac{\cos\frac{3\pi\ell}{4L}}{\left(\sin\frac{\pi\ell}{L}\right)^{9/16}}\,,
\end{aligned} \tag{4.25}$$

where the interval ℓ starts at the $\alpha = +$ boundary. The expressions for the bare twist correlators are in accord with the equivalent results obtained in [94].

With this mention, we show in Figure 4.4 the remarkable agreement between our CFT calculations for the two terms contributing to the second Rényi entropy $S_2^{\alpha\beta} = -\log\langle\hat{\sigma}(m,0)\rangle^{(\alpha\beta)}$ of the interval $[0,m]$ on the lattice, and the numerical results for the critical Ising chain from the exact diagonalization of the Hamiltonian. Figure 4.4a illustrates the case of different ($\pm$) fixed BC on the two sides of the chain, while Figure 4.4b corresponds to letting the $m = 0$ site free and applying a magnetic field at the boundary site $m = M - 1$.

To illustrate the large amplitude of finite-size effects, we show in Figure 4.5 how the CFT prediction fares against the lattice results with and without the incorporation of the subleading term. Even for the curve including both subleading and leading terms in (4.24), the agreement with lattice data is not perfect close to the boundary. This can be traced to the presence of corrections from *descendants* of twist operators, which introduce terms of $O(M^{-h_\epsilon-1})$ relative to the bare twist contribution.

We can repeat the same kind of analysis for the third Rényi entropy, related to the $\mathbb{Z}_3$-orbifold one-point function by $S_3^{\alpha\beta} = -\frac{1}{2}\log\langle\hat{\sigma}(m,0)\rangle^{(\alpha\beta)}$. The Ising orbifold correlators in this case are given by:

$$\begin{aligned}
\langle\sigma_1(\ell,\ell)\rangle^{+-}_{\mathbb{S}_L} &= 3^{-2}\left(\frac{2L}{\pi}\right)^{-1/9}\frac{7+2\cos\frac{2\pi\ell}{L}}{\left(\sin\frac{\pi\ell}{L}\right)^{1/9}}\,,\\
\langle\sigma_\varepsilon(\ell,\ell)\rangle^{+-}_{\mathbb{S}_L} &= 3^{-2}\left(\frac{2L}{\pi}\right)^{-4/9}\frac{1+8\cos\frac{2\pi\ell}{L}}{\left(\sin\frac{\pi\ell}{L}\right)^{4/9}}\,,\\
\langle\sigma_1(\ell,\ell)\rangle^{+f}_{\mathbb{S}_L} &= 2\left(\frac{2L}{\pi}\right)^{-1/9}\frac{\cos\frac{\pi\ell}{3L}}{\left(\sin\frac{\pi\ell}{L}\right)^{1/9}}\,,\\
\langle\sigma_1(\ell,\ell)\rangle^{+f}_{\mathbb{S}_L} &= 2^{1/9}\left(\frac{2L}{\pi}\right)^{-4/9}\frac{\cos\frac{2\pi\ell}{3L}}{\left(\sin\frac{\pi\ell}{L}\right)^{4/9}}\,.
\end{aligned} \tag{4.26}$$

In Figure 4.6, we once again compare our CFT calculations (including both the leading and subleading term) with the critical chain results for the third Rényi entropy $S_3^{\alpha\beta}$, to good agreement for mixed fixed BC (Fig. 4.6a) and mixed free fixed

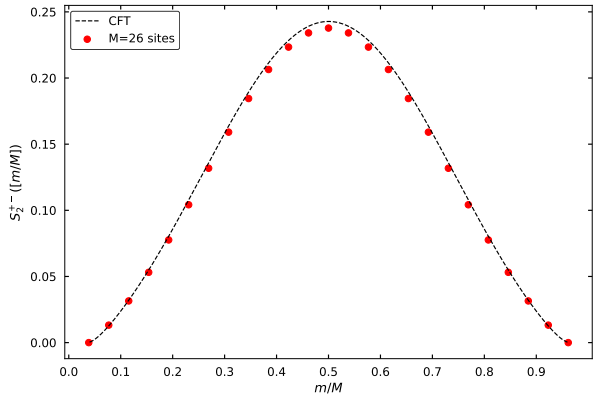

(a) Fixed mixed BC

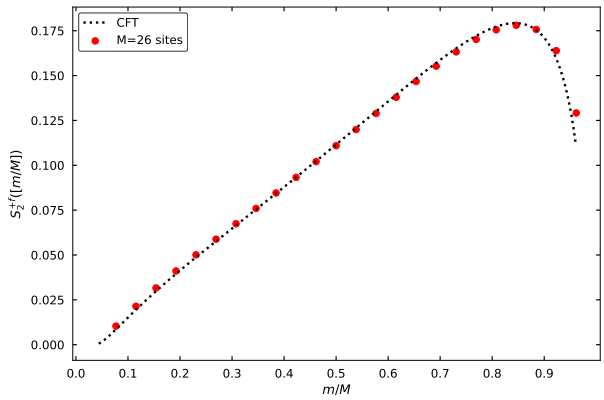

(b) Fixed-free mixed BC

Figure 4.4: Plots of the second Rényi entropy $S_2^{\alpha\beta}([m/M])$ in the critical Ising chain with two types of mixed BC for a chain of size $M = 26$. The interval is grown from the $\alpha = +$ boundary. We stress that the CFT prediction contains both the leading and subleading BCFT contributions to $S_2^{\alpha\beta}([m/M])$

BC (Fig. 4.6b). As for the $\mathbb{Z}_2$ results, including the CFT subleading contribution to $S_3^{\alpha\beta}$ is necessary to find a satisfying match with the lattice results. Further finite-size corrections in this case decay as $O\left(M^{-\frac{2h_\varepsilon}{3}-1}\right)$.

As advertised at the beginning of the section, our results for the bare twist correlators (for all configurations of mixed BC) are compatible with the ones of [94]. The subleading contribution to the Rényi entropies from the excited twist correlator is largely responsible for the mismatch between the lattice and CFT data in the aforementioned article.

4.3.2 The three-state Potts quantum chain with mixed BC

A natural extension of the Ising chain, the three-state Potts model allows the spins at each site to take one of three possible values $\{R, G, B\}$, which we can also conveniently parametrize by third roots of unity $\{1, \omega, \bar{\omega}\}$, with $\omega = \exp(2\pi i/3)$. The Hamiltonian of the three-state Potts model, tuned to its bulk critical point

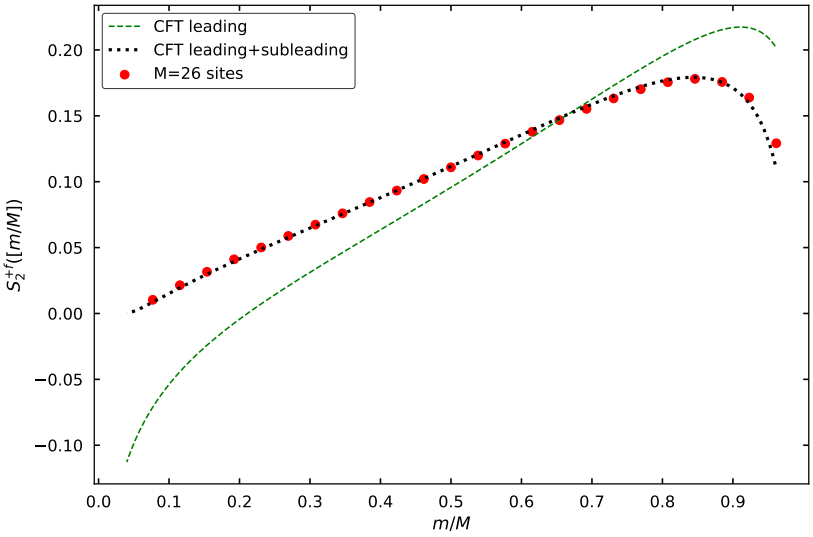

Figure 4.5: Comparison of the second Rényi entropy in the critical Ising chain of size $M = 26$ with mixed free fixed BC with CFT results. Inclusion of the subleading term in the expansion 4.24 is crucial for obtaining a satisfying agreement with lattice data

[216][217],[14] is given by:

$$H_{\alpha\beta} = -\zeta\left[\sum_{j=1}^{M-1}\left(Z_j Z_{j+1}^{\dagger} + Z_j^{\dagger} Z_{j+1}\right) + \sum_{j=2}^{M-1}\left(X_j + X_j^{\dagger}\right) + hH_1^{(\alpha)} + hH_M^{(\beta)}\right], \tag{4.27}$$

where h are boundary couplings, $\zeta = \frac{\sqrt{3}}{2\pi^{3/2}}$ is the conformal normalization factor [14] and the operators Z_j and X_j act at site j as:

$$Z = \begin{pmatrix} 1 & 0 & 0 \\ 0 & \omega & 0 \\ 0 & 0 & \omega^2 \end{pmatrix}, \qquad X = \begin{pmatrix} 0 & 1 & 0 \\ 0 & 0 & 1 \\ 1 & 0 & 0 \end{pmatrix}. \tag{4.28}$$

The terms $H_1^{(\alpha)}$ and $H_M^{(\beta)}$ set the BCs at the ends of the chain. For this analysis, we will set *fixed* BC of type R at site M and *restricted* boundary conditions of type $\{G, B\}$ at site 1 – the spin at site 1 is forbidden from taking the value R. The critical points of interest for the boundaries correspond to $h = +\infty$. However, for any $h > 0$, the boundaries will flow towards the same critical points, up to irrelevant boundary perturbations[143] . These are typically inconsequential for h a large positive value. Furthermore, in our numerical analysis we can, in fact, implement $|h| \to \infty$ by restricting the local Hilbert spaces of the boundary sites to exclude the $\{G, B\}$ and $\{R\}$ configurations on the left and, respectively, right boundary.

The scaling limit $M \to \infty$, $\epsilon \to 0$ (with $L = M\epsilon$ fixed) of this critical chain is also well understood. It is given by the D-series BCFT $\mathcal{M}(6, 5)$ with central charge $c = 4/5$ and a bulk primary operator spectrum that contains the scalar fields given in Table 4.2 as well as the non-diagonal fields $\{\phi_{2/5,7/5}, \phi_{7/5,2/5}, \phi_{3,0}, \phi_{0,3}\}$ whose labels indicate their respective holomorphic and antiholomorphic conformal dimensions. One can, as shown in Table 4.2, assign a $\mathbb{Z}_3$ charge to the scalar fields, and their respective conformal families, that is consistent with the fusion rules

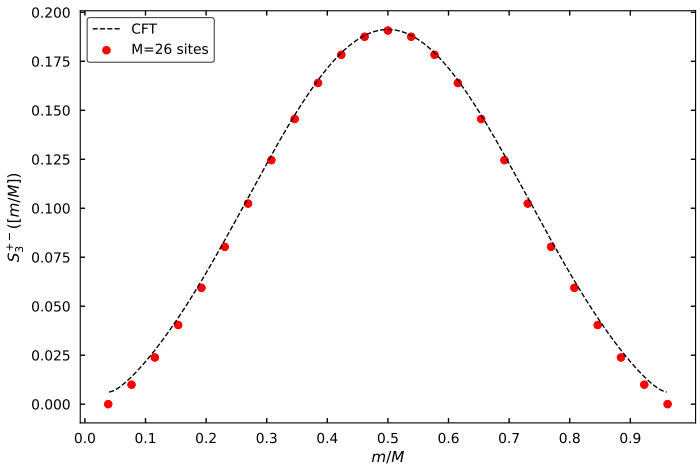

(a) Fixed mixed BC

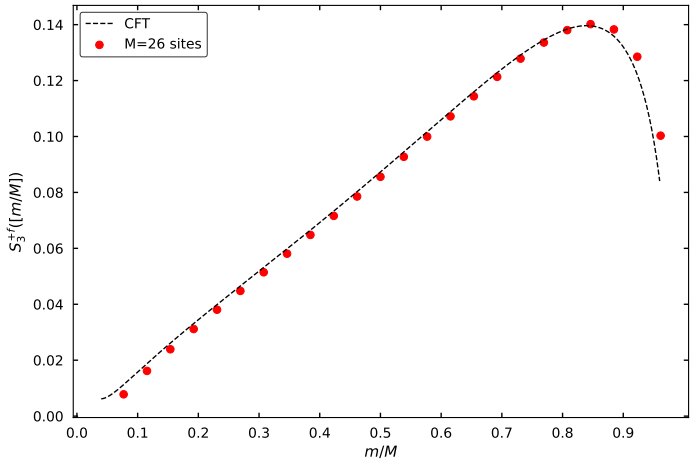

(b) Fixed-free mixed BC

Figure 4.6: Plots of the third Rényi entropy $S_3^{\alpha\beta}([m/M])$ in the critical Ising chain with two types of mixed BC for a chain of size $M = 26$. The interval is grown from the $\alpha = +$ boundary.

between them. The conjugation in Table 4.2 is, therefore, used to differentiate the fields with the same conformal dimension, but opposite $\mathbb{Z}_3$ charge.

Diagonal fields	$(h, \bar{h})$	$\mathbb{Z}_3$ charge
$\mathbf{1}$	$(0, 0)$	0
$\varepsilon \equiv \phi_{12}$	$(\frac{2}{5}, \frac{2}{5})$	0
ϕ_{13}	$(\frac{7}{5}, \frac{7}{5})$	0
ϕ_{14}	$(3, 3)$	0
$s, s^\dagger \equiv \phi_{33}$	$(\frac{1}{15}, \frac{1}{15})$	± 1
$\psi, \psi^\dagger \equiv \phi_{34}$	$(\frac{2}{3}, \frac{2}{3})$	± 1

Table 4.2: Spectrum of spinless primary operators in the three-state Potts CFT

In the scaling limit, the fixed and restricted[6] boundary critical points will correspond, naturally, to the conformal boundary states [108, 218].

$$
\begin{aligned}
|\mathbf{1}\rangle &= \mathcal{N}[(|\mathbf{1}\rangle\!\rangle + |\psi\rangle\!\rangle + |\psi^\dagger\rangle\!\rangle) + \lambda(|\epsilon\rangle\!\rangle + |s\rangle\!\rangle + |s^\dagger\rangle\!\rangle)] && \text{(fixed } R\text{)}\\
|\psi\rangle &= \mathcal{N}[(|\mathbf{1}\rangle\!\rangle + \omega|\psi\rangle\!\rangle + \bar\omega|\psi^\dagger\rangle\!\rangle) + \lambda(|\epsilon\rangle\!\rangle + \omega|s\rangle\!\rangle + \bar\omega|s^\dagger\rangle\!\rangle)] && \text{(fixed } G\text{)}\\
|\psi^\dagger\rangle &= \mathcal{N}[(|\mathbf{1}\rangle\!\rangle + \bar\omega|\psi\rangle\!\rangle + \omega|\psi^\dagger\rangle\!\rangle) + \lambda(|\epsilon\rangle\!\rangle + \bar\omega|s\rangle\!\rangle + \omega|s^\dagger\rangle\!\rangle)] && \text{(fixed } B\text{)}\\
|\varepsilon\rangle &= \mathcal{N}[\lambda^2(|\mathbf{1}\rangle\!\rangle + |\psi\rangle\!\rangle + |\psi^\dagger\rangle\!\rangle) - \lambda^{-1}(|\epsilon\rangle\!\rangle + |s\rangle\!\rangle + |s^\dagger\rangle\!\rangle)] && \text{(restricted } GB\text{)}\\
|s\rangle &= \mathcal{N}[\lambda^2(|\mathbf{1}\rangle\!\rangle + \omega|\psi\rangle\!\rangle + \bar\omega|\psi^\dagger\rangle\!\rangle) - \lambda^{-1}(|\epsilon\rangle\!\rangle + \omega|s\rangle\!\rangle + \bar\omega|s^\dagger\rangle\!\rangle)] && \text{(restricted } RB\text{)}\\
|s^\dagger\rangle &= \mathcal{N}[\lambda^2(|\mathbf{1}\rangle\!\rangle + \bar\omega|\psi\rangle\!\rangle + \omega|\psi^\dagger\rangle\!\rangle) - \lambda^{-1}(|\epsilon\rangle\!\rangle + \bar\omega|s\rangle\!\rangle + \omega|s^\dagger\rangle\!\rangle)] && \text{(restricted } RG\text{)}\,,
\end{aligned}
\tag{4.29}
$$

where

$$
\mathcal{N} = \sqrt{\frac{2}{\sqrt{15}}\sin\frac{\pi}{5}}\,, \qquad \lambda = \sqrt{\frac{\sin(2\pi/5)}{\sin(\pi/5)}}\,, \tag{4.30}
$$

and the $|i\rangle\!\rangle$'s are the Ishibashi states defined in [108]. These conformal boundary states are labelled by the primary fields of Table 4.2.

Due to the $\mathbb{Z}_3$ symmetry of our model, we have some freedom to set which conformal boundary state corresponds to the *fixed* boundary condition R in the chain. However, this uniquely determines the CFT boundary state that corresponds to the *restricted* boundary conditions GB. This can be understood by considering the spectrum of boundary fields that can interpolate between these conformal BC [31], and ensuring the results are consistent with the underlying $\mathbb{Z}_3$ symmetry. In our case, choosing *fixed* $R \leftrightarrow |\mathbf{1}\rangle$ forces us to assign *restricted* $GB \leftrightarrow |\varepsilon\rangle$. The most relevant boundary field interpolating between these BCs is $\psi_{12}^{(GB,R)}$ [31] with conformal dimension $h_\varepsilon = 2/5$.

We will now compare the quantum chain data for the second Rényi entropy in the critical Potts chain with our correlator calculations in the $\mathbb{Z}_2$ orbifold of the BCFT defined above. Our analysis will parallel the one for the Ising critical chain. We first hypothesize the form of the local expansion (4.22) of the lattice twist operator $\hat\sigma_{m,n}$ in the case of the three-state Potts model:

$$
\hat\sigma(m,n) = c_2\,\epsilon^{2h_\sigma}\sigma(w,\bar w) + c_2^\varepsilon\,\epsilon^{2h_{\sigma_\varepsilon}}\sigma_\varepsilon(w,\bar w) + \text{less relevant terms}\,, \tag{4.31}
$$

where $h_\sigma = 1/20$, and the composite twist operator σ_ε is built with the energy operator ε of the Potts model so that $h_{\sigma_\varepsilon} = 1/4$. We've numerically estimated the parameters c_2, c_2^ε by a simple analysis of the critical three-state Potts critical chain with *periodic boundary conditions*. Following this, the one-point lattice twist correlator with our choice of mixed BC can be calculated from:

$$
\langle\hat\sigma(m,0)\rangle^{(GB,R)} = c_2\left(\frac{M}{\pi}\right)^{-2h_{\sigma_\mathbf{1}}}\langle\sigma(z,\bar z)\rangle_{\mathbb{H}}^{(GB,R)} + c_2^\varepsilon\left(\frac{M}{\pi}\right)^{-2h_{\sigma_\varepsilon}}\langle\sigma_\varepsilon(z,\bar z)\rangle_{\mathbb{H}}^{(GB,R)} + \ldots \tag{4.32}
$$

The correlators in (4.32) satisfy the second order (4.87) and fourth order (4.114) ODEs with $g = 6/5$. While the solutions to equation (4.87) are known exactly (4.92), one needs to solve (4.114) numerically to find the conformal blocks in the expansion (4.81) of the excited twist correlator $\langle\sigma_\varepsilon(z,\bar z)\rangle_{\mathbb{H}}^{\alpha\beta}$. This is done by a standard numerical implementation of the Frobenius method, whose details we leave for Appendix C.7.

[6] In [108] they are referred to as "mixed" BC.

As in the case of the Ising BCFT, not all the solutions of these differential equations are needed to build the twist field correlators in (4.32). Crucially, we note that in the three-state Potts mother BCFT, there is no boundary operator $\psi_{7/5}^{(RR)}$ living on the fixed conformal boundary of type R [31]. This means, as discussed at the end of Section 4.5.1, that the expression for the leading BCFT to the second Rényi entropy is given by (4.10) with the extra constraint (4.16). The relevant ground state degeneracies were calculated in [217] and we reproduce them here for convenience:

$$g_R = \left(\frac{5-\sqrt{5}}{30}\right)^{\frac{1}{4}} \qquad g_{GB} = 2g_R \cos(\pi/5) \tag{4.33}$$

Consequently, one finds the leading BCFT contribution in this case to be:

$$S_2^{GB|R}(\ell) \sim \frac{c}{8}\log\frac{2L}{\pi a}\sin\left(\frac{\pi\ell}{L}\right) - \log F_2^{(GB,R)}(l/L) \tag{4.34}$$

with:

$$F_2^{(GB,R)}\left(\frac{\ell}{L}\right) = \frac{1}{g_{GB}}\left(-2\cos\pi\frac{6}{5}\right) I_{\frac{6}{5}}\left(\cos\frac{\pi l}{L}\right) \tag{4.35}$$

where I_g is defined in (4.13). For the excited twist correlator, we do not have a closed form expression, but the relevant expression (4.126) can be evaluated numerically, as explained in Section 4.5.2.

Putting everything together, we can compare the lattice prediction for the second Rényi entropy $S_2^{GB|R} = -\log\langle\hat{\sigma}(m,0)\rangle^{(GB,R)}$ with our analytic results in Figure 4.7. While the CFT prediction does not satisfyingly match the lattice data at all points, we observe that the inclusion of the subleading term gives an analytic curve that is closer to the lattice data. However, it is not enough to make up for the severe finite-size effects.

Firstly, due to the operator content of the D-series $\mathcal{M}_{6,5}$ CFT, we expect the higher order corrections in 4.32 to have a slower power law decay than in the case of the Ising CFT. We conjecture that the next-to-subleading contribution to (4.32) will decay as $\sim M^{-2(h_{\sigma_\varepsilon}+1/2)}$. These corrections, we believe, arise from the combined contribution of the $\langle\sigma_{\phi_{13}}(w,\bar{w})\rangle_{\mathbb{S}}^{(GB,R)}$ and $\langle L_{-1/2}^{(1)}\bar{L}_{-1/2}^{(1)}\sigma_{\phi_{12}}(w,\bar{w})\rangle_{\mathbb{S}}^{(GB,R)}$. While the first correlator can be calculated by a repeat of the method employed for the subleading term, the correlator involving the descendant twist field requires the derivation of a new differential equation. Such an endeavour is beyond the scope of this chapter.

Furthermore, the quantum chain sizes we can reach are diminished in the case of the three-state Potts model, since the size of the space of states grows as $\sim 3^M$. This memory constraint prevents us from reaching sizes at which higher-order corrections are suppressed, using our computational methods. This limitation can be, perhaps, bypassed through the usage of more sophisticated numerical tools, such as DMRG or tensor network methods, to access system sizes M for which the unknown higher-order correction terms are further suppressed.

Finally, one can use the method of Appendix C.7, applied this time to the third order ODE of Section 4.5.3 to derive the leading CFT contribution to the $S_3^{GB|R}([0,\ell])$ Rényi entropy. Since in this case, we have not derived an ODE for the excited twist correlator, we have no handle on the finite-size corrections to the lattice data, which should be even more severe for $n = 3$.

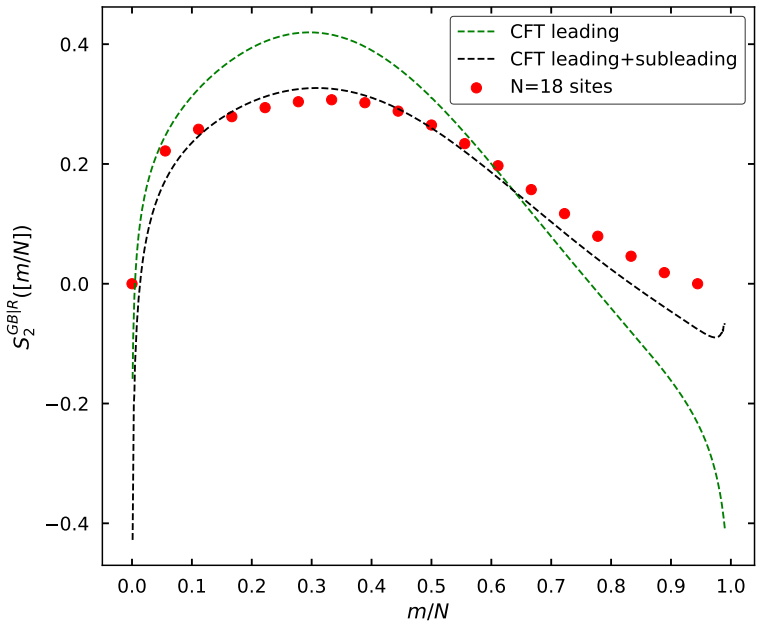

Figure 4.7: Comparison of the second Rényi entropy in the critical three-state Potts chain of size $M = 18$ with mixed (GB, R) BC with CFT results.

Instead, we have just checked that the CFT result for mixed BC matches the values for the third Rényi entropies for identical GB and R boundaries:

$$S_3^{\alpha}([0,\ell]) = \frac{c}{9}\log\left[\frac{2L}{\pi\epsilon}\sin\left(\frac{\pi\ell}{L}\right)\right] + \log g_{\alpha} \tag{4.36}$$

in the asymptotic regimes $\ell \to 0$ and $\ell \to L$ respectively.

Our expectations are met, as Figure 4.8 confirms.

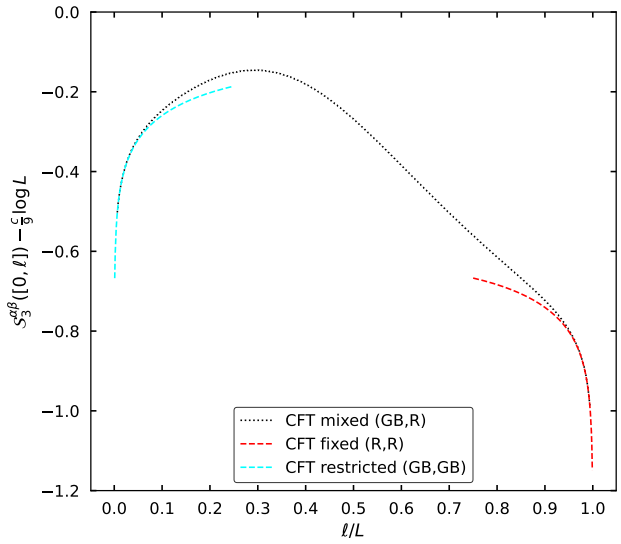

Figure 4.8: Comparison of shifted third Rényi entropies for (GB, R), (R, R) and (GB, GB) BC. The mixed BC curve can be seen to interpolate between the identical BC results

4.4 The cyclic orbifold

In this section, we will present the construction of the cyclic orbifold BCFT on the upper half-plane $\mathbb{H}$. After reviewing a few essential features of the $\mathbb{Z}_n$ orbifold on the Riemann sphere, we will discuss conformal boundary conditions, boundary operators as well as bulk-boundary and boundary-boundary operator algebras.

4.4.1 The cyclic orbifold on the Riemann sphere

To build a cyclic orbifold CFT, one starts from any mother CFT $\mathcal{M}$ and constructs the tensor product theory $\mathcal{M}^{\otimes n}$. Then one considers all the $\mathbb{Z}_n$ equivalent ways of connecting the copies of the product theory, which creates n different sectors, each with its corresponding operator families and labelled by a $\mathbb{Z}_n$ *twist charge* $[k]$. The spectrum of the cyclic orbifold $\mathcal{M}_n$ is then built as a reunion of the operator families from all the sectors $[k]$.

Symmetry algebra and operator content

In $\mathcal{M}_n$, each copy a of the mother CFT carries the components of the stress-energy tensor $T_a(z), \overline{T}_a(\bar{z})$. We define the discrete Fourier modes of these currents as

$$T^{(r)}(z) = \sum_{a=0}^{n-1} \omega^{ar}\, T_a(z)\,, \qquad \overline{T}^{(r)}(\bar{z}) = \sum_{a=0}^{n-1} \omega^{ar}\, \overline{T}_a(\bar{z})\,, \tag{4.37}$$

where r is considered modulo n, and we have used the notation $\omega = \exp(2i\pi/n)$. They satisfy the OPEs

$$\begin{aligned} T^{(r)}(z)T^{(s)}(w) &= \frac{\delta_{r+s,0}\, nc/2}{(z-w)^4} + \frac{2T^{(r+s)}(w)}{(z-w)^2} + \frac{\partial T^{(r+s)}(w)}{z-w} + \mathrm{reg}_{z\to w}\,, \\ \overline{T}^{(r)}(\bar{z})\overline{T}^{(s)}(\bar{w}) &= \frac{\delta_{r+s,0}\, nc/2}{(\bar{z}-\bar{w})^4} + \frac{2\overline{T}^{(r+s)}(\bar{w})}{(\bar{z}-\bar{w})^2} + \frac{\partial \overline{T}^{(r+s)}(\bar{w})}{\bar{z}-\bar{w}} + \mathrm{reg}_{\bar{z}\to\bar{w}}\,, \end{aligned} \tag{4.38}$$

where the Kronecker symbols $\delta_{r+s,0}$ are understood modulo n. The symmetric modes $T^{(0)}(z)$ and $\overline{T}^{(0)}(\bar{z})$ are the components of the stress-energy tensor of $\mathcal{M}_n$ with central charge nc, whereas the other Fourier modes $T^{(r)}(z), \overline{T}^{(r)}(\bar{z})$ with $r \neq 0$ should be regarded as additional conserved currents. Altogether, these Fourier modes encode an extended conformal symmetry. The modes associated with these currents are defined in the usual way:

$$\begin{aligned} L_m^{(r)} &= \frac{1}{2i\pi} \oint dz\, z^{m+1}\, T^{(r)}(z)\,, \\ \bar{L}_m^{(r)} &= \frac{1}{2i\pi} \oint d\bar{z}\, \bar{z}^{m+1}\, \overline{T}^{(r)}(\bar{z})\,. \end{aligned} \tag{4.39}$$

In the sector of twist charge $[k]$ one has the following mode decompositions

$$\begin{aligned} T^{(r)}(z) &= \sum_{m\in -kr/n+\mathbb{Z}} z^{-m-2}\, L_m^{(r)} \\ \overline{T}^{(r)}(\bar{z}) &= \sum_{m\in +kr/n+\mathbb{Z}} \bar{z}^{-m-2}\, \bar{L}_m^{(r)} \end{aligned} \tag{4.40}$$

and the commutation relations

$$\begin{aligned}\left[L_m^{(r)}, L_p^{(s)}\right] &= (m-p)L_{m+p}^{(r+s)} + \frac{nc}{12}m(m^2-1)\,\delta_{m+p,0}\,\delta_{r+s,0}\,,\\ \left[\bar{L}_m^{(r)}, \bar{L}_p^{(s)}\right] &= (m-p)\bar{L}_{m+p}^{(r+s)} + \frac{nc}{12}m(m^2-1)\,\delta_{m+p,0}\,\delta_{r+s,0}\,.\end{aligned} \tag{4.41}$$

Hermitian conjugation of the modes acts as:

$$\left(L_m^{(r)}\right)^\dagger = L_{mn}^{(-r)}\,, \qquad \left(\bar{L}_m^{(r)}\right)^\dagger = \bar{L}_{-m}^{(-r)}\,. \tag{4.42}$$

Orbifold *primary operators* are, by definition, annihilated by the action of all the positive modes of $\mathrm{OVir}\otimes\overline{\mathrm{OVir}}$. Descendant operators with respect to this algebra are constructed by the action of the negative m modes. We establish the notation for descendants of a scaling (primary or not) operator $\mathcal{O}$:

$$\begin{aligned}\left(L_m^{(r)}\cdot\mathcal{O}\right)(z,\bar{z}) &:= \frac{1}{2i\pi}\oint_{C_z} dw\,(w-z)^{m+1}\,T^{(r)}(w)\mathcal{O}(z,\bar{z})\,,\\ \left(\bar{L}_m^{(r)}\cdot\mathcal{O}\right)(z,\bar{z}) &:= \frac{1}{2i\pi}\oint_{C_z} d\bar{w}\,(\bar{w}-\bar{z})^{m+1}\,\overline{T}^{(r)}(\bar{w})\mathcal{O}(z,\bar{z})\,,\end{aligned} \tag{4.43}$$

where the contour C_z encloses the point z.

It will be useful to work with the primary operator spectrum with respect to the *neutral subalgebra* $A\otimes\bar{A}$ generated by the algebra elements

$$L_{m_1}^{(r_1)}\ldots L_{m_p}^{(r_p)} \quad\text{and}\quad \bar{L}_{m_1}^{(r_1)}\ldots\bar{L}_{m_p}^{(r_p)}\,, \qquad \text{with } r_1+\cdots+r_p = 0 \mod n\,. \tag{4.44}$$

One can classify all $\mathbb{Z}_n$-symmetric operators of $\mathcal{M}_n$ into representations of $A\otimes\bar{A}$. This organization, described in detail in [211], distinguishes between three types of operators. First, we have identified the *untwisted non-diagonal operators* $\Phi_{[j_1\ldots j_n]}$. These operators are built from $\mathbb{Z}_n$-symmetrized combinations of products of mother CFT primary operators ϕ_j (with $j=1$ referring to the identity operator $\mathbf{1}$):

$$\Phi_{[j_1\ldots j_n]} := \frac{1}{\sqrt{n}}\sum_{a=0}^{n-1}(\phi_{j_{1+a}}\otimes\cdots\otimes\phi_{j_{n+a}})\,, \tag{4.45}$$

in which at least one pair satisfies $j_i\neq j_k$. Its conformal dimension is given by $h_{[j_1\ldots j_n]} = \sum_s h_{j_s}$.

The second type of primary operators under the neutral algebra are the *untwisted diagonal fields* $\Phi_j^{(r)}$, where the Fourier replica index r takes values in $\mathbb{Z}_n$. The $r=0$ diagonal fields are defined to be:

$$\Phi_j^{(0)} = \Phi_j := \phi_j\otimes\cdots\otimes\phi_j\,, \tag{4.46}$$

while for $r\neq 0$, they are constructed as:

$$\Phi_j^{(r)} := \frac{1}{2nh_j}L_{-1}^{(r)}\bar{L}_{-1}^{(-r)}\cdot\Phi_j\,, \qquad \mathbf{1}^{(r)} := \frac{2}{nc}L_{-2}^{(r)}\bar{L}_{-2}^{(-r)}\cdot\Phi_{\mathbf{1}}\,, \tag{4.47}$$

The conformal dimension of a diagonal operator $\Phi_j^{(r)}$ is then generically given by

$$h_j^{(r)} = nh_j + \delta_{r,0}\left(1+\delta_{j,1}\right) \tag{4.48}$$

We should note that the diagonal operators with $r = 0$ and the non-diagonal operators are also primary under $\mathrm{OVir} \otimes \overline{\mathrm{OVir}}$.

Finally, we have to consider twist operators, which come in distinct flavours. For this chapter, we will mostly work with twist operators with Fourier replica index $r = 0$. Thereupon, just as for the diagonal fields, we will drop this specification when the context heavily implies it, to decongest the notation.

We first consider the ubiquitous bare twist operators [46, 70, 87, 123] which are denoted in our conventions $\sigma^{[k]} = \sigma_{\mathbf{1}}^{[k]}$, or, in light notation, $\sigma = \sigma^{[1]}$ and $\sigma^\dagger = \sigma^{[-1]}$. We have also the composite twist fields $\sigma_j^{[k]}$, which can be defined through point-splitting as in [219]:

$$\sigma_j^{[k]}(z,\bar{z}) := \mathcal{A}_j \lim_{\epsilon\to 0}\left[\epsilon^{2(1-n^{-1})h_j}\Phi_{[j,\mathbf{1},\ldots,\mathbf{1}]}(z+\epsilon,\bar{z}+\bar{\epsilon})\cdot\sigma^{[k]}(z,\bar{z})\right], \tag{4.49}$$

where the constant $\mathcal{A}_j = n^{-2(1-n^{-1})h_j - 1/2}$ ensures that non-vanishing two-point functions of twist operators are normalized to one. If n and k are coprime, the conformal dimension of the bare twist operator is

$$h_\sigma = \frac{c}{24}\left(n - \frac{1}{n}\right), \tag{4.50}$$

while for composite twist operators one has:

$$h_{\sigma_j} = h_\sigma + \frac{h_j}{n}. \tag{4.51}$$

Having established the primary operator spectrum of the orbifold, we will now review how the null vectors of the diagonal and twisted fields in $\mathcal{M}_n$ are inferred from the ones of the mother theory $\mathcal{M}$.

Null vectors for untwisted operators

Let us consider a generic mother CFT $\mathcal{M}$, with central charge

$$c = 1 - \frac{6(1-g)^2}{g}, \qquad 0 < g \leq 1. \tag{4.52}$$

The conformal dimensions of degenerate primary operators are given by the Kac formula

$$h_{rs} = \frac{(r-sg)^2 - (1-g)^2}{4g}, \tag{4.53}$$

where r, s are positive integers. The corresponding operator ϕ_{rs} is degenerate at level rs. If the parameter g is rational, i.e. $g = p/p'$ with coprime p and p', then the set of operators ϕ_{rs} with $1 \leq r \leq p-1$ and $1 \leq s \leq p'-1$ generates a closed operator algebra, and the related CFT is the minimal model $\mathcal{M}_{p,p'}$. While we do employ this parametrization extensively, in the present work we will consider a more generic mother CFT, and we *do not assume* that it is a minimal model—unless explicitly indicated.

Consider the situation when the mother CFT includes the degenerate operator ϕ_{12}, with null-vector condition

$$\left(L_{-2} - \frac{1}{g}L_{-1}^2\right)\phi_{12} = 0. \tag{4.54}$$

In the untwisted sector of the orbifold CFT, we have

$$L_n^{(r)} = \sum_{a=1}^{n} e^{2i\pi ra/n} \left(1 \otimes \dots 1 \otimes \underset{(a-\text{th})}{L_n} \otimes 1 \otimes \dots 1 \right), \qquad n \in \mathbb{Z}, \tag{4.55}$$

and the diagonal untwisted operator associated to ϕ_{12} is

$$\Phi_{12} = \phi_{12} \otimes \dots \otimes \phi_{12}. \tag{4.56}$$

Using an inverse discrete Fourier transform, one easily finds, for any $r \in \mathbb{Z}_n$,

$$\left[L_{-2}^{(r)} - \frac{1}{ng} \sum_{s=0}^{n-1} L_{-1}^{(s)} L_{-1}^{(r-s)} \right] \cdot \Phi_{12} = 0. \tag{4.57}$$

When inserted into a correlation function, the modes $L_m^{(0)}$ act as linear differential operators. The treatment of the modes $L_m^{(r)}$ with $r \neq 0$ introduces an additional difficulty, that we will address case by case, with the help of orbifold Ward identities.

The induction procedure

The null vectors of the mother CFT also determine the null vector conditions on twist operators in $\mathcal{M}_n$, through the *induction procedure*[119].

In the present work, we shall only be concerned with the twist sectors with charges [±1]. In the notations of [211], induction can be expressed in terms of a norm-preserving, invertible linear map Θ from the Hilbert space of the mother CFT to that of the twisted sector [1], defined by

$$\Theta |\phi\rangle = |\sigma_\phi\rangle, \qquad \Theta L_m \Theta^{-1} = n \left(L_{m/n}^{(-m)} - h_\sigma \, \delta_{m0} \right), \tag{4.58}$$

where ϕ is any primary operator in the mother CFT, and σ_ϕ is the associated composite twist operator in the orbifold CFT.

The simplest application to null-vectors is the case of the identity:

$$L_{-1} \cdot \mathbf{1} = 0 \qquad \Rightarrow \qquad L_{-1/n}^{(1)} \cdot \sigma = 0. \tag{4.59}$$

For a degenerate operator at level two, applying the induction map on (4.54) yields

$$\left[L_{-2/n}^{(2)} - \frac{n}{g} (L_{-1/n}^{(1)})^2 \right] \cdot \sigma_{12} = 0. \tag{4.60}$$

The corresponding null-vector conditions for the operators $\sigma^\dagger$ and $\sigma_{12}^\dagger$ are easily obtained by conjugation.

4.4.2 The cyclic orbifold on the upper half plane

To construct the cyclic orbifold BCFT, we will work on the upper half-plane $\mathbb{H}$, with the boundary along the real axis. We parametrize $\mathbb{H}$ by $z = x + iy$ with $x \in \mathbb{R}$ and $y > 0$, and we impose the gluing condition on the boundary for the stress-energy tensor components:

$$T^{(0)}(x) = \overline{T}^{(0)}(x) \quad \text{for} \quad x \in \mathbb{R}, \tag{4.61}$$

which ensures that the boundary is conformal i.e., preserves a copy of the Virasoro algebra [220]. The $\mathbb{Z}_n$ orbifold, however, has an extended symmetry, and we must choose if and how the components of the additional currents $T^{(r\neq 0)}$ are glued at the boundary. Our usage of the replica trick provides a clear indication for these choices: since we are considering n copies of the *same* mother BCFT, we must impose the gluing condition $T_a(x) = \bar{T}_a(x)$ on each of them. By taking the Fourier transform of this relation, we find that in the orbifold CFT we are effectively imposing:

$$T^{(r)}(x) = \overline{T}^{(r)}(x) \quad \text{for} \quad x \in \mathbb{R}\,, \tag{4.62}$$

for all the discrete Fourier modes of the stress-energy tensor components defined in (4.37). This implies that the boundary preserves a full copy of the OVir algebra.

By the same reasoning on CFT replicas, the orbifold boundary states we are interested in correspond to having the same conformal BC on the n copies of the mother CFT. They are simply given by $|\alpha\rangle^{\otimes n}$ and $|\beta\rangle^{\otimes n}$.

On the upper half-plane, we will set the conformal BC α on the positive real axis $x > 0$ and the conformal BC β on $x < 0$. To implement such mixed conformal BC in a BCFT, we will have to work with the formalism of BCCOs [108]. These operators, restricted to live on the boundary, are placed at the points of suture of regions of different BC. The full operator algebra of a BCFT is then formed by considering the OPEs between both BCCOs and bulk operators, as detailed in Appendix C.1. For a given pair of conformal BCs (α, β), there can be several primary BCCOs implementing the change $\alpha \to \beta$: we denote such an operator $\psi_h^{(\alpha\beta)}$, where h specifies its conformal dimension. The most relevant BCCO implementing $\alpha \to \beta$ is simply referred to as $\psi^{(\alpha\beta)}$.

In the $\mathbb{Z}_n$ orbifold CFT, we will be concerned with the calculation of correlators with insertions of *diagonal BCCOs*, namely :

$$\Psi_h^{(\alpha\beta)} = \underbrace{\psi_h^{(\alpha\beta)} \otimes \cdots \otimes \psi_h^{(\alpha\beta)}}_{\text{n times}}\,. \tag{4.63}$$

Then, orbifold correlators with mixed BC are obtained by inserting the most relevant diagonal BCCO:

$$\langle \mathcal{O}_1(z_1,\bar{z}_1)\dots\mathcal{O}_n(z_n,\bar{z}_n)\rangle_{\mathbb{H}}^{\alpha\beta} = \langle \Psi^{(\alpha\beta)}(\infty)\,\mathcal{O}_1(z_1,\bar{z}_1)\dots\mathcal{O}_n(z_n,\bar{z}_n)\Psi^{(\beta\alpha)}(0)\rangle_{\mathbb{H}}\,. \tag{4.64}$$

By Cardy's doubling trick [28], [124], such $(n+2)$-point correlators satisfy the same Ward identities as any of the $(2n+2)$-point conformal blocks on the Riemann sphere $\mathbb{C}$ with external operators

$$\Phi(\infty), \mathcal{O}_1(z_1), \overline{\mathcal{O}}_1(\bar{z}_1), \dots, \mathcal{O}_n(z_n), \overline{\mathcal{O}}_n(\bar{z}_n), \Phi(0)\,, \tag{4.65}$$

where $\overline{\mathcal{O}_i}(\bar{z})$ is the antiholomorphic counterpart of $\mathcal{O}_i(z)$, and $\Phi(z)$ is the holomorphic part of the diagonal primary operator defined in (4.46), with the conformal dimension of $\Psi^{(\alpha\beta)}$. In more precise terms, $\overline{\mathcal{O}_i}$ is the operator conjugate to $\mathcal{O}_i$ with respect to the symmetry algebra preserved by the boundary [221]. For $\mathbb{Z}_n$ twist operators, conjugation acts as $\overline{\sigma}_i = \sigma_i^\dagger$ [70], so that the one-twist function

$$\langle \sigma_i(z,\bar{z})\rangle_{\mathbb{H}}^{(\alpha\beta)} = \langle \Psi^{(\alpha\beta)}(\infty)\sigma_i(z,\bar{z})\Psi^{(\alpha\beta)}(0)\rangle_{\mathbb{H}} \tag{4.66}$$

satisfies the same Ward identities as the functions $\bar{z}^{-2h_{\sigma_i}} \times \mathcal{F}_k(z/\bar{z})$, where $\mathcal{F}_k$ is the rescaled conformal block:

$$\mathcal{F}_k(\eta) = \quad \Phi(\infty) \quad \Phi(0) \quad \Phi_k \quad \sigma_i(1) \quad \sigma_i^\dagger(\eta) \quad = \langle \Phi | \sigma_i(1) \mathcal{P}_k \sigma_i^\dagger(\eta) | \Phi \rangle \,, \tag{4.67}$$

$\mathcal{P}_k$ is the projector onto the $(A \otimes \bar{A})$-module of Φ_k, and $\{\Phi_k\}$ is the set of allowed intermediary untwisted (diagonal or not) primary operators. In the following, it will also be necessary to consider the conformal blocks in the channel $\eta \to 1$, namely

$$\widetilde{\mathcal{F}}_\ell(\eta) = \quad \sigma_i^\dagger(\eta) \quad \Phi(0) \quad \Phi_\ell \quad \sigma_i(1) \quad \Phi(\infty) \quad = \langle \Phi | \Phi(1) \mathcal{P}_\ell \sigma_i^\dagger(1-\eta) | \sigma_i \rangle \,. \tag{4.68}$$

Using the Ward identities implied by the OVir algebra (discussed in detail in Section 4.5) for these functions, together with the null-vectors of the previous section, will allow us to extract an ODE that the functions (4.67–4.68) satisfy.

To understand the structure of the conformal blocks, we also need to define *non-diagonal* BCCOs, paralleling (4.45):

$$\Psi^{(\alpha\beta)}_{[j_1 \cdots j_n]} := \frac{1}{\sqrt{n}} \sum_{\ell=0}^{n-1} (\psi^{(\alpha\beta)}_{j_{1+\ell}} \otimes \cdots \otimes \psi^{(\alpha\beta)}_{j_{n+\ell}}) \,, \tag{4.69}$$

where the $1/\sqrt{n}$ factor ensures that the non-vanishing two-point functions of these BCCOs are normalized to one. These operators appear in the OPE of the diagonal boundary fields $\Psi^{(\alpha\beta)}_j$, and thus their conformal dimension determines the leading singular behaviour of the conformal blocks. Naturally, we should now discuss the operator algebra of the $\mathbb{Z}_n$ orbifold BCFT.

4.4.3 Operator algebra of the cyclic orbifold BCFT

In the orbifold BCFT, the operator algebra consists of OPEs of three types. First, there is the operator subalgebra of bulk operators, inherited from the $\mathbb{Z}_n$ orbifold CFT on $\mathbb{C}$. We shall not directly use the structure constants of this subalgebra in this chapter, but they have been discussed in [118, 119, 123, 222]. The second type of OPE we need to consider in the orbifold BCFT is the bulk-boundary OPE which encapsulates the singular behaviour of a bulk field as it approaches a conformal boundary. In our calculations, we will only need to work with the OPEs of primary twist operators $\sigma_i(z, \bar{z})$ as they are sent towards a conformal boundary α:

$$\sigma_i(x, y) \underset{y \to 0}{\sim} \sum_j \mathcal{A}^{(\alpha)}_{\sigma_i, \Psi_j} (2y)^{h_j - 2h_{\sigma_i}} \Psi^{(\alpha\alpha)}_j(x) \tag{4.70}$$

where the sum runs over all the boundary operators $\Psi^{(\alpha\alpha)}_j$ and their descendants under OVir, and we have denoted the *bulk-boundary structure constants* by $\mathcal{A}^{(\alpha)}_{\sigma_i, \Psi_j}$.

Finally, we need to consider the OPEs of orbifold boundary operators. For generic diagonal BCCOs, this takes the form

$$\Psi_{i_1}^{(\alpha\beta)}(x_1)\Psi_{i_2}^{(\beta\gamma)}(x_2) \underset{x_1\to x_2}{\sim} \sum_j \mathcal{B}_{\Psi_{i_1},\Psi_{i_2}}^{(\beta\gamma)\Psi_j}(x_1-x_2)^{-h_{i_1}-h_{i_2}+h_j}\Psi_j^{(\alpha\gamma)}(x_2) \tag{4.71}$$

with the index j running over all the orbifold BCCOs interpolating between the conformal boundary conditions α and γ. We have denoted the *boundary-boundary structure constants* by $\mathcal{B}_{\Psi_{i_1},\Psi_{i_2}}^{(\alpha\beta\gamma)\Psi_j}$. To calculate the structure constants of the OPEs that are relevant for the present work, we will need to use factorization and unfolding arguments for the correlator that determine them, along the lines of [211],[223] and [123].

Calculation of boundary-boundary structure constants

Let us consider the calculation of boundary-boundary structure constants of the type $\mathcal{B}_{\Psi_*,\Psi_j}^{(\beta\beta\alpha)\Psi_k}$, where Ψ_* denotes a generic untwisted orbifold primary BCCO. We can express this as a three-point function on the upper half-plane $\mathbb{H}$:

$$\mathcal{B}_{\Psi_*,\Psi_j}^{(\beta\beta\alpha)\Psi_k} = \langle \Psi_k^{(\alpha\beta)}(\infty)\Psi_j^{(\beta\beta)}(1)\Psi_*^{(\beta\alpha)}(0)\rangle_{\mathbb{H}}\,. \tag{4.72}$$

Since there are no twist insertions in the above correlator, it just factorizes into a linear combination of products of mother BCFT three-point functions. Let us first consider the case of a diagonal BCCO, with $\Psi_*^{(\beta\alpha)} = \Psi_i^{(\beta\alpha)}$. Then, the orbifold correlator factorizes into mother CFT three-point functions as:

$$\mathcal{B}_{\Psi_i,\Psi_j}^{(\beta\beta\alpha)\Psi_k} = \left(\langle \psi_k^{(\alpha\beta)}(\infty)\psi_j^{(\beta\beta)}(1)\psi_i^{(\beta\alpha)}(0)\rangle_{\mathbb{H}}\right)^n\,, \tag{4.73}$$

so we find a simple expression for these coefficients, in terms of mother BCFT boundary-boundary structure constants:

$$\boxed{\mathcal{B}_{\Psi_i,\Psi_j}^{(\beta\beta\alpha)\Psi_k} = \left(B_{ij}^{(\beta\beta\alpha)\,k}\right)^n\,.} \tag{4.74}$$

By similar considerations, the structure constants involving a non-diagonal BCCO $\Psi_{[i_1\ldots i_n]}^{(\beta\alpha)}$ can be expressed as:

$$\boxed{\mathcal{B}_{\Psi_{[i_1\ldots i_n]},\Psi_j}^{(\beta\beta\alpha)\Psi_k} = \sqrt{n}\prod_{a=1}^{n} B_{i_a j}^{(\beta\beta\alpha)\,k}} \tag{4.75}$$

The rest of the boundary-boundary structure constants of untwisted BCCOs can similarly be expressed in terms of mother BCFT quantities, but we will not need them in this work.

Orbifold bulk-boundary structure constants

The first bulk-boundary structure constant we need to calculate is $\mathcal{A}_{\sigma,\Psi_\mathbf{1}}^{(\alpha)}$, where $\Psi_\mathbf{1}^{(\alpha\alpha)}$ is just the identity boundary field. This can be expressed as the one-point function on the unit disk $\mathbb{D}$:

$$\mathcal{A}_{\sigma,\Psi_\mathbf{1}}^{(\alpha)} = \langle \sigma(0,0)\rangle_{\mathbb{D}}^{\alpha}\,, \tag{4.76}$$

which is just the ratio of mother CFT partition functions:

$$\langle \sigma(0,0) \rangle^{\alpha}_{\mathbb{D}} = \frac{\mathcal{Z}^{(\alpha)}_{\mathbb{D}_n}}{\left[\mathcal{Z}^{(\alpha)}_{\mathbb{D}}\right]^n}\,, \tag{4.77}$$

where $\mathbb{D}_n$ denotes the n-th covering of the unit disk with branch points at 0 and 1. As shown in [110], we can express (4.76) in terms of the *ground state degeneracy* $g_\alpha = \langle 0|\alpha\rangle$ [217] (which is defined as the overlap between the vacuum state $|0\rangle$ and the boundary state $|\alpha\rangle$ in the mother BCFT):

$$\mathcal{A}^{(\alpha)}_{\sigma,\Psi_{\mathbf{1}}} = g_\alpha^{1-n}\,. \tag{4.78}$$

Using this result, we can calculate the one-point structure constants of composite twist operators σ_i, by using the definition (4.49) and the relation between twist correlators on the disk $\mathbb{D}$ and the mother CFT partition function on $\mathbb{D}_n$, which simply gives:

$$\mathcal{A}^{(\alpha)}_{\sigma_i,\Psi_{\mathbf{1}}} = \mathcal{A}^{(\alpha)}_{\sigma,\Psi_{\mathbf{1}}} A^{\alpha}_{\phi_i}\,, \tag{4.79}$$

where $A^{\alpha}_{\phi_i}$ is the mother CFT one-point structure constant of ϕ_i with conformal boundary condition α. The proof is relegated to Appendix C.2.1.

Extending these results to more complicated bulk-boundary structure constants $\mathcal{A}^{(\alpha)}_{\sigma_i^{[k]},\Psi_j}$ for generic choices of mother CFT and cyclic group $\mathbb{Z}_n$ is not usually straightforward and depends on our knowledge of correlation functions in the mother CFT. For example, in Appendix C.2.2 we calculate the structure constant $\mathcal{A}^{(\alpha)}_{\sigma,\Psi_{13}}$ in the $\mathbb{Z}_2$ orbifold BCFT since it can be expressed in terms of a two-point function of boundary operators in the mother CFT. For generic n and composite twist operator $\sigma_i^{[k]}$, knowledge of higher-point correlators in the mother CFT is required to compute such structure constants through the same unfolding methods.

4.5 Differential equations in the $\mathbb{Z}_2$ and $\mathbb{Z}_3$ orbifold BCFT

We consider the case of a generic BCFT, with central charge c. The model is defined on the upper half plane, with conformal boundary conditions α and β set on the negative $\Re(z) < 0$ and positive $\Re(z) > 0$ parts of the real axis, respectively. We will work, for the entirety of this section, under the assumption that the most relevant BCCO interpolating between these boundary conditions is $\psi^{(\alpha\beta)}_{12}$, with conformal dimension h_{12}. This implies that the BCCO has a null vector at level 2. Of course, our results also apply to the case where the BCCO is $\psi^{(\alpha\beta)}_{21}$, up to changing $g \to 1/g$.

In the $\mathbb{Z}_n$ orbifold of this theory, we will consider one-point correlators of generic *composite twist operators* σ_i of twist charge $[k = 1]$, in a background with mixed BC α and β, corresponding to the replicated boundary conditions of the mother BCFT. The change in boundary conditions in the orbifold theory will be implemented by the diagonal BCCO $\Psi^{(\alpha\beta)}_{12}$ defined in (4.63), with conformal dimension $h_{\Psi_{12}} = nh_{12}$. In this setup, we aim to calculate:

$$\langle \sigma_i(z,\bar{z}) \rangle^{\alpha\beta}_{\mathbb{H}} = \langle \Psi^{(\alpha\beta)}_{12}(\infty)\, \sigma_i(z,\bar{z}) \Psi^{(\beta\alpha)}_{12}(0) \rangle_{\mathbb{H}}\,, \tag{4.80}$$

Using the information about the operator algebra of the orbifold BCFT we have presented in Section 4.4.3, we can write the following block expansion for (4.80)

$$\langle \sigma_i(\ell,\ell)\rangle^{\alpha\beta}_{\mathbb{H}} = \mathcal{J}_{SL(2,\mathbb{C})} \sum_{\ell} \mathcal{A}^{(\beta)}_{\sigma_i,\Psi_\ell} \mathcal{B}^{(\beta\beta\alpha)\Psi_{12}}_{\Psi_\ell,\Psi_{12}} \widetilde{\mathcal{F}}_\ell(\eta)\,, \tag{4.81}$$

where $\eta = \bar{z}/z$, and $\mathcal{J}_{SL(2,\mathbb{C})} = (z)^{-2h_{\sigma_i}}$ is the Jacobian associated to the Möbius map $\zeta \mapsto \zeta/z$ that takes $(0, z, \bar{z}, \infty) \mapsto (0, 1, \eta, \infty)$. As per Cardy's doubling argument [220], the functions $\tilde{\mathcal{F}}_k(\eta)$ are four-point conformal blocks (4.67) with $\Phi = \Phi_{12}$, in the channel $\eta \to 1$.

To proceed, we need to determine the differential equation satisfied by these functions. To this end, we will use a combination of the null-vector conditions and the orbifold Ward identities of [118]

4.5.1 The function $\langle \Psi_{12} \cdot \sigma \cdot \Psi_{12}\rangle$ in a generic $\mathbb{Z}_2$ orbifold

Following the general approach described above, the function $\langle \Psi_{12}(\infty)\sigma(z,\bar{z})\Psi_{12}(0)\rangle_{\mathbb{H}}$ is given, up to the overall factor z^{-2h_σ}, by a linear combination of the conformal blocks

$$\mathcal{F}_k(\eta) = \langle \Phi_{12}|\sigma(1)\mathcal{P}_k\sigma(\eta)|\Phi_{12}\rangle\,. \tag{4.82}$$

It turns out that this family of conformal blocks was already studied in [118], for the calculation of the single-interval Rényi entropy in the excited state $|\Phi_{12}\rangle$ with periodic BC. Let us recall how the derivation of the corresponding ODE goes. The null-vectors at level two of the untwisted chiral state $|\Phi_{12}\rangle$ are:

$$\begin{aligned} &\left[L^{(0)}_{-2} - \frac{1}{2g}\left(L^{(0)}_{-1}\right)^2 - \frac{1}{2g}\left(L^{(1)}_{-1}\right)^2\right]\cdot|\Phi_{12}\rangle \equiv 0,\\ &\left[L^{(1)}_{-2} - \frac{1}{g}L^{(0)}_{-1}L^{(1)}_{-1}\right]\cdot|\Phi_{12}\rangle \equiv 0\,, \end{aligned} \tag{4.83}$$

while the null vector at level $1/n$ of the bare twist operator σ is :

$$L^{(1)}_{-1/2}\cdot\sigma \equiv 0\,. \tag{4.84}$$

We combine these with the orbifold Ward identity for the *chiral* correlator:

$$\mathcal{G}^{(1)}(w,\eta) = \langle \Phi_{12}|\,\sigma(1)\mathcal{P}_k\sigma(\eta)T^{(1)}(w)L^{(1)}_{-1}\,|\Phi_{12}\rangle\,, \tag{4.85}$$

with $(m_1, m_2, m_3, m_4) = (0, -1/2, -1/2, -1)$ in the notation of (C.22). This gives, after taking into account (4.84):

$$\sum_{p=0,1,2} d_p\,\langle \Phi_{12}|\,\sigma(1)\mathcal{P}_k\sigma(\eta)L^{(1)}_{-p+2}L^{(1)}_{-1}\,|\Phi_{12}\rangle = 0\,, \tag{4.86}$$

with d_p calculated from the series (C.27).

By substituting the null vectors (4.54–4.84) and employing the identity (C.28), one obtains the differential equation:

$$\begin{aligned} &64g^2\eta^2(\eta-1)^2\,\partial^2_\eta\mathcal{F} + 16g\eta(\eta-1)\left[(-14g^2+23g-6)\eta + 2g(1-4g)\right]\partial_\eta\mathcal{F}\\ &+ (3g-2)\left[+3(5g-6)(1-2g)^2\eta^2 + 12g(1-2g)\eta + 16g^2(g-1)\right]\mathcal{F} = 0\,, \end{aligned} \tag{4.87}$$

whose Riemann scheme is given by:

0	1	∞
$-2h_{12}$	$-2h_\sigma$	$2h_\sigma - 2h_{12}$
$-2h_{12} + h_{13}/2$	$-2h_\sigma + 2h_{13}$	$2h_\sigma - 2h_{12} + h_{13}/2$

This corresponds to the intermediary states $\{\sigma, \sigma_{13}\}$ in the channels $\eta \to 0$ and $\eta \to \infty$, and $\{\mathbf{1}, \Phi_{13}\}$ in the channel $\eta \to 1$. Note that, when the mother CFT is a minimal model $\mathcal{M}_{p,p'}$, one can check for various values of (p, p') that these are exactly the intermediary states allowed by the orbifold fusion given in (5.4), and that they all have multiplicity one.

To proceed, one can define the shifted function $f(\eta)$:

$$\mathcal{F}(\eta) = (1-\eta)^{-2h_\sigma} \eta^{-2h_{12}} f(\eta)\,, \tag{4.88}$$

and substitute in (4.87) to find that $f(\eta)$ satisfies a second order hypergeometric equation (C.41) with parameters:

$$a = 2 - 3g\,, \qquad b = \frac{3}{2} - 2g\,, \qquad c = \frac{3}{2} - g\,. \tag{4.89}$$

Since these coefficients are related via

$$a + 1 = b + c \tag{4.90}$$

we can exploit Kummer's quadratic transformation formula (see Appendix C.5), leading to

$$\boxed{\langle \Psi_{12}^{(\alpha\beta)}(\infty)\sigma(z,\bar{z})\Psi_{12}^{(\alpha\beta)}(0)\rangle_{\mathbb{H}} = \frac{1}{|z-\bar{z}|^{2h_\sigma}}\Big(A^{\alpha\beta}\,K_1(\zeta) + B^{\alpha\beta}\,K_2(\zeta)\Big)\,, \qquad \zeta = \frac{(z+\bar{z})^2}{4|z|^2}} \tag{4.91}$$

where

$$\boxed{\begin{aligned} K_1(\zeta) &= {}_2\mathrm{F}_1\left(\frac{a}{2}, b - \frac{a}{2}; \frac{1}{2}\middle|\,\zeta\right) \\ K_2(\zeta) &= \sqrt{\zeta}\;{}_2\mathrm{F}_1\left(\frac{a+1}{2}, b - \frac{a-1}{2}; \frac{3}{2}\middle|\,\zeta\right) \end{aligned}} \tag{4.92}$$

To determine the coefficients $A^{\alpha\beta}$ and $B^{\alpha\beta}$, we exploit the known behaviour in the limit where the twist field σ approaches the boundary, that is $z = x + iy \to x$. We have to distinguish between two situations, as σ can either approach the β boundary ($x > 0$) or the α boundary ($x < 0$).

In the former case, we expect, from the block expansion (4.81):

$$|z-\bar{z}|^{2h_\sigma}\langle \Psi_{12}(\infty)\sigma(z,\bar{z})\Psi_{12}(0)\rangle_{\mathbb{H}} \xrightarrow{z\to\bar{z}} \left(\mathcal{A}^{(\beta)}_{\sigma,\Psi_{\mathbf{1}}}\mathcal{B}^{(\beta\beta\alpha)\Psi_{12}}_{\Psi_{\mathbf{1}},\Psi_{12}} + |z-\bar{z}|^{2h_{13}}x^{2h_{13}}\mathcal{A}^{(\beta)}_{\sigma,\Psi_{13}}\mathcal{B}^{(\beta\beta\alpha)\Psi_{12}}_{\Psi_{13},\Psi_{12}}\right) \tag{4.93}$$

where the various structure constants are expressed in terms of the mother BCFT data as

$$\mathcal{A}^{(\beta)}_{\sigma,\Psi_{\mathbf{1}}} = g_\beta^{-1}\,, \qquad \mathcal{A}^{(\beta)}_{\sigma,\Psi_{13}} = g_\beta^{-1}2^{-4h_{13}}\,, \qquad \mathcal{B}^{(\beta\beta\alpha)\Psi_{12}}_{\Psi_{\mathbf{1}},\Psi_{12}} = 1\,, \qquad \mathcal{B}^{(\beta\beta\alpha)\Psi_{12}}_{\Psi_{13},\Psi_{12}} = \left(B^{(\beta\beta\alpha)\,\psi_{12}}_{\psi_{13}\psi_{12}}\right)^2. \tag{4.94}$$

while the corresponding expressions for $x < 0$ are obtained by swapping $\alpha \leftrightarrow \beta$ in the above equations.

For the task of fixing $A^{\alpha\beta}$ and $B^{\alpha\beta}$ only the leading behaviour in (4.93) is needed:

$$|z-\bar{z}|^{2h_\sigma}\langle \Psi_{12}(\infty)\sigma(z,\bar{z})\Psi_{12}(0)\rangle_{\mathbb{H}} \sim_{z\to\bar{z}} \begin{cases} \frac{1}{g_\beta} & \text{if} \quad \mathrm{Re}(z) > 0 \\ \frac{1}{g_\alpha} & \text{if} \quad \mathrm{Re}(z) < 0 \end{cases} \tag{4.95}$$

Furthermore, it will be convenient to switch to the following basis of solutions :

$$\begin{aligned} H_1(\zeta) &= {}_2\mathrm{F}_1\left(\frac{a}{2}, b-\frac{a}{2}; b+\frac{1}{2} \mid 1-\zeta\right) \\ H_2(\zeta) &= (1-\zeta)^{\frac{1}{2}-b}\ {}_2\mathrm{F}_1\left(\frac{a+3}{2}-b, \frac{3-a}{2}; \frac{3}{2}-b \mid 1-\zeta\right) \end{aligned} \tag{4.96}$$

When $x > 0$ one can directly use the relation

$$K_i = P_{ij} H_j \tag{4.97}$$

to transform to (4.96). The matrix P is given in (C.45), up to changing $a \to a/2$, $b \to b - a/2$ and $c \to 1/2$. For $x < 0$ on the other hand one must first analytically continue (4.91) around $\zeta = 0$, which simply changes $B^{\alpha\beta} \to -B^{\alpha\beta}$ in (4.91) , and only then use (4.97). Then imposing the constraint (4.95), the constants $A^{\alpha\beta}$ and $B^{\alpha\beta}$ are found to be

$$\boxed{A^{\alpha\beta} = \frac{\Gamma\left(\frac{g}{2}\right)\Gamma\left(\frac{3g}{2}-\frac{1}{2}\right)}{2\sqrt{\pi}\Gamma(2g-1)}\left(\frac{1}{g_\alpha}+\frac{1}{g_\beta}\right), \qquad B^{\alpha\beta} = \frac{\Gamma\left(\frac{3g}{2}\right)\Gamma\left(\frac{g+1}{2}\right)}{\sqrt{\pi}\Gamma(2g-1)}\left(\frac{1}{g_\beta}-\frac{1}{g_\alpha}\right)} \tag{4.98}$$

Splitting the contributions proportional to $1/g_\alpha$ and $1/g_\beta$ leads to

$$F_2^{(\alpha\beta)}(\zeta) = \frac{1}{g_\alpha} G_g\left(\sqrt{\zeta}\right) + \frac{1}{g_\beta} G_g\left(-\sqrt{\zeta}\right) \tag{4.99}$$

and where the function G_g is given by

$$\begin{aligned} G_g(\chi) = [2\sqrt{\pi}\Gamma(2g-1)]^{-1} \Bigg[&\Gamma\left(\frac{g}{2}\right)\Gamma\left(\frac{3g}{2}-\frac{1}{2}\right) {}_2\mathrm{F}_1\left(1-\frac{3g}{2}, \frac{1-g}{2}; \frac{1}{2}\middle| \chi^2\right) + \\ &+ \Gamma\left(\frac{3g}{2}\right)\Gamma\left(\frac{g+1}{2}\right) 2\chi\ \ {}_2\mathrm{F}_1\left(\frac{3-3g}{2}, 1-\frac{g}{2}; \frac{3}{2}\middle| \chi^2\right)\Bigg] \end{aligned} \tag{4.100}$$

The expression (4.100) can be further simplified using standard results for hypergeometric functions from [224] to arrive at:

$$G_g(\chi) = \frac{\sin 2\pi g}{\sin 3\pi g}\left(I_g(-\chi) + 2\cos \pi g\, I_g(\chi)\right) \tag{4.101}$$

where

$$I_g(\chi) = \left(\frac{1+\chi}{2}\right)^{2g-1} {}_2\mathrm{F}_1\left(g, 1-g; 2-2g\middle| \frac{1-\chi}{2}\right) \tag{4.102}$$

which leads to the main result (4.11).

By comparing the subleading terms in (4.91) with the ones in the expansion (4.93) (and its $x < 0$ analogue) one can determine the orbifold boundary-boundary OPE coefficients directly:

$$\begin{aligned} \mathcal{B}^{(\beta\beta\alpha)\Psi_{12}}_{\Psi_{13},\Psi_{12}} &= \langle \Psi_{12}^{\beta\alpha}(\infty)\Psi_{13}^{\alpha\alpha}(-1)\Psi_{12}^{\alpha\beta}(0)\rangle = \frac{\Gamma(3g-1)\Gamma(1-2g)}{\Gamma(1-g)\Gamma(2g-1)}\left(1+2\cos(\pi g)\frac{g_\beta}{g_\alpha}\right) \\ \mathcal{B}^{(\alpha\alpha\beta)\Psi_{12}}_{\Psi_{13},\Psi_{12}} &= \langle \Psi_{12}^{\beta\alpha}(\infty)\Psi_{13}^{\beta\beta}(1)\Psi_{12}^{\alpha\beta}(0)\rangle = \frac{\Gamma(3g-1)\Gamma(1-2g)}{\Gamma(1-g)\Gamma(2g-1)}\left(1+2\cos(\pi g)\frac{g_\alpha}{g_\beta}\right) \end{aligned} \tag{4.103}$$

The results (4.103) are just the square of mother BCFT structure constants as per (4.74). As a cross-check, we have verified that the above expressions are compatible with the ones obtained by standard bootstrap methods [124, 130] in the mother BCFT.

Moving on, we've found that, for some pairs of conformal BCs (α, β), the expressions in (4.98) simplify because the boundary-boundary structure constant $\mathcal{B}^{(\beta\beta\alpha)\Psi_{12}}_{\Psi_{13},\Psi_{12}}$ vanishes. At the level of the mother BCFT, this is equivalent to demanding that the operator $\psi^{(\beta\beta)}_{13}$ is not allowed in the theory.

For BCFTs based on A-series minimal models $\mathcal{M}(p, p')$, this holds for any pair of mixed conformal BCs $(\alpha, \beta) \equiv ((r, 2), (r, 1))$, labelled by bulk primary fields with $1 \leq r < p$. One can use well-established results about fusion rules in such models [23], to check that:

$$\phi_{12} \in \phi_{r1} \times \phi_{r2} \tag{4.104}$$

so that these BCs are interpolated by $\psi^{(\alpha\beta)}_{12}$ and

$$\phi_{13} \notin \phi_{r1} \times \phi_{r1} \tag{4.105}$$

which implies that $\psi^{(\beta\beta)}_{13}$ is not in the boundary operator spectrum of the BCFT. This is reflected in the vanishing of the orbifold structure constant $\mathcal{B}^{(\beta\beta\alpha)\Psi_{12}}_{\Psi_{13},\Psi_{12}} = 0$, since:

$$g_{(r,1)} = -g_{(r,2)}(2\cos(\pi g)) \tag{4.106}$$

so that the function $F^{\alpha\beta}_2$ will only depend on the conformal BC through $g_{(r,2)}$. We note that such simplification is not necessarily restricted to A-series models. Let us consider the D-series BCFT $\mathcal{M}(6, 5)$ (three-state Potts), with mixed BC $(\alpha, \beta) \equiv (\phi_{12}, \phi_{11}) \equiv (GB, R)$, for which there is no boundary operator $\psi^{(RR)}_{13}$ (with conformal dimension $h_{13} = 7/5$) living on the conformal boundary of type R [31]. At the level of the operator algebra, this translates, once again, into the vanishing of the boundary-boundary structure constants $B^{(\beta\beta\alpha),\psi_{12}}_{\psi_{13},\psi_{12}}$ as we have checked using the results of [213], so that the same considerations as above will apply.

4.5.2 The function $\langle \Psi_{12} \cdot \sigma_h \cdot \Psi_{12} \rangle$ in a generic $\mathbb{Z}_2$ orbifold

From the perspective of critical quantum chains, the result in (4.10) only determines the leading contribution to the second Rényi entropy. To understand finite-size corrections to this result, we should also study the one-point function of subleading primary twist operators, namely $\langle \sigma_h(z, \bar{z}) \rangle^{\alpha\beta}_{\mathbb{H}}$.

We shall derive an ODE for the conformal blocks

$$\mathcal{F}_k(\eta) = \langle \Phi_{12} | \sigma_h(1) \mathcal{P}_k \sigma_h(\eta) | \Phi_{12} \rangle \,. \tag{4.107}$$

Here we consider the case of a generic composite twist operator σ_h with conformal dimension

$$\widehat{h} = h_\sigma + \frac{h}{n} \,, \tag{4.108}$$

and thus we do not assume any null-vector condition on σ_h. Besides the null-vector conditions at level two (4.83), we will need the null-vector at level three in the module of $|\Phi_{12}\rangle$:

$$L^{(1)}_{-2} L^{(1)}_{-1} |\Phi_{12}\rangle = \left[-L^{(0)}_{-3} + \frac{1}{g} \left(2g L^{(0)}_{-1} L^{(0)}_{-2} - \left(L^{(0)}_{-1} \right)^3 \right) \right] |\Phi_{12}\rangle \,, \tag{4.109}$$

and two Ward identities obtained from:

$$\langle\Phi_{12}|\,\sigma_h(1)\mathcal{P}_k\sigma_h(\eta)T^{(1)}(z)L^{(1)}_{-1}\,|\Phi_{12}\rangle\,, \tag{4.110}$$

with $(m_1,m_2,m_3,m_4)=(-1,1/2,1/2,-2)$:

$$a_{0|1}\,\langle\Phi_{12}|\,L^{(1)}_1\sigma_h(1)\mathcal{P}_k\sigma_h(\eta)L^{(1)}_{-1}\,|\Phi_{12}\rangle=\sum_{p=0}^{3}d_{p|1}\,\langle\Phi_{12}|\,\sigma_h(1)\mathcal{P}_k\sigma_h(\eta)L^{(1)}_{-2+p}L^{(1)}_{-1}\,|\Phi_{12}\rangle \tag{4.111}$$

and $(m_1,m_2,m_3,m_4)=(-2,1/2,1/2,-1)$:

$$\begin{aligned}a_{0|2}\,\langle\Phi_{12}|\,L^{(1)}_2\sigma_h(1)\mathcal{P}_k\sigma_h(x)L^{(1)}_{-1}\,|\Phi_{12}\rangle+a_{1|2}\,\langle\Phi_{12}|\,L^{(1)}_1\sigma_h(1)\mathcal{P}_k\sigma_h(x)L^{(1)}_{-1}\,|\Phi_{12}\rangle=\\ =d_{0|2}\,\langle\Phi_{12}|\,\sigma_h(1)\mathcal{P}_k\sigma_h(\eta)L^{(1)}_{-1}L^{(1)}_{-1}\,|\Phi_{12}\rangle+d_{1|2}\,\langle\Phi_{12}|\,\sigma_h(1)\mathcal{P}_k\sigma_h(\eta)L^{(1)}_0L^{(1)}_{-1}\,|\Phi_{12}\rangle+\\ +d_{2|2}\,\langle\Phi_{12}|\,\sigma_h(1)\mathcal{P}_k\sigma_h(\eta)L^{(1)}_1L^{(1)}_{-1}\,|\Phi_{12}\rangle\end{aligned} \tag{4.112}$$

Putting everything together, and applying the change of function

$$\mathcal{F}(\eta)=\eta^{-2h_{12}}\,(1-\eta)^{4h_{12}-2\widehat{h}}\,f(\eta)\,, \tag{4.113}$$

we obtain the fourth-order ODE

$$\begin{aligned}&(\eta-1)^4\eta^3\,\partial^4_\eta f+\frac{1}{2}(\eta-1)^3\eta^2\left[(2g+13)\eta+(2g-11)\right]\partial^3_\eta f\\ &-\frac{1}{8}(\eta-1)^2\eta\left[(16g\widehat{h}+6g^2-45g-60)\eta^2+(20g^2+34g+96)\eta+(16g\widehat{h}+6g^2+3g-36)\right]\partial^2_\eta f\\ &-\frac{g}{16}(\eta-1)\Big[(48\widehat{h}+18g-75)\eta^3+(16g^2-18g-112\widehat{h}+167)\eta^2\\ &\qquad+(80\widehat{h}+16g^2-74g-53)\eta+(-16\widehat{h}-6g+9)\Big]\,\partial_\eta f\\ &+\frac{g}{8}\Big[(16g^2\widehat{h}+6g^3-13g^2+4)\eta^2+(-32g^2\widehat{h}+12g^3+34g^2-64g+24)\eta\\ &\qquad+(24+16g^2\widehat{h}+6g^3-13g^2+4)\Big]\,f=0\,.\end{aligned} \tag{4.114}$$

At this stage, it will be convenient to use the Coulomb-Gas parametrization to analyse the local exponents of the ODE. Recall the relation between the mother CFT central charge and the parameter g:

$$c=1-24Q^2\,,\qquad Q=\frac{1}{2}(1/b-b)\,,\qquad b=\sqrt{g}\,. \tag{4.115}$$

The conformal dimensions in the mother CFT are parametrized by the *vertex charge* α as

$$h_\alpha=\alpha(\alpha-2Q)\,, \tag{4.116}$$

and we use the shorthand notation for the conformal dimension of composite twisted operators

$$\widehat{h}_\alpha=h_\sigma+\frac{h_\alpha}{n}\,. \tag{4.117}$$

In this parametrization, the Riemann scheme for $\mathcal{F}(\eta)$ is given in Table 4.3.

0	1	∞
$-2h_{12}$	$-2\widehat{h}_\alpha$	$2\widehat{h}_\alpha - 2h_{12}$
$-2h_{12}+\frac{1}{2}$	$-2\widehat{h}_\alpha + h_{13}$	$2\widehat{h}_\alpha - 2h_{12}+\frac{1}{2}$
$-\widehat{h}_\alpha - 2h_{12} + \widehat{h}_{\alpha+b}$	$-2\widehat{h}_\alpha + 2h_{13}$	$\widehat{h}_\alpha - 2h_{12} + \widehat{h}_{\alpha+b}$
$-\widehat{h}_\alpha - 2h_{12} + \widehat{h}_{\alpha-b}$	$-2\widehat{h}_\alpha + 2h_{13} + 2$	$\widehat{h}_\alpha - 2h_{12} + \widehat{h}_{\alpha-b}$

Table 4.3: Singular exponents around $\eta = 0, 1, \infty$

These exponents correspond to the intermediary states (counted with their multiplicities):

$$\begin{aligned} &\{\mathbf{1}, [\mathbf{1}, \phi_{13}], \Phi_{13}, \Phi_{13}\} \quad \text{in the channel } \eta \to 1\,, \\ &\{\sigma_h, L^{(1)}_{-1/2}\cdot\sigma_h, \sigma_{h'}, \sigma_{h''}\} \quad \text{in the channels } \eta \to 0 \text{ and } \eta \to \infty\,. \end{aligned} \tag{4.118}$$

Here, we have defined $h' = h_{\alpha+b}$ and $h'' = h_{\alpha-b}$. Recall that the conformal blocks are labelled by primary operators under the neutral subalgebra A, and that $L^{(1)}_{-1/2}\cdot\sigma_h$ is one of these operators. When the mother CFT is a minimal model, one can check on various examples that the orbifold fusion rules derived in [211] from the Verlinde formula are consistent with these intermediary states.

While an analytic solution to the differential equation is not known, one can determine the conformal blocks $\mathcal{F}_k(\eta)$ around $\eta = 0$ and $\widetilde{\mathcal{F}}(\eta)$ around $\eta = 1$ numerically to arbitrary precision. Assuming this step has been performed, all that is left is to calculate the structure constants in the block expansion (4.81). The boundary-boundary structure constants are calculated from (4.74) and (4.75), while the bulk-boundary structure constants can be calculated analytically through unfolding, as shown, for some cases in Appendix C.2.2 and C.2.1. For numerical studies, however, it is simpler to bootstrap some of the coefficients in the block expansion (4.81) rather than to calculate all of them analytically.

To implement this method, as detailed in [130], one needs to compare the block expansions in (4.81) with the block expansion corresponding to sending the twist field to the part of the boundary, endowed with the α BC. The crucial point here is that the conformal blocks $\mathcal{F}_k(\eta)$ are branched functions on $\mathbb{C}$, with branch points $\{0, 1, \infty\}$, and, thus, sending the twist field to the boundary with BC α is equivalent to crossing to the other branch of the function. This is marked by appending the phase factor $e^{2\pi i}$ to the variable η to get:

$$\langle \sigma_h(z,\bar{z})\rangle^{\alpha\beta}_{\mathbb{S}} = \mathcal{J}_{SL(2,\mathbb{C})} \sum_\ell \mathcal{A}^{(\alpha)}_{\sigma_h,\Psi_\ell} \mathcal{B}^{(\alpha\alpha\beta)\Psi_{12}}_{\Psi_\ell,\Psi_{12}} \widetilde{\mathcal{F}}_\ell(e^{2\pi i}\eta)\,. \tag{4.119}$$

To proceed, one needs to find the *monodromy matrix* X around zero for the basis $\widetilde{\mathcal{F}}_\ell(\eta)$, which encodes the behaviour of the conformal blocks as the branch cut is crossed:

$$\widetilde{\mathcal{F}}_\ell(e^{2\pi i}\eta) = \sum_m X_{\ell m}\widetilde{\mathcal{F}}_m(\eta)\,. \tag{4.120}$$

Since the monodromy of the blocks $\widetilde{\mathcal{F}}_\ell$ around zero is non-diagonal, we can use the fusing matrix P_{ij} to express the blocks $\widetilde{\mathcal{F}}_\ell$ in terms of a basis of the blocks $\mathcal{F}_k$, which have diagonal monodromy around $\eta = 0$:

$$\widetilde{\mathcal{F}}_\ell(\eta) = \sum_k P_{\ell k}\mathcal{F}_k(\eta)\,. \tag{4.121}$$

The blocks $\mathcal{F}_k(\eta)$ simply acquire a phase under $z \to e^{2\pi i} z$, so their monodromy matrix Y is diagonal:

$$\mathcal{F}_k(e^{2i\pi}\eta) = \sum_j Y_{kj}\mathcal{F}_j(\eta)\,, \qquad Y_{kj} = \delta_{kj}\,\exp\left[2\pi i\left(-\widehat{h}_\alpha - 2h_{12} + \widehat{h}_k\right)\right], \tag{4.122}$$

where the exponents in the exponential above, are simply read off from the Riemann scheme. Then, the monodromy matrix of the blocks $\widetilde{\mathcal{F}}_\ell(\eta)$ is found from the matrix product:

$$X = P \cdot Y \cdot P^{-1}\,, \tag{4.123}$$

which allows us to compare the block expansions in (4.81) and (4.119) to find a duality relation, of the type presented in [130]:

$$\mathcal{A}^{(\beta)}_{\sigma_h,\Psi_i}\mathcal{B}^{(\beta\beta\alpha)\Psi_i}_{\Psi_{12},\Psi_{12}} = \sum_j \mathcal{A}^{(\alpha)}_{\sigma_h,\Psi_j}\mathcal{B}^{(\alpha\alpha\beta)\Psi_j}_{\Psi_{12},\Psi_{12}} X_{ji}\,. \tag{4.124}$$

Using the numerical determinations for $\mathcal{F}_k(\eta)$ and $\widetilde{\mathcal{F}}_\ell(\eta)$, one can find a good estimate for the fusing matrix P_{ij}, and, consequently, X_{ij}. A more fleshed-out example of how the determination of P_{ij} works has been relegated to the Appendix C.7, where this equation is used for the case of the $\mathbb{Z}_2$ orbifold of the three-state Potts model BCFT.

After solving the linear system in (4.124) one can evaluate the unknown structure constants $\mathcal{A}^{(\beta)}_{\sigma_h,\Psi_i}$ and $\mathcal{A}^{(\alpha)}_{\sigma_h,\Psi_i}$. At this point, we stress that (4.124) gives, at most, *four* constraints between the unknown structure constants. To fully determine all these quantities, one should calculate the remaining four structure constants through other methods.

Example: Three-state Potts model

Let us once again consider the 3-state Potts model BCFT with mixed BC $(\alpha,\beta) \equiv (GB, R)$ as mother theory. We are interested in this case in the one-point function of the excited twist operator σ_ε where $\varepsilon \equiv \phi_{12}$ is a primary field in $\mathcal{M}(6,5)$.

The non-existence of a boundary field $\psi^{(RR)}_{13}$ in this theory implies, through the relations between mother BCFT and orbifold structure constants derived in Section 4.4.3, the vanishing of some of the coefficients in the block expansions (4.81) of the correlators in (4.32). In effect, only the block corresponding to the identity operator contributes to these expressions when the twist field is sent to the β boundary. This corresponds to the following fusion rules σ_ε:

$$\sigma_\varepsilon\Big|_\beta \to \Psi^{(\beta\beta)}_{\mathbf{1}} \tag{4.125}$$

Hence, we are led to obtain the following expressions for the excited twist correlator on the UHP:

$$\langle\sigma_\varepsilon(z,\bar{z})\rangle^{\alpha\beta} = z^{-2h_{\sigma_\varepsilon}}\mathcal{A}^{(\beta)}_{\sigma_\varepsilon,\Psi_{\mathbf{1}}}\mathcal{B}^{(\beta\beta\alpha)\Psi_{12}}_{\Psi_{\mathbf{1}},\Psi_{12}}\tilde{\mathcal{F}}^{(\varepsilon)}_{\mathbf{1}}(\eta)\,, \tag{4.126}$$

where we have:

$$\tilde{\mathcal{F}}^{(\varepsilon)}_{\mathbf{1}}(\eta) = J_1(u(\eta)) = (1-u)^{-2h_{\sigma_\varepsilon}}\sum_{n=0}^{\infty} a_n(1-u)^n\,, \tag{4.127}$$

with the coefficients determined by the recursion relation (C.74), derived in Appendix C.7. The structure constants can be expressed in terms of known quantities for the $\mathcal{M}(6,5)$ BCFT, obtained in Appendix B:

$$\mathcal{A}^{(\beta)}_{\sigma_\varepsilon,\Psi_{\mathbf{1}}} = g_R^{-1} A^R_\varepsilon \,, \qquad \mathcal{B}^{(\beta\beta\alpha)\Psi_{12}}_{\Psi_{\mathbf{1}},\Psi_{12}} = 1 \,. \tag{4.128}$$

where the bulk-boundary structure constant A^R_ε has been calculated in [218, 225] to be:

$$A^R_\varepsilon = \left(\frac{1+\sqrt{5}}{2}\right)^{\frac{3}{2}} \,. \tag{4.129}$$

4.5.3 The function $\langle \Psi_{12} \cdot \sigma \cdot \Psi_{12} \rangle$ in a generic $\mathbb{Z}_3$ orbifold

Here the relevant conformal blocks are

$$\mathcal{F}_k(\eta) = \langle \Phi_{12} | \sigma(1) \mathcal{P}_k \sigma^\dagger(\eta) | \Phi_{12} \rangle \,. \tag{4.130}$$

We give the null vectors of $|\Phi_{12}\rangle$ at levels two and three:

$$L^{(r)}_{-2} |\Phi_{12}\rangle = \frac{1}{3g} \sum_{s=0}^{2} L^{(r-s)}_{-1} L^{(s)}_{-1} |\Phi_{12}\rangle \,, \tag{4.131}$$

$$L^{(3-r)}_{-1} L^{(r)}_{-2} |\Phi_{12}\rangle = \frac{1}{3g} \left[2 L^{(0)}_{-1} L^{(1)}_{-1} L^{(2)}_{-1} + \left(L^{(3-r)}_{-1}\right)^3 \right] |\Phi_{12}\rangle \,, \tag{4.132}$$

for $r \in \{0,1,2\}$. We will also need the null vectors for the out-state $\langle \Phi_{12}|$, which can be obtained by Hermitian conjugation (4.42).

To derive an ODE for the conformal blocks, we had to employ seven orbifold Ward identities, together with six of the null-vector conditions above. To not overload the presentation of this section with technical details, we relegate the specifics of the derivation to Appendix C.6. We apply the change of function

$$\mathcal{F}(\eta) = \eta^{-8h_{12}/3} (1-\eta)^{16h_{12}/3 - 2h_\sigma} f(\eta) \,. \tag{4.133}$$

The function f satisfies the ODE

$$\begin{aligned} &(\eta-1)^3 \eta^2 \, \partial_\eta^3 f + (\eta-1)^2 \eta \left[(g+3)\eta + (g-3) \right] \partial_\eta^2 f \\ &+ \frac{2}{9} (\eta-1) \left[2(2+3g)\eta^2 - 2(7-15g+18g^2)\eta + (4-3g) \right] \partial_\eta f \\ &+ \frac{4}{27} (1-6g)(2-3g)(\eta+1) \, f = 0 \,. \end{aligned} \tag{4.134}$$

The Riemann scheme for $\mathcal{F}$ is

0	1	∞
$-\frac{8}{3}h_{12}$	$-2h_\sigma$	$2h_\sigma - \frac{8}{3}h_{12}$
$-\frac{8}{3}h_{12} + \frac{1}{3}$	$-2h_\sigma + 2h_{13}$	$2h_\sigma - \frac{8}{3}h_{12} + \frac{1}{3}$
$-3h_{12} + \frac{h_{14}}{3}$	$-2h_\sigma + 3h_{13}$	$2h_\sigma - 3h_{12} + \frac{h_{14}}{3}$

The local exponents correspond to the intermediary states:

$$\begin{aligned} &\{\mathbf{1}, [\mathbf{1}, \phi_{13}, \phi_{13}], \Phi_{13}\} \quad \text{in the channel } \eta \to 1 \,, \\ &\{\sigma_{12}, L^{(1)}_{-1/3} \cdot \sigma_{12}, \sigma_{14}\} \quad \text{in the channels } \eta \to 0 \text{ and } \eta \to \infty \,. \end{aligned} \tag{4.135}$$

In the orbifold BCFT, this translates into the following fusion rules for the twist operator with the boundary β:

$$\sigma_{\mathbf{1}}\Big|_{\beta} \to \Psi_{\mathbf{1}}^{(\beta\beta)} + \Psi_{[\mathbf{1},\phi_{13},\phi_{13}]}^{(\beta\beta)} + \Psi_{13}^{(\beta\beta)} . \tag{4.136}$$

The analytic solutions to the differential equation (4.134) are not known, but they can be evaluated numerically, to arbitrary precision. Then, one can use the bootstrap to determine some relations between the unknown structure constants in the expansion (4.81), as outlined in the previous section, and determine the rest analytically, by unfolding methods, to complete the calculation of the mixed BC correlator of the bare twist.

We note that a fourth-order differential equation that the correlator (4.64) satisfies has already been found in [223], where it plays a role in the determination of the leading contribution to the third Rényi entropy of an excited state in a periodic 1D critical chain. As predicted in [223], there is no degeneracy in the exponents in the more constraining third-order differential equation we have found here. Note that these exponents are the ones expected from the orbifold fusion rules[211].

4.5.4 The function $\langle \Psi_{12} \cdot \sigma_{13} \cdot \Psi_{12} \rangle$ in the $\mathbb{Z}_3$ orbifold of the Ising model

In this section, we will work with the $\mathbb{Z}_3$ orbifold of the Ising BCFT. The bulk primary fields of this BCFT are $\phi_{11} \equiv \mathbf{1}$, $\phi_{12} \equiv s$ and $\phi_{13} \equiv \varepsilon$ with $h_s = 1/16$ and $h_\varepsilon = 1/2$. We will keep labelling the fields by their Kac indices, to not overcomplicate the notation.

We will provide here an alternative method for finding a differential equation for the one-point function:

$$\langle \sigma_{13}(z,\bar{z}) \rangle_{\mathbb{H}}^{f+} , \tag{4.137}$$

where the orbifold conformal boundary conditions $\alpha = f$ and $\beta = +$ correspond to setting fixed and free BC respectively, on all the copies of the Ising mother BCFT. The diagonal BCCO $\Psi_{12}^{(f+)}$ is the one interpolating between them in the orbifold, since in the Ising BCFT only the $\psi_{12}^{(f+)}$ primary boundary field can change between the CBCs $(+) \leftrightarrow (f)$ [130]. As in the previous sections, we aim to find a differential equation satisfied by the conformal blocks

$$\mathcal{F}_k(\eta) = \langle \Phi_{12} | \sigma_{13}(1) \mathcal{P}_k \sigma_{13}^\dagger(\eta) | \Phi_{12} \rangle . \tag{4.138}$$

First, we use the fusion numbers in (5.4) to infer the dimension of the space of conformal blocks for (4.137):

$$\sum_i \mathcal{N}_{\sigma_{13},\sigma_{13}^\dagger}^{i} \mathcal{N}_{i,\Phi_{12}}^{\Phi_{12}} = 2 , \tag{4.139}$$

which means the differential equation we seek should be second order.

By using the null-vectors induced on σ_{13} together with the right combination of Ward identities, one should be able to rigorously derive it. Instead, we will assume this equation exists and is of Fuchsian type – a linear homogenous ODE whose three singular points are regular. The latter assumption is based on the observation

that the method exploited in the previous sections relies on expressing orbifold modes $L_m^{(r\neq 0)}$ in terms of Virasoro generators, whose combined differential action on correlators is well-understood in the literature [23],[226] to be of Fuchsian type.

Now, using the fusion numbers of (5.4), the fusion rules are

$$\begin{aligned} \sigma_{13} \times \Phi_{12} &\to \sigma_{12} + L^{(2)}_{-2/3} \cdot \sigma_{12} \,, \\ \sigma_{13} \times \sigma^{\dagger}_{13} &\to \mathbf{1} + [\mathbf{1}, \phi_{13}, \phi_{13}] \,, \end{aligned} \tag{4.140}$$

so we can determine the asymptotic behaviour of the solutions around the regular singular points $\eta \in \{0, 1, \infty\}$ of the differential equation and infer the Riemann scheme:

0	1	∞
$-h_{\sigma_{13}} - 3h_{12} + h_{\sigma_{12}}$	$-2h_{\sigma_{13}}$	$h_{\sigma_{13}} - 3h_{12} + h_{\sigma_{12}}$
$-h_{\sigma_{13}} - 3h_{12} + h_{\sigma_{12}} + \frac{2}{3}$	$-2h_{\sigma_{13}} + 2h_{13}$	$h_{\sigma_{13}} - 3h_{12} + h_{\sigma_{12}} + \frac{2}{3}$

One can readily check that the entries of this Riemann scheme sum up to one, so, by a general theorem on Fuchsian ODEs (see [227]), there is a unique second-order Fuchsian ODE with this set of singular exponents. If we define the shifted function $f(\eta)$:

$$f(\eta) = \eta^{h_{\sigma_{13}} + 3h_{12} - h_{\sigma_{12}}} (1-\eta)^{2h_{\sigma_{13}}} \mathcal{F}(\eta) \,, \tag{4.141}$$

we find, by the same considerations, that it should satisfy a second-order Fuchsian differential equation with the Riemann scheme

0	1	∞
0	0	$-2h_{\sigma_{13}} - 6h_{12} + 2h_{\sigma_{12}}$
$\frac{2}{3}$	$2h_{13}$	$-2h_{\sigma_{13}} - 6h_{12} + 2h_{\sigma_{12}} + \frac{2}{3}$

This is just the canonical Riemann scheme of a hypergeometric differential equation (C.41), with coefficients:

$$\begin{aligned} a &= -2h_{\sigma_{13}} - 6h_{12} + 2h_{\sigma_{12}} = -2/3 \,, \\ b &= -2h_{\sigma_{13}} - 6h_{12} + 2h_{\sigma_{12}} + \frac{2}{3} = 0 \,, \\ c &= \frac{1}{3} \,, \end{aligned} \tag{4.142}$$

in the conventions of Appendix C.5. We notice that the exponents in the $\eta \to 1$ channel are spaced by one, so we will have to deal with the *degenerate exponents* to arrive at a closed-form solution. To do this, we will use the basis of solutions in the $\eta \to 0$ channel – given in (C.42) – to construct a linearly independent basis of solutions around $\eta \to 1$. The solutions for f can be simplified, in this case, to:

$$I_1(\eta) = 1 \,, \qquad I_2(\eta) = \eta^{2/3} \,, \tag{4.143}$$

which gives the conformal blocks around $\eta \to 0$:

$$\mathcal{F}_1(\eta) = \eta^{-1/3}(1-\eta)^{-4/9} \,, \qquad \mathcal{F}_2(\eta) = \eta^{1/3}(1-\eta)^{-4/9} \,. \tag{4.144}$$

in our normalisation convention.

To build the basis of solutions around $\eta = 1$, we look for the linear combinations $\tilde{\mathcal{F}}_i(\eta) = \sum_j P^{-1}_{ij} \mathcal{F}_j(\eta)$ that have the following series expansion around $\eta = 1$:

$$\tilde{\mathcal{F}}_1(\eta) = (1-\eta)^{-4/9} \left(1 + O[(1-\eta)^2]\right) \,, \qquad \tilde{\mathcal{F}}_2(\eta) \sim (1-\eta)^{5/9} \,, \tag{4.145}$$

since the power series associated with the orbifold identity should have no $(1-\eta)$ term due to the null-vectors $L_{-1}^{(r)}\cdot\mathbf{1}\equiv 0$, and both solutions should have the leading coefficient normalised to one, in our convention for the conformal blocks. With these requirements, one finds the fusing matrix P_{ij}^{-1} to be:

$$P^{-1}=\frac{1}{2}\begin{pmatrix}1 & 1\\ 3 & -3\end{pmatrix}. \tag{4.146}$$

Thus, the conformal blocks of (4.137) around $\eta=1$ are found to be:

$$\tilde{\mathcal{F}}_1(\eta)=\frac{\eta^{-1/3}+\eta^{1/3}}{2(1-\eta)^{4/9}}\,,\qquad \tilde{\mathcal{F}}_2(\eta)=\frac{3(\eta^{-1/3}-\eta^{1/3})}{2(1-\eta)^{4/9}}\,. \tag{4.147}$$

For the physical correlation function, we write

$$\langle\sigma_{13}(z,\bar{z})\rangle_{\mathbb{H}}^{f+}=\bar{z}^{-2h_{\sigma_{13}}}\left[\mathcal{A}^{(+)}_{\sigma_{13},\Psi_{\mathbf{1}}}\mathcal{B}^{(++f)\Psi_{12}}_{\Psi_{\mathbf{1}},\Psi_{12}}\tilde{\mathcal{F}}_1(\eta)+\mathcal{A}^{(+)}_{\sigma_{13},[\psi_{\mathbf{1}},\psi_{13},\psi_{13}]}\mathcal{B}^{(++f)\Psi_{12}}_{[\psi_{\mathbf{1}},\psi_{13},\psi_{13}],\Psi_{12}}\tilde{\mathcal{F}}_2(\eta)\right]. \tag{4.148}$$

Finally, we observe that $B^{(++f)\psi_{12}}_{\psi_{13}\psi_{12}}$ vanishes, and hence $\mathcal{B}^{(++f)\Psi_{12}}_{[\psi_{\mathbf{1}},\psi_{13},\psi_{13}],\Psi_{12}}=0$, so the expression (4.148) simplifies to:

$$\boxed{\langle\sigma_{13}(z,\bar{z})\rangle_{\mathbb{H}}^{f+}=2^{5/9}\times\frac{\cos(2\theta/3)}{(r\sin\theta)^{4/9}}\,,\qquad z=re^{i\theta}} \tag{4.149}$$

where we have also used:

$$\mathcal{A}^{(+)}_{\sigma_{13},\Psi_{\mathbf{1}}}=g_+^{-2}\,,\qquad \mathcal{B}^{(++f)\Psi_{12}}_{\Psi_{\mathbf{1}},\Psi_{12}}=1\,, \tag{4.150}$$

and the value of the ground-state degeneracy for fixed BC $g_+=1/\sqrt{2}$ in the Ising BCFT [217].

4.5.5 More hypergeometric differential equations in the Ising cyclic orbifold BCFTs

We have managed, in Sections 4.5.2 and 4.5.3 to obtain differential equations for cyclic orbifolds of generic mother BCFTs, but have not been able to provide analytic solutions for them.

One can, however, find second-order differential equations for particular choices of $\mathcal{M}_{p,p'}$ and composite twist fields (for the correlators of Section 4.5.2), in the manner presented in Section 4.5.4, which allow us to *exactly* determine the correlators. Since we want to compare the results of this section with lattice data of the critical Ising spin chain with mixed BC, it will be particularly satisfying to find such equations for the cyclic orbifolds of the Ising BCFT.

Let's first consider the correlator:

$$\langle\sigma_{13}(z,\bar{z})\rangle_{n=2}^{\alpha\beta} \tag{4.151}$$

in the $\mathbb{Z}_2$ Ising orbifold BCFT which should satisfy, up to a Möbius map, the same differential equation as:

$$\langle\Phi_{12}|\,\sigma_{13}(1)\sigma_{13}(\eta)\,|\Phi_{12}\rangle \tag{4.152}$$

The orbifold fusion rules of [119], imply that the space of conformal blocks is two-dimensional since:

$$\sum_i \mathcal{N}^i_{\sigma_{13},\sigma_{13}} \mathcal{N}^{\Phi_{12}}_{i,\Phi_{12}} = 2 \tag{4.153}$$

By the same type of arguments and assumptions as in Section 4.5.4, we infer that (4.152) satisfies a second-order Fuchsian differential equation with the following Riemann scheme:

0	1	∞
$-h_{\sigma_{13}} - 2h_{12} + h_{\sigma_\mathbf{1}}$	$-2h_{\sigma_{13}}$	$h_{\sigma_{13}} - 2h_{12} + h_{\sigma_{1,1}}$
$-h_{\sigma_{13}} - 2h_{12} + h_{\sigma_{13}} + \frac{1}{2}$	$-2h_{\sigma_{13}} + 2h_{13}$	$h_{\sigma_{13}} - 2h_{12} + h_{\sigma_{12}} + \frac{1}{2}$

so that we eventually find the one-point twist correlator to be

$$\langle \sigma_{13}(z,\bar{z})\rangle^{\alpha\beta}_{(n=2)} = \bar{z}^{-2h_{\sigma_{13}}} g_+^{-1} \tilde{\mathcal{F}}^{n=2}_{\Psi_\mathbf{1}}(\eta) \tag{4.154}$$

with

$$\boxed{\tilde{\mathcal{F}}^{(n=2)}_{\Psi_\mathbf{1}}(\eta) = \frac{1+\eta^{3/4}}{2(1-\eta)^{9/16}\eta^{3/8}}} \tag{4.155}$$

Finally, we can find an exact expression for the bare twist correlator:

$$\langle \sigma_\mathbf{1}(z,\bar{z})\rangle^{\alpha\beta}_{n=3} \tag{4.156}$$

in the $\mathbb{Z}_3$ Ising orbifold BCFT since it also satisfies a second order differential equation with Riemann scheme:

0	1	∞
$-h_{\sigma_\mathbf{1}} - 3h_{12} + h_{\sigma_{12}}$	$-2h_{\sigma_\mathbf{1}}$	$h_{\sigma_\mathbf{1}} - 3h_{12} + h_{\sigma_{12}}$
$-h_{\sigma_\mathbf{1}} - 3h_{12} + h_{\sigma_{12}} + \frac{1}{3}$	$-2h_{\sigma_\mathbf{1}} + 2h_{13}$	$h_{\sigma_\mathbf{1}} - 3h_{\Psi_{12}} + h_{\sigma_{12}} + \frac{1}{3}$

We find:

$$\langle \sigma_\mathbf{1}(z,\bar{z})\rangle^{\alpha\beta}_{n=3} = \bar{z}^{-1/9} g_+^{-2} \tilde{\mathcal{F}}^{n=3}_{\Psi_\mathbf{1}}(\eta) \tag{4.157}$$

with

$$\boxed{\tilde{\mathcal{F}}^{n=3}_{\Psi_\mathbf{1}}(\eta) = \frac{1+\eta^{1/3}}{2(1-\eta)^{1/9}\eta^{1/6}}} \tag{4.158}$$

Other results for the Ising BCFT. We have also obtained results specific to the $\mathbb{Z}_2$ and $\mathbb{Z}_3$ orbifolds of the Ising BCFT with fixed mixed BC with $\alpha = +$ and $\beta = -$, for which the most relevant primary BCCO is $\psi^{(+-)}_{2,1}$. Since these results are not based on deriving differential equations, it felt thematically appropriate to leave their presentation for the Appendix C.4.

4.6 Conclusion

In this chapter, we have presented a general method for calculating Rényi entropies $S_n^{\alpha\beta}$ in the ground state of a 1D critical system with mixed open boundaries, for an interval starting at one of its ends. This required computing three-point

functions of one twist operator and two BCCOs on the upper-half plane $\mathbb{H}$ with mixed BCs (α, β) in the $\mathbb{Z}_n$ cyclic orbifold.

For this purpose, we have derived ODEs satisfied by these correlation functions, by exploiting the null-vectors of the twisted and untwisted representations of its symmetry algebra OVir_n, together with Ward identities obtained from the additional conserved currents of the theory. We used a combination of analytical and numerical methods to find a basis of solutions (*a.k.a* conformal blocks) of these ODEs.

For the examples provided in this chapter, we have calculated the boundary and bulk-boundary structure constants needed to build the physical correlators as linear combinations of the blocks. Among the setups we have analysed are the leading and subleading contributions to the one-interval second and third Rényi entropies of the Ising model, and the second Rényi entropy for the three-state Potts model. We have also derived differential equations for mixed BC twist field correlators in the $\mathbb{Z}_2$ and $\mathbb{Z}_3$ orbifolds of generic BCFTs, and obtained an explicit expression for the second Rényi entropy valid for any diagonal minimal model, but with a particular set of mixed boundary conditions.

We have compared the CFT results against critical Ising and three-state Potts spin chain data. Since finite size effects are quite significant for open chains, we have included both the leading and subleading contributions to the lattice twist field correlator in our analytical prediction. In the Ising case, the agreement was excellent for all choices of mixed BC, even though the system sizes we could reach were limited. For the three-state Potts chain, however, the finite size effects are even more severe, and as a consequence, the matching is less satisfactory. This could be improved by using more sophisticated numerical techniques such as DMRG [49, 228] or tensor network methods [210].

The clearest limitation of our method, first identified in [118], is that the process for obtaining a differential equation becomes more difficult as n is increased. We have checked using the fusion rules in (5.4) for $n > 3$ that the expected order of the ODEs increases with n for generic minimal models, which implies that more orbifold Ward identities will be needed to obtain the ODEs.

There are several possible extensions of the work presented in this chapter. A possibility would be to generalize the setup for the calculation of Rényi entropies of an interval *contained in the bulk*, with mixed BC. However, in this situation, one would have to find a differential equation that a four-point function with two twist fields and two BCCOs satisfies. Cardy's doubling trick suggests that such a correlator satisfies the same Ward identities as a six-point conformal block on the complex plane, so the corresponding differential equation would be partial instead of ordinary.

Chapter 5

Operator algebra of the cyclic orbifold

5.1 Summary

In this chapter, we shall present a more detailed treatment of cyclic orbifold CFTs. Such theories have been of interest for the construction of certain types of superstring theories [70, 229], and constitute an active topic of research in the mathematical community [230][231] [232].

Our main motivation for better understanding them, is, as explained in Chapter 1, the study of entanglement in 1D critical systems. Beyond the examples presented in Sections 1.3, 1.4 (1.36), most situations involving boundaries [110, 152, 173], finite size and finite temperature [233–238], or simply several intervals [71, 84, 88, 123, 127, 132, 153, 163, 198–200, 239–241] are much more complicated and to this day remain mostly unsolved for generic CFTs. The main difficulty in such cases is that the Rényi entropy involves either the two-point function of twist fields on non-trivial surfaces (such as the upper-half-plane or the torus), or higher-point correlation functions. To make progress in such cases, a more comprehensive understanding of fusion rules and their multiplicities in the $\mathbb{Z}_n$ orbifold, as well as a full characterization of the conformal blocks is of crucial importance.

In this chapter, an adaptation of [211], we report some progress in that direction based on the identification of the maximal chiral algebra of the cyclic orbifold. Naively, the Virasoro algebra OVir_n is extended by $n-1$ simple currents, whose modes $L_m^{(r)}$ obey the following commutation relations [119]

$$\left[L_m^{(r)}, L_p^{(s)}\right] = (m-p)L_{m+p}^{(r+s)} + \frac{nc}{12} m(m^2-1)\,\delta_{m+p,0}\,\delta_{r+s,0}\,, \tag{5.1}$$

with $r, s \in \mathbb{Z}_n$. There is however an important caveat: these $n-1$ additional currents are not local, as they have non-trivial monodromies around the twist fields. This implies that acting with a mode $L_m^{(r)}$ on a local field yields a non-local one. Therefore, it is not possible to arrange *local fields* into modules of the orbifold chiral algebra OVir_n. The cornerstone of this chapter is to identify the maximal subalgebra of (the universal enveloping algebra of) OVir_n that acts locally on fields. It is generated by monomials of the form

$$L_{m_1}^{(r_1)} \dots L_{m_p}^{(r_p)} \quad \text{such that} \quad r_1 + \dots + r_p \equiv 0 \mod n\,, \tag{5.2}$$

In the following, we refer to this algebra as the *neutral algebra* and denote it by A_n.

For simplicity, we restrict our investigation to mother CFTs $\mathcal{M}$ which are diagonal and rational (*w.r.t.* to the action of the Virasoro algebra), thus containing finitely many primary fields ϕ_j. One of the main results is that the cyclic orbifold $\mathcal{M}_n$ is then also rational and diagonal *w.r.t.* the neutral algebra A_n. In particular, there are finitely many A_n-primary fields, i.e. annihilated by all monomials of the form (5.2) with $\sum_p m_p > 0$. These primary operators come in three varieties:

- *untwisted non-diagonal* $\Phi_{[j_1 \dots j_n]}$,
- *untwisted diagonal* $\Phi_j^{(r)}$,
- and *twisted* $\sigma_j^{[k](r)}$,

where $[j_1, \dots j_n]$ denotes the equivalence class of $(j_1, \dots, j_n)$ under $\mathbb{Z}_n$ permutations, $j, j_1, \dots, j_n$ run over the primary operator spectrum of the mother theory $\mathcal{M}$, while the Fourier replica index r and twist charge k take values in $\mathbb{Z}_n$ and $\mathbb{Z}_n^\times$, respectively. If we denote by $\chi_{[j_1 \dots j_n]}$, $\chi_j^{(r)}$ and $\chi_j^{[k](r)}$ the characters of the corresponding A_n-modules, the torus partition function is diagonal :

$$Z_{\text{orb}} = \sum_{J=[j_1 \dots j_n]} |\chi_J|^2 + \sum_j \sum_{r=0}^{n-1} |\chi_j^{(r)}|^2 + \sum_j \sum_{k=1}^{n-1} \sum_{r=0}^{n-1} |\chi_j^{[k](r)}|^2 \,, \tag{5.3}$$

As we shall argue, this classification of primary operators is particularly well suited for the determination of fusion rules, and the decomposition of correlation functions into conformal blocks. This classification has been suggested by the work of [119], which did not explicitly identify the neutral algebra A_n, but in fact determined the modular data and fusion rules for precisely the same set of operators, in the case $n = 2$. In this sense, the present chapter generalizes the results of [119] to any prime n. We give then a summary of our results:

Summary of results

- We establish the operator content of the $\mathbb{Z}_n$ orbifold CFT built from an arbitrary rational, diagonal Virasoro CFT model. The $\mathbb{Z}_n$ invariant primary operators are identified as the primary operators of the $A_n \oplus \bar{A}_n$ neutral algebra.
- We build the modules under the chiral algebra A_n, and the decomposition of the Hilbert space over these modules, for any prime n.
- We use the above decomposition property to characterize orbifold conformal blocks. This allows us to decompose any four-point correlation function of local primary operators in terms of finitely many holomorphic and antiholomorphic conformal blocks, indexed by A_n- and $\bar{A}_n$-modules, respectively.
- By studying the modular characters, and applying constraints arising from unitarity and modular relations to lift degeneracies, we obtain the orbifold $\mathcal{T}$ and $\mathcal{S}$ matrices. This leads, through the Verlinde formula, to explicit expressions of the orbifold fusion numbers $\mathcal{N}_{\alpha\beta}^{\gamma}$.

These fusion rules, in their most compact form, are given by:

Fusion rules in the cyclic orbifold

$$
\begin{aligned}
\mathcal{N}_{[i_1\dots i_n],[j_1\dots j_n]}^{[k_1\dots k_n]} &= \sum_{a,b=0}^{n-1} n_{i_{1+a},j_{1+b}}^{k_1}\dots n_{i_{n+a},j_{n+b}}^{k_n}\,,\\
\mathcal{N}_{[i_1\dots i_n],[j_1\dots j_n]}^{k^{(r)}} &= \sum_{a=0}^{n-1} n_{i_{1+a},j_1}^{k}\dots n_{i_{n+a},j_n}^{k}\,,\\
\mathcal{N}_{[i_1\dots i_n],j^{(r)}}^{k^{(s)}} &= n_{i_1,j}^{k}\dots n_{i_n,j}^{k}\,,\\
\mathcal{N}_{i^{(r)},j^{(s)}}^{k^{(t)}} &= \delta_{r+s,t}\, n_{ij}^{k}\,.\\
\mathcal{N}_{i^{[p](r)}j^{[q](s)}}^{[k_1\dots k_n]} &= \delta_{p+q,0}\sum_{\ell}\frac{S_{i\ell}S_{j\ell}\cdot S_{k_1\ell}\dots S_{k_n\ell}}{S_{1\ell}^{n}}\,,\\
\mathcal{N}_{i^{[p](r)}j^{[q](s)}}^{k^{(t)}} &= \frac{\delta_{p+q,0}}{n}\sum_{\ell}\left[\frac{S_{i\ell}S_{j\ell}S_{k\ell}^{n}}{S_{1\ell}^{n}}+\sum_{a=1}^{n-1}\omega^{np(r+s-t)}\frac{(P_{-a})_{i\ell}(P_{a})_{j\ell}S_{k\ell}}{S_{1\ell}}\right],\\
\mathcal{N}_{i^{[p](r)}j^{[q](s)}}^{k^{[m](t)}} &= \frac{\delta_{p+q,m}}{n}\sum_{\ell}\left[\frac{S_{i\ell}S_{j\ell}S_{k\ell}}{S_{1\ell}^{n}}+\sum_{a=1}^{n-1}\omega^{n(r+s-t)}\frac{(P^{\dagger}_{pa^{-1}})_{i\ell}(P^{\dagger}_{qa^{-1}})_{j\ell}(P_{ma^{-1}})_{k\ell}}{S_{1\ell}}\right].
\end{aligned}
\tag{5.4}
$$

Here n_{ij}^{k} and S_{ij} are, respectively, the fusion numbers and modular S-matrix of the mother theory, and ω stands for the first n$^{\text{th}}$ root of unity $\omega = \exp(2\pi i/n)$. The matrices P_a's, which are labelled by $a \in \mathbb{Z}_n^{\times}$ (*the multiplicative group of integers modulo n*) , are also modular matrices acting on characters of the mother CFT – see (5.118–5.119), and a^{-1} stands for the inverse of a in $\mathbb{Z}_n^{\times}$. The sums over ℓ run over the primary operators of the mother CFT.

The chapter is organized as follows. In Section 5.2, we define, for a generic integer n, the basic properties of the cyclic orbifold such as twist operators, the conserved currents $T^{(r)}$, the orbifold Virasoro algebra OVir_n, and the neutral algebras A_n. In Section 5.3, we restrict the discussion to n prime and describe the operator content, OPEs and conformal blocks. In Section 5.4, we analyse the modular properties of the torus partition function and derive the fusion numbers. In Section 5.5, we give some applications of our results for fusion rules and conformal blocks of the $\mathbb{Z}_3$ orbifold of minimal CFTs. In Section 5.6, we conclude with a recapitulation of our results and comment on possible refinements and extensions. We have relegated to the Appendix the more technical proofs, to avoid congesting the logical flow of the chapter.

5.2 Cyclic orbifolds

In this section, we provide some basic background on cyclic orbifolds $\mathcal{M}_n$, such as twist operators, the conserved currents, the symmetry algebra OVir_n, and the induction procedure.

5.2.1 The cyclic orbifold CFT

With the above motivation in mind, we define cyclic orbifold CFTs as follows. Let $\mathcal{M}$ be any CFT with central charge c and primary operator content $\{\phi_1, \phi_2, \phi_3, \dots\}$,

which we call the mother CFT. By convention, we always take ϕ_1 to be the identity operator: $\phi_1 = \mathbf{1}$. The cyclic orbifold CFT $\mathcal{M}$ for a positive integer n, which is usually denoted as

$$\mathcal{M}_n = \mathcal{M}^{\otimes n}/\mathbb{Z}_n\,, \tag{5.5}$$

is most easily defined in the path-integral formalism. If the configurations of the mother theory are described by a field $\varphi(r)$ with action $\mathcal{A}[\varphi]$, then the configurations of $\mathcal{M}^{\otimes n}$ are (locally) described by n independent copies $(\varphi_1(r), \dots \varphi_n(r))$, with action $\mathcal{A}[\varphi_1] + \cdots + \mathcal{A}[\varphi_n]$. Furthermore, the modding out by $\mathbb{Z}_n$ means that configurations with topological defects (as described in the previous section) are to be included. In particular, on the cylinder (and the torus, see section 5.4.1) this implies that one must consider all possible $\mathbb{Z}_n$ twisted boundary conditions. Accordingly, the Hilbert space (for a closed system) splits into n distinct sectors labelled by the *twist charge* $[k] \in \mathbb{Z}_n$, corresponding to boundary conditions twisted by the permutation of copies $a \mapsto a + k$. Via the state-operator correspondence, local fields also carry a twist charge.

In the untwisted sector $[k = 0]$, the Hilbert space is simply the n^{th} tensor product of the mother theory Hilbert space. The associated operators are called *untwisted* operators and are spanned by products of local operators acting on each copy. These are generated, under the Operator Product Expansion (OPE), by operators acting on a single copy a

$$\phi_a = \mathbf{1} \otimes \cdots \otimes \mathbf{1} \otimes \underset{(a)}{\phi} \otimes \mathbf{1} \otimes \cdots \otimes \mathbf{1}\,. \tag{5.6}$$

By contrast, the Hilbert space in the twisted sector $[k = 1]$ is in one-to-one correspondence with the mother theory Hilbert space [119]. Indeed, one can untangle the n copies coupled via the twist $a \to a+1$ into a single copy, at the cost of making the system n times larger. More generally, the Hilbert space in the twisted sector $[k]$ maps to the tensor product of C_k copies of the mother theory Hilbert space, where C_k is the number of cycles of the permutation $a \to a+k$ (in particular $C_k = 1$ exactly when k and n are coprime).

A generic operator $\mathcal{O}^{[k]}$ with twist charge $[k]$ inserts a defect line as explained above, and hence its monodromy relative to a diagonal operator ϕ_a reads:

$$\phi_a(e^{2i\pi}z, e^{-2i\pi}\bar{z}) \cdot \mathcal{O}^{[k]}(0) = \phi_{a-k}(z, \bar{z}) \cdot \mathcal{O}^{[k]}(0)\,. \tag{5.7}$$

being understood that upon going around the twisted field $\mathcal{O}^{[k]}(0)$, the field $\phi_a(z, \bar{z})$ does not encircle any other (twisted) field.

note that the twist charge $[k]$ is conserved under fusion, in the sense that

$$\langle \mathcal{O}_1^{[k_1]}(z_1, \bar{z}_1) \dots \mathcal{O}_m^{[k_n]}(z_n, \bar{z}_n)\rangle = 0 \quad \text{if} \quad k_1 + \cdots + k_m \neq 0 \mod n\,. \tag{5.8}$$

Of particular interest is the bare twist operator $\sigma^{[k]}$, which is simply the most relevant operator with twist charge $[k]$. Under the state-operator correspondence, it maps to the lowest energy state in the twisted sector $[k]$. In the untwisted sector, this is simply the identity $\sigma^{[0]} = \mathbf{1}$. Moreover, to lighten the notation, we write σ and $\sigma^\dagger$ instead of $\sigma^{[1]}$ and $\sigma^{[-1]}$, respectively. The conformal dimension of the twist operators σ and $\sigma^\dagger$ is

$$h_\sigma = \frac{c}{24}\left(n - \frac{1}{n}\right). \tag{5.9}$$

This fundamental result, which is at the heart of the universal behaviour 1.36 of entanglement entropy for 1D critical systems, is surprisingly easy to establish.

Indeed, it is a simple consequence of the finite-size scaling of eigenenergies in CFT. For a periodic system of size L, the orbifold Hamiltonian is $\frac{2\pi}{L}(L_0 + \overline{L}_0 - nc/12)$, as the orbifold central charge is nc, where c is the central charge of the mother theory. Thus, the lowest energy in the sector $[k = 1]$ is

$$E = \frac{4\pi}{L}\left(h_\sigma - \frac{nc}{24}\right). \tag{5.10}$$

since σ is a scalar field ($h_\sigma = \bar{h}_\sigma$). But as stated above, the twisted sector [1] for a system of size L is nothing but the Hilbert space of the mother theory for a system of size nL. From this perspective the Hamiltonian is $\frac{2\pi}{nL}(L_0 + \overline{L}_0 - c/12)$, and the state with the lowest energy is the vacuum, therefore

$$E = -\frac{4\pi}{nL}\frac{c}{24}. \tag{5.11}$$

Equating these two expressions yields (5.9). The argument is easy to generalize to arbitrary k, and one finds

$$h_{\sigma^{[k]}} = \frac{c}{24}\sum_{\text{cycle } j}\left(n_{kj} - \frac{1}{n_{kj}}\right). \tag{5.12}$$

where the sum is over all cycles of the permutation $a \mapsto a + k$, and n_{kj} is the length of the j^{th} cycle. In particular, when n is prime, one gets $h_{\sigma^{[k]}} = h_\sigma$ for all $k \in \mathbb{Z}_n^\times$.

5.2.2 Orbifold Virasoro algebra

now that we have discussed the splitting of the Hilbert space into twisted sectors, we can describe the action of the extended orbifold algebra. In the orbifold CFT $\mathcal{M}_n$, each copy a of the mother CFT carries the components $T_a(z), \overline{T}_a(\bar{z})$ of the stress-energy tensor, with OPEs

$$\begin{aligned} T_a(z)T_b(w) &= \delta_{ab}\left[\frac{c/2}{(z-w)^4} + \frac{2T_b(w)}{(z-w)^2} + \frac{\partial T_b(w)}{z-w}\right] + \mathrm{reg}_{z\to w}, \\ \overline{T}_a(\bar{z})\overline{T}_b(\bar{w}) &= \delta_{ab}\left[\frac{c/2}{(\bar{z}-\bar{w})^4} + \frac{2\overline{T}_b(\bar{w})}{(\bar{z}-\bar{w})^2} + \frac{\bar{\partial}\overline{T}_b(\bar{w})}{\bar{z}-\bar{w}}\right] + \mathrm{reg}_{\bar{z}\to\bar{w}}, \end{aligned} \tag{5.13}$$

where c is the central charge of the mother CFT, and $\mathrm{reg}_{z\to w}$ denotes a function which is regular as z tends to w. It turns out to be convenient to work with the discrete Fourier modes of these currents, namely

$$T^{(r)}(z) = \sum_{a=0}^{n-1}\omega^{ar}\,T_a(z), \qquad \overline{T}^{(r)}(\bar{z}) = \sum_{a=0}^{n-1}\omega^{ar}\,\overline{T}_a(\bar{z}), \tag{5.14}$$

where $\omega = \exp(2i\pi/n)$ and $r \in \mathbb{Z}_n$. We get the OPEs

$$\begin{aligned} T^{(r)}(z)T^{(s)}(w) &= \frac{\delta_{r+s,0}\,nc/2}{(z-w)^4} + \frac{2T^{(r+s)}(w)}{(z-w)^2} + \frac{\partial T^{(r+s)}(w)}{z-w} + \mathrm{reg}_{z\to w}, \\ \overline{T}^{(r)}(\bar{z})\overline{T}^{(s)}(\bar{w}) &= \frac{\delta_{r+s,0}\,nc/2}{(\bar{z}-\bar{w})^4} + \frac{2\overline{T}^{(r+s)}(\bar{w})}{(\bar{z}-\bar{w})^2} + \frac{\partial\overline{T}^{(r+s)}(\bar{w})}{\bar{z}-\bar{w}} + \mathrm{reg}_{\bar{z}\to\bar{w}}. \end{aligned} \tag{5.15}$$

The invariant modes $T^{(0)}(z)$ and $\overline{T}^{(0)}(\bar{z})$ are the components of the total stress-energy tensor of $\mathcal{M}_n$, with central charge nc, whereas the other Fourier modes $T^{(r)}(z), \overline{T}^{(r)}(\bar{z})$ with $r \neq 0 \mod n$ can be regarded as additional conserved currents. Altogether, these Fourier modes encode an extended conformal symmetry.

The Laurent expansion of the currents $T^{(r)}(z)$ depends on the twist sector in which they act. Indeed, since by definition an operator $\mathcal{O}^{[k]}$ with charge $[k]$ inserts a defect line connecting copies a and $a+k$, we have the monodromy conditions (in the absence of other twist operators in the vicinity of the origin)

$$T^{(r)}(e^{2i\pi}z) \cdot \mathcal{O}^{[k]}(0) = \omega^{kr} T^{(r)}(z) \cdot \mathcal{O}^{[k]}(0) \,. \tag{5.16}$$

As a result, the mode decomposition is of the form

$$T^{(r)}(z) \cdot \mathcal{O}^{[k]}(0) = \sum_{m \in -kr/n+\mathbb{Z}} z^{-m-2} \, (L_m^{(r)} \cdot \mathcal{O}^{[k]})(0) \ . \tag{5.17}$$

with $L_m^{(r)\dagger} = L_{-m}^{(-r)}$. Likewise, for $\overline{T}^{(r)}$ we have

$$\overline{T}^{(r)}(\bar{z}) \cdot \mathcal{O}^{[k]}(0) = \sum_{m \in +kr/n+\mathbb{Z}} \bar{z}^{-m-2} \, (\bar{L}_m^{(r)} \cdot \mathcal{O}^{[k]})(0) \ . \tag{5.18}$$

Importantly, in the twist sector $[k]$, the allowed indices for $L_m^{(r)}$ (resp. $\bar{L}_m^{(r)}$) are $m \in -kr/n + \mathbb{Z}$ (resp. $m \in +kr/n + \mathbb{Z}$). The OPEs (5.15) yield the commutation relations

$$\begin{aligned} \left[L_m^{(r)}, L_p^{(s)}\right] &= (m-p) L_{m+p}^{(r+s)} + \frac{nc}{12} m(m^2-1)\, \delta_{m+p,0}\, \delta_{r+s,0} \,, \\ \left[\bar{L}_m^{(r)}, \bar{L}_p^{(s)}\right] &= (m-p) \bar{L}_{m+p}^{(r+s)} + \frac{nc}{12} m(m^2-1)\, \delta_{m+p,0}\, \delta_{r+s,0} \,, \\ \left[L_m^{(r)}, \bar{L}_p^{(s)}\right] &= 0 \,, \end{aligned} \tag{5.19}$$

where the Kronecker symbols $\delta_{r+s,0}$ are understood modulo n. These relations define the two commuting orbifold Virasoro algebras OVir_n and $\overline{\mathrm{OVir}}_n$.

The invariant modes $L_m^{(0)}$ are the modes of the total stress-energy tensor, and their index m is always an integer, as it should be. Of course, they form a Virasoro algebra, with central charge nc:

$$\left[L_m^{(0)}, L_p^{(0)}\right] = (m-p) L_{m+p}^{(0)} + \frac{nc}{12} m(m^2-1)\, \delta_{m+p,0} \,, \qquad m \in \mathbb{Z} \,, \tag{5.20}$$

and similarly for the $\bar{L}_m^{(0)}$'s.

Due to the conservation of Fourier indices in the commutation relations (5.19), the two families of algebra elements

$$L_{m_1}^{(r_1)} \dots L_{m_p}^{(r_p)} \quad \text{and} \quad \bar{L}_{m_1}^{(r_1)} \dots \bar{L}_{m_p}^{(r_p)} \,, \qquad \text{with } r_1 + \dots + r_p = 0 \mod n \tag{5.21}$$

generate algebras of the universal enveloping algebra of OVir_n and $\overline{\mathrm{OVir}}_n$, which we shall call the *neutral algebras* A_n and $\bar{A}_n$, respectively. These neutral algebras are of key importance for the classification of operators and the description of correlations in the cyclic orbifold CFT.

5.2.3 Orbifold induction procedure

As mentioned above, the Hilbert space $\mathcal{H}^{[1]}$ of the twisted sector $[k = 1]$ is in one-to-one correspondence with the Hilbert space $\mathcal{H}$ of the mother theory [119]. More precisely, there is an isomorphism $\Theta_1 : \mathcal{H} \to \mathcal{H}^{[1]}$, that is a norm-preserving, invertible linear map. This map is quite simple: it encodes the identification of states between $\mathcal{H}^{[1]}$ and $\mathcal{H}$ that follows from unfolding the n copies of the cylinder with twisted boundary conditions into a single copy of the cylinder.

In particular, we get the following identification between the stress-tensor T of the mother theory (on the cylinder of perimeter nL) and the stress-tensor T_a acting on the a^{th} copy of the orbifold on the cylinder of perimeter L:

$$T_a(x,t) = \Theta_1\, T(aL + x, t)\, \Theta_1^{-1}\,, \tag{5.22}$$

where $0 \leq x < L$ and $a = 0, \cdots, n-1$. In terms of modes, this means

$$\left(L_m^{(r)} - \delta_{m,0}\frac{nc}{24}\right) = \frac{1}{n}\Theta_1\left(L_{nm} - \delta_{m,0}\frac{c}{24}\right)\Theta_1^{-1}\,, \qquad m \in -r/n + \mathbb{Z}\,, \tag{5.23}$$

that is to say

$$L_m^{(r)} = \frac{1}{n}\Theta_1 L_{nm}\Theta_1^{-1} + \frac{c}{24}\left(n - \frac{1}{n}\right)\delta_{m0}\,, \qquad m \in -r/n + \mathbb{Z}\,. \tag{5.24}$$

It follows that there is a one-to-one correspondence between Virasoro primary states $|\phi_j\rangle$ in the mother theory and primary states under the orbifold algebra in the twisted sector $[k = 1]$ of the cyclic orbifold, which we will denote by $|\sigma_j^{[1]}\rangle$:

$$|\sigma_j^{[1]}\rangle = \Theta_1\,|\phi_j\rangle\ . \tag{5.25}$$

The same elementary argument of finite-size scaling is used to derive (5.9) yields

$$h_{\sigma_j} = \frac{c}{24}\left(n - \frac{1}{n}\right) + \frac{h_j}{n} = h_\sigma + \frac{h_j}{n}\,. \tag{5.26}$$

The identification map Θ_1 provides a comprehensive and explicit construction of the twisted sector $[k = 1]$ in terms of states of the mother theory, known as the *orbifold induction procedure* [119]. Furthermore, since Θ_1 is norm-preserving, a state in the twisted sector is a null state if and only if it is the image (under Θ_1) of a null state in the mother theory. In that sense, the induction procedure provides a full description of all null states in the twisted sector. Such null states are important, as they can be exploited to derive differential equations for twist correlation functions [118].

Of course, the above discussion can be adapted to all twisted sectors $[k]$. In particular, when k and n are coprime (that is when the permutation $a \to a + k$ mod n has a unique cycle), the Hilbert space $\mathcal{H}^{[k]}$ can still be identified with $\mathcal{H}$, via a map $\Theta_k : \mathcal{H} \to \mathcal{H}^{[k]}$. The relation between modes becomes simply

$$L_m^{(r)} = \frac{1}{n}\Theta_k L_{nm}\Theta_k^{-1} + \frac{c}{24}\left(n - \frac{1}{n}\right)\delta_{m0}\,, \qquad m \in -kr/n + \mathbb{Z}\,. \tag{5.27}$$

The state $|\sigma_j^{[k]}\rangle = \Theta_k\,|\phi_j\rangle$ has the same conformal dimension as $|\sigma_j^{[1]}\rangle$.

5.3 Operator content, OPEs and conformal blocks

From now on, we restrict to the case when the number of copies is a prime integer n. We shall describe the operator content of the cyclic orbifold CFT $\mathcal{M}_n$, in terms of the primary operators $\{\phi_j\}$ of the mother CFT $\mathcal{M}$. In $\mathcal{M}_n$, operators and states will be organized into representations of the neutral algebras $A_n \oplus \bar{A}_n$ defined in Sec. 5.2.2.

To simplify the discussion, we suppose that the mother CFT is diagonal, namely every primary operator ϕ_j is scalar, so that its conformal dimensions obey $h_j = \bar{h}_j$, and all primaries correspond to distinct Virasoro modules. This is the case in particular for all diagonal minimal models. Under these assumptions, the torus partition function is a diagonal modular invariant

$$Z = \sum_j |\chi_j|^2 \tag{5.28}$$

and the modular S-matrix is real symmetric. The fusion numbers n_{ij}^k, as given by the Verlinde formula

$$n_{ij}^k = \sum_m \frac{S_{im} S_{jm} \bar{S}_{mk}}{S_{\mathbf{1}m}}\,, \tag{5.29}$$

can only take the values 0 or 1.

5.3.1 Invariant operators

Local operators in the $\mathbb{Z}_n$ orbifold must form a set of mutually local fields. In particular, they must be local with respect to the twist fields, *i.e.* be invariant under cyclic permutations. In that sense, gauging the $\mathbb{Z}_n$ symmetry in the replicated theory $\mathcal{M}^{\otimes n}$ removes [1] all fields in $\mathcal{M}^{\otimes n}$ that are not $\mathbb{Z}_n$ invariant. It turns out that this condition is also sufficient: all invariant fields are local, as we will show in section 5.4.1. Throughout the chapter, we will use the terms *local* and *invariant* interchangeably when referring to fields/operators.

Importantly, the currents $T^{(r)}(z)$ themselves are *not local* for $r \neq 0$, since they have non-trivial monodromies around twist fields (5.16). This means that acting with a mode $L_m^{(r)}$ on a local field yields a non-local one, and therefore it is not possible to decompose local fields into modules of the full orbifold algebra $\mathrm{OVir}_n \oplus \overline{\mathrm{OVir}}_n$. Instead, one has to work with the neutral algebra A_n.

Invariant operators can be classified into three families of primary operators and their descendants, with respect to the neutral algebras $A_n \oplus \bar{A}_n$. In this section, we enumerate all $(P^n - P)/n + n^2 P$ primary invariant operators, where P is the number of primary fields in the mother theory.

The proofs that these operators are primary and that the action of $A_n \oplus \bar{A}_n$ on them generates all invariant operators, are given in Appendix D.1.

The non-diagonal untwisted operators $\Phi_{[j_1 \dots j_n]}$. They are defined as

$$\Phi_J = \Phi_{[j_1,\cdots,j_n]} := \frac{1}{\sqrt{n}} \sum_{a=0}^{n-1} (\phi_{j_{1+a}} \otimes \cdots \otimes \phi_{j_{n+a}})\,, \tag{5.30}$$

[1] Such fields are not really removed: they are downgraded to semilocal fields in the cyclic orbifold. At the level of states, while they do not contribute to the torus partition function, they do contribute to twisted partition functions [36].

where $J = [j_1, \cdots, j_n]$ stands for the n-tuple $(j_1, \cdots, j_n)$ modulo $\mathbb{Z}_n$, that is the equivalence class of $(j_1, \ldots, j_n)$ under cyclic permutations. The indices $(1+a), \ldots, (n+a)$ in (5.30) are understood modulo n. Part of the definition is to demand that at least two labels among $(j_1, \cdots, j_n)$ are distinct, ensuring that the fields $\phi_{j_{1+a}} \otimes \cdots \otimes \phi_{j_{n+a}}$, for $0 \leq a \leq n-1$ are linearly independent. Each ϕ_j stands for a primary operator in the mother CFT. The conformal dimension of Φ_J is

$$h_{[j_1,\cdots,j_n]} = h_{j_1} + \cdots + h_{j_n}\,, \tag{5.31}$$

where h_j is the conformal dimension of ϕ_j.

The diagonal untwisted operators $\Phi_j^{(r)}$, with $r \in \mathbb{Z}_n$. For $r = 0$, let

$$\Phi_j^{(0)} = \Phi_j := \phi_j \otimes \cdots \otimes \phi_j\,, \tag{5.32}$$

where ϕ_j is a primary operator in the mother CFT. For $r \neq 0 \mod n$, we define

$$\Phi_j^{(r)} := \frac{1}{2nh_j} L_{-1}^{(r)} \bar{L}_{-1}^{(-r)} \cdot \Phi_j \qquad \text{for } \phi_j \neq \mathbf{1}\,, \tag{5.33}$$

and

$$\mathbf{1}^{(r)} := \frac{2}{nc} L_{-2}^{(r)} \bar{L}_{-2}^{(-r)} \cdot \mathbf{1} = \frac{2}{nc} T^{(r)} \overline{T}^{(-r)}\,. \tag{5.34}$$

Recall that by convention, $\phi_1 = \mathbf{1}$ in the mother CFT. The reason for introducing a specific definition of the operators $\mathbf{1}^{(r)}$ is the fact that $L_{-1}^{(r)} \cdot \mathbf{1} = \bar{L}_{-1}^{(r)} \cdot \mathbf{1} = 0$, due to the null-vector conditions $L_{-1} \cdot \mathbf{1} = \bar{L}_{-1} \cdot \mathbf{1} = 0$ in the mother CFT. The corresponding conformal dimensions are

$$h_j^{(r)} = nh_j + (1 - \delta_{r0}) \qquad \text{for } \phi_j \neq \mathbf{1}\,, \tag{5.35}$$

$$h_1^{(r)} = 2(1 - \delta_{r0})\,. \tag{5.36}$$

The prefactors in (5.33–5.34) are chosen to normalize the two-point function – see below.

The twist operators $\sigma_j^{[k](r)}$. These operators are indexed by three labels: j identifies a primary field ϕ_j in the mother theory, $k \neq 0 \mod n$ labels the twisted sector, and r takes values in $\mathbb{Z}_n$. When $j = 1$ and $r = 0$, they simply correspond to the "bare" twist operators

$$\sigma_{\mathbf{1}}^{[k](0)} := \sigma^{[k]}\,, \tag{5.37}$$

and they all have conformal dimension

$$h_\sigma = \frac{c}{24}\left(n - \frac{1}{n}\right). \tag{5.38}$$

as follows from the state-operator correspondence and the finite size scaling argument above (5.9). For $j \neq 1$ and $r = 0$, the twist operator $\sigma_j^{[k](0)} := \sigma_j^{[k]}$ is the field associated to the state $|\sigma_j^{[k]}\rangle$ (as defined in section (5.2.3)) under the state-operator correspondence. This defines a *composite twist operator*, with conformal dimension given by (5.26), that is :

$$h_{\sigma_j} = h_\sigma + \frac{h_j}{n}\,. \tag{5.39}$$

Alternatively, this composite twist field can be constructed as the most relevant field obtained in the fusion

$$\Phi_{[j,\mathbf{1},\dots,\mathbf{1}]} \times \sigma_{\mathbf{1}}^{[k](0)} \tag{5.40}$$

where the field $\Phi_{[j,\mathbf{1},\dots,\mathbf{1}]}$ is defined at (5.30). Formally [219, 242] :

$$\sigma_j^{[k](0)}(z,\bar{z}) = \mathcal{A}_j \lim_{\epsilon\to 0}\left[\epsilon^{2(1-n^{-1})h_j}\Phi_{[j,\mathbf{1},\dots,\mathbf{1}]}(z+\epsilon,\bar{z}+\bar{\epsilon})\cdot\sigma^{[k]}(z,\bar{z})\right], \tag{5.41}$$

where $\Phi_{[j,\mathbf{1},\dots,\mathbf{1}]}$ is the non-diagonal untwisted operator given above, and h_j is the conformal dimension of ϕ_j, and the constant prefactor is $\mathcal{A}_j = n^{-2(1-n^{-1})h_j - 1/2}$. As explained in section (5.2.3), the operators $\sigma_j^{[k]}$ are also primary under $\mathrm{OVir}_n \oplus \overline{\mathrm{OVir}}_n$.

For $r \neq 0$ the twist operators $\sigma_j^{[k](r)}$ are given by

$$\sigma_j^{[k](r)} := \begin{cases} \mathcal{B}_{j,[\![kr]\!]}\, L^{(r)}_{-[\![kr]\!]/n}\bar{L}^{(-r)}_{-[\![kr]\!]/n}\cdot\sigma_j^{[k]} & \text{if } \phi_j \neq \mathbf{1} \text{ or } kr \neq 1 \mod n\,, \\ \mathcal{B}_{1,n+1}\, L^{(r)}_{-1-1/n}\bar{L}^{(-r)}_{-1-1/n}\cdot\sigma^{[k]} & \text{otherwise,}\end{cases} \tag{5.42}$$

or equivalently as states

$$|\sigma_j^{[k](r)}\rangle := n^{-2}\Theta_k \begin{cases} \mathcal{B}_{j,[\![kr]\!]}\, L_{-[\![kr]\!]}\bar{L}_{-[\![kr]\!]}\,|\phi_j\rangle & \text{if } \phi_j \neq \mathbf{1} \text{ or } kr \neq 1 \mod n\,, \\ \mathcal{B}_{1,n+1}\, L_{-(n+1)}\bar{L}_{-(n+1)}\,|0\rangle & \text{otherwise.}\end{cases} \tag{5.43}$$

where $[\![m]\!]$ stands for the remainder of the Euclidean division of m by n, that is the unique integer in the interval $\{0,\dots,n-1\}$ such that $[\![m]\!] = m \mod n$. The constant prefactors $\mathcal{B}_{j,m} = n^2\left[2mh_j + cm(m^2-1)/12\right]^{-1}$ are included to normalize the two-point function in the usual way (5.47).

The case $j = \mathbf{1}$ has to be treated separately because of the null-vector relations obeyed by the bare twist operators [118, 119]:

$$L^{(k^{-1})}_{-1/n}\cdot\sigma^{[k]} = 0\,, \qquad \bar{L}^{(-k^{-1})}_{-1/n}\cdot\sigma^{[k]} = 0\,. \tag{5.44}$$

The conformal dimension of $\sigma_j^{[k](r)}$ is

$$h_j^{[k](r)} = \begin{cases} h_{\sigma_j} + \frac{[\![kr]\!]}{n} & \text{if } \phi_j \neq \mathbf{1} \text{ or } kr \neq 1 \mod n\,, \\ h_\sigma + \frac{n+1}{n} & \text{otherwise.}\end{cases} \tag{5.45}$$

Property. All the operators in the above list are primary under the neutral algebra $A_n \oplus \bar{A}_n$. They are local, by virtue of being invariant under cyclic permutations of copies. They are scalar operators, namely they have conformal dimensions $h = \bar{h}$. Moreover, these are the only fields with these properties: any invariant operator in $\mathcal{M}_n$ can be obtained by acting with $A_n \oplus \bar{A}_n$ on one of these invariant primary operators. These fundamental properties are proven in Appendix D.1.

Two-point functions. The normalization factors have been chosen so that the two-point functions are given by

$$\begin{aligned}
&\langle\Phi_{[j_1,\dots,j_n]}(z,\bar{z})\Phi_{[j_1,\dots,j_n]}(w,\bar{w})\rangle = |z-w|^{-4h_{[j_1,\dots,j_n]}}\,, \\
&\langle\Phi_j^{(r)}(z,\bar{z})\Phi_j^{(-r)}(w,\bar{w})\rangle = |z-w|^{-4h_j^{(r)}}\,, \\
&\langle\sigma_j^{[k](r)}(z,\bar{z})\sigma_j^{[-k](-r)}(w,\bar{w})\rangle = |z-w|^{-4h_j^{[k](r)}}\,,
\end{aligned} \tag{5.46}$$

where $r \in \mathbb{Z}_n$ and $k \in \mathbb{Z}_n^\times$. Any other two-point function of invariant primary operators vanishes. This can be summarized by writing

$$\langle \Phi_\alpha(z,\bar{z}) \Phi_\beta^\dagger(w,\bar{w}) \rangle = \delta_{\alpha\beta} \, |z-w|^{-4h_\alpha} \,, \tag{5.47}$$

where Φ_α denotes an operator of the form $\Phi_{[j_1\dots j_n]}$, $\Phi_j^{(r)}$ or $\sigma_j^{[k](r)}$, and the conjugation $\alpha \to \alpha^\dagger$ acts as

$$[j_1 \dots j_n] \to [j_1 \dots j_n] \tag{5.48}$$
$$j,(r) \to j,(-r) \tag{5.49}$$
$$j,[k],(r) \to j,[-k],(-r) \tag{5.50}$$

5.3.2 Invariant Hilbert space

In any *chiral* OVir_n-module with a lowest-weight state $|h_\alpha\rangle$, we can define a formal cyclic permutation operator π by

$$\pi \cdot |h_\alpha\rangle := |h_\alpha\rangle \,, \qquad \pi \cdot L_m^{(r)} := \omega^r \, L_m^{(r)} \cdot \pi \,, \tag{5.51}$$

and similarly for an $\overline{\mathrm{OVir}}_n$-module. With this definition, we have $\pi^n = \mathbf{1}$, and hence the operator

$$P_r = \frac{1}{n} \sum_{a=0}^{n-1} \omega^{-ar} \, \pi^a \,. \tag{5.52}$$

is the projector on the eigenspace of π corresponding to the eigenvalue ω^r.

For any invariant primary operator Φ_α of the form $\Phi_{[j_1\dots j_n]}$, $\Phi_j^{(r)}$ or $\sigma_j^{[k](r)}$, we denote by $\mathcal{V}_\alpha$ the corresponding $(A_n \oplus \bar{A}_n)$-module. The action of A_n (resp. $\bar{A}_n$) on the highest weight state $|h_\alpha\rangle$ generates an A_n-module (resp. $\bar{A}_n$-module), which we denote as V_α (resp. $\bar{V}_\alpha$). Since A_n and $\bar{A}_n$ commute, we have

$$\mathcal{V}_\alpha \simeq V_\alpha \otimes \bar{V}_\alpha \,. \tag{5.53}$$

It turns out that the A_n-modules V_α associated to the three types of invariant primary operators Φ_α in the orbifold model can be viewed as eigenspaces of π in OVir_n-modules, namely

$$V_{[j_1,\dots,j_n]} \simeq P_0 \cdot (v_{j_1} \otimes \dots \otimes v_{j_n}) \,, \quad V_j^{(r)} \simeq P_r \cdot (v_j \otimes \dots \otimes v_j) \,, \quad V_j^{[k](r)} \simeq P_r \cdot \Theta_k \cdot v_j \,. \tag{5.54}$$

Here, we have denoted by v_j the Vir-module associated with the primary operator ϕ_j in the mother CFT, and we have used the induction isomorphisms Θ_k introduced in Sec. 5.2.3. For $\bar{A}_n$-modules we have

$$\bar{V}_{[j_1,\dots,j_n]} \simeq P_0 \cdot (\bar{v}_{j_1} \otimes \dots \otimes \bar{v}_{j_n}) \,, \quad \bar{V}_j^{(r)} \simeq P_{-r} \cdot (\bar{v}_j \otimes \dots \otimes \bar{v}_j) \,, \quad \bar{V}_j^{[k](r)} \simeq P_{-r} \cdot \Theta_k \cdot \bar{v}_j \,, \tag{5.55}$$

where the $\bar{v}_j$'s are the mother CFT's $\overline{\mathrm{Vir}}$-modules.

Let $\mathcal{H}_0$ be the space of $\mathcal{M}_n$ states which are invariant under cyclic permutations. We shall refer to $\mathcal{H}_0$ as the *invariant Hilbert space*. As a consequence of the classification of invariant operators presented in Sec. 5.3.1, one gets the $(A_n \oplus \bar{A}_n)$-module decomposition of $\mathcal{H}_0$:

$$\mathcal{H}_0 = \bigoplus_{J=[j_1\dots j_n]} \mathcal{V}_J \quad \oplus \quad \bigoplus_j \bigoplus_{r=0}^{n-1} \mathcal{V}_j^{(r)} \quad \oplus \quad \bigoplus_j \bigoplus_{k=1}^{n-1} \bigoplus_{r=0}^{n-1} \mathcal{V}_j^{[k](r)} \,. \tag{5.56}$$

In this expression, the sums on j run over the primary operators ϕ_j of the mother CFT, whereas the sum on $[j_1 \dots j_n]$ runs over the equivalence classes of n-tuples $(j_1, \dots, j_n)$ under cyclic permutations, where the j_a's are indices of primary operators of the mother CFT, and with at least two distinct indices $j_a \neq j_b$.

5.3.3 On fusion numbers

Before moving on to operator product expansions and conformal blocks, it is useful to discuss fusion numbers. From the above discussion, the cyclic orbifold is a diagonal theory with respect to the extended symmetry $A_n \oplus \bar{A}_n$, therefore operators $\{\Phi_\alpha\}$ are labelled by a single symbol α, also labelling the irreducible A_n-modules $\{V_\alpha\}$. The fusion rules are generically of the form

$$\Phi_\alpha \times \Phi_\beta \to \sum_\gamma \mathcal{N}_{\alpha\beta}^\gamma \, \Phi_\gamma \,, \tag{5.57}$$

where the sum is over all primary invariant operators Φ_γ, and the non-negative integers $\mathcal{N}_{\alpha\beta}^\gamma$ are the fusion numbers. They obey

$$\mathcal{N}_{\alpha\beta}^\gamma = \mathcal{N}_{\beta\alpha}^\gamma \,, \qquad \mathcal{N}_{\alpha\beta}^\gamma = \mathcal{N}_{\alpha\gamma^\dagger}^{\beta^\dagger} \,. \tag{5.58}$$

Recall that we are assuming that, in the mother theory, all fusion numbers n_{ij}^k are 0 or 1. But in the orbifold, non-trivial multiplicities (*i.e.* $\mathcal{N}_{\alpha\beta}^\gamma > 1$) are expected to appear. The fusion number $\mathcal{N}_{\alpha\beta}^\gamma$ is the dimension of the space of chiral vertex operators [243] of type $\binom{\gamma}{\alpha\beta}$. Chiral three-point functions

$$C_{\alpha\beta}^\gamma(\lambda, \mu, \nu) = \langle \Phi_\gamma | \nu^\dagger \, (\lambda \cdot \Phi_\alpha)(1) \, \mu | \Phi_\beta \rangle \tag{5.59}$$

for $\lambda, \mu, \nu \in A_n$ are not all linearly independent. Indeed, they satisfy many linear relations following from:

1. The commutation rules of A_n, which follow from

$$\left[L_m^{(r)}, L_p^{(s)} \right] = (m-p) L_{m+p}^{(r+s)} + \frac{nc}{12} m(m^2-1) \, \delta_{m+p,0} \, \delta_{r+s,0} \,. \tag{5.60}$$

2. The properties of primary operators and states

$$[L_m^{(0)}, \Phi_\alpha(z,\bar{z})] = z^m \left((m+1) h_\alpha + z\partial_z \right) \Phi_\alpha(z,\bar{z}) \,, \tag{5.61}$$

$$\langle \Phi_\gamma | \, L_{m<0}^{(r)} = 0 \,, \qquad \langle \Phi_\gamma | \, L_0^{(0)} = h_\gamma \, \langle \Phi_\gamma | \,, \tag{5.62}$$

$$L_{m>0}^{(r)} \, | \Phi_\alpha \rangle = 0 \,, \qquad L_0^{(0)} \, | \Phi_\alpha \rangle = h_\alpha \, | \Phi_\alpha \rangle \,. \tag{5.63}$$

3. The Ward identities associated with the OVir_n currents. These can be expressed generally as closed contour identities, for any m-tuple of operators $\Phi_1, \dots, \Phi_m$ (primary or not) with twist charges $k_1, \dots, k_m$:

$$\oint dz \, (z-z_1)^{q_1} \dots (z-z_m)^{q_m} \, \langle T^{(r)}(z) \Phi_1(z_1,\bar{z}_1) \dots \Phi_m(z_m,\bar{z}_m) \rangle = 0 \,,$$
$$\text{if } q_j \in -\frac{rk_j}{n} + \mathbb{Z} \text{ and } q_1 + \dots + q_m \leq 2 \,. \tag{5.64}$$

4. The decoupling of null-vectors (*e.g.* if $\mu|\Phi_\beta\rangle$ is null, then $C^\gamma_{\alpha\beta}(\lambda,\mu,\nu)=0$).

For instance, using (5.61) and (5.63), we have for $m>0$:

$$C^\gamma_{\alpha\beta}(\mathbf{1},\mathbf{1},L^{(0)}_{-m})=\langle\Phi_\gamma|L_m\Phi_\alpha(1)|\Phi_\beta\rangle=\Big((m+1)h_\alpha-2h_\alpha-2h_\beta+2h_\gamma\Big)C^\gamma_{\alpha\beta}(\mathbf{1},\mathbf{1},\mathbf{1})\,. \quad (5.65)$$

Consider the whole set of constraints (5.60–5.64) plus the decoupling of null-vectors as a linear system of equations for the function

$$\begin{cases} A_n\otimes A_n\otimes A_n & \to & \mathbb{C} \\ (\lambda,\mu,\nu) & \mapsto & C^\gamma_{\alpha\beta}(\lambda,\mu,\nu)=\langle\Phi_\gamma|\nu^\dagger\,(\lambda\cdot\Phi_\alpha)(1)\,\mu|\Phi_\beta\rangle\,. \end{cases}$$

Then $\mathcal{N}^\gamma_{\alpha\beta}$ is the dimension of the solution space of this linear system. By the use of orbifold Ward identities, one can show that the subset of coefficients

$$C^\gamma_{\alpha\beta}(\mu):=C^\gamma_{\alpha\beta}(\mathbf{1},\mu,\mathbf{1})=\langle\Phi_\gamma|\Phi_\alpha(1)\mu|\Phi_\beta\rangle\,, \quad (5.66)$$

determines uniquely all the other coefficients $C^\gamma_{\alpha\beta}(\lambda,\mu,\nu)$. Hence, $\mathcal{N}^\gamma_{\alpha\beta}$ corresponds to the number of linearly independent solutions for the function $\mu\mapsto C^\gamma_{\alpha\beta}(\mu)$, subject to (5.60–5.64). Let $\left(C_{\alpha\beta}\right)_m$, with $m=1,\cdots,\mathcal{N}^\gamma_{\alpha\beta}$, denote a basis of these solutions.

If we now return to the physical three-point function (that is including the anti-holomorphic degrees of freedom), generically we have

$$\langle\Phi_\gamma|\Phi_\alpha(1,\bar1)\mu\bar\mu|\Phi_\beta\rangle=\sum_{m,n=1}^{\mathcal{N}^\gamma_{\alpha\beta}}\kappa_{m,p}\left(C^\gamma_{\alpha\beta}\right)_m(\mu)\left(C^\gamma_{\alpha\beta}\right)_p(\bar\mu)\,. \quad (5.67)$$

However since the application $(\mu,\bar\mu)\to\langle\Phi_\gamma|\Phi_\alpha(1,\bar1)\mu\bar\mu|\Phi_\beta\rangle$ is bilinear and symmetric, there exists a (real) basis $\left(X_{\alpha\beta}\right)_m$, such that

$$\langle\Phi_\gamma|\Phi_\alpha(1,\bar1)\mu\bar\mu|\Phi_\beta\rangle=\sum_{m=1}^{\mathcal{N}^\gamma_{\alpha\beta}}\epsilon_m\left(X^\gamma_{\alpha\beta}\right)_m(\mu)\left(X^\gamma_{\alpha\beta}\right)_m(\bar\mu)\,, \quad (5.68)$$

where $\epsilon_m\in\{-1,0,1\}$. The naturality theorem [244] implies that the above bilinear form has maximal rank, thus $\epsilon_m=0$ must be excluded.

Let's consider for instance the fusion process involving three non-diagonal untwisted operators

$$\Phi_{[i_1\ldots i_n]}\times\Phi_{[j_1\ldots j_n]}\to\Phi_{[k_1\ldots k_n]}\,. \quad (5.69)$$

For compactness we introduce the shorthand notation $I=[i_1\ldots i_n]$, $J=[j_1\ldots j_n]$ and $K=[k_1\ldots k_n]$. Consider the following physical three-point function

$$C^K_{IJ}(\mu,\bar\mu)=\langle\Phi_K\Phi_I(\mu\,\bar\mu\cdot\Phi_J)\rangle\,, \quad (5.70)$$

for $\mu\in A_n$ and $\bar\mu\in\bar A_n$. Using the definition of $\Phi_{[i_1\ldots i_n]},\Phi_{[j_1\ldots j_n]},\Phi_{[k_1\ldots k_n]}$ and the fact that $\mu,\bar\mu$ are invariant under the cyclic permutation Π, one can write

$$C^K_{IJ}(\mu,\bar\mu)=\sum_{a,b=0}^{n-1}\left(C^K_{IJ}\right)_{ab}(\mu,\bar\mu)\,, \quad (5.71)$$

where (with a slight abuse of notation, as we now treat I, J and K as n-tuples)

$$\left(C_{IJ}^{K}\right)_{ab}(\mu,\bar{\mu}) := \frac{1}{\sqrt{n}}\langle \Pi^{a}[\phi_{k_1}\otimes\cdots\otimes\phi_{k_n}]\,\Pi^{b}[\phi_{i_1}\otimes\cdots\otimes\phi_{i_n}]\,(\mu\,\bar{\mu}\cdot(\phi_{j_1}\otimes\cdots\otimes\phi_{j_n}))\rangle\,. \quad (5.72)$$

and Π is the generator of cyclic permutations : $\Pi[\phi_{i_1}\otimes\cdots\otimes\phi_{i_n}] = [\phi_{i_2}\otimes\phi_{i_3}\otimes\cdots\otimes\phi_{i_1}]$. A closer inspection reveals that each symmetric bilinear form $\left(C_{IJ}^{K}\right)_{ab}$ is rank at most one. Indeed, decomposing

$$\mu = L_{m_1}^{(r_1)}\ldots L_{m_p}^{(r_p)} \quad (5.73)$$

together with

$$L_{m}^{(r)} = \sum_{j=0}^{n-1}\omega^{jr}\,\mathbf{1}\otimes\cdots\otimes\underset{(j)}{L_m}\otimes\cdots\otimes\mathbf{1}\,, \quad (5.74)$$

and likewise for $\bar{\mu}$, one ends up with a sum of products of three-point functions in the mother theory of the form

$$\prod_{c}\langle\phi_{k_{c+a}}\phi_{i_{c+b}}\left(\lambda_c\bar{\lambda}_c\cdot\phi_{j_c}\right)\rangle \quad (5.75)$$

where $\lambda,\bar{\lambda}$ are in (the enveloping algebra of) Virasoro. For each term in the product, we have

$$\langle\phi_k\phi_i(\lambda\,\bar{\lambda}\cdot\phi_j)\rangle = \begin{cases}\langle\phi_k\phi_i\phi_j\rangle\,x_{ij}^{k}(\lambda)x_{ij}^{k}(\bar{\lambda}) & \text{if } n_{ij}^{k}=1\,,\\ 0 & \text{if } n_{ij}^{k}=0\,,\end{cases} \quad (5.76)$$

where $x_{ij}^{k}(\lambda)$ is uniquely determined by the Virasoro analogue of (5.60–5.64). Clearly $\left(C_{IJ}^{K}\right)_{ab}$ vanishes unless

$$\langle\phi_{k_{1+a}}\phi_{i_{1+b}}\phi_{j_1}\rangle\ldots\langle\phi_{k_{c+a}}\phi_{i_{c+b}}\phi_{j_c}\rangle\ldots\langle\phi_{k_{n+a}}\phi_{i_{n+b}}\phi_{j_n}\rangle\neq 0 \quad (5.77)$$

Moreover, when it does not vanish, it factorizes as

$$\left(C_{IJ}^{K}\right)_{ab}(\mu,\bar{\mu}) := \left(X_{IJ}^{K}\right)_{ab}(\mu)\left(X_{IJ}^{K}\right)_{ab}(\bar{\mu}) \quad (5.78)$$

where the linear forms $\left(X_{IJ}^{K}\right)_{ab}$ can be computed explicitly in terms of the x_{ij}^{k}'s. For instance, one has

$$\left(X_{IJ}^{K}\right)_{ab}(L_m^{(0)}) \propto \sum_{c=0}^{n-1} x_{i_{c+b},j_c}^{k_{c+a}}(L_m) \quad (5.79)$$

and

$$\left(X_{IJ}^{K}\right)_{ab}(L_m^{(r)}L_n^{(-r)}) \propto \sum_{c,d=0}^{n-1}\left[(1-\delta_{cd})\omega^{(c-d)r}x_{i_{c+b},j_c}^{k_{c+a}}(L_m)x_{i_{d+b},j_d}^{k_{d+a}}(L_n)+\delta_{cd}x_{i_{c+b},j_c}^{k_{c+a}}(L_mL_n)\right]. \quad (5.80)$$

We have decomposed the physical three point function $\langle\Phi_\gamma|\Phi_\alpha(1,\bar{1})\mu\bar{\mu}|\Phi_\beta\rangle$ in terms of a family of solutions $\left(X_{IJ}^{K}\right)_{ab}(\mu)$ of (5.60–5.64), and shown how to compute them. The cardinal of this family is

$$\sum_{a,b} n_{i_{1+a},j_{1+b}}^{k_1}\ldots n_{i_{n+a},j_{n+b}}^{k_n}\,, \quad (5.81)$$

where n_{ij}^k is the fusion number for $\phi_i \times \phi_j \to \phi_k$ in the mother CFT. By the naturality theorem [244], the forms $\left(X_{IJ}^K\right)_{ab}(\mu)$ span the whole space of solutions. But, as we did not prove that the $\left(X_{IJ}^K\right)_{ab}(\mu)$ are linearly independent, (5.81) is only an upper bound for the fusion number $\mathcal{N}_{IJ}^K$. The fact that $\mathcal{N}_{IJ}^K$ indeed equals (5.81), and therefore the $\left(X_{IJ}^K\right)_{ab}(\mu)$ are linearly independent, will be proved indirectly in Sec. 5.4.3 via the Verlinde formula.

The above arguments can be easily extended to construct a family of independent OPE coefficients $(C_{\alpha\beta}^{\gamma})_m(\mu)$ for a fusion process involving any kind of untwisted operators, leading to the fusion numbers

$$\mathcal{N}_{[i_1\dots i_n],[j_1\dots j_n]}^{[k_1\dots k_n]} = \sum_{a,b} n_{i_{1+a},j_{1+b}}^{k_1} \dots n_{i_{n+a},j_{n+b}}^{k_n}\,, \tag{5.82}$$

$$\mathcal{N}_{[i_1\dots i_n],[j_1\dots j_n]}^{k^{(r)}} = \sum_{a=0}^{n-1} n_{i_{1+a},j_1}^{k} \dots n_{i_{n+a},j_n}^{k}\,, \tag{5.83}$$

$$\mathcal{N}_{[i_1\dots i_n],j^{(r)}}^{k^{(s)}} = n_{i_1,j}^{k} \dots n_{i_n,j}^{k}\,, \tag{5.84}$$

$$\mathcal{N}_{j^{(r)},k^{(s)}}^{\ell^{(t)}} = \delta_{r+s,t}\, n_{ij}^{k}\,. \tag{5.85}$$

Fusion number involving twist fields on the other hand cannot be inferred using the same elementary approach, because for such three-point functions the copies of the mother CFT within the orbifold CFT are no longer decoupled. The answer, as provided by Verlinde's formula, will turn out to be more complicated, and not expressible in terms of the fusion numbers of the mother theory alone. But while we cannot at this stage easily compute the fusion numbers involving twist fields, we can at least argue that they are finite, by showing that correlation functions in the orbifold always involve finitely many (extended) conformal blocks.

Holomorphic factorization property and rationality Conformal field theories obey the holomorphic factorization property [245]. On the plane/sphere, it means that correlation functions can be decomposed as

$$\langle \Phi_{i_1}(z_1,\bar{z}_1)\cdots\Phi_{i_m}(z_m,\bar{z}_m)\rangle = \sum_{I,J} F_I(\mathbf{z})\rho_{IJ}\overline{F}_J(\bar{\mathbf{z}}) \tag{5.86}$$

where the (extended) conformal blocks F_I are holomorphic functions of $\mathbf{z} = (z_1,\cdots,z_n)$, and $\overline{F}_J$ are anti-holomorphic. More generally, on a Riemann surface Σ the factorization property becomes

$$Z_\Sigma\ \langle \Phi_{i_1}(z_1,\bar{z}_1)\cdots\Phi_{i_m}(z_m,\bar{z}_m)\rangle_\Sigma = \sum_{I,J} F_I(\mathbf{z},\mathbf{p})\rho_{IJ}\overline{F}_J(\bar{\mathbf{z}},\bar{\mathbf{p}}) \tag{5.87}$$

where Z_Σ stands for the partition function on Σ, and the conformal blocks F_I depend also holomorphically on the analytic coordinates $\mathbf{p}$ of the moduli of Σ. The above holds in particular in the absence of field insertion ($m = 0$), meaning that the partition function itself obeys the holomorphic factorization property. For instance in genus one, with a flat metric, this is simply

$$Z(\tau,\bar{\tau}) = \sum_{i,j} \chi_i(\tau)\rho_{ij}\overline{\chi}_j(\bar{\tau})\,. \tag{5.88}$$

A CFT is said to be *rational* when all the sums involved above are finite.

Provided the mother theory $\mathcal{M}$ obeys the holomorphic factorization property, then so does its cyclic orbifold $\mathcal{M}_n$. Consider for instance a generic correlation function of twists fields on a Riemann surface Σ

$$\langle \sigma_{i_1}^{k_1}(z_1, \bar{z}_1) \cdots \sigma_{i_m}^{k_m}(z_m, \bar{z}_m) \rangle_\Sigma \tag{5.89}$$

One can reinterpret this correlation function as a correlation function in the mother theory on the n-sheeted branched cover $\pi : \Sigma' \to \Sigma$, with ramification index k_j at z_j. We then have

$$Z_\Sigma \, \langle \sigma_{i_1}^{k_1}(z_1, \bar{z}_1) \cdots \sigma_{i_m}^{k_n}(z_m, \bar{z}_m) \rangle_\Sigma = Z_{\Sigma'} \langle \phi_{i_1}(z_1, \bar{z}_1) \cdots \phi_{i_m}(z_m, \bar{z}_m) \rangle_{\Sigma'} \,, \tag{5.90}$$

where in the *r.h.s.* both the correlation function and the partition function involve the mother theory on the covering surface Σ', with the metric $g' = \pi^* g$ being the pull-back of the metric g on Σ. In practice, the picture above is slightly more complicated, as the pull-back metric g' has conical singularities at the ramification points, but these can be regularized [122].

Exploiting the holomorphic factorization property of the mother theory then yields

$$Z_\Sigma \, \langle \sigma_{i_1}^{k_1}(z_1, \bar{z}_1) \cdots \sigma_{i_m}^{k_m}(z_m, \bar{z}_m) \rangle_\Sigma = \sum_{I,J} F_I(\mathbf{z}, \mathbf{p}') \rho_{IJ} \overline{F}_J(\bar{\mathbf{z}}, \bar{\mathbf{p}}') \tag{5.91}$$

The factorization property of the *l.h.s.* then follows from the fact that the moduli $\mathbf{p}' = \mathbf{p}'(\mathbf{p}, \mathbf{z})$ of the branched covering Σ' depends holomorphically on the moduli $\mathbf{p}$ of Σ and the positions $\mathbf{z}$ of the branched points. For instance, the 2-sheeted cover of the sphere with four branch points at positions z_i is a torus with moduli

$$\tau(x) = i \frac{{}_2\mathrm{F}_1\left(\frac{1}{2}, \frac{1}{2}, 1; 1 - x\right)}{{}_2\mathrm{F}_1\left(\frac{1}{2}, \frac{1}{2}, 1; x\right)}, \qquad x = \frac{(z_1 - z_2)(z_3 - z_4)}{(z_1 - z_3)(z_2 - z_4)}$$

The above argument is easily adapted to the generic case involving descendants of twist fields and/or untwisted fields. The last quantity to consider is the partition function itself, but this is simply obtained by summing all twisted partition functions of n copies of the mother theory, each of which obeys the factorization property.

Furthermore, it is clear that if the mother theory is rational, then so is the orbifold. As a consequence, all fusion numbers in the cyclic orbifold are finite when the mother theory is rational.

5.3.4 (Extended) conformal blocks on the sphere

The computation of entanglement entropies in the case of a single interval embedded in an infinite line (or a circle) at zero temperature boils down to a two-point function of twist fields on the sphere [46, 87, 214]. The main simplification in that case is that such two-point functions are completely fixed by conformal invariance. In contrast, if the system has boundaries, or is at finite temperature with periodic boundary conditions, the CFT computation involves two point functions of twist fields on more complicated Riemann surfaces, namely, the upper half plane or the torus[110, 152, 173, 233, 234, 236–238, 246]. Likewise, if the region A consists of several disjoint intervals, Rényi entropies involve higher-point correlation

functions of twist fields, or equivalently the partition function on higher genus Riemann surfaces [71, 84, 85, 88, 123, 127, 132, 153, 163, 187, 198–200, 239, 240]. In such cases, conformal invariance alone is no longer sufficient, and the full resources of two-dimensional CFT have to be brought to bear on the computation. One practical approach is to expand correlation functions using standard Virasoro conformal blocks, either to produce asymptotic expansions in some limiting cases (such as a small interval, for instance) [85, 212, 247–251] or to implement a numerical bootstrap approach[222]. However, by building on the present work, one can exploit the extended A_n symmetry and use extended conformal blocks instead of a brute force expansion employing just Virasoro blocks.

As we shall now explain, the diagonal decomposition (5.68) of OPE coefficients is a key property for the analysis of correlation functions and allows for a systematic description of orbifold conformal blocks. Consider the four-point function

$$G(z,\bar{z}) = \langle \Phi_1^\dagger(\infty)\Phi_2(1)\Phi_3(z,\bar{z})\Phi_4(0)\rangle\,, \tag{5.92}$$

where $\Phi_1,\dots,\Phi_4$ are (twisted or untwisted) invariant primary operators in $\mathcal{M}_n$. Inserting a resolution of the identity, we get

$$G(z,\bar{z}) = \sum_{\alpha,\mu,\bar{\mu}} z^{-h^\alpha_{34}+|\mu|}\, z^{-h^\alpha_{34}+|\bar{\mu}|}\, \langle \Phi_1^\dagger \Phi_2(\mu\cdot\bar{\mu}\cdot\Phi_\alpha)\rangle\, \langle (\mu\cdot\bar{\mu}\cdot\Phi_\alpha)^\dagger \Phi_3\Phi_4\rangle\,, \tag{5.93}$$

where we have used the notation $h^c_{ab} = h_a + h_b - h_c$, and $|\mu|, |\bar{\mu}|$ denote the levels of $\mu, \bar{\mu}$ respectively. In this expansion, Φ_α runs over all the invariant primary operators, and $\{\mu\,|\Phi_\alpha\rangle\}$ (resp. $\{\bar{\mu}\,|\Phi_\alpha\rangle\}$) is an *orthonormal* basis of V_α (resp. $\bar{V}_\alpha$). We now use the decomposition (5.68) for the three-point functions, which gives

$$\langle \Phi_1^\dagger \Phi_2(\mu\cdot\bar{\mu}\cdot\Phi_\alpha)\rangle = \sum_{m=1}^{\mathcal{N}^1_{2\alpha}} (\epsilon^1_{2\alpha})_m \left(X^1_{2\alpha}\right)_m(\mu)\left(X^1_{2\alpha}\right)_m(\bar{\mu})\,, \tag{5.94}$$

$$\langle (\mu\cdot\bar{\mu}\cdot\Phi_\alpha)^\dagger \Phi_3\Phi_4\rangle = \sum_{n=1}^{\mathcal{N}^\alpha_{34}} (\epsilon^4_{3^\dagger,\alpha})_n\, (X^4_{3^\dagger,\alpha})^*_n(\mu)\, (X^4_{3^\dagger,\alpha})^*_n(\bar{\mu})\,. \tag{5.95}$$

where we have used $\langle (\mu\cdot\bar{\mu}\cdot\Phi_\alpha)^\dagger\Phi_3\Phi_4\rangle = \langle \Phi_4^\dagger\Phi_3^\dagger(\mu\cdot\bar{\mu}\cdot\Phi_\alpha)\rangle^*$. We get the decomposition

$$G(z,\bar{z}) = \sum_\alpha \sum_{m=1}^{\mathcal{N}^1_{2\alpha}} \sum_{p=1}^{\mathcal{N}^\alpha_{34}} (\epsilon^1_{2\alpha})_m\, (\epsilon^4_{3^\dagger,\alpha})_p\, \mathcal{F}_{\alpha,m,p}(z)\, \bar{\mathcal{F}}_{\alpha,m,p}(\bar{z})\,, \tag{5.96}$$

where the conformal blocks are defined by

$$\mathcal{F}_{\alpha,m,p}(z) = \sum_\mu z^{-h^\alpha_{34}+|\mu|}\, (X^1_{2\alpha})_m(\mu)\, (X^4_{3^\dagger,\alpha})^*_n(\mu)\,, \tag{5.97}$$

$$\bar{\mathcal{F}}_{\alpha,m,p}(\bar{z}) = \sum_{\bar{\mu}} \bar{z}^{-h^\alpha_{34}+|\bar{\mu}|}\, (X^1_{2\alpha})_m(\bar{\mu})\, (X^4_{3^\dagger,\alpha})^*_n(\bar{\mu})\,, \tag{5.98}$$

and the sums run over orthonormal bases $\{\mu\,|\Phi_\alpha\rangle\}$ and $\{\bar{\mu}\,|\Phi_\alpha\rangle\}$ of V_α and $\bar{V}_{\alpha^*}$, respectively.

note that each of the conformal blocks $\mathcal{F}_{\alpha,m,p}(z)$ has the form of an integer power series in z, multiplied by a factor $z^{-h^\alpha_{34}}$. The conformal block decomposition (5.96) is indexed by the invariant primary operators Φ_α under the $A_n \oplus \bar{A}_n$ neutral algebra. Each internal primary state $|\Phi_\alpha\rangle$ contributes with a multiplicity (*i.e.* number of independent conformal blocks) given by the product of fusion numbers $\mathcal{N}^1_{2\alpha}\times\mathcal{N}^\alpha_{34}$.

5.4 Modular properties and Verlinde's formula

In this section, we recall the modular properties of the cyclic orbifold and obtain the orbifold fusion rules from the Verlinde formula.

5.4.1 Torus partition function

Consider the torus of modular parameter τ

$$\mathbb{T}_\tau = \mathbb{C}/(\mathbb{Z} + \tau\mathbb{Z})\,, \tag{5.99}$$

with $\mathrm{Im}\,\tau > 0$, and let us use the notations $q = e^{2i\pi\tau}$ and $\bar{q} = e^{-2i\pi\bar{\tau}}$. We denote by $Z_{m,p}(\tau)$ the partition function of $\mathcal{M}_n$, where the copy a is connected to the copy $a+m$ (resp. $a+p$) along the cycle $z \to z+\tau$ (resp. $z \to z+1$). Since changing the orientation of both cycles yields the same torus, clearly $Z_{m,p}(\tau) = Z_{-m,-p}(\tau)$. Furthermore, the elementary modular transformations act as:

$$Z_{mp}(\tau+1) = Z_{m-p,p}(\tau)\,, \qquad Z_{mp}(-1/\tau) = Z_{p,-m}(\tau)\,. \tag{5.100}$$

For a general modular transformation, we have:

$$Z_{mp}\,(\tau) = Z_{am+bp,cm+dp}\left(\frac{a\tau+b}{c\tau+d}\right), \qquad (a,b,c,d) \in \mathbb{Z}^4\,, \qquad ad-bc = 1\,. \tag{5.101}$$

The full partition function of the orbifold CFT is defined as the sum over all possible defects:

$$Z_{\mathrm{orb}}(\tau) = \frac{1}{n}\sum_{m,p=0}^{n-1} Z_{mp}(\tau)\,, \tag{5.102}$$

and it is manifestly modular invariant.

Denoting by $Z(\tau)$ the mother CFT partition function, we have the identities

$$Z_{m0}(\tau) = Z(n\tau)\,, \qquad Z_{0m}(\tau) = Z(\tau/n)\,, \qquad m \neq 0 \mod n\,. \tag{5.103}$$

Using these, together with the relations (5.101), we can express $Z_{\mathrm{orb}}(\tau)$ as:

$$\begin{aligned} Z_{\mathrm{orb}}(\tau) &= \frac{1}{n}\left[Z_{00}(\tau) + \sum_{m=1}^{n-1} Z_{m0}(\tau) + \sum_{m=0}^{n-1}\sum_{p=1}^{n-1} Z_{mp}(\tau)\right] \\ &= \frac{1}{n}Z(\tau)^n + \frac{n-1}{n}\left[Z(n\tau) + \sum_{k=0}^{n-1} Z\left(\frac{\tau+k}{n}\right)\right], \end{aligned} \tag{5.104}$$

which is the standard result [229] for the partition function of the $\mathbb{Z}_n$ orbifold. Recall the definition (D.3) for the cyclic permutation of copies, and the family of projectors

$$\mathcal{P}_r = \frac{1}{n}\sum_{a=0}^{n-1} \omega^{-ar}\,\Pi^a\,, \tag{5.105}$$

on the eigenspaces of eigenvalue ω^r of Π. By construction, each individual twisted partition function $Z_{mp}(\tau)$ reads

$$Z_{mp}(\tau) = \mathrm{Tr}_{\mathcal{H}[p]}\left[\Pi^m\, q^{L_0^{(0)}-nc/24}\,\bar{q}^{\bar{L}_0^{(0)}-nc/24}\right], \tag{5.106}$$

where $\mathcal{H}^{[n]}$ is the space of $\mathcal{M}_n$ states with twist charge n. Therefore, the orbifold partition function (5.102) can be rewritten as

$$Z_{\rm orb}(\tau) = \sum_{p=0}^{n-1} {\rm Tr}_{\mathcal{H}^{[p]}} \left[\mathcal{P}_0 \, q^{L_0^{(0)} - nc/24} \, \bar{q}^{\bar{L}_0^{(0)} - nc/24} \right] . \tag{5.107}$$

Hence we get the simple identity

$$Z_{\rm orb}(\tau) = {\rm Tr}_{\mathcal{H}_0} \left[q^{L_0^{(0)} - nc/24} \, \bar{q}^{\bar{L}_0^{(0)} - nc/24} \right] , \tag{5.108}$$

where $\mathcal{H}_0$ is the invariant Hilbert space defined in Sec. 5.3.2. We recover that local fields coincide with invariant fields.

5.4.2 Modular characters

Let us first fix the notations for the characters of the mother CFT, in the case when it is rational, *i.e.* with a finite set of primary operators $\{\phi_1, \dots, \phi_M\}$. We denote by χ_j the Virasoro character of the module associated to ϕ_j in the mother CFT:

$$\chi_j(\tau) = {\rm Tr}_{v_j} \left(q^{L_0 - c/24} \right) . \tag{5.109}$$

The χ_j's transform under the elementary modular maps as

$$\chi_j(\tau + 1) = t_j \, \chi_j(\tau) , \qquad \chi_i(-1/\tau) = \sum_{j=1}^{M} S_{ij} \, \chi_j(\tau) , \tag{5.110}$$

where $t_j = \exp[2i\pi(h_j - c/24)]$, and S is a unitary matrix. Moreover, since we assume that the mother theory $\mathcal{M}$ is diagonal, the matrix S is real symmetric, and satisfies $(ST)^3 = \mathbf{1}$, where $T = {\rm diag}(t_1, \dots, t_M)$.

In the orbifold CFT, the characters associated to the A_n-modules V_J, $V_j^{(r)}$, $V_j^{[k](r)}$ are, respectively:

$$\chi_J(\tau) = \chi_{j_1}(\tau) \dots \chi_{j_n}(\tau) , \tag{5.111}$$

$$\chi_j^{(r)}(\tau) = \frac{1}{n} \left[\chi_j(\tau)^n + (n\delta_{r0} - 1) \chi_j(n\tau) \right] , \tag{5.112}$$

$$\chi_j^{[k](r)}(\tau) = \frac{1}{n} \sum_{m=0}^{n-1} t_j^{-m/n} \, \omega^{-krm} \, \chi_j \left(\frac{\tau + m}{n} \right) . \tag{5.113}$$

The proof for these expressions is given in [119]. and they can be considered as a special case of [252, 253] (which are also employed in [254] and [230])

From the decomposition of the invariant Hilbert space $\mathcal{H}_0$, we can write the partition function (5.108) as

$$Z_{\rm orb}(\tau) = \sum_{J=[j_1 \dots j_n]} |\chi_J|^2 + \sum_j \sum_{r=0}^{n-1} |\chi_j^{(r)}|^2 + \sum_j \sum_{k=1}^{n-1} \sum_{r=0}^{n-1} |\chi_j^{[k](r)}|^2 , \tag{5.114}$$

where the notations for the sums are the same as in (5.56). The orbifold characters transform under the elementary modular maps as

$$\chi_\alpha(\tau + 1) = \mathcal{T}_\alpha \, \chi_\alpha(\tau) , \qquad \chi_\alpha(-1/\tau) = \sum_\beta \mathcal{S}_{\alpha\beta} \, \chi_\beta(\tau) , \tag{5.115}$$

with

$$\mathcal{T}_J = t_{j_1} \dots t_{j_n} , \qquad \mathcal{T}_j^{(r)} = t_j^n , \qquad \mathcal{T}_j^{[k](r)} = \omega^{kr}\, t_j^{1/n} , \tag{5.116}$$

and

$$\begin{aligned}
\mathcal{S}_{I,J} &= \sum_{a=0}^{n-1} S_{i_1,j_{1+a}} \dots S_{i_n,j_{n+a}} , \\
\mathcal{S}_{I,j^{(r)}} &= \mathcal{S}_{j^{(r)},[i_1 \dots i_n]} = S_{i_1,j} \dots S_{i_n,j} , \\
\mathcal{S}_{i^{(r)},j^{(s)}} &= \frac{S_{ij}^n}{n} , \\
\mathcal{S}_{i^{(r)},j^{[k](s)}} &= \mathcal{S}_{j^{[k](s)},i^{(r)}} = \frac{\omega^{-kr}\, S_{ij}}{n} , \\
\mathcal{S}_{i^{[k](r)},j^{[\ell](s)}} &= \frac{\omega^{-ks-\ell r}\, (P_{\ell.k^{-1}})_{ij}}{n} , \\
\mathcal{S}_{I,j^{[k](r)}} &= \mathcal{S}_{j^{[k](r)},I} = 0 .
\end{aligned} \tag{5.117}$$

The matrices P_m appearing in this expression are defined as

$$P_m = T^{-m/n} \cdot Q_m \cdot T^{[[-m^{-1}]]/n} , \qquad m \in \mathbb{Z}_n^\times , \tag{5.118}$$

where $[[-m^{-1}]]$ denotes the inverse of $(-m)$ modulo n, with $0 < [[-m^{-1}]] < n$, and Q_m is the matrix representing the linear action of the modular map

$$\tau \mapsto q_m(\tau) = \frac{m\tau - (m[[-m^{-1}]] + 1)/n}{n\tau - [[-m^{-1}]]} \tag{5.119}$$

on the characters χ_j of the mother CFT. We introduce the conjugation matrix C, with matrix elements

$$C_{\alpha\beta} = \delta_{\alpha,\beta^\dagger} , \tag{5.120}$$

and the diagonal matrix $\mathcal{T}$ with matrix elements $\mathcal{T}_\alpha$. The orbifold modular matrices $\mathcal{S}$ and $\mathcal{T}$ satisfy the properties

$$\mathcal{S}^t = \mathcal{S} , \tag{5.121}$$

$$\mathcal{S}^2 = C , \tag{5.122}$$

$$\mathcal{S}^\dagger \mathcal{S} = \mathbf{1} , \tag{5.123}$$

$$(\mathcal{S}\mathcal{T})^3 = C , \tag{5.124}$$

where $\mathcal{S}^t$ denotes the transpose of $\mathcal{S}$.

The main arguments for the proofs of these properties are given in the Appendix D.3. note that the relations (5.115) are not sufficient to determine completely the matrices $\mathcal{S}$ and $\mathcal{T}$, because some distinct A_n-modules have the same characters, namely

$$\chi_{[j_1 \dots j_n]}(\tau) = \chi_{[j_{p(1)} \dots j_{p(n)}]}(\tau) \quad \text{for any permutation } p \text{ of } \{1, \dots, n\}, \tag{5.125}$$

$$\chi_j^{(r)}(\tau) = \chi_j^{(s)}(\tau) \quad \text{if } r, s \neq 0 , \tag{5.126}$$

$$\chi_j^{[k](r)}(\tau) = \chi_j^{[\ell](s)}(\tau) \quad \text{if } rk = s\ell \mod n . \tag{5.127}$$

However, the expressions (5.116–5.117) define a simple and elegant solution to the constraints (5.121–5.124) in terms of the modular matrices of the mother CFT. Furthermore, it agrees with the S matrix given in equation (10) of [253].

5.4.3 Fusion rules

Recall our notation for the fusion numbers:

$$\Phi_\alpha \times \Phi_\beta \to \sum_\gamma \mathcal{N}_{\alpha\beta}^{\gamma}\, \Phi_\gamma\,, \tag{5.128}$$

where $\Phi_\alpha, \Phi_\beta, \Phi_\gamma$ are invariant primary operators. The fusion numbers can be computed through the Verlinde formula

$$\mathcal{N}_{\alpha\beta}^{\gamma} = \sum_\delta \frac{\mathcal{S}_{\alpha\delta}\,\mathcal{S}_{\beta\delta}\,\mathcal{S}^\dagger_{\gamma\delta}}{\mathcal{S}_{\mathbf{1}\delta}}\,, \tag{5.129}$$

where the sum runs over all possible invariant primary operators Φ_δ described in Section 5.3.1. This formula, together with (5.121–5.124), directly ensures that the properties are satisfied

$$\mathcal{N}_{\alpha\beta}^{\gamma} = \mathcal{N}_{\beta\alpha}^{\gamma}\,, \qquad \mathcal{N}_{\alpha\beta}^{\gamma} = \mathcal{N}_{\alpha\gamma^\dagger}^{\beta^\dagger}\,, \tag{5.130}$$

are satisfied. In the case of untwisted operators, we get

$$\mathcal{N}_{I,J}^{K} = \sum_{a,b=0}^{n-1} n_{i_{1+a},j_{1+b}}^{k_1} \dots n_{i_{n+a},j_{n+b}}^{k_n}\,, \tag{5.131}$$

$$\mathcal{N}_{I,J}^{k^{(r)}} = \sum_{a=0}^{n-1} n_{i_{1+a},j_1}^{k} \dots n_{i_{n+a},j_n}^{k}\,, \tag{5.132}$$

$$\mathcal{N}_{I,j^{(r)}}^{k^{(s)}} = n_{i_1,j}^{k} \dots n_{i_n,j}^{k}\,, \tag{5.133}$$

$$\mathcal{N}_{i^{(r)},j^{(s)}}^{k^{(t)}} = \delta_{r+s,t}\, n_{ij}^{k}\,, \tag{5.134}$$

which confirms the hypothesis that the OPE coefficients constructed in Sec. 5.3.3 span the solution space of the linear system of equations which derive from the orbifold algebraic rules and Ward identities. The fusion numbers involving twist operators are given by

$$\mathcal{N}_{i^{[p](r)}j^{[q](s)}}^{K} = \delta_{p+q,0} \sum_{\ell=1}^{M} \frac{S_{i\ell}S_{j\ell}\cdot S_{k_1\ell}\dots S_{k_n\ell}}{S_{1\ell}^{n}}\,, \tag{5.135}$$

$$\mathcal{N}_{i^{[p](r)}j^{[q](s)}}^{k^{(t)}} = \frac{\delta_{p+q,0}}{n} \sum_{\ell=1}^{M} \left[\frac{S_{i\ell}S_{j\ell}S^{n}_{k\ell}}{S_{1\ell}^{n}} + \sum_{a=1}^{n-1} \omega^{ap(r+s-t)} \frac{(P_{-a})_{i\ell}(P_a)_{j\ell}S_{k\ell}}{S_{1\ell}} \right], \tag{5.136}$$

$$\mathcal{N}_{i^{[p](r)}j^{[q](s)}}^{k^{[m](t)}} = \frac{\delta_{p+q,m}}{n} \sum_{\ell=1}^{M} \left[\frac{S_{i\ell}S_{j\ell}S_{k\ell}}{S_{1\ell}^{n}} + \sum_{a=1}^{n-1} \omega^{a(r+s-t)} \frac{(P^\dagger_{pa^{-1}})_{i\ell}(P^\dagger_{qa^{-1}})_{j\ell}(P_{ma^{-1}})_{k\ell}}{S_{1\ell}} \right]. \tag{5.137}$$

The fusion numbers (5.136) depend on the Fourier indices r, s, t only through the combination $(r + s - t)$, as expected from the discussion in Sec. 5.3.3. Using the unitarity of S, some of the terms can be expressed using the fusion numbers of the mother CFT:

$$\sum_{\ell=1}^{M} \frac{S_{i\ell}S_{j\ell}\cdot S_{k_1\ell}\dots S_{k_n\ell}}{S_{1\ell}^{n}} = \sum_{\ell_1,\dots,\ell_{n-1}=1}^{M} n_{ij}^{\ell_1} \times n_{\ell_1 k_1}^{\ell_2} n_{\ell_2 k_2}^{\ell_3} \dots n_{\ell_{n-2}k_{n-2}}^{\ell_{n-1}} \times n_{\ell_{n-1}k_{n-1}}^{k_n}\,, \tag{5.138}$$

$$\sum_{\ell=1}^{M} \frac{S_{i\ell}S_{j\ell}S^{n}_{k\ell}}{S_{1\ell}^{n}} = \sum_{\ell_1,\dots,\ell_{n-1}=1}^{M} n_{ij}^{\ell_1} \times n_{\ell_1 k}^{\ell_2} n_{\ell_2 k}^{\ell_3} \dots n_{\ell_{n-2}k}^{\ell_{n-1}} \times n_{\ell_{n-1}k}^{k}\,. \tag{5.139}$$

This is also the case for the first term in (5.137). For instance, for $n = 3$, we have

$$\sum_{\ell=1}^{M} \frac{S_{i\ell} S_{j\ell} S_{k\ell}}{S_{1\ell}^3} = \sum_{\ell_1,\ell_2,\ell_3=1}^{M} n_{i\ell_1}^{\ell_2} n_{j\ell_2}^{\ell_3} n_{k\ell_3}^{\ell_1} , \tag{5.140}$$

and similar but more complicated expressions hold for $n > 3$.

5.5 Example applications

In this section, we shall present some applications of our results on the $\mathbb{Z}_3$ orbifolds of minimal CFTs.

5.5.1 The $\mathbb{Z}_3$ orbifold of the Yang-Lee CFT

In this section, we shall present a simple application of our results for the operator algebra of the cyclic orbifold CFT. We choose as mother theory the Yang-Lee minimal model $\mathcal{M}(5,2)$ with central charge $c = -22/5$, and primary operator content $\{\mathbf{1}, \phi\}$ with conformal dimensions $h_{\mathbf{1}} = 0$ and $h_\phi = -1/5$. The modular S-matrix associated to this CFT is given by:

$$S = \frac{2}{\sqrt{5}} \begin{pmatrix} -\sin(2\pi/5) & \sin(4\pi/5) \\ \sin(4\pi/5) & \sin(2\pi/5) \end{pmatrix} . \tag{5.141}$$

The non-trivial fusion rule in the Yang-Lee CFT is

$$\phi \times \phi \to \mathbf{1} + \phi \, . \tag{5.142}$$

We will consider the $\mathbb{Z}_3$ cyclic orbifold of the above CFT. Its primary operator content (with respect to the neutral algebra $A_n \oplus \bar{A}_n$) consists of:

- 2 non-diagonal untwisted operators: $[\mathbf{1}, \mathbf{1}, \phi]$ and $[\mathbf{1}, \phi, \phi]$,
- 6 diagonal untwisted operators: $\mathbf{1}^{(r)}, \Phi^{(r)}$ with $r \in \mathbb{Z}_3$,
- 12 twist operators: $\sigma_{\mathbf{1}}^{(r)}, \sigma_{\mathbf{1}}^{\dagger(r)}, \sigma_\phi^{(r)} \sigma_\phi^{\dagger(r)}$ with $r \in \mathbb{Z}_3$.

Recall the definition of non-diagonal untwisted operators, e.g.

$$[\mathbf{1}, \mathbf{1}, \phi] := \frac{1}{\sqrt{3}} (\mathbf{1} \otimes \mathbf{1} \otimes \phi + \mathbf{1} \otimes \phi \otimes \mathbf{1} + \phi \otimes \mathbf{1} \otimes \mathbf{1}) \, . \tag{5.143}$$

Using the results of Sec. 5.4.3, we get the fusion rules between untwisted

operators:

$$
\begin{aligned}
&[\mathbf{1},\mathbf{1},\phi]\times[\mathbf{1},\mathbf{1},\phi]\to[\mathbf{1},\mathbf{1},\phi]+2[\mathbf{1},\phi,\phi]+\sum_{r\in\mathbb{Z}_3}\mathbf{1}^{(r)}\,,\\
&[\mathbf{1},\mathbf{1},\phi]\times[\mathbf{1},\phi,\phi]\to[\mathbf{1},\mathbf{1},\phi]+2[\mathbf{1},\phi,\phi]+\sum_{r\in\mathbb{Z}_3}\Phi^{(r)}\,,\\
&[\mathbf{1},\phi,\phi]\times[\mathbf{1},\phi,\phi]\to 2[\mathbf{1},\mathbf{1},\phi]+3[\mathbf{1},\phi,\phi]+\sum_{r\in\mathbb{Z}_3}\mathbf{1}^{(r)}+2\sum_{r\in\mathbb{Z}_3}\Phi^{(r)}\,,\\
&[\mathbf{1},\mathbf{1},\phi]\times\mathbf{1}^{(r)}\to[\mathbf{1},\mathbf{1},\phi]\,,\\
&[\mathbf{1},\phi,\phi]\times\mathbf{1}^{(r)}\to[\mathbf{1},\phi,\phi]\,,\\
&\mathbf{1}^{(r)}\times\mathbf{1}^{(s)}\to\mathbf{1}^{(r+s)}\,,\\
&\Phi^{(r)}\times\mathbf{1}^{(s)}\to\Phi^{(r+s)}\,,\\
&[\mathbf{1},\mathbf{1},\phi]\times\Phi^{(r)}\to[\mathbf{1},\phi,\phi]+\sum_{s\in\mathbb{Z}_3}\Phi^{(s)}\,,\\
&[\mathbf{1},\phi,\phi]\times\Phi^{(r)}\to[\mathbf{1},\mathbf{1},\phi]+2[\mathbf{1},\phi,\phi]+\sum_{s\in\mathbb{Z}_3}\Phi^{(s)}\,,\\
&\phi^{(r)}\times\phi^{(s)}\to[\mathbf{1},\mathbf{1},\phi]+[\mathbf{1},\phi,\phi]+2\times\mathbf{1}^{(r+s)}+\Phi^{(r+s)}\,.
\end{aligned}
\tag{5.144}
$$

The fusion rules between untwisted and twisted operators read

$$
\begin{aligned}
&[\mathbf{1},\mathbf{1},\phi]\times\sigma_{\mathbf{1}}^{(s)}\to\sum_r\sigma_\phi^{(r)}\,,\\
&[\mathbf{1},\phi,\phi]\times\sigma_{\mathbf{1}}^{(s)}\to\sum_r\sigma_{\mathbf{1}}^{(r)}+\sum_{r\in\mathbb{Z}_3}\sigma_\phi^{(r)}\,,\\
&[\mathbf{1},\mathbf{1},\phi]\times\sigma_{\phi}^{(s)}\to\sum_r\sigma_{\mathbf{1}}^{(r)}+\sum_{r\in\mathbb{Z}_3}\sigma_\phi^{(r)}\,,\\
&[\mathbf{1},\phi,\phi]\times\sigma_{\phi}^{(s)}\to\sum_r\sigma_{\mathbf{1}}^{(r)}+2\sum_{r\in\mathbb{Z}_3}\sigma_\phi^{(r)}\,,\\
&\mathbf{1}^{(r)}\times\sigma_{\mathbf{1}}^{(s)}\to\sigma_{\mathbf{1}}^{(s+r)}\,,\\
&\Phi^{(r)}\times\sigma_{\mathbf{1}}^{(s)}\to\sigma_{\mathbf{1}}^{(s+r)}+\sigma_\phi^{(s+r)}+\sigma_\phi^{(s+r+1)}\,,\\
&\mathbf{1}^{(r)}\times\sigma_{\phi}^{(s)}\to\sigma_{\phi}^{(s+r)}\,,\\
&\Phi^{(r)}\times\sigma_{\phi}^{(s)}\to\sigma_{\mathbf{1}}^{(s+r-1)}+\sigma_{\mathbf{1}}^{(s+r)}+\sum_{t\in\mathbb{Z}_3}\sigma_\phi^{(t)}\,.
\end{aligned}
\tag{5.145}
$$

Finally, the fusion rules between twist operators read

$$
\begin{aligned}
&\sigma_{\mathbf{1}}^{(r)}\times\sigma_{\mathbf{1}}^{\dagger(s)}\to[\mathbf{1},\phi,\phi]+\mathbf{1}^{(s+r)}+\Phi^{(s+r)}\,,\\
&\sigma_{\phi}^{(r)}\times\sigma_{\mathbf{1}}^{\dagger(s)}\to[\mathbf{1},\mathbf{1},\phi]+[\mathbf{1},\phi,\phi]+\Phi^{(s+r-1)}+\Phi^{(s+r)}\,,\\
&\sigma_{\phi}^{(r)}\times\sigma_{\phi}^{\dagger(s)}\to[\mathbf{1},\mathbf{1},\phi]+2[\mathbf{1},\phi,\phi]+\mathbf{1}^{(s+r)}+\sum_{r\in\mathbb{Z}_3}\Phi^{(r)}\,,\\
&\sigma_{\mathbf{1}}^{(r)}\times\sigma_{\mathbf{1}}^{(s)}\to\sigma_{\mathbf{1}}^{\dagger(r+s)}+\sigma_{\mathbf{1}}^{\dagger(r+s+1)}+\sigma_{\phi}^{\dagger(r+s)}\,,\\
&\sigma_{\phi}^{(r)}\times\sigma_{\mathbf{1}}^{(s)}\to\sigma_{\mathbf{1}}^{\dagger(r+s)}+\sum_{t\in\mathbb{Z}_3}\sigma_\phi^{\dagger(t)}\,,\\
&\sigma_{\phi}^{(r)}\times\sigma_{\phi}^{(s)}\to\sum_{t\in\mathbb{Z}_3}\sigma_{\mathbf{1}}^{\dagger(t)}+\sigma_\phi^{\dagger(r+s)}+\sigma_\phi^{\dagger(r+s+1)}+2\sigma_\phi^{\dagger(r+s+2)}\,.
\end{aligned}
\tag{5.146}
$$

The other fusion rules are easily obtained by symmetry under conjugation.

As pointed out in Sec. 5.3.3, one may treat the OPE of twist operators $\sigma_i^{(r)} \times \sigma_j^{\dagger(s)}$ or $\sigma_i^{(r)} \times \sigma_j^{(s)}$, by "unfolding" the three-point correlator corresponding to a particular orbifold fusion rule, as a mother CFT correlator. This is done in two steps: first, one translates the orbifold correlation function into an expectation value on the replicated surface Σ_n. Then, one conformally maps this quantity to a correlator defined on a Riemann surface that is more amenable to calculations (the Riemann sphere $\mathbb{C}$ in our first example). This approach is exemplified in Appendix D.2 for the calculation of the orbifold structure constant

$$C^{[\mathbf{1},\phi,\phi]}_{\sigma_\phi^{(0)},\sigma_\phi^{\dagger(0)}} = \langle [\mathbf{1},\phi,\phi] \cdot \sigma_\phi^{(0)} \cdot \sigma_\phi^{\dagger(0)} \rangle \neq 0\,. \tag{5.147}$$

Since the structure constant is non-vanishing, we can conclude that indeed the OPE $\sigma_\phi^{(0)} \times \sigma_\phi^{\dagger(0)}$ produces the module $[\mathbf{1},\phi,\phi]$. However, this unfolding does not allow us to extract the value of the associated multiplicity. From (5.146), we see that this multiplicity is two. Furthermore, using this technique to infer the fusion rules of the cyclic orbifold CFT from the mother CFT data is only feasible provided the resulting correlator can be calculated, and the unfolding map is known.

One encounters both of these difficulties in trying to find the fusion rules between twist operators in the same twist charge sector. Let us consider the following orbifold three-point function of twist operators:

$$C^{\sigma_i^\dagger}_{\sigma_j\sigma_k} = \langle \sigma_i \cdot \sigma_j \cdot \sigma_k \rangle\,. \tag{5.148}$$

This translates into a three-point function on the three-sheeted cover of the Riemann sphere, with branch points at $(0,1,\infty)$, which we denote by Σ_3:

$$\langle \phi_i \cdot \phi_j \cdot \phi_k \rangle_{\Sigma_3}\,. \tag{5.149}$$

We can now calculate the genus of this surface Σ_3, using the Riemann-Hurwitz formula

$$2g - 2 = n(2h-2) + \sum_{i=1}^{p}(k_i - 1)\,, \tag{5.150}$$

giving the genus g of an n-sheeted cover of a surface of genus h, with p branch points having ramification indices k_i. In our case, all the branch points have ramification indices $k_i = 3$, so that we find $g = 1$. Thus, there exists a conformal map $z \mapsto t(z)$ between the surface Σ_3 and a torus $\mathbb{T}_\tau$ which allow us to relate (5.149) to the following three-point function on the torus

$$\langle \phi_i(t_1,\bar{t}_1)\phi_j(t_2,\bar{t}_2)\phi_k(t_3,\bar{t}_3)\rangle_{\mathbb{T}_\tau}\,. \tag{5.151}$$

To complete such a calculation, one would have two non-trivial problems to solve: finding the conformal map $z \mapsto t(z)$, and calculating the three-point correlator (5.151). Assuming the conformal map has been found, one needs to calculate the torus correlators on a case-by-case basis. For example, when $(\phi_i,\phi_j,\phi_k) = (\mathbf{1},\mathbf{1},\mathbf{1})$ or $(\mathbf{1},\mathbf{1},\phi)$, results are already known – they correspond respectively to the partition function of the Yang-Lee CFT, and the torus one-point function $\langle\phi\rangle_{\mathbb{T}_\tau}$, which have been calculated in [255].

However, the issue of counting multiplicities remains, and as we go beyond this relatively simple example of the $\mathbb{Z}_3$ orbifold of the Yang-Lee CFT, to higher $\mathbb{Z}_n$ orbifolds, the formula (5.150) shows that unfolding would require the calculation of correlators on surfaces of genus $g \geq 2$, for which few exact results are available in the literature.

5.5.2 Counting conformal blocks of twist correlators

We will provide a few examples of conformal block counting for four-point correlators in $\mathbb{Z}_3$ cyclic orbifolds.

The $\mathbb{Z}_3$ cyclic orbifold of the Ising CFT. We will first illustrate this by using the minimal model $\mathcal{M}(4,3)$ (Ising CFT) as mother theory, with central charge $c = 1/2$, and primary operator content $\{\mathbf{1}, s, \varepsilon\}$ with conformal dimensions $h_{\mathbf{1}} = 0, h_s = 1/16$, $h_\varepsilon = 1/2$. To avoid confusion with the twist operators, we d The modular S-matrix associated to this CFT is given by:

$$S = \frac{1}{2}\begin{pmatrix} 1 & 1 & \sqrt{2} \\ 1 & 1 & -\sqrt{2} \\ \sqrt{2} & -\sqrt{2} & 0 \end{pmatrix}, \tag{5.152}$$

and the fusion rules are

$$s \times s \to \mathbf{1} + \varepsilon\,, \qquad s \times \varepsilon \to s\,, \qquad \varepsilon \times \varepsilon \to \mathbf{1}\,. \tag{5.153}$$

We remind that for a four-point function $\langle \Phi_1 \Phi_2 \Phi_3 \Phi_4 \rangle$, the dimension of its space of conformal blocks can be calculated from the fusion numbers of the theory [23]:

$$\mathcal{D}^{\Phi_3,\Phi_4}_{\Phi_1,\Phi_2} = \sum_\alpha \mathcal{N}^{\Phi_\alpha}_{\Phi_1,\Phi_2} \mathcal{N}^{\Phi_4}_{\Phi_\alpha,\Phi_3}\,, \tag{5.154}$$

where the sum on α runs over all the primary fields in the CFT. Using the above, we will calculate the dimensions of the space of conformal blocks for a few correlators of physical interest in the $\mathbb{Z}_3$ orbifold of the Ising CFT.

Let us first consider the four-point functions of twist operators:

$$\langle \sigma_j(z_1,\bar{z}_1)\sigma_k^\dagger(z_2,\bar{z}_2)\sigma_j(z_3,\bar{z}_3)\sigma_k^\dagger(z_4,\bar{z}_4)\rangle\,, \tag{5.155}$$

with $j,k \in \{\mathbf{1}, \varepsilon\}$. In this case, one finds:

$$\boxed{\mathcal{D}^{\sigma_j,\sigma_k^\dagger}_{\sigma_j,\sigma_k^\dagger} = \sum_\alpha \left(\mathcal{N}^{\Phi_\alpha}_{\sigma_j,\sigma_k^\dagger}\right)^2 = 4\,,} \tag{5.156}$$

where the sum runs over the untwisted operators. The correlator with $j = k = \mathbf{1}$ gives the leading universal contribution in the calculation of the third Rényi entropy of two disjoint intervals in the ground state of a quantum spin chain with periodic boundary conditions, while the correlators with composite twist insertions (i.e. for which j,k can be ε) provide expressions for the universal parts of the first two subleading terms, as per the reasoning of [118].

Also of physical relevance are correlators of the type:

$$\langle \sigma_j(z_1,\bar{z}_1)\sigma_j^\dagger(z_2,\bar{z}_2)\Phi_i^{(0)}(z_3,\bar{z}_3)\Phi_i^{(0)}(z_4,\bar{z}_4)\rangle\,, \tag{5.157}$$

with $j \in \{\mathbf{1}, \varepsilon\}$ and $i \in \{s, \epsilon\}$. These allow for the calculation of leading and subleading contributions to the third Rényi entropy of a single interval in an excited state of the quantum Ising chain with periodic boundary conditions. We find:

$$\mathcal{D}^{\varepsilon^{(0)},\varepsilon^{(0)}}_{\sigma_{\mathbf{1}},\sigma_{\mathbf{1}}^\dagger} = \mathcal{D}^{\varepsilon^{(0)},\varepsilon^{(0)}}_{\sigma_\varepsilon,\sigma_\varepsilon^\dagger} = \mathcal{D}^{s^{(0)},s^{(0)}}_{\sigma_{\mathbf{1}},\sigma_\varepsilon^\dagger} = 1\,, \tag{5.158}$$

and

$$\mathcal{D}^{s^{(0)},s^{(0)}}_{\sigma_{\mathbf{1}},\sigma_{\mathbf{1}}^\dagger} = \mathcal{D}^{s^{(0)},s^{(0)}}_{\sigma_\varepsilon,\sigma_\varepsilon^\dagger} = 2\,. \tag{5.159}$$

The $\mathbb{Z}_3$ orbifold of a Virasoro minimal model $\mathcal{M}_{p,q}$. One can furthermore provide numerical checks[2] for the claims of [118] at $n = 3$.

Provided the mother CFT is a diagonal Virasoro minimal model $\mathcal{M}_{p,q}$ [23], the cyclic orbifold correlation function:

$$\langle \sigma_{\mathbf{1}}(z_1,\bar{z}_1), \sigma_{\mathbf{1}}^{\dagger}(z_2,\bar{z}_2), \Phi_{21}^{(0)}(z_3,\bar{z}_3), \Phi_{21}^{(0)}(z_4,\bar{z}_4)\rangle \,, \tag{5.160}$$

where ϕ_{21} is the primary field with Kac indices $(m,n) = (2,1)$ (see [23]). According to [118], this correlator should satisfy a third-order differential equation. We've found evidence for this claim by calculating the dimension of the space of conformal blocks of this correlator for a few minimal models. The results are given in Table 5.1. We see that indeed the space of conformal dimensions satisfies the

$\mathcal{M}(p,q)$	$\mathcal{M}(4,3)$	$\mathcal{M}(5,4)$	$\mathcal{M}(6,5)$	$\mathcal{M}(7,5)$	$\mathcal{M}(7,6)$	$\mathcal{M}(8,7)$
$\mathcal{D}^{\Phi_{21}^{(0)},\Phi_{21}^{(0)}}_{\sigma_{\mathbf{1}},\sigma_{\mathbf{1}}^{\dagger}}$	1	2	2	3	3	3

Table 5.1: Dimension of the space of conformal blocks for the correlator (5.160) in diverse minimal models $\mathcal{M}(p,q)$.

bound

$$\mathcal{D}^{\Phi_{21}^{(0)},\Phi_{21}^{(0)}}_{\sigma_{\mathbf{1}},\sigma_{\mathbf{1}}^{\dagger}} \leq 3 \,, \tag{5.161}$$

conjectured in [118] for all the cases we've checked. We should mention, as well, that we've managed to derive the equation conjectured in [173], and it is part of the results presented in Chapter 5. Furthermore, the conformal blocks in the $z_1 \to z_2$ channel were found in [173] to correspond to the following twist field fusion rules:

$$\sigma_{\mathbf{1}} \times \sigma_{\mathbf{1}}^{\dagger} \to \Phi_{\mathbf{1}} + \Phi_{[\mathbf{1}\,\phi_{1,3}\,\phi_{1,3}]} + \Phi_{1,3} \tag{5.162}$$

in agreement with the results of (5.4).

In general, knowing the dimension of the space of conformal blocks can be a useful guide in determining the BPZ-type differential equation that an orbifold correlator involving twist fields satisfies. This is because conformal blocks form bases of solutions around the singular points of these equations, so their order can be inferred from the dimensions $\mathcal{D}$. This, in turn, provides hints for finding which combination of orbifold null-vectors and Ward identities [118] one should manipulate to recover the BPZ-type equation.

5.6 Conclusion

In this chapter, we have provided a formal analysis of the $\mathcal{M}_n$ orbifold CFT, with prime n, of a diagonal and rational mother CFT $\mathcal{M}$. We have classified the operators of the theory under the neutral algebra of the full orbifold symmetry algebra. Analysing the spectrum of primary operators under $A_n \oplus \bar{A}_n$, we have found exact solutions for its modular data, as well as closed expressions for the fusion numbers of $\mathcal{M}_n$. Our results are consistent with the ones obtained for $n = 2$ in [119][3].

[2] if the number of primary fields of the mother CFT has a reasonable value

[3] note that since at $n = 2$ there is only one twist charge sector, there are no fusion rules involving three twist fields.

To showcase the use of our results, we have explicitly given all the fusion rules in the $\mathbb{Z}_3$-orbifold of the Yang-Lee CFT. We have also commented on the limitations of the unfolding approach, which requires, even in this relatively simple case, the computation of correlators on surfaces with genus $g \geq 1$. As a second example, we have shown how the fusion numbers can be used to count conformal blocks and commented on applications to the calculation of Rényi entropies. The block counting examples we have presented are consistent with previous results in the literature [118].

natural directions for investigations can be realized by considering more intricate mother CFTs as starting points. One could consider CFTs which are non-diagonal, non-rational or have extended symmetries as mother CFTs and generalize the results of this chapter. Alternatively, one could consider orbifolding by a generic $\mathbb{Z}_n$ group, i.e. removing the restriction of n to prime values: this will cause each twist sector $[k]$ to depend on the greatest common divisor $\gcd(k, n)$.

Finally, it would be mathematically interesting to find an interpretation for the expressions of the fusion numbers (5.136) and (5.137) in terms of fusion processes in the mother CFT. For $n = 2$, this has been done in [256], and the relevant surface is the crosscap. To our knowledge, generalizing this argument to generic n remains an open problem.

Chapter 6

Epilogue

In this thesis, we have investigated the properties of entanglement for pure states in critical systems by using the methods of two-dimensional conformal field theory. While the calculation of entanglement through these methods commenced almost two decades ago [46], for models with open boundaries few *exact* results have been obtained for all but the simplest bipartitions. This is because the presence of the boundary introduces additional technical complications for the field theoretical description of the system, discussed in detail in Chapter 1.

Let us now recap the results we've obtained, despite these obstacles. In Chapter 2, we've derived the leading contribution to the second Rényi entropy of an interval A in the bulk of a critical 1D system with open BC. This was done by relating $S_2^\alpha(A)$ to the annulus partition function of the BCFT that describes this system in the scaling limit. In Chapter 3 we have restricted our interests to models whose scaling limit is given by the free massless scalar of compactified with radius R with Neumann or Dirichlet BC. What we've gained by imposing this restriction, is that we've managed to obtain an *exact* result for the REE for *all* integer $n \geq 2$. As a by-product of this calculation, we've also obtained results in the $R \to \infty$ (decompactification limit) which are important for numerical studies of harmonic chains with open BC. These two projects were predominantly grounded in the replicated surface framework.

In Chapter 4, we've considered a different setup: an interval A containing one of the boundaries of a 1D critical system with *mixed BC*. For this project, we've obtained results for the second and third Rényi entropy for a variety of mixed BC setups, by using bootstrap methods in the cyclic orbifold BCFT. While this method does not seem to conveniently extend to generic n, it does provide a good handle on finite-size corrections.

From a more formal point of view, it would be interesting to use the treatment of Chapter 5 and an extension of the methods of Chapter 4 to formally "solve" the cyclic orbifold BCFT, at least for rational seed BCFTs. In principle, after properly classifying the boundary states of the theory, one should be able to use the sewing constraints of [130] and unfolding methods as employed in Section 4.4.3, to fix the bulk and boundary structure constants.

As the previous chapters have shown, determining the REE rests on either the evaluation of the partition function of a BCFT $\mathcal{M}$ on a replicated Riemann surface Σ_n or the calculation of a correlator in the $\mathbb{Z}_n$ orbifold of $\mathcal{M}$ on one copy of Σ_n. For the derivations of Chapters 2 and 3 we have benefited from the fact that the expressions for the annulus partition function (for generic BCFTs) and, respectively, the $\mathbb{D}_n$ partition function for the compact boson are relatively easy to

handle analytically. Furthermore, at least in the case of the compact boson, it seems that one could extend the results to address setups at finite temperatures and more general bipartitions (multiple disjoint intervals) with a reasonable amount of effort. However, even if one is to calculate the partition function through Riemann surface methods, finding the analytic continuation to $n \to 1$ might turn out to be a difficult task, as is already the case for the result [87] and our expressions for the REE of the compact boson of finite radius R in Chapter 3.

While obtaining exact and explicit expressions for the EE is the ideal outcome for these types of investigations, one can still learn a great deal about the properties of entanglement in a system from other types of results. For example, the predictions of [121] , given *implicitly* as solutions to an integral equation that needs to be solved numerically, are in agreement with our analytical results for the REE of a compact boson with Dirichlet BC.

There are also setups, in which the interesting information is already captured in some limiting regime of the model so that more approximate methods are sufficient for physical interests. For example, for AdS_3/CFT_2 investigations [97], the interest is mostly in the large central charge behaviour of the entanglement entropies so that one sets up a series expansion for them in $1/c$ whose coefficients are fixed by the structure constants of the orbifold operator algebra. For these types of applications [110], extending the investigations of Chapters 4 and 5 to BCFTs with $c \geq 1$ could be useful.

To wrap up, we hope that this work has shown that there is still a lot of "juice" to squeeze from the methods of two-dimensional conformal field theory for the exploration of entanglement in critical quantum systems with open boundaries. We hope that the work presented in this thesis will foster further investigations on these topics, as well as clarify certain murky details of some well-established results.

Acknowledgements

I would first like to thank my advisors, *Benoît Estienne* and *Yacine Ikhlef*, for accepting to take me in as a PhD student. Without exaggeration, I consider myself lucky to have been guided and supported by them for these three years, both on a personal and professional level. I am grateful for your availability, pedagogy and sense of humour manifested during the countless long discussions and coffee chats we've had.

Moving on, I would like to acknowledge Pasquale Calabrese and German Sierra for accepting to review my thesis. I also want to thank Jérôme Dubail, Jesper Jacobsen, Vincent Pasquier, Didina Serban, Jean-Marie Stéphan for their contributions as thesis jurors.

I would like to thank my collaborator, Erik Tonni, for illuminating early morning chats and for hosting me at SISSA. I also want to acknowledge Raoul Santachiara for inviting me to LPTMS, and Gregory Schehr and Benoît Douçot from LPTHE for interesting conversations.

Now, I will focus my thanks on the ephemeral members of the lab. It is beyond the scope of this section to express personalized gratitude for all the moments we've shared, be they in the kitchen, the bar, the boulder or the uncanny valley. I'd rather say that during those years, the lab felt less like a workplace and more like a sitcom – one in which the characters have great chemistry and the jokes are often good [1]. In the spirit of this comparison, I will let the credits roll:

Main cast: *Andriani*, *Anthony*, Carlo, Dîyar, Francesco C., Francesco M., Greivin, Jordan, Jules, Léo, Mathis, Maxl, Pierre, *Simon*, *Thorsten*, Tom, Vincent, Wenqi, Yann, Yehudi

Recurring roles: Andrea, Christiana, Davide, Luca, Sebastian.

Beyond this sizeable cast, there is a big world outside the lab. I would like to thank Abhinav, Anna, Cristi, Diana, Doriane, Ephraim, Erik, Federico, Georgiana, Jenna, Juan, Mariam, Pulkit, Romain, Rômullo, Wendy for populating it.

I also express my gratitude to my family for supporting me all these years. To my mother and father, for many teachable moments. To Alex for explaining essential teen slang to me. To Maria, for unmatched sense of humor. I would also like to acknowledge Dan and Sandu, as they bear some moral responsibility for my choice of career.

Finally, I would like to thank *Bianca*, my partner, for everything she has contributed and put up with during our shared life in Paris. Sa nu stricam prietenia!

[1] i.e. the opposite of Friends(1994-2002)

Appendix A

Appendix for chapter 2

A.1 Conventions and identities for elliptic functions

In this Appendix, we fix our notations and conventions for elliptic functions.

A.1.1 Jacobi theta functions

We use the following conventions for the Jacobi theta functions $\theta_i(t|\tau)$:

$$\begin{aligned}
\theta_1(t|\tau) &= -i \sum_{r\in\mathbb{Z}+1/2} (-1)^{r-1/2} y^r q^{r^2/2}\,, \qquad & \theta_2(t|\tau) &= \sum_{r\in\mathbb{Z}+1/2} y^r q^{r^2/2}\,,\\
\theta_3(t|\tau) &= \sum_{n\in\mathbb{Z}} y^n q^{n^2/2}\,, & \theta_4(t|\tau) &= \sum_{n\in\mathbb{Z}} (-1)^n y^n q^{n^2/2}\,,
\end{aligned} \tag{A.1}$$

where $q = e^{2i\pi\tau}$ and $y = e^{2i\pi t}$. Here, t is a complex variable and τ is a complex parameter living in the upper half-plane. Theta functions have a single zero, located at $z = 0, 1/2, (1+\tau)/2$ and $\tau/2$, respectively. They have no pole. Using Jacobi's triple product identity one can rewrite them as

$$\begin{aligned}
\theta_1(t|\tau) &= -iy^{1/2}q^{1/8}\prod_{n=1}^{\infty}(1-q^n)\prod_{n=0}^{\infty}(1-yq^{n+1})(1-y^{-1}q^n)\,,\\
\theta_2(t|\tau) &= y^{1/2}q^{1/8}\prod_{n=1}^{\infty}(1-q^n)\prod_{n=0}^{\infty}(1+yq^{n+1})(1+y^{-1}q^n)\,,\\
\theta_3(t|\tau) &= \prod_{n=1}^{\infty}(1-q^n)\prod_{r\in\mathbb{N}+1/2}^{\infty}(1+yq^r)(1+y^{-1}q^r)\,,\\
\theta_4(t|\tau) &= \prod_{n=1}^{\infty}(1-q^n)\prod_{r\in\mathbb{N}+1/2}^{\infty}(1-yq^r)(1-y^{-1}q^r)\,.
\end{aligned} \tag{A.2}$$

They satisfy the following half-period relations

$$\begin{aligned}
\theta_1(t|\tau) &= -i\,e^{i\pi(t+\tau/4)}\,\theta_4(t+\tau/2|\tau)\,,\\
\theta_2(t|\tau) &= \;e^{i\pi(t+\tau/4)}\,\theta_3(t+\tau/2|\tau)\,,\\
\theta_3(t|\tau) &= \;e^{i\pi(t+\tau/4)}\,\theta_2(t+\tau/2|\tau)\,,\\
\theta_4(t|\tau) &= -i\,e^{i\pi(t+\tau/4)}\,\theta_1(t+\tau/2|\tau)\,.
\end{aligned} \tag{A.3}$$

The functions $\theta_i(0|\tau) \equiv \theta_i(\tau)$ are

$$\begin{aligned}
\theta_2(\tau) &= \sum_{n\in\mathbb{Z}} q^{(n+1/2)^2/2} = 2q^{1/8}\prod_{n=1}^{\infty}(1-q^n)\,(1+q^n)^2\,, \\
\theta_3(\tau) &= \sum_{n\in\mathbb{Z}} q^{n^2/2} \quad\;\; = \prod_{n=1}^{\infty}(1-q^n)\left(1+q^{n-1/2}\right)^2\,, \\
\theta_4(\tau) &= \sum_{n\in\mathbb{Z}} (-1)^n q^{n^2/2} = \prod_{n=1}^{\infty}(1-q^n)\left(1-q^{n-1/2}\right)^2\,.
\end{aligned} \tag{A.4}$$

Finally, we note the following relations

$$\theta_3^4(\tau) = \theta_2^4(\tau) + \theta_4^4(\tau)\,, \qquad 2\eta^3(\tau) = \theta_2(\tau)\theta_3(\tau)\theta_4(\tau)\,, \tag{A.5}$$

where $\eta(\tau)$ is the Dedekind eta function :

$$\eta(\tau) = q^{\frac{1}{24}}\prod_{n=1}^{\infty}(1-q^n)\,. \tag{A.6}$$

A.1.2 Elliptic integral of the first kind

The elliptic integral of the first kind $K(x)$ is given by:

$$K(x) = \int_0^{\frac{\pi}{2}} \frac{\mathrm{d}\theta}{\sqrt{1-x^2\sin^2\theta}} = \frac{\pi}{2}\,{}_2F_1\left(\frac{1}{2},\frac{1}{2},1;x^2\right) = \frac{\pi}{2}\theta_3^2(\tau)\,. \tag{A.7}$$

This means

$$x = \frac{\theta_2^2(\tau)}{\theta_3^2(\tau)}\,. \tag{A.8}$$

The parameter x is called the elliptic modulus. The inverse relation is

$$q = e^{2i\pi\tau} = \exp\left(-2\pi\frac{K(x')}{K(x)}\right), \qquad x' = \sqrt{1-x^2} \tag{A.9}$$

or equivalently

$$\tau = i\frac{K(\sqrt{1-x^2})}{K(x)}\,. \tag{A.10}$$

In particular one can check that

$$x(1-x^2)\frac{d\tau}{dx} = \frac{2}{i\pi\theta_3^4(\tau)}\,. \tag{A.11}$$

A.1.3 Weierstrass elliptic function

One possible way to derive the differential equation (2.36) is to express the function $g(t)$ defined in (2.21) in terms of the Weierstrass elliptic function $\wp(t)$. The function $\wp : \mathbb{T}_\tau \to \widehat{\mathbb{C}}$ is defined on the complex torus $\mathbb{T}_\tau = \mathbb{C}/(\mathbb{Z}+\tau\mathbb{Z})$ and takes values in the Riemann sphere $\widehat{\mathbb{C}} = \mathbb{C}\cup\{\infty\}$:

$$\wp(t) = \frac{1}{t^2} + \sum_{(m,n)\in\mathbb{Z}^2\setminus(0,0)} \frac{1}{(t-m-n\tau)^2} - \frac{1}{(m+n\tau)^2}\,. \tag{A.12}$$

This is a covering map of the two-sphere $\widehat{\mathbb{C}}$ with 4 ramification points :

$$e_1 = \wp(1/2)\,, \qquad e_2 = \wp\left(\frac{1+\tau}{2}\right), \qquad e_3 = \wp\left(\frac{\tau}{2}\right), \qquad \infty = \wp(0)\,. \tag{A.13}$$

The lattice roots e_i can be expressed in terms of the theta functions as :

$$e_1 = \frac{\pi^2}{3}\left(\theta_2^4(\tau) + 2\theta_4^4(\tau)\right), \quad e_2 = \frac{\pi^2}{3}\left(\theta_2^4(\tau) - \theta_4^4(\tau)\right), \quad e_3 = -\frac{\pi^2}{3}\left(2\theta_2^4(\tau) + \theta_4^4(\tau)\right). \tag{A.14}$$

The function $g(t)$ as defined in (2.21) is simply the composition of $\wp(t)$ with a particular Möbius transformation that sends the ramification points to $0, 1/x, x$ and ∞ :

$$g(t) = \frac{1}{x}\frac{\wp(t) - e_3}{e_1 - e_3}, \qquad x = \sqrt{\frac{e_2 - e_3}{e_1 - e_3}} = \left(\frac{\theta_2(\tau)}{\theta_3(\tau)}\right)^2, \tag{A.15}$$

as follows from the fact that $(\wp(t) - e_3)/g(t)$ is constant by virtue of being doubly periodic and holomorphic (*i.e.* with no pole). Now from the differential equation obeyed by $\wp(t)$, namely

$$\wp'^2(t) = 4\left(\wp(t) - e_1\right)\left(\wp(t) - e_2\right)\left(\wp(t) - e_3\right), \tag{A.16}$$

we get

$$\left(\frac{dg}{dt}\right)^2 = -4\pi^2\theta_3^4(\tau)g(g-x)(1-xg)\,, \tag{A.17}$$

from which (2.36) follows.

A.2 Alternative derivation of the second Rényi entropy for A_n minimal models

In this Appendix, we present an alternative computation of the two-twist correlation function (2.44) based on the mirror trick [30] and BCFT bootstrap methods [130]. The conformal blocks are obtained in terms of the modular characters (see also [118, 123]). The other key ingredients are the bulk and bulk-boundary structure constants appearing in the conformal block expansion. We note that the correspondence between conformal blocks and characters has also been employed in the recent work of [222] for the evaluation of twist correlators on manifolds without boundaries.

To avoid some technicalities, we restrict our attention to Virasoro minimal models in the A_n series, for which the torus partition function is a diagonal modular invariant. On the unit disk, the mirror trick amounts to replacing the disk by its Schottky double [115], namely a sphere, and bulk fields $\phi(z, \bar{z})$ by a pair of chiral fields, one at position z and the other at its mirror image $1/\bar{z}$:

$$\phi(z, \bar{z}) \to \phi(z)\,\bar{z}^{-2h}\phi(1/\bar{z})\,. \tag{A.18}$$

Thus we can decompose $\langle\sigma(0,0)\sigma(x,\bar{x})\rangle_{\mathbb{D}}^{(\alpha,\alpha)}$ as a linear combination of conformal blocks on the sphere

$$\langle\sigma(0,0)\sigma(x,\bar{x})\rangle_{\mathbb{D}}^{(\alpha,\alpha)} = \sum_j X_j^\alpha f_j(x,\bar{x})\,, \tag{A.19}$$

$$f_j(x,\bar{x}) = \bar{x}^{-2h_\sigma} \quad \begin{matrix} \sigma(0) & & \sigma(\infty) \\ & \phi_j\otimes\phi_j & \\ \sigma(x) & & \sigma(1/\bar{x}) \end{matrix} \,. \tag{A.20}$$

Indeed, for the $\mathbb{Z}_2$ orbifold of a minimal model in the A_n series, the fusion $\sigma\times\sigma$ is of the form [118]

$$\sigma\times\sigma = \sum_{\phi_j \text{ primary}} \phi_j\otimes\phi_j\,, \tag{A.21}$$

where the sum runs over the primary operators of the mother CFT. We shall denote by h_j the conformal dimension of ϕ_j (recall that for A_n minimal models, all primary operators are scalar, so $\bar{h}_j = h_j$). The expansion coefficients X_j^α in (A.19) are obtained in terms of OPE structure constants as

$$X_j^\alpha = C_{\sigma\sigma}^{\phi_j\otimes\phi_j} A_{\phi_j\otimes\phi_j}^{(\alpha,\alpha)}, \tag{A.22}$$

which in turn can be expressed as [123]

$$A_{\phi_j\otimes\phi_j}^{(\alpha,\alpha)} = \langle(\phi_j\otimes\phi_j)(0)\rangle_{\mathbb{D}}^{(\alpha,\alpha)} = \left(\langle\phi_j(0)\rangle_{\mathbb{D}}^{\alpha}\right)^2 = \left(A_j^\alpha\right)^2\,, \tag{A.23}$$

$$C_{\sigma\sigma}^{\phi_j\otimes\phi_j} = \langle\sigma(\infty)(\phi_j\otimes\phi_j)(1)\sigma(0)\rangle_{\mathbb{C}} = 2^{-4h_j}\langle\phi_j(-1)\phi_j(1)\rangle_{\mathbb{C}} = 2^{-8h_j}\,, \tag{A.24}$$

so that

$$X_j^\alpha = 2^{-8h_j}\,(A_j^\alpha)^2\,. \tag{A.25}$$

The OPE coefficient A_j^α is very much related to coefficients Ψ_j^α appearing in the decomposition of the boundary state $|\alpha\rangle$ in terms of the Ishibashi states $|j\rangle\!\rangle$:

$$A_j^\alpha = \frac{\Psi_j^\alpha}{\Psi_0^\alpha}, \qquad |\alpha\rangle = \sum_j \Psi_j^\alpha\,|j\rangle\!\rangle\,. \tag{A.26}$$

For minimal models in the A_n series, these coefficients are given in terms of the modular S-matrix elements [257]:

$$\Psi_j^\alpha = \frac{S_{j\alpha}}{\sqrt{S_{0j}}}, \qquad A_j^\alpha = \frac{S_{j\alpha}}{S_{0\alpha}}\sqrt{\frac{S_{00}}{S_{j0}}}\,, \tag{A.27}$$

where the index 0 corresponds to the identity operator.

Let us turn to the expression of the conformal blocks f_j in terms of the characters of the mother CFT. By a simple rescaling, we have

$$f_j(x,\bar{x}) = \mathcal{F}_j(\eta), \qquad \eta = |x|^2\,, \tag{A.28}$$

where $\mathcal{F}_j(\eta)$ is the standard conformal block

$$\mathcal{F}_j(\eta) = \quad \begin{matrix} \sigma(0) & & \sigma(\infty) \\ & \phi_j\otimes\phi_j & \\ \sigma(\eta) & & \sigma(1) \end{matrix} \,. \tag{A.29}$$

These conformal blocks are known [123] to be related to the characters $\chi_j(\tau)$ of the mother theory via

$$\mathcal{F}_j(\eta) = 2^{8h_j - c/3}\,[\eta\,(1-\eta)]^{-c/24}\,\chi_j(\tau)\,, \qquad \eta = [\theta_2(\tau)/\theta_3(\tau)]^4\,. \tag{A.30}$$

Assembling the above results, we obtain the expression

$$\langle\sigma(0,0)\sigma(x,\bar{x})\rangle_{\mathbb{D}}^{(\alpha,\alpha)} = 2^{-\frac{c}{3}}\left[|x|^2(1-|x|^2)\right]^{-\frac{c}{24}} \sum_j (A_j^\alpha)^2\,\chi_j(\tau)\,. \tag{A.31}$$

The last step is to relate the above linear combination of characters to the annulus partition function:

$$Z_{\alpha|\alpha}(\tau) = \langle\alpha|e^{i\pi\tau(L_0+\bar{L}_0-c/12)}|\alpha\rangle = \sum_j (\Psi_j^\alpha)^2\,\langle\!\langle j|e^{i\pi\tau(L_0+\bar{L}_0-c/12)}|j\rangle\!\rangle = \sum_j (\Psi_j^\alpha)^2\,\chi_j(\tau)\,, \tag{A.32}$$

using (A.26), and $g_\alpha = \Psi_0^\alpha$.

A.3 Annulus partition function for the compact boson

For the following discussion, it is useful to have in mind a lattice model whose scaling limit is given by the free compact boson – we take for example the six-vertex (6V) model on the square lattice. It is well established (see [258] for instance) that the 6V model with homogeneous Boltzmann weights

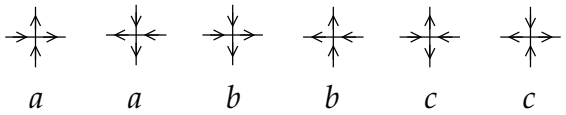

is critical in the regime

$$|\Delta| < 1\,, \qquad \Delta = \frac{a^2+b^2-c^2}{2ab}\,, \tag{A.33}$$

and is described in the scaling limit by a free compact boson with action

$$S[\phi] = \frac{1}{8\pi}\int d^2r\,\partial_\mu\phi\,\partial^\mu\phi\,, \qquad \phi \equiv \phi + 2\pi R\,, \tag{A.34}$$

where the compactification radius is given by $R = \sqrt{(2/\pi)\cos^{-1}\Delta}$. We consider the 6V model on a rectangle of $M \times N$ sites, with periodic boundary conditions in the horizontal direction, and reflecting boundary conditions at the top and bottom edges, for even M, N. Any 6V configuration defines (up to a global shift) a height function on the dual lattice, with steps $\pm\pi R$ between neighbouring heights. Since the local arrow flux into each of the boundaries is zero, the height function is constant along each boundary, and it is periodic in the horizontal direction. However, there can be a flux of $2m$ arrows (with $m \in \mathbb{Z}$) going between the two boundaries, and hence the height difference between the boundaries is of the form $2\pi mR$. In the scaling limit $N, M \to \infty$ with $N/M = \operatorname{Im}\tau/2$, the height function renormalizes to the free boson ϕ, and we get

$$Z_{6V}(M/N) \to \sum_{m\in\mathbb{Z}} Z_{\alpha|\alpha+m}(\tau)\,, \tag{A.35}$$

where α is an arbitrary integer, and $Z_{\alpha|\beta}(\tau)$ denotes the partition function of (A.34) on the annulus of Figure 2.4 with Dirichlet boundary conditions $\phi(x,0) = 2\pi R\alpha$ and $\phi(x, \mathrm{Im}\,\tau/2) = 2\pi R\beta$. A path integral computation gives

$$Z_{\alpha|\beta}(\tau) = \frac{e^{-i\pi R^2(\alpha-\beta)^2/\tau}}{\eta(-1/\tau)}\,. \tag{A.36}$$

Hence, the scaling limit of the 6V partition function is

$$Z_{6V}(M/N) \to Z(\tau) = \frac{\sum_{m\in\mathbb{Z}} e^{-i\pi R^2 m^2/\tau}}{\eta(-1/\tau)} = \frac{\theta_3(-R^2/\tau)}{\eta(-1/\tau)}\,. \tag{A.37}$$

In the geometry of the infinite strip of width N sites, the 6V transfer matrix generates the XXZ spin-chain Hamiltonian

$$H_{XXZ} = -\sum_{j=1}^{N-1}\left(s_j^x s_{j+1}^x + s_j^x s_{j+1}^x + \Delta s_j^z s_{j+1}^z\right), \tag{A.38}$$

where $s_j^{x,y,z}$ are Pauli matrices acting on site j. Reflecting boundary conditions for the 6V model (and thus Dirichlet boundary conditions for the boson) correspond to free boundary conditions on the spins.

Appendix B

Appendix for Chapter 3

B.1 An insight from the six-vertex model

The Hamiltonian of the spin-$\frac{1}{2}$ XXZ spin chain with open BC is [217]

$$H_{\text{XXZ}} = \sum_{j=1}^{N-1} \left(\sigma_j^x \sigma_{j+1}^x + \sigma_j^y \sigma_{j+1}^y + \Delta\, \sigma_j^z \sigma_{j+1}^z \right) - h_1 \sigma_1^x - h_N \sigma_N^x \tag{B.1}$$

where $\sigma_j^{x,y,z}$ denote the Pauli matrices acting on the j-th site, $\{h_1, h_N\}$ are boundary fields and the anisotropy parameter Δ lies in the critical regime $|\Delta| < 1$. The model (B.1) is a gapless one-dimensional quantum system belonging to the Luttinger liquid universality class. The related discrete 2D classical model is the six-vertex model on the square lattice with Boltzmann weights

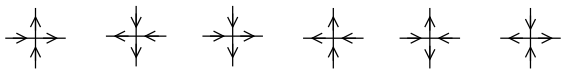

such that

$$\frac{a^2 + b^2 - c^2}{2ab} = \Delta\,. \tag{B.2}$$

The six-vertex model is mapped to a height model on the dual lattice, with height values $\varphi(p) \in \mathbb{Z}$, through the following simple rule. For any pair on neighbouring faces p, p', we set $\varphi(p') = \varphi(p) + 1$ (resp. $\varphi(p') = \varphi(p) - 1$) if p' is above or to the right of (resp. below or to the left of) p , following the reasoning of [258]. The arrow conservation around each vertex ensures that the height ϕ is well defined, up to an overall additive constant.

In the scaling limit, the height variable $\varphi(p)$ provides a real compact boson $\varphi(p) \to \phi(p)/(\pi R)$, with renormalised radius $R = \sqrt{(2/\pi)\arccos(-\Delta)}$ [217]. Note also that setting free BC in the XXZ chain ($h_1 = h_N = 0$) corresponds to Dirichlet BC in the compact boson [259], while turning on the boundary fields leads to Neumann BC [217].

From the above mapping, we see that in any partition function, the variation $\delta\phi$ along any trivial cycle is zero, whereas for non-trivial cycles or open paths joining two boundary points this variation $\delta\phi$ is a multiple of $2\pi R$ (by convention, we only consider lattices for which these non-trivial cycles and open paths have even length so that the configuration with $\delta\phi = 0$ along each of these cycles and paths is allowed). In the scaling limit, this corresponds to (3.38).

B.2 Period matrix

In this Appendix, we discuss the derivation of the period matrix (3.25). This is a standard computation (see for instance [71]) that we report here for the sake of completeness.

We are interested in the period matrix of the Riemann surface Σ_n given by the n-sheeted covering surface over the Riemann sphere $\mathbb{CP}^1$ with four branch points at $0, x, 1/\bar{x}, \infty$ and a branch cut connecting 0 to x and another connecting $1/\bar{x}$ to ∞. Without loss of generality, we could assume x real positive. The Riemann surface Σ_n can be defined as the algebraic curve $w^n = z(z-x)(z-1/\bar{x})^{n-1}$ with $(z,w) \in \mathbb{C}^2$ (up to compactification and resolution of the singularity at the origin by a blow-up). It is a compact Riemann surface with genus $n-1$. This can be obtained from the Riemann-Hurwitz theorem, which provides the Euler characteristics of the n-sheeted covering $\mathscr{P}_n$ of a generic Riemann surface $\mathscr{P}_1$ as follows

$$\chi(\mathscr{P}_n) = n\,\chi(\mathscr{P}_1) - 4(n-1) \tag{B.3}$$

where $\chi(\mathscr{P}) = 2-2g$ is the Euler characteristic of a Riemann surface $\mathscr{P}$ without boundaries. In our case $\Sigma_1 = \mathbb{CP}^1$; hence $\chi(\Sigma_n) = 4-2n$.

A compact Riemann surface of genus g supports g linearly independent holomorphic one-forms. The ones for Σ_n have been constructed explicitly and read [70]

$$\omega_k = \frac{1}{z^{k/n}(z-x)^{(n-k)/n}(z-1/\bar{x})^{k/n}}\,dz \qquad\qquad k \in \{1,\cdots,n-1\} \tag{B.4}$$

This is the basis of holomorphic one-forms diagonalising the holomorphic deck transformation f that sends the j-th sheet to the $(j+1)$-th sheet; indeed, we have that $f^*\omega_k = e^{-2\pi i k/n}\,\omega_k$, being f^* defined as the pullback of the deck transformation.

We work with the cycles $\mathcal{A}_j, \mathcal{B}_j$ and C_j described in section 3.2.1 and depicted in figure 3.4. The period matrix $\boldsymbol{\tau}$ of Σ_n is then

$$\boldsymbol{\tau} = \boldsymbol{A}^{-1}\cdot\boldsymbol{B} \qquad\qquad \boldsymbol{A}_{k,j} = \int_{\mathcal{A}_j}\omega_k \qquad\qquad \boldsymbol{B}_{k,j} = \int_{\mathcal{B}_j}\omega_k \tag{B.5}$$

The integrals

$$\oint_{C_j}\omega_k \qquad\qquad \oint_{\mathcal{B}_j}\omega_k \tag{B.6}$$

can be computed exactly [70]. Indeed, by using that $f^*\omega_k = e^{-2\pi i k/n}\,\omega_k$, we have

$$\oint_{C_j}\omega_k = \mathrm{e}^{-2\pi i k(j-1)/n}\oint_{C_1}\omega_k \qquad\qquad \oint_{\mathcal{B}_j}\omega_k = \mathrm{e}^{-2\pi i k(j-1)/n}\oint_{\mathcal{B}_1}\omega_k \tag{B.7}$$

which tells us that just two contour integrals in the r.h.s. must be computed. These integrals can be calculated by deforming the contours down to the branch cut and using the integral representation of the Gauss hypergeometric function. This gives

$$\oint_{C_1}\omega_k = 2\,\mathrm{i}\sin(\pi k/n)\int_0^x\omega_k = 2\pi\,\mathrm{i}\,\bar{x}^{k/n}F_{k/n}(|x|^2) \tag{B.8}$$

and

$$\oint_{\mathcal{B}_1}\omega_k = -2\pi\mathrm{i}\,\bar{x}^{k/n}\,\mathrm{e}^{-\pi i k/n}\,F_{k/n}(1-|x|^2) \tag{B.9}$$

where we remind that $F_a(y) \equiv {}_2F_1(a, 1-a; 1; y)$. The final result for the generic element of the $(n-1)\times(n-1)$ period matrix reads

$$\boldsymbol{\tau}_{i,j}(|x|^2) = \mathrm{i}\,\frac{2}{n}\sum_{k=1}^{n-1}\sin(\pi k/n)\,\frac{F_{k/n}(1-|x|^2)}{F_{k/n}(|x|^2)}\,\cos\Big[2\pi k(i-j)/n\Big] \tag{B.10}$$

which is the result obtained in [71]. The period matrix (B.10) satisfies the following relation

$$\boldsymbol{\tau}(1-|x|^2) \;=\; -\,\boldsymbol{T}\cdot\boldsymbol{\tau}(|x|^2)^{-1}\cdot\boldsymbol{T}^{\mathrm{t}} \tag{B.11}$$

where the generic element of the matrix $\boldsymbol{T}$ is $\boldsymbol{T}_{j,k} \equiv \delta_{j,k} - \delta_{j,k+1}$. This is reminiscent of the relations found in Appendix C.3.3 of [88] in the special case of two disjoint intervals on the line.

B.3 Green function in the presence of twist fields

Consider a non-compact complex scalar field Φ on the unit disk $\mathbb{D}$ satisfying the following condition after a rotation of the complex coordinate z around a branch point at $z = 0$ [70] (see also (3.53))

$$\Phi(e^{2i\pi}z, e^{-2i\pi}\bar{z}) = \mathrm{e}^{2\pi\mathrm{i}\,k/n}\,\Phi(z,\bar{z}) \tag{B.12}$$

and a similar condition with opposite phase after a rotation around $z = x \in (0,1)$. To have a simpler notation and to prevent any potential confusion with the mirror image, we will use the notation $\Phi(z)$ instead of $\Phi(z,\bar{z})$. However, it is important to note that this does not imply that the field $\Phi(z)$ depends holomorphically on the position z.

These conditions define the occurrence of a twist field $\sigma_{k/n}$ at $z = 0$ and of its conjugate field $\sigma^\dagger_{k/n}$ at $z = x$. The holomorphic part of the stress-energy tensor $T(z)$ for the complex boson we are considering is

$$T(z) = -\frac{1}{2}:\partial_z\Phi(z)\partial_z\overline{\Phi}(z): \;=\; -\lim_{w\to z}\left[\frac{\partial_z\Phi(z)\,\partial_w\overline{\Phi}(w)}{2} + \frac{1}{(z-w)^2}\right] \tag{B.13}$$

By adapting the analysis of [70] to the case where a conformal boundary occurs, in the following, we show that

$$\frac{\langle T(z)\,\sigma_{k/n}(0)\,\sigma^\dagger_{k/n}(x)\rangle_{\mathbb{D}}}{\langle\sigma_{k/n}(0)\,\sigma^\dagger_{k/n}(x)\rangle_{\mathbb{D}}} = \frac{h_{k/n}\left[x(1/\bar{x}-2z)+z^2\right]^2}{z^2(z-x)^2(z-1/\bar{x})^2} - \frac{x(x-1/\bar{x})}{z(z-x)(z-1/\bar{x})}\,\partial_x\log E^{(\alpha)}_{k/n}(x) \tag{B.14}$$

where $h_{k/n}$ and $E^{(\alpha)}_{k/n}(x)$ have been defined in (3.57). Then, taking the residue of (B.14) at $z \to x$ leads to (3.56).

Let us consider the following Green functions on the unit disk $\mathbb{D}$

$$G_{k/n}(z,w) \;=\; \frac{\langle\partial_z\Phi(z)\,\partial_w\overline{\Phi}(w)\,\sigma_{k/n}(0)\,\sigma^\dagger_{k/n}(x)\rangle_{\mathbb{D}}}{\langle\sigma_{k/n}(0)\,\sigma^\dagger_{k/n}(x)\rangle_{\mathbb{D}}} \tag{B.15}$$

$$H_{k/n}(z,w) \;=\; \frac{\langle\partial_{\bar{z}}\Phi(z)\,\partial_w\overline{\Phi}(w)\,\sigma_{k/n}(0)\,\sigma^\dagger_{k/n}(x)\rangle_{\mathbb{D}}}{\langle\sigma_{k/n}(0)\,\sigma^\dagger_{k/n}(x)\rangle_{\mathbb{D}}} \tag{B.16}$$

where $|z| \leqslant 1$, $|w| \leqslant 1$ and the boundary condition on $\partial\mathbb{D}$ reads

$$z\,\partial_z\Phi = \pm\,\bar{z}\,\partial_{\bar{z}}\Phi \tag{B.17}$$

with + and − corresponding respectively to Dirichlet BC and Neumann BC . As remarked above, the notation $H_{k/n}(z,w)$ does not mean that $H_{k/n}$ is holomorphic in z (as a matter of fact it is antiholomorphic in z). On the other hand, the function $G_{k/n}$ is holomorphic in z and w; hence the Schwarz reflection principle can be employed to obtain its analytic continuation to the whole Riemann sphere, via

$$G_{k/n}(z,w) = \begin{cases} \pm\,\dfrac{1}{z^2}\,\dfrac{\langle\partial_{\bar{z}}\Phi(1/\bar{z})\,\partial_w\overline{\Phi}(w)\,\sigma_{k/n}(0)\,\sigma^\dagger_{k/n}(x)\rangle_{\mathbb{D}}}{\langle\sigma_{k/n}(0)\,\sigma^\dagger_{k/n}(x)\rangle_{\mathbb{D}}} & |z|\geqslant 1,\ |w|\leqslant 1 \\ \pm\,\dfrac{1}{w^2}\,\dfrac{\langle\partial_z\Phi(z)\,\partial_{\bar{w}}\overline{\Phi}(1/\bar{w})\,\sigma_{k/n}(0)\,\sigma^\dagger_{k/n}(x)\rangle_{\mathbb{D}}}{\langle\sigma_{k/n}(0)\,\sigma^\dagger_{k/n}(x)\rangle_{\mathbb{D}}} & |z|\leqslant 1,\ |w|\geqslant 1 \\ \pm\,\dfrac{1}{w^2\,z^2}\,\dfrac{\langle\partial_{\bar{z}}\Phi(1/\bar{z})\,\partial_{\bar{w}}\overline{\Phi}(1/\bar{w})\,\sigma_{k/n}(0)\,\sigma^\dagger_{k/n}(x)\rangle_{\mathbb{D}}}{\langle\sigma_{k/n}(0)\,\sigma^\dagger_{k/n}(x)\rangle_{\mathbb{D}}} & |z|\geqslant 1,\ |w|\geqslant 1 \end{cases} \tag{B.18}$$

The Green function $H_{k/n}$, which is anti-holomorphic in z and holomorphic in w, can be analytically continued similarly. Moreover, these two Green functions are related through a mirror relation as follows

$$G_{k/n}(z,w) = \pm\frac{1}{z^2}\,H_{k/n}(1/\bar{z},w) \tag{B.19}$$

whenever they are well defined functions, namely for $z\neq w$ and $z,w\notin\{0,x,1/\bar{x},\infty\}$. The r.h.s. of (B.19) is indeed holomorphic in z as $H_{k/n}(1/\bar{z},w)$ is the composition of two anti-holomorphic functions, namely $H_{k/n}(z,w)$ and $\zeta(z)=1/\bar{z}$.

Now one observes that $z^{k/n}(z-x)^{1-k/n}(z-1/\bar{x})^{k/n}\,G_{k/n}(z,w)$ is holomorphic on the whole Riemann sphere except for $z=w$, where a second-order pole occurs. Hence, for $G_{k/n}(z,w)$ we must have

$$G_{k/n}(z,w) = f_{k/n}(z)\left(\frac{\alpha_{k/n}}{(z-w)^2}+\frac{\beta_{k/n}}{(z-w)}+\gamma_{k/n}\right) \tag{B.20}$$

where $\alpha_{k/n},\beta_{k/n}$ and $\gamma_{k/n}$ are independent of z, while

$$f_{k/n}(z) = \frac{1}{z^{k/n}(z-x)^{(1-k/n)}(z-1/\bar{x})^{k/n}} \tag{B.21}$$

From the OPE of $\partial_z\Phi(z)\,\partial_w\overline{\Phi}(w)$ as $z\to w$, we have that $G_k(z,w) = -2/(z-w)^2 + O(1)$. This condition gives $\alpha_{k/n}$ and $\beta_{k/n}$, which can be plugged into (B.20), finding

$$G_{k/n}(z,w) = -\frac{2f_{k/n}(z)}{f_{k/n}(w)}\left(\frac{1}{(z-w)^2}-\frac{f'_{k/n}(w)/f_{k/n}(w)}{z-w}+f_{k/n}(w)\,f_{1-k/n}(w)\,\mu_{k/n}(w)\right) \tag{B.22}$$

for some unknown function $\mu_{k/n}$. The same argument for the complex variable w leads to

$$G_{k/n}(z,w) = -\frac{2f_{1-k/n}(w)}{f_{1-k/n}(z)}\left(\frac{1}{(z-w)^2}-\frac{f'_{1-k/n}(z)/f_{1-k/n}(z)}{w-z}+f_{1-k/n}(z)\,f_{k/n}(z)\,\mu_{1-k/n}(z)\right) \tag{B.23}$$

Comparing (B.22) and (B.23), one obtains

$$\mu_{k/n}(z) = \frac{k}{n}(z-x) + A_{k/n}(x) \qquad\qquad A_{k/n} = A_{1-k/n} \tag{B.24}$$

Finally, combining (B.21)-(B.24), we arrive to

$$\begin{aligned} G_{k/n}(z,w) \;&=\; \\ &= -2\, f_{k/n}(z) f_{1-k/n}(w) \left[\frac{k}{n}\, \frac{z(z-1/\bar{x})(w-x)}{(z-w)^2} + \left(1-\frac{k}{n}\right) \frac{w(w-1/\bar{x})(z-x)}{(z-w)^2} + A_{k/n}(x) \right] \end{aligned} \tag{B.25}$$

Then, it follows from (B.13) that

$$\frac{\langle T(z)\, \sigma_{k/n}(0)\, \sigma^{\dagger}_{k/n}(x)\rangle_{\mathbb{D}}}{\langle \sigma_{k/n}(0)\, \sigma^{\dagger}_{k/n}(x)\rangle_{\mathbb{D}}} = \frac{h_{k/n}\left[x(1/\bar{x}-2z)+z^2\right]^2}{z^2(z-x)^2(z-1/\bar{x})^2} + \frac{A_{k/n}(x)}{z(z-x)(z-1/\bar{x})} \tag{B.26}$$

where the dependence on the boundary condition is encoded only in $A_{k/n}(x)$.

In the case of Neumann BC, we can determine $A_{k/n}(x)$ by exploiting the fact that the field $\Phi(z)$ has no windings. In particular, $\langle \Phi(z)\, \partial_w \overline{\Phi}(w)\, \sigma_{k/n}(0)\, \sigma^{\dagger}_{k/n}(x)\rangle_{\mathbb{D}}$ must be a single-valued function of z. By using that $d\Phi = \partial_z \Phi\, dz + \partial_{\bar{z}} \Phi(z)\, d\bar{z}$ and comparing with (B.15) and (B.16), we find that the above condition implies

$$\oint_{C_1} \Big[\, G_{k/n}(z,w)\, dz + H_{k/n}(z,w)\, d\bar{z} \,\Big] = 0 \tag{B.27}$$

To evaluate the l.h.s., one can first change variable to $\xi \equiv \zeta(z) = 1/\bar{z}$ and using (B.19), finding

$$\oint_{C_1} H_{k/n}(z,w)\, d\bar{z} \;=\; \oint_{C_1} H_{k/n}(1/\bar{\xi},w)\, d(1/\xi) \;=\; \oint_{C_1} G_{k/n}(\xi,w)\, d\xi \qquad \text{Neumann BC} \tag{B.28}$$

where we used that $\zeta(C_1) = C_1$. Thus, the constraint (B.27) boils down to

$$\oint_{C_1} G_{k/n}(z,w)\, dz = 0 \qquad \text{Neumann BC} \tag{B.29}$$

In the case of Dirichlet BC, the constraint (B.27) is automatically satisfied; indeed the above change of variable leads to

$$\oint_{C_1} H_{k/n}(z,w)\, d\bar{z} = -\oint_{C_1} G_{k/n}(\xi,w)\, d\xi \tag{B.30}$$

Now, since $\Phi(z)$ vanishes on all boundary components, we have that

$$\int_{\mathcal{B}_1^+} \Big[\, G_{k/n}(z,w)\, dz + H_{k/n}(z,w)\, d\bar{z} \,\Big] = 0 \qquad \text{Dirichlet BC} \tag{B.31}$$

where $\mathcal{B}_1^+$ is the part of $\mathcal{B}_1$ located inside the white region in Fig. 3.4, which connects the two red points located on two different components of the boundary.

Using the above change of variable, the condition (B.31) becomes

$$\oint_{\mathcal{B}_1} G_{k/n}(z,w)\, dz = 0 \qquad \text{Dirichlet BC} \tag{B.32}$$

where we used the fact that mirror image of $\mathcal{B}_1^+$ is the remaining part of $\mathcal{B}_1$ with the opposite orientation.

By using (B.25), the constraints (B.29) and (B.32) become

$$\oint_C f_{k/n}(z)\left[\frac{k}{n}\,\frac{z(z-1/\bar{x})(w-x)}{(z-w)^2}+\left(1-\frac{k}{n}\right)\frac{w(w-1/\bar{x})(z-x)}{(z-w)^2}+A_{k/n}(x)\right]dz\;=\;0 \tag{B.33}$$

where the contour is either $C = C_1$ for Neumann BC or $C = \mathcal{B}_1$ for Dirichlet BC; hence

$$\begin{aligned} A_{k/n}(x)\oint_C f_{k/n}(z)\,dz \;&= \\ &= -\oint_C f_{k/n}(z)\left[\frac{k}{n}\,\frac{z(z-1/\bar{x})(w-x)}{(z-w)^2}+\left(1-\frac{k}{n}\right)\frac{w(w-1/\bar{x})(z-x)}{(z-w)^2}\right]dz \end{aligned} \tag{B.34}$$

The analysis of this equation has been already carried out in [70]. However, in the following, we report a detailed derivation for the sake of completeness.

The first important feature to highlight is the fact that the r.h.s. of (B.34) does not depend on w. This follows from the relation

$$\begin{aligned} \frac{\partial}{\partial w}\left[f_{k/n}(z)\left(\frac{k}{n}\frac{z(z-1/\bar{x})(w-x)}{(z-w)^2}+\left(1-\frac{k}{n}\right)\frac{w(w-1/\bar{x})(z-x)}{(z-w)^2}\right)\right] \;&= \\ &= -\frac{\partial}{\partial z}\left[\frac{z(z-x)(z-1/\bar{x})f_{k/n}(z)}{(z-w)^2}\right] \end{aligned} \tag{B.35}$$

Since (B.34) is independent of w, we can choose convenient points for w on the Riemann sphere. In particular, considering $w = x$, we obtain

$$A_{k/n}(x)\oint_C f_{k/n}(z)\,dz = -\left(1-\frac{k}{n}\right)x\,(x-1/\bar{x})\oint_C \frac{f_{k/n}(z)}{z-x}\,dz \tag{B.36}$$

Now one observes that the definition of $f_{k/n}(z)$ in (B.21) straightforwardly leads to

$$\partial_x f_{k/n}(z) = \left(1-\frac{k}{n}\right)\frac{f_{k/n}(z)}{z-x} \tag{B.37}$$

which can be employed in (B.36), finding that

$$A_{k/n}(x) = -\,(x-1/\bar{x})\,x\,\partial_x \log\oint_C f_{k/n}(z)dz \tag{B.38}$$

Since the integrals $\oint_C f_{k/n}(z)dz$ have already been evaluated in (B.8) and (B.9), we arrive to

$$A_k(x) = -\,(x-1/\bar{x})\,x\,\partial_x \log E^{(\alpha)}_{k/n}(x) \tag{B.39}$$

where $E^{(\alpha)}_{k/n}(x)$ has been defined in (3.57). This concludes the derivation of (B.14), whose residue at $z \to x$ leads to (3.56).

B.4 Interval adjacent to the boundary

The entanglement entropies of the interval $A = [0, v]$ for a BCFT with central charge c defined on the segment $[0, L]$ are [46] (see also (B.40))

$$S_n(\ell) = \frac{c}{12}\left(1+\frac{1}{n}\right)\log\left[\frac{2L}{\pi\epsilon}\,\sin\left(\frac{\pi v}{L}\right)\right]+\log(g) \tag{B.40}$$

up to subleading terms, where g is the boundary entropy of [32]. Focussing on the case of the massless boson, which has $c = 1$, in the following we recover (B.40) for this model by taking the limit $u \to 0$ of $\langle \sigma_n(u)\, \sigma_n^\dagger(v) \rangle_{s_L}^{(\alpha)}$ for a finite value of R. This provides an important consistency check of our BCFT results (3.23).

By employing (3.65), the expressions in (3.23) can be written respectively as follows

$$\mathcal{F}_n^{(\mathrm{D})}(r) = R^{n-1}\, \frac{\Theta\Big(-R^2 \boldsymbol{\tau}(r)^{-1}\Big)}{\Theta\Big(-\boldsymbol{\tau}(r)^{-1}\Big)} \qquad\qquad \mathcal{F}_n^{(\mathrm{N})}(r) = \left(\frac{2}{R}\right)^{n-1} \frac{\Theta\Big(-4\boldsymbol{\tau}(r)^{-1}/R^2\Big)}{\Theta\Big(-\boldsymbol{\tau}(r)^{-1}\Big)} \tag{B.41}$$

whose prefactors can be written in terms of the ground state degeneracies [32] for this model, which are [142, 217]

$$g_{\mathrm{D}} \equiv \sqrt{\frac{1}{R}} \qquad\qquad g_{\mathrm{N}} \equiv \sqrt{\frac{R}{2}} \tag{B.42}$$

for Dirichlet and Neumann BC respectively,

From (3.10), we have that $r \to 1^-$ when $u \to 0^+$. Taking this limit in (B.41), one finds

$$\mathcal{F}_n^{(\mathrm{D})}(r) \to g_{\mathrm{D}}^{2(1-n)} \qquad\qquad \mathcal{F}_n^{(\mathrm{N})}(r) \to g_{\mathrm{N}}^{2(1-n)} \tag{B.43}$$

(in the numerical checks of the Dirichlet BC case, R should not be too small).

The bulk-boundary Operator Product Expansion (OPE) of the twist field $\sigma(u)$ reads [110]

$$\sigma(u) \sim \mathcal{A}_{n;\alpha} (2u)^{-\Delta_n}\, \mathbb{I} + \dots \qquad\qquad u \to 0^+ \tag{B.44}$$

where $\mathbb{I}$ denotes the identity operator on the boundary, the dots indicate subleading contributions that have been neglected and $\mathcal{A}_{n;\alpha}$ is the one-point structure constant, which can be expressed in terms of the ground state degeneracy g_α as $\mathcal{A}_{n;\alpha} = g_\alpha^{1-n}$ [46, 110]. In our case, combining this observation with (B.43), one concludes that $\mathcal{F}_n^{(\alpha)}(r) \to \mathcal{A}_{n;\alpha}^2$ as $r \to 1$, for $\alpha \in \{\mathrm{D}, \mathrm{N}\}$. This observation and (3.9) lead to

$$\langle \sigma_n(u)\, \sigma_n^\dagger(v) \rangle_{s_L}^{(\alpha)} \sim (2u)^{-\Delta_n} \mathcal{A}_{n;\alpha}^2\, [s(2v)]^{-\Delta_n} + \dots \tag{B.45}$$

From the bulk-boundary OPE (B.44), it is straightforward to find that

$$\langle \sigma_n(u)\, \sigma_n^\dagger(v) \rangle_{\mathrm{s}}^{(\alpha)} \sim \mathcal{A}_{n;\alpha} (2u)^{-\Delta_n} \langle \sigma_n^\dagger(v) \rangle_{s_L}^{(\alpha)} + \dots \tag{B.46}$$

Finally, (B.45) and (B.46) are consistent when $\langle \sigma_n^\dagger(v) \rangle_{s_L}^{(\alpha)} = g_\alpha^{(1-n)} / s(2v)^{\Delta_n}$, in agreement with (1.52).

B.5 Limits in the decompactified case

B.5.1 Normalization of twist 2-point function

In this section, we determine the overall normalization of the two-point functions of twist fields in the decompactified regime. In the finite R case, we have used the $x \to 0$ behaviour of the twist correlator to fix such constants, and we shall pursue the same strategy here, with a few modifications.

The extra difficulty arises due to the *continuous* primary operator spectrum of the non-compact boson CFT, which is formed by vertex operators $V_\gamma =: \exp i\gamma\Phi(z,\bar{z}) :$, with scaling dimensions $\Delta_\gamma = \gamma^2$ and $\gamma \in \mathbb{R}$. Thus, in the $\mathbb{Z}_N$ orbifold of this theory [118, 211, 235], the untwisted sector is built from operators [1]:

$$\mathcal{V}_\gamma = V_{\gamma_1} \otimes \cdots \otimes V_{\gamma_n} \tag{B.47}$$

with $\gamma = \{\gamma_1, \ldots, \gamma_n\}$ and the identity field given by $\mathbb{I} = \mathcal{V}_0$.

The leading $x \to 0$ behaviour in (3.71) will then be obtained by considering the OPE of the twist fields, which, by twist charge conservation can only contain fields of type (B.47)[2]. Since the spectrum of untwisted primary fields is continuous, the OPE should be given by a weighted integral over the $\mathcal{V}_\gamma$ operators. We conjecture, then, encouraged by previous works [235], that the contribution of untwisted primary operators to the OPE of conjugate twist fields is :

$$\sigma(0,0)\sigma_n^\dagger(x) \sim x^{-2\Delta_n} \int_{\mathbb{R}^n} \prod_{i=1}^n d\gamma_i \, \delta\left(\sum_i \gamma_i\right) x^{\gamma^2} C_{\sigma,\sigma_n^\dagger}^{\mathcal{V}_\gamma} \mathcal{V}_\gamma(0,0) \tag{B.48}$$

where the δ function appears as a consequence of $U(1)$ charge conservation in the non-compact boson CFT, and we work with the usual conventions that the structure constant $C_{\sigma,\sigma_n^\dagger}^{\mathbb{I}} = 1$.

Now we plug (B.48) in the twist field two-point functions (3.71) to find the primary field contribution to the limit $x \to 0$ for Neumann and Dirichlet BC:

$$\langle \sigma(0,0)\sigma_n^\dagger(x)\rangle_{\mathbb{D}}^{(\alpha)} \underset{x\to 0}{\sim} x^{-2\Delta_n} \int_{\mathbb{R}^n} \prod_{i=1}^n d\gamma_i \, \delta\left(\sum_i \gamma_i\right) x^{\gamma^2} C_{\sigma,\sigma_n^\dagger}^{\mathcal{V}_\gamma} \langle \mathcal{V}_\gamma(0,0)\rangle_{\mathbb{D}}^{\alpha} \tag{B.49}$$

Conveniently, the correlators in (B.49) factorize into one-point functions of the non-compact boson BCFT:

$$\langle \mathcal{V}_\gamma(0,0)\rangle_{\mathbb{D}}^{\alpha} = \prod_{i=1}^n \langle V_{\gamma_i}(0,0)\rangle_{\mathbb{D}}^{\alpha} \tag{B.50}$$

which are given by [24]:

$$\langle V_\gamma(0,0)\rangle_{\mathbb{D}}^{(\mathrm{N})} = \delta(\gamma) \qquad \langle V_\gamma(0,0)\rangle_{\mathbb{D}}^{(D,\phi_0)} = e^{i\gamma\phi_0} \tag{B.51}$$

for Neumann BC and Dirichlet BC with $\phi_0 = constant$. Thus, we find:

$$\langle \mathcal{V}_\gamma(0,0)\rangle_{\mathbb{D}}^{(\mathrm{N})} = \prod_{i=1}^n \delta(\gamma_i) \qquad \langle \mathcal{V}_\gamma(0,0)\rangle_{\mathbb{D}}^{(D,\phi_0)} = \exp\left(i\sum_{i=1}^n \gamma_i\phi_0\right) = 1 \tag{B.52}$$

and the dependence on ϕ_0 drops, as it should. Thus, we find for Neumann BC:

$$\langle \sigma(0,0)\sigma_n^\dagger(x)\rangle_{\mathbb{D}}^{(\mathrm{N})} \underset{x\to 0}{\sim} x^{-2\Delta_n} + \ldots \tag{B.53}$$

and comparing with the straightforward $x \to 0$ limit of (3.64), we find $c_n^{(\mathrm{N})} = 1$.

[1] strictly speaking only $\mathbb{Z}_N$ invariant linear combinations of such fields are local in the orbifold but this subtlety can be ignored at this level.

[2] and their descendants, but their contribution in the $x \to 0$ limit is subldeading

For Dirichlet BC, we arrive at:

$$\langle\sigma(0,0)\sigma_n^\dagger(x)\rangle_{\mathbb{D}}^{(\mathrm{D})} \underset{x\to 0}{\sim} x^{-2\Delta_n}\int_{\mathbb{R}^n}\prod_{i=1}^n d\gamma_i\,\delta\left(\sum_i\gamma_i\right)x^{\gamma^2}C^{\mathcal{V}_\gamma}_{\sigma,\sigma_n^\dagger} \tag{B.54}$$

The structure constant $C^{\mathcal{V}_\gamma}_{\sigma,\sigma_n^\dagger}$ depends smoothly on γ. Indeed it can be unfolded to an n-point correlator of vertex operators on the Riemann sphere in the non-compact boson CFT:

$$C^{\mathcal{V}_\gamma}_{\sigma,\sigma_n^\dagger} = n^{-\sum_i^2\gamma_i^2/2}\left\langle V_{\gamma_1}\left(e^{2\pi i/n}\right)V_{\gamma_2}\left(e^{4\pi i/n}\right)\cdots V_{\gamma_n}(1)\right\rangle_{\mathbb{C}} \tag{B.55}$$

Now, using the classical CFT result [23]:

$$\left\langle V_{\gamma_1}(z_1)\cdots V_{\gamma_n}z_n\right\rangle_{\mathbb{C}} = \prod_{i<j}|z_i-z_j|^{2\gamma_i\gamma_j} \tag{B.56}$$

we find the behaviour of the structure constants close to $\gamma_i = 0$:

$$C^{\mathcal{V}_\gamma}_{\sigma,\sigma_n^\dagger} \underset{\gamma_i\to 0}{\sim} 1 \tag{B.57}$$

which is all we need, since we are interested in the leading $x\to 0$ behaviour of (B.54). Now, we integrate over the Dirac-δ function to arrive at:

$$\langle\sigma(0,0)\sigma_n^\dagger(x)\rangle_{\mathbb{D}}^{(\mathrm{D})} \underset{x\to 0}{\sim} x^{-2\Delta_n}\int_{\mathbb{R}^{n-1}}\prod_{i=1}^{n-1}d\gamma_i\,\exp\{-1/2|\log x^2|\sum_{i,j=1}^{n-1}\gamma_i A_{ij}\gamma_j\} \tag{B.58}$$

where the matrix $A_{ij} = 1+\delta_{ij}$ has $\det A = n$. The leading asymptotic behaviour of such an integral as $x\to 0$ follows from Laplace's method

$$\langle\sigma(0,0)\sigma_n^\dagger(x)\rangle_{\mathbb{D}}^{(\mathrm{D})} \underset{x\to 0}{\sim} x^{-2\Delta_n}\frac{1}{\sqrt{n}}\left(\frac{2\pi}{|\log x^2|}\right)^{(n-1)/2} \tag{B.59}$$

Now, we need to compare (B.59) with the $x\to 0$ limit of (3.63). We have:

$$\langle\sigma(0,0)\sigma_n^\dagger(x)\rangle_{\mathbb{D}}^{(\mathrm{D})} \underset{x\to 0}{\sim} x^{-2\Delta_n}\frac{1}{\sqrt{\det(-i\tau)}}(c_n^{(\mathrm{D})}+\dots) \tag{B.60}$$

From the relations (3.60), we have that:

$$\frac{1}{\sqrt{\det(-i\tau(x))}} = \prod_{k=1}^{n-1}\sqrt{\frac{F_{k/n}(x^2)}{F_{k/n}(1-x^2)}} \underset{x\to 0}{\sim} \frac{1}{\sqrt{n}}\left(\frac{2\pi}{|\log x^2|}\right)^{(n-1)/2} \tag{B.61}$$

where we have used the $\det(-i\tau(x))$ identities of sections 4.5. in[71]. Thus, by comparing (B.60) with (B.59) we fix $c_n^{(\mathrm{D})} = 1$.

B.5.2 The $x\to 1$ behaviour

The $x\to 1$ behaviour of (3.71) is also of interest, as it provides information about the one-point structure constants of the twist fields. Using the normalized two-point functions in (3.72), we find, for Dirichlet BC:

$$\langle\sigma(0,0)\sigma_n^\dagger(x)\rangle_{\mathbb{D}}^{(\mathrm{D})} \underset{x\to 1}{\sim} (1-x^2)^{-\Delta_n} \tag{B.62}$$

since $\Theta(-\boldsymbol{\tau}^{-1}(x)) \to 1$ as $x \to 1$.

Then, for Neumann BC, by using the property (3.65) in the second equation of (3.72) we arrive at:

$$\langle\sigma(0,0)\sigma_n^\dagger(x)\rangle_{\mathbb{D}}^{(\mathrm{N})} \underset{x\to 1}{\sim} (1-x^2)^{-\Delta_n}\sqrt{\det(-i\boldsymbol{\tau}(x))} \tag{B.63}$$

with

$$\det(-i\boldsymbol{\tau}(x)) = \prod_{k=1}^{n-1}\frac{F_{k/n}(1-x^2)}{F_{k/n}(x^2)} \underset{x\to 1}{\sim} \frac{1}{n}\left(\frac{2\pi}{|\log(1-x^2)|}\right)^{(n-1)} \tag{B.64}$$

easily found from (B.61)

We now want to see how the above expressions fare against the $x \to 1$ behaviour implied by the bulk-boundary OPE of $\sigma_n^\dagger(x)$ fields, which has contributions from *untwisted boundary fields* exclusively.

To proceed, we need to present a few facts on the boundary field spectrum of the non-compact boson BCFT which we dn $\psi^{(\alpha)}(e^{i\theta})$, with $\theta \in (0, 2\pi)$ a coordinate parametrizing the boundary of the unit disk $\mathbb{D}$. We use as reference [24], where these concepts are explained in detail.

For Dirichlet BC, the spectrum of boundary operators only contains the boundary identity operator $\psi_0^{(\mathrm{D})}$ and its descendants, since we have $\Phi_0 = const.$ along the boundary. On the other hand, for Neumann BC, any boundary vertex operator $\psi_\gamma^{(\mathrm{N})} =: \exp i\gamma\Phi(e^{i\theta}) :$, with scaling dimension $\Delta_\gamma = \gamma^2/2$ is allowed. Then, in the $\mathbb{Z}_n$ orbifold of this BCFT, the untwisted sector of primary boundary fields consists of the identity operator $\Psi_0^{(\mathrm{D})}$ for Dirichlet b.c, while for Neumann BC we have :

$$\Psi_\gamma^{(\mathrm{N})} = \psi_{\gamma_1}^{\alpha} \otimes \dots \psi_{\gamma_n}^{\alpha} \tag{B.65}$$

For Dirichlet BC, the leading contribution to the bulk-boundary OPE of $\sigma_n^\dagger$ is given by:

$$\sigma_n^\dagger(x) \sim (1-x^2)^{-\Delta_n}\mathcal{A}_{n,\mathbb{I}}^{(\mathrm{D})}\,\mathbb{I}(1) \tag{B.66}$$

In the Neumann BC setup, there are issues with the continuous spectrum of boundary operators analogous to the ones outlined in Appendix B.5.1. To bypass them, we conjecture the following continuum version of the bulk-boundary OPE :

$$\sigma^\dagger(x) \sim (1-x^2)^{-\Delta_n}\int_{-\infty}^{+\infty}(\prod_{i=1}^{n}d\gamma_i)\,\delta\left(\sum_i\gamma_i\right)(1-x^2)^{\gamma^2/2}\,\mathcal{A}_{n,\Psi_\gamma}^{(\mathrm{N})}\Psi_\gamma^{(\mathrm{N})}(1) \tag{B.67}$$

where $\mathcal{A}_{n,\Psi_\gamma}^{(\mathrm{N})}$ are bulk-boundary structure constants, and we have used that $U(1)$ charge neutrality holds on the boundary.

Now, we plug the OPEs (B.66) and (B.67) into their respective correlators and find for the Dirichlet case:

$$\langle\sigma(0,0)\sigma_n^\dagger(x)\rangle_{\mathbb{D}}^{(\mathrm{D})} \underset{x\to 1}{\sim} (1-x^2)^{-\Delta_n}\left(\mathcal{A}_{n,\mathbb{I}}^{(\mathrm{D})}\right)^2 \tag{B.68}$$

and we have used [173]

$$\langle\sigma(0,0)\rangle_{\mathbb{D}}^{\alpha} = \mathcal{A}_{n,\mathbb{I}}^{(\alpha)} \tag{B.69}$$

which, upon comparison with (B.62) fixes $\left(\mathcal{A}_{n,\mathbb{I}}^{(\mathrm{D})}\right)^2 = 1$.

For Neumann BC, the result is slightly more involved:

$$\langle\sigma(0,0)\sigma_n^\dagger(x)\rangle_{\mathbb{D}}^{(\mathrm{N})} \underset{x\to 1}{\sim} (1-x^2)^{-\Delta_n}\int_{-\infty}^{+\infty}(\prod_{i=1}^{n}d\gamma_i)\,\delta\left(\sum_i\gamma_i\right)(1-x^2)^{\gamma^2/2}\left(\mathcal{A}_{n,\Psi_\gamma}^{(\mathrm{N})}\right)^2 \tag{B.70}$$

where we have used that[173]:

$$\langle \sigma(0,0)\Psi_{\gamma}^{(\alpha)}(1)\rangle_{\mathbb{D}}^{\alpha} = \mathcal{A}_{n,\Psi_\gamma}^{(\alpha)} \tag{B.71}$$

The rest of this derivation is analogous to the one of Appendix B.5.1. The correlator in (B.71) unfolds to a n-point function of boundary vertex operators on the unit disk [173] which should be smooth in γ_i. Thus, we can approximate $\mathcal{A}_{n,\Psi_\gamma}^{(\mathrm{N})} \approx \mathcal{A}_{n,\mathbb{I}}^{(\mathrm{N})}$ for $\gamma_i \to 0$ small, since we are only interested in the leading $x \to 1$ behaviour. Then, we calculate the Gaussian integral as in Appendix B.5.1 to arrive at:

$$\langle \sigma(0,0)\sigma_n^{\dagger}(x)\rangle_{\mathbb{D}}^{(\mathrm{N})} \underset{x\to 1}{\sim} \left(\mathcal{A}_{n,\mathbb{I}}^{(\mathrm{N})}\right)^2 (1-x^2)^{-\Delta_n} \left(\frac{2\pi}{|\log(1-x^2)|}\right)^{(n-1)/2} \tag{B.72}$$

and by comparing with (B.63) we conclude that $\left(\mathcal{A}_{n,\mathbb{I}}^{(\mathrm{N})}\right)^2 = 1$.

Finally, since the one-point structure constants of twist fields are related to the ground state degeneracies g_α as $\mathcal{A}_{n,\mathbb{I}}^{(\alpha)} = g_\alpha^{1-n}$ we obtain:

$$g_D = 1 \qquad g_N = 1 \tag{B.73}$$

which is compatible with well-established results in the literature [24].

Appendix C

Appendix for chapter 4

C.1 Mother BCFT conventions

We will define here our mother BCFT conventions on the upper-half plane $\mathbb{H}$ parametrized by the coordinate $z = x + iy$. The boundary is aligned with the real axis.

Bulk operators in the mother CFT are denoted by $\phi_i(z, \bar{z})$ while boundary operators are written as $\psi_j^{(ab)}(x)$. The operator algebra consists of three types of OPE, which we explicitate, to fix the notations for the corresponding structure constants.

First, we have the *bulk-bulk OPEs*:

$$\phi_i(z,\bar{z})\phi_j(0,0) = \sum_{\phi_k \text{ scaling op.}} C_{ij}^k z^{-h_i-h_j+h_k} \bar{z}^{-\bar{h}_i-\bar{h}_j+\bar{h}_k} \phi_k(0,0) \tag{C.1}$$

where C_{ij}^k are the *bulk structure constants*.

The second type of OPE are **boundary-boundary OPEs** between BCCOs interpolating different boundary conditions:

$$\psi_i^{(ab)}(x)\psi_j^{(dc)}(y) = \delta_{bd} \sum_k B_{\psi_i\psi_j}^{(abc)\psi_k} (x-y)^{h_k-h_i-h_j} \psi_k^{(ac)}(y) \tag{C.2}$$

for $x > y$. The $B_{\psi_i\psi_j}^{(abc)\psi_k}$ are the *boundary-boundary structure constants*. The Kronecker delta formally expresses the fact that it only makes sense to consider correlations of boundary operators ordered such that their BCs change consistently with their labelling.

Finally, we consider the third kind of OPE, between the bulk and the boundary:

$$\phi_i(z) = \sum_k A_{\phi_i,\psi_k}^{(a)} (2y)^{h_k-\Delta_i} \cdot \psi_k^{(aa)}(x) \tag{C.3}$$

with $A_{\phi_i,\psi_k}^{(a)}$ the bulk-boundary structure constants.

In [257],[213] all the structure constants $A_{\phi_i,\psi_k}^{(a)}$ and $B_{\psi_i\psi_j}^{(abc)\psi_k}$ have been determined for A-series and D-series BCFTs, in terms of fusion matrix elements of bulk CFT four-point functions, and the entries of the modular S matrix. Relevant to this paper are the results:

$$\boxed{B_{\psi_i\psi_j}^{(abc)\psi_k} = \mathbf{F}_{bk}\begin{bmatrix} a & c \\ i & j \end{bmatrix}} \tag{C.4}$$

where the fusion matrix relates bases of conformal blocks around $z = 0$ and $z = 1$

$$\mathcal{I}^{r}_{ia,cj}(z) = \sum_{rs} \mathbf{F}_{rs} \begin{bmatrix} a & c \\ i & j \end{bmatrix} \mathcal{J}^{s}_{ij,ac}(1-z) \tag{C.5}$$

defined in the bulk.

We also give the expressions for the 1-point structure constants of the BCFT in terms of S-matrix elements of the mother CFT

$$\boxed{A^{(a)}_{\phi_i} \equiv A^{(a)}_{\phi_i,\psi_{\mathbb{I}}} = \frac{S_{ai}}{S_{a1}} \sqrt{\frac{S_{11}}{S_{i1}}}} \tag{C.6}$$

C.2 Computation of orbifold structure constants

C.2.1 Composite twist one-point structure constant in the $\mathbb{Z}_N$ orbifold BCFT

Assuming the one-point structure constant $\mathcal{A}^{(\alpha)}_{\sigma_{\mathbf{1}},\psi_{\mathbf{1}}}$ is known, let's consider the correlator:

$$\left\langle \sigma_j(0,0) \right\rangle^{\alpha}_{\mathbb{D}} = \mathcal{A}^{(\alpha)}_{\sigma_j,\psi_{\mathbf{1}}} \tag{C.7}$$

We now use (4.49) to write the LHS of (C.7) as:

$$\left\langle \sigma_j(0,0) \right\rangle^{\alpha}_{\mathbb{D}} = \mathcal{A}_j \lim_{\epsilon\to 0} \epsilon^{2(1-N^{-1})h_j} \left\langle \Phi_{[j,\mathbf{1},\ldots,\mathbf{1}]}(\epsilon,\bar{\epsilon}) \sigma^{[k]}(0,0) \right\rangle^{\alpha}_{\mathbb{D}} \tag{C.8}$$

Substituting the definition (4.45) of non-diagonal fields, we find:

$$\left\langle \sigma_j(0,0) \right\rangle^{\alpha}_{\mathbb{D}} = N^{-2(1-N^{-1})h_j - 1} \lim_{\epsilon\to 0} \epsilon^{2(1-N^{-1})h_j} \sum_{a=0}^{N-1} \left\langle \left(\phi_{j+a} \otimes \phi_{\mathbf{1}+a} \otimes \ldots \phi_{\mathbf{1}+a} \right)(\epsilon,\bar{\epsilon}) \sigma^{[k]}(0,0) \right\rangle^{\alpha}_{\mathbb{D}} \tag{C.9}$$

Each correlator in the sum above can be written as:

$$\left\langle \left(\phi_{j+a} \otimes \phi_{\mathbf{1}+a} \otimes \ldots \phi_{\mathbf{1}+a} \right)(\epsilon,\bar{\epsilon}) \sigma^{[k]}(0,0) \right\rangle^{\alpha}_{\mathbb{D}} = \frac{Z_{N,a}}{Z^{N}_{1,a}} \langle \phi_j(\epsilon,\bar{\epsilon}) \rangle_{\mathbb{D}_N} = \mathcal{A}^{(\alpha)}_{\sigma_{\mathbf{1}},\psi_{\mathbf{1}}} \langle \phi_j(\epsilon,\bar{\epsilon}) \rangle^{a}_{\mathbb{D}_N} \tag{C.10}$$

where $Z_{N,a}$ denotes the partition function on the N-sheeted disk with conformal BC a, and branch point at 0. Now, we can unfold the disk correlator through the conformal map $w \to w^{1/N}$ and substitute back in (C.9) to find:

$$\left\langle \sigma_j(0,0) \right\rangle^{\alpha}_{\mathbb{D}} = \mathcal{A}^{(\alpha)}_{\sigma_{\mathbf{1}},\psi_{\mathbf{1}}} \langle \phi_j(0,0) \rangle^{a}_{\mathbb{D}} \tag{C.11}$$

so that we finally find:

$$\boxed{\mathcal{A}^{(\alpha)}_{\sigma_j,\psi_{\mathbf{1}}} = \mathcal{A}^{(\alpha)}_{\sigma_{\mathbf{1}},\psi_{\mathbf{1}}} A^{a}_{\phi_j}} \tag{C.12}$$

C.2.2 Bulk-boundary structure constant in the $\mathbb{Z}_2$ orbifold CFT

In this section we compute the structure constant $\mathcal{A}^{(\alpha)}_{\sigma_{\mathbf{1}},\Psi_k}$, which is given by the UHP correlator:

$$\left\langle \sigma_{\mathbf{1}}(i/2,-i/2) \Psi^{(\alpha\alpha)}_{k}(1) \right\rangle^{\alpha}_{\mathbb{H}} = \mathcal{A}^{(\alpha)}_{\sigma_{\mathbf{1}},\Psi_k} \tag{C.13}$$

where we have implicitly assumed that the boundary field Ψ_k of scaling dimension $2h_k$ can leave on α - otherwise the structure $\mathcal{A}^{(\alpha)}_{\sigma_1,\Psi_k}$ constant is trivially zero.

We can now map the LHS of (C.13) to the unit disk through:

$$z \to \frac{z - i/2}{z + i/2} \tag{C.14}$$

and then use the partition function expression of the correlator (as in the previous section) to find (after a global rotation):

$$\left\langle \sigma_1(0,0)\Psi^{\alpha}_{13}(-i)\right\rangle_{\mathbb{D}} = \langle \sigma_1(0,0)\rangle^{\alpha}_{\mathbb{D}} \left\langle \psi^{\alpha}_{13}(-i)\psi^{\alpha}_{13}(-ie^{2i\pi})\right\rangle_{\mathbb{D}_{2,a}} \tag{C.15}$$

where $D_{2,a}$ is a 2-sheeted disk with branch point at 0. We unfold the correlator of boundary fields through the map $w \to w^{1/2}$ to find:

$$\left\langle \psi^{\alpha}_{13}(-i)\psi^{\alpha}_{13}(-ie^{2i\pi})\right\rangle_{\mathbb{D}_{2,a}} = \left(2i^{-1/2}\right)^{-2h_{13}} \left\langle \psi^{(aa)}_{13}(i^{1/2})\psi^{(aa)}_{13}(-i^{1/2})\right\rangle_{\mathbb{D}} \tag{C.16}$$

The 2-point function of boundary fields on the disk can then be mapped to the UHP, through:

$$w \to z = \frac{i(w+1)}{2(1-w)} \tag{C.17}$$

and calculated to be:

$$\left\langle \psi^{(aa)}_{13}(i^{1/2})\psi^{(aa)}_{13}(-i^{1/2})\right\rangle_{\mathbb{D}} = 2^{-2h_{13}} \tag{C.18}$$

so that, by putting everything together, we arrive at:

$$\boxed{\mathcal{A}^{(\alpha)}_{\sigma_1,\Psi_{13}} = \mathcal{A}^{(\alpha)}_{\sigma_1,\Psi_1} 2^{-4h_{13}}} \tag{C.19}$$

We note that (C.19) can be obtained from the result of [120] for the twist 2-point function on the strip $\mathbb{S}_L$ of width L with conformal BC α. In the limit $L \to \infty$, one obtains the right half plane (RHP) correlator

$$\langle \sigma(u,\bar{u})\sigma(v,\bar{v})\rangle_{RHP} = (u+v)^{-4h_\sigma}\, g_\alpha^{-2}\, 2^{-c/3}[|x|^2(1-|x|^2)]^{-2h_\sigma} \mathcal{Z}_{\alpha|\alpha}(-1/\tau) \tag{C.20}$$

with $0 < u \leq v$ and

$$x = \frac{v-u}{v+u} \qquad \tau(|x|) = i\frac{{}_2\,\mathrm{F}_1\left(\frac{1}{2},\frac{1}{2},1;1-|x|^2\right)}{{}_2\,\mathrm{F}_1\left(\frac{1}{2},\frac{1}{2},1;|x|^2\right)} \tag{C.21}$$

One can then compare the limit $u \to 0$ in the above expression with the expression obtained by employing the bulk-boundary OPEs of the twist fields in the LHS of (C.20) to recover the result (C.19).

For generic n, expressing the bulk-boundary structure constant $\mathcal{A}^{(\alpha)}_{\sigma_1,\Psi_{13}}$ in terms of mother BCFT quantities depends on our ability to calculate n-point functions of boundary operators. For $n \geq 5$, this becomes difficult to solve for generic mother BCFTs.

C.3 Orbifold Ward identities for bulk fields

Following [118], we give here the **orbifold Ward identities for 4-point bulk correlators**:

$$\begin{aligned}\sum_{p=0}^{\infty} a_p \left\langle O_1 \left| L^{(r)}_{-m_1-p} O_2(1) O_3(x,\bar{x}) \right| O_4 \right\rangle = &\sum_{p=0}^{\infty} b_p \left\langle O_1 \left| \left[L^{(r)}_{m_2+p} O_2 \right](1) O_3(x,\bar{x}) \right| O_4 \right\rangle \\ &+ \sum_{p=0}^{\infty} c_p \left\langle O_1 \left| O_2(1) \left[L^{(r)}_{m_3+p} O_3 \right](x,\bar{x}) \right| O_4 \right\rangle \\ &+ \sum_{p=0}^{\infty} d_p \left\langle O_1 \left| O_2(1) O_3(x,\bar{x}) L^{(r)}_{m_4+p} \right| O_4 \right\rangle\end{aligned} \tag{C.22}$$

where the *levels* $m_i \in \mathbb{Z} + rk_i/N$ satisfy:

$$m_1 + m_2 + m_3 + m_4 = -2 \tag{C.23}$$

and the coefficients a_p, b_p, c_p and d_p are defined from the Taylor series:

$$(1-z)^{m_2+1}(1-xz)^{m_3+1} = \sum_{p=0}^{\infty} a_p z^p \tag{C.24}$$

$$(z-x)^{m_3+1} z^{m_4+1} = \sum_{p=0}^{\infty} b_p (z-1)^p \tag{C.25}$$

$$(z-1)^{m_2+1} z^{m_4+1} = \sum_{p=0}^{\infty} c_p (z-x)^p \tag{C.26}$$

$$(z-1)^{m_2+1}(z-x)^{m_3+1} = \sum_{p=0}^{\infty} d_p z^p \tag{C.27}$$

A useful identity

We give here the following commutation identity [118]:

$$\begin{aligned}&\langle O_1 | O_2(1) O_3(x,\bar{x}) L_n | O_4 \rangle - \langle O_1 | L_n O_2(1) O_3(x,\bar{x}) | O_4 \rangle \\ &\quad = \left\{ (1-x^n)\left[x\partial_x + (n+1)h_3 \right] + (h_4 - h_1) - n(h_2 + h_3) \right\} \langle O_1 | O_2(1) O_3(x,\bar{x}) | O_4 \rangle\end{aligned} \tag{C.28}$$

where O_2 and O_3 are primary fields and $|O_2\rangle$, $|O_4\rangle$ are generic states. This commutator identity allows one to express insertions of Virasoro modes L_n *inside* a correlation function in terms of differential operators acting *on* them.

C.4 Rényi entropies for the critical Ising chain with mixed fixed BC

In this section, we will derive the bare and excited twist contributions to the second and third Rényi entropy in the critical Ising chain with fixed mixed BC $a = +, b = -$. In the Ising BCFT, the boundary field that interpolates between the corresponding conformal BC $|\pm\rangle$ is the operator $\psi^{(+-)}_{2,1}$, with conformal dimension

$h_{2,1} = 1/2$. In the $\mathbb{Z}_N$ orbifold of this theory, the change in boundary conditions is implemented by the diagonal operator $\Psi_{2,1}^{(\alpha\beta)}$ defined as in (4.63).

The essential observation for the derivation of this section is that the space of conformal blocks is one-dimensional for the chiral correlators

$$\left\langle \Phi_{1,3} | \sigma_j^{[-k]}(1) \sigma_j^{[k]}(\eta) | \Phi_{1,3} \right\rangle \tag{C.29}$$

with $j \in \{\mathbf{1}, \phi_{1,3}\}$in the $\mathbb{Z}_2$ and $\mathbb{Z}_3$ Ising orbifold CFTs. The result is obtained, as in the discussion of Section 3, from the fusion rules of these theories, found in [119] and [211]. These fusion rules also imply the leading singular behaviour of the conformal block around the points $\eta \in \{0, 1, \infty\}$. The corresponding exponents are given in Table C.1.

	0	1	∞
$N = 2, j = \mathbf{1}$	-1	$-\frac{1}{16}$	$-\frac{15}{16}$
$N = 2, j = \phi_{1,3}$	-1	$-\frac{9}{16}$	$-\frac{7}{16}$
$N = 3, j = \mathbf{1}$	-1	$-\frac{1}{9}$	$-\frac{8}{9}$
$N = 3, j = \phi_{1,3}$	-1	$-\frac{4}{9}$	$-\frac{5}{9}$

Table C.1: Singular behaviour of the conformal block of (C.29) for different N and twist field insertions $\sigma_j^{[k]}(\eta)$

In the $\eta \to 1$ channel, the exponent corresponds to the fusion

$$\sigma_j^{[k]} \times \sigma_j^{[-k]} \to \Phi_{\mathbf{1}} \tag{C.30}$$

for all the chiral correlators we are considering in this section. The diagonal operator $\Phi_{\mathbf{1}}$ is defined as in (4.46).

From the exponents around $\eta \to 0$ and $\eta \to 1$ we can determine the generic form of the conformal blocks for the four cases enumerated above to be:

$$f_j^{(N)}(\eta) = \eta^{-1}(1-\eta)^{-2h_{\sigma_j}} P(\eta) \tag{C.31}$$

where $P(\eta)$ is a generic polynomial in η. Furthermore, taking into account the singular behaviour of $f_j^{(N)}(\eta)$ around $\eta \to \infty$, one can constrain its degree in all four cases to be ≤ 2, so that we have:

$$f_j^{(N)}(\eta) = \eta^{-1}(1-\eta)^{-2h_{\sigma_j}} (a_2\,\eta^2 + a_1\,\eta + a_0) \tag{C.32}$$

Around $\eta \to 1$, this function behaves as:

$$f_j^{(N)}(\eta) \sim (1-\eta)^{-2h_{\sigma_j}} \left[(a_2 + a_1 + a_0) + (a_2 - a_0)(1-\eta) + a_2(1-\eta)^2 + \dots \right] \tag{C.33}$$

To find a_i, we will need to consider the first few results in the module of $\Phi_{\mathbf{1}}$ from the OPE of twist fields in the $\mathbb{Z}_N$ orbifold:

$$\sigma_j^{[k]}(\eta)\sigma_j^{[-k]}(1) = \Phi_{\mathbf{1}}(1) + \frac{2h_{\sigma_j}}{Nc}(1-\eta)^2\, T^{(0)}(1) + \dots \tag{C.34}$$

where $T^{(0)}(z) = L_{-2}^{(0)}\Phi_{\mathbf{1}}(z)$ is the SET of the chiral $\mathbb{Z}_N$ orbifold CFT. The corresponding structure constant has been determined by applying a $L_2^{(0)}$ from the left on both sides of the OPE, and power matching in $(1-\eta)$. Finally, the term at level

1 has vanished because the null vector $L_{-1}\mathbf{1} \equiv 0$ in the mother CFT induces the null-vectors $L_{-1}^{(r)}\Phi_{\mathbf{1}} \equiv 0$ in the orbifold.

Inserting (C.34) into (C.29) one finds, the coefficients

$$a_0 = a_2 = \frac{2h_{\sigma_j}}{Nc} \quad a_1 = 1 - 2a_0 \tag{C.35}$$

with which we fix the conformal blocks for all the cases presented in Table C.1. We then use the block expansions for the mixed BC correlators to find:

$$\left\langle \sigma_j^{[k]}(z,\bar{z}) \right\rangle_N^{\alpha\beta} = g_+^{1-N} f_j^N(\eta) \tag{C.36}$$

where we have also used, notably, the results of (4.78) for the 1-point structure constant of twist fields. After mapping to the strip through (4.3), we find for $N = 2$:

$$\langle \sigma_{\mathbf{1}}(\ell,\ell)\rangle_{\mathbb{S}_L}^{+-} = 2^{-5/2}\left(\frac{2L}{\pi}\right)^{-1/16} \frac{7 + \cos\frac{2\pi\ell}{L}}{\left(\sin\frac{\pi\ell}{L}\right)^{1/16}} \tag{C.37}$$

$$\langle \sigma_{\varepsilon}(\ell,\ell)\rangle_{\mathbb{S}_L}^{+-} = 2^{-5/2}\left(\frac{2L}{\pi}\right)^{-9/16} \frac{1 - 9\cos\frac{2\pi\ell}{L}}{\left(\sin\frac{\pi\ell}{L}\right)^{9/16}} \tag{C.38}$$

and $N = 3$:

$$\langle \sigma_{\mathbf{1}}(\ell,\ell)\rangle_{\mathbb{S}_L}^{+-} = 3^{-2}\left(\frac{2L}{\pi}\right)^{-1/9} \frac{7 + 2\cos\frac{2\pi\ell}{L}}{\left(\sin\frac{\pi\ell}{L}\right)^{1/9}} \tag{C.39}$$

$$\langle \sigma_{\varepsilon}(\ell,\ell)\rangle_{\mathbb{S}_L}^{+-} = 3^{-2}\left(\frac{2L}{\pi}\right)^{-4/9} \frac{1 + 8\cos\frac{2\pi\ell}{L}}{\left(\sin\frac{\pi\ell}{L}\right)^{4/9}} \tag{C.40}$$

C.5 Hypergeometric differential equation

The hypergeometric differential equation is canonically defined as:

$$\eta(\eta-1)f''(\eta) + [(a+b+1)\eta - c]f'(\eta) + ab\, f(\eta) = 0 \tag{C.41}$$

with the Riemann scheme:

0	1	∞
0	0	a
$1-c$	$c-a-b$	b

The solutions are constructed using the Gauss hypergeometric function ${}_2\,\mathrm{F}_1(a,b;c \mid \eta)$. Following the conventions of [224], we give a standard basis of fundamental solutions to (C.41) around the singular point $\eta = 0$:

$$\begin{aligned} I_1(\eta) &= {}_2\,\mathrm{F}_1(a,b;c \mid \eta) \\ I_2(\eta) &= \eta^{1-c}\,{}_2\,\mathrm{F}_1(b-c+1, a-c+1; 2-c \mid \eta) \end{aligned} \tag{C.42}$$

and around $\eta = 1$:

$$\begin{aligned} J_1(\eta) &= {}_2\,\mathrm{F}_1(a,b;a+b-c+1 \mid 1-\eta) \\ J_2(\eta) &= (1-\eta)^{c-a-b}\,{}_2\,\mathrm{F}_1(c-b, c-a; c-a-b+1 \mid 1-\eta) \end{aligned} \tag{C.43}$$

The two bases of solutions are linearly related as

$$I_i(\eta) = \sum_{j=1}^{2} P_{ij} J_j(\eta) \tag{C.44}$$

with the fusing matrix P

$$\mathrm{P} = \begin{bmatrix} \frac{\Gamma(c)\Gamma(d)}{\Gamma(c-a)\Gamma(c-b)} & \frac{\Gamma(c)\Gamma(-d)}{\Gamma(a)\Gamma(b)} \\ \frac{\Gamma(2-c)\Gamma(d)}{\Gamma(1-a)\Gamma(1-b)} & \frac{\Gamma(2-c)\Gamma(-d)}{\Gamma(1-c+a)\Gamma(1-c+b)} \end{bmatrix} \tag{C.45}$$

and its inverse:

$$\mathrm{P}^{-1} = \begin{bmatrix} \frac{\Gamma(1-c)\Gamma(1-d)}{\Gamma(1-c+a)\Gamma(1-c+b)} & \frac{\Gamma(c-1)\Gamma(1-d)}{\Gamma(a)\Gamma(b)} \\ \frac{\Gamma(1-c)\Gamma(1+d)}{\Gamma(1-a)\Gamma(1-b)} & \frac{\Gamma(c-1)\Gamma(1+d)}{\Gamma(c-a)\Gamma(c-b)} \end{bmatrix} \tag{C.46}$$

expressed in terms of Euler's Gamma function Γ, with $d = c - a - b$.

C.6 Derivation of differential equation in the Z_3 orbifold BCFT

We present in this section all the orbifold Ward identities and null-vector conditions necessary to derive the third-order differential equation (4.134).

The Ward identities

Ward 1 The correlator to integrate over is:

$$\langle \Phi_{12}| L_1^{(1)} \sigma_{\mathbf{1}}(1) T^{(1)}(z) \tilde{\sigma}_{\mathbf{1}}(\eta) L_{-1}^{(1)} |\Phi_{12}\rangle \tag{C.47}$$

with $(m_1, m_2, m_3, m_4) = (-1, 1/3, -1/3, -1)$, to find:

$$\begin{aligned} a_{0|1} \langle \Phi_{12}| (L_1^{(1)})^2 \sigma_{\mathbf{1}}(1) \tilde{\sigma}_{\mathbf{1}}(\eta) L_{-1}^{(1)} |\Phi_{12}\rangle + a_{1|1} \langle \Phi_{12}| L_1^{(1)} L_0^{(1)} \sigma_{\mathbf{1}}(1) \tilde{\sigma}_{\mathbf{1}}(\eta) L_{-1}^{(1)} |\Phi_{12}\rangle = \\ d_{0|1} \langle \Phi_{12}| L_1^{(1)} \sigma_{\mathbf{1}}(1) \tilde{\sigma}_{\mathbf{1}}(\eta) L_{-1}^{(1)} L_{-1}^{(1)} |\Phi_{12}\rangle + d_{1|1} \langle \Phi_{12}| L_1^{(1)} \sigma_{\mathbf{1}}(1) \tilde{\sigma}_{\mathbf{1}}(\eta) L_0^{(1)} L_{-1}^{(1)} |\Phi_{12}\rangle \end{aligned} \tag{C.48}$$

Ward 2 The correlator to integrate over is:

$$\langle \Phi_{12}| \sigma_{\mathbf{1}}(1) T^{(1)}(z) \tilde{\sigma}_{\mathbf{1}}(\eta) L_{-1}^{(1)} L_{-1}^{(1)} |\Phi_{12}\rangle \tag{C.49}$$

with $(m_1, m_2, m_3, m_4) = (-1, 1/3, -1/3, -1)$ to find:

$$\begin{aligned} a_{0|2} \langle \Phi_{12}| L_1^{(1)} \sigma_{\mathbf{1}}(1) \tilde{\sigma}_{\mathbf{1}}(\eta) \left(L_{-1}^{(1)}\right)^2 |\Phi_{12}\rangle = d_{0|2} \langle \Phi_{12}| \sigma_{\mathbf{1}}(1) \tilde{\sigma}_{\mathbf{1}}(\eta) \left(L_{-1}^{(1)}\right)^3 |\Phi_{12}\rangle \\ + d_{1|2} \langle \Phi_{12}| \sigma_{\mathbf{1}}(1) \tilde{\sigma}_{\mathbf{1}}(\eta) L_0^{(1)} \left(L_{-1}^{(1)}\right)^2 |\Phi_{12}\rangle + d_{2|2} \langle \Phi_{12}| \sigma_{\mathbf{1}}(1) \tilde{\sigma}_{\mathbf{1}}(\eta) L_1^{(1)} \left(L_{-1}^{(1)}\right)^2 |\Phi_{12}\rangle \\ + d_{3|2} \langle \Phi_{12}| \sigma_{\mathbf{1}}(1) \tilde{\sigma}_{\mathbf{1}}(\eta) L_2^{(1)} \left(L_{-1}^{(1)}\right)^2 |\Phi_{12}\rangle \end{aligned} \tag{C.50}$$

Ward 3 The correlator to integrate over is

$$\langle \Phi_{12}| L_1^{(1)} L_1^{(1)} \sigma_{\mathbf{1}}(1) T^{(1)}(z) \tilde{\sigma}_{\mathbf{1}}(\eta) |\Phi_{12}\rangle \tag{C.51}$$

with $(m_1, m_2, m_3, m_4) = (-1, 1/3, -1/3, -1)$ to find:

$$d_{0|3} \langle \Phi_{12}| \left(L_1^{(1)}\right)^2 \sigma_{\mathbf{1}}(1)\tilde{\sigma}_{\mathbf{1}}(\eta) L_{-1}^{(1)} |\Phi_{12}\rangle = a_{0|3} \langle \Phi_{12}| \left(L_1^{(1)}\right)^3 \sigma_{\mathbf{1}}(1)\tilde{\sigma}_{\mathbf{1}}(\eta) |\Phi_{12}\rangle$$
$$+a_{1|3} \langle \Phi_{12}| \left(L_1^{(1)}\right)^2 L_0^{(1)} \sigma_{\mathbf{1}}(1)\tilde{\sigma}_{\mathbf{1}}(\eta) |\Phi_{12}\rangle + a_{2|3} \langle \Phi_{12}| \left(L_1^{(1)}\right)^2 L_{-1}^{(1)} \sigma_{\mathbf{1}}(1)\tilde{\sigma}_{\mathbf{1}}(\eta) |\Phi_{12}\rangle$$
$$+ a_{3|3} \langle \Phi_{12}| \left(L_1^{(1)}\right)^2 L_{-2}^{(1)} \sigma_{\mathbf{1}}(1)\tilde{\sigma}_{\mathbf{1}}(\eta) |\Phi_{12}\rangle \tag{C.52}$$

Ward 4 The correlator to integrate over is:

$$\langle \Phi_{12}| \sigma_{\mathbf{1}}(1) T^{(2)}(z) \tilde{\sigma}_{\mathbf{1}}(\eta) L_{-1}^{(1)} |\Phi_{12}\rangle \tag{C.53}$$

with $(m_1, m_2, m_3, m_4) = (0, -1/3, 1/3, -2)$ so we find:

$$d_{0|4} \langle \Phi_{12}| \sigma_{\mathbf{1}}(1)\tilde{\sigma}_{\mathbf{1}}(\eta) L_{-2}^{(2)} L_{-1}^{(1)} |\Phi_{12}\rangle + d_{1|4} \langle \Phi_{12}| \sigma_{\mathbf{1}}(1)\tilde{\sigma}_{\mathbf{1}}(\eta) L_{-1}^{(2)} L_{-1}^{(1)} |\Phi_{12}\rangle +$$
$$d_{2|4} \langle \Phi_{12}| \sigma_{\mathbf{1}}(1)\tilde{\sigma}_{\mathbf{1}}(\eta) L_0^{(2)} L_{-1}^{(1)} |\Phi_{12}\rangle + d_{3|4} \langle \Phi_{12}| \sigma_{\mathbf{1}}(1)\tilde{\sigma}_{\mathbf{1}}(\eta) L_1^{(2)} L_{-1}^{(1)} |\Phi_{12}\rangle = 0 \tag{C.54}$$

Ward 5 The correlator to integrate over is:

$$\langle \Phi_{12}| L_1^{(1)} T^{(2)}(z) \sigma_{\mathbf{1}}(1)\tilde{\sigma}_{\mathbf{1}}(\eta) |\Phi_{12}\rangle \tag{C.55}$$

with $(m_1, m_2, m_3, m_4) = (-2, -1/3, 1/3, 0)$ so we find:

$$a_{0|5} \langle \Phi_{12}| L_1^{(1)} L_2^{(2)} \sigma_{\mathbf{1}}(1)\tilde{\sigma}_{\mathbf{1}}(\eta) |\Phi_{12}\rangle + a_{1|5} \langle \Phi_{12}| L_1^{(1)} L_1^{(2)} \sigma_{\mathbf{1}}(1)\tilde{\sigma}_{\mathbf{1}}(\eta) |\Phi_{12}\rangle +$$
$$a_{2|5} \langle \Phi_{12}| L_1^{(1)} L_0^{(2)} \sigma_{\mathbf{1}}(1)\tilde{\sigma}_{\mathbf{1}}(\eta) |\Phi_{12}\rangle + a_{3|5} \langle \Phi_{12}| L_1^{(1)} L_{-1}^{(2)} \sigma_{\mathbf{1}}(1)\tilde{\sigma}_{\mathbf{1}}(\eta) |\Phi_{12}\rangle = 0 \tag{C.56}$$

Ward 6 The correlator to integrate over is:

$$\langle \Phi_{12}| \sigma_{\mathbf{1}}(1) T^{(2)}(z) \tilde{\sigma}_{\mathbf{1}}(\eta) L_{-1}^{(1)} |\Phi_{12}\rangle \tag{C.57}$$

with $(m_1, m_2, m_3, m_4) = (-1, -1/3, 1/3, -1)$ to find:

$$a_{0|6} \langle \Phi_{12}| L_1^{(2)} \sigma_{\mathbf{1}}(1)\tilde{\sigma}_{\mathbf{1}}(\eta) L_{-1}^{(1)} |\Phi_{12}\rangle = d_{0|6} \langle \Phi_{12}| \sigma_{\mathbf{1}}(1)\tilde{\sigma}_{\mathbf{1}}(\eta) L_{-1}^{(2)} L_{-1}^{(1)} |\Phi_{12}\rangle$$
$$+d_{1|6} \langle \Phi_{12}| \sigma_{\mathbf{1}}(1)\tilde{\sigma}_{\mathbf{1}}(\eta) L_0^{(2)} L_{-1}^{(1)} |\Phi_{12}\rangle + d_{2|6} \langle \Phi_{12}| \sigma_{\mathbf{1}}(1)\tilde{\sigma}_{\mathbf{1}}(\eta) L_1^{(2)} L_{-1}^{(1)} |\Phi_{12}\rangle \tag{C.58}$$

Ward 7 The correlator to integrate over is:

$$\langle \Phi_{12}| \sigma_{\mathbf{1}}(1) T^{(1)}(z) \tilde{\sigma}_{\mathbf{1}}(\eta) L_{-1}^{(2)} |\Phi_{12}\rangle \tag{C.59}$$

with $(m_1, m_2, m_3, m_4) = (-1, 1/3, -1/3, -1)$ to find:

$$a_{0|7} \langle \Phi_{12}| L_1^{(1)} \sigma_{\mathbf{1}}(1)\tilde{\sigma}_{\mathbf{1}}(\eta) L_{-1}^{(2)} |\Phi_{12}\rangle = d_{0|7} \langle \Phi_{12}| \sigma_{\mathbf{1}}(1)\tilde{\sigma}_{\mathbf{1}}(\eta) L_{-1}^{(1)} L_{-1}^{(2)} |\Phi_{12}\rangle$$
$$+d_{1|7} \langle \Phi_{12}| \sigma_{\mathbf{1}}(1)\tilde{\sigma}_{\mathbf{1}}(\eta) L_0^{(1)} L_{-1}^{(2)} |\Phi_{12}\rangle + d_{2|7} \langle \Phi_{12}| \sigma_{\mathbf{1}}(1)\tilde{\sigma}_{\mathbf{1}}(\eta) L_1^{(1)} L_{-1}^{(2)} |\Phi_{12}\rangle \tag{C.60}$$

The null-vector conditions

$$L_{-1}^{(1)} L_{-1}^{(2)} |\Phi_{12}\rangle = \frac{1}{2}\left[3g L_{-2}^{(0)} - \left(L_{-1}^{(0)}\right)^2\right] |\Phi_{12}\rangle \tag{C.61}$$

$$\langle \Phi_{12}| L_1^{(1)} L_1^{(2)} = \langle \Phi_{12}| \frac{1}{2}\left[3g L_2^{(0)} - \left(L_1^{(0)}\right)^2\right] \tag{C.62}$$

$$2\, L_{-1}^{(0)} L_{-1}^{(2)} L_{-1}^{(1)} |\Phi_{12}\rangle = \left[3g L_{-1}^{(0)} L_{-2}^{(0)} - \left(L_{-1}^{(0)}\right)^3\right] |\Phi_{12}\rangle \tag{C.63}$$

$$2\, L_{-1}^{(0)} L_{-1}^{(2)} L_{-1}^{(1)} |\Phi_{12}\rangle = \left[3g L_{-1}^{(1)} L_{-2}^{(2)} - \left(L_{-1}^{(1)}\right)^3\right] |\Phi_{12}\rangle \tag{C.64}$$

$$2 \langle \Phi_{12}| L_1^{(0)} L_1^{(2)} L_1^{(1)} = \langle \Phi_{12}| \left[3g L_2^{(0)} L_1^{(0)} - \left(L_1^{(0)}\right)^3\right] \tag{C.65}$$

$$2 \langle \Phi_{12}| L_1^{(0)} L_1^{(2)} L_1^{(1)} = \langle \Phi_{12}| \left[3g L_2^{(2)} L_1^{(1)} - \left(L_1^{(1)}\right)^3\right] \tag{C.66}$$

By removing from this linear system of 13 equations all terms containing modes $L_n^{(r)}$ with $r \neq 0$, one indeed obtains (4.134).

C.7 Numerical implementation of the Frobenius method

We want to find a basis of solutions to the differential equation (4.114) that converge on the entire range of interest - the unit circle $|\eta| = 1$.

The Fuchsian ODE (4.114) has singular points $0, 1, \infty$. The solutions around $\eta = 0$ and $\eta = 1$ converge on the disks $|\eta| < 1$ and $|\eta - 1| < 1$ respectively. Thus, only a portion of the unit semicircle, namely $0 < \text{Arg}(\eta) < \pi/3$, is contained in the convergence disk around $\eta = 1$. We can circumvent this problem by observing that the solutions around $\eta = \infty$ can be convergent on the whole unit circle $|\eta| = 1$. Even better, we can implement the change of variable

$$\eta \mapsto \frac{1+u}{2u}, \qquad \partial_\eta \mapsto -2u^2 \partial_u \,. \tag{C.67}$$

so that the new ODE, in the variable u has singular points at $u = 0, 1, -1$. The original unit circle $|\eta| = 1$ is mapped to $|u - 1/3| = 2/3$, which is contained in the convergence disk $|u| < 1$. Hence, applying the Froebenius method, and expressing the solutions around $u = 1$ in terms of those around $u = 0$ will give the appropriate numerical evaluation of the desired values of η.

Now, as explained in [118], a convenient way of finding power series solutions around a point $u = u_0$ is to rewrite the differential equation (4.114) in terms of the operator $\theta = (u - u_0)\partial_u$, which satisfies:

$$(u - u_0)^n \partial_u^n = \prod_{k=0}^{n-1} (\theta - k) \tag{C.68}$$

Most importantly, we have that any polynomial $P(\theta)$ satisfies:

$$P(\theta)(u - u_0)^r = P(r)(u - u_0)^r \tag{C.69}$$

For $u_0 = 0$, we can then rewrite the equation as:

$$\left[\sum_{i=0}^{8} u^i P_i(\theta) \right] = 0 \tag{C.70}$$

where:

$$\begin{aligned}
P_0(\theta) &= 250\theta^4 - 125\theta^3 - 130\theta^2 - \theta + 6 \\
P_1(\theta) &= -\theta\left(-2125\theta^2 + 450\theta + 997\right) - 174 \\
P_2(\theta) &= -250\theta^4 + 125\theta^3 + 130\theta^2 - \left(750\theta^3 + 1250\theta^2 - 2415\theta + 4264\right)\theta + \theta - 3123 \\
P_3(\theta) &= -\theta\left(4250\theta^2 + 5925\theta + 6016\right) + \theta\left(-2125\theta^2 + 450\theta + 997\right) - 8511 \\
P_4(\theta) &= 5\,\theta\left(150\theta^3 + 575\theta^2 + 93\theta - 332\right) + \theta\left(750\theta^3 + 1250\theta^2 - 2415\theta + 4264\right) - 6000 \\
P_5(\theta) &= 2125\,\theta\left(\theta^2 + 3\theta + 2\right) + \theta\left(4250\theta^2 + 5925\theta + 6016\right) \\
P_6(\theta) &= -250\,\theta\left(\theta^3 + 6\theta^2 + 11\theta + 6\right) - 5\theta\left(150\theta^3 + 575\theta^2 + 93\theta - 332\right) \\
P_7(\theta) &= -2125\,\theta\left(\theta^2 + 3\theta + 2\right) \\
P_8(\theta) &= 250\,\theta\left(\theta^3 + 6\theta^2 + 11\theta + 6\right)
\end{aligned} \tag{C.71}$$

We now seek power series solutions around $u = 0$ of the form:

$$I_i(u) = u^{r_i} \sum_{n=0}^{\infty} a_n u^n \quad \text{with} \quad a_0 = 1 \tag{C.72}$$

where the r_i are the roots of the *characteristic polynomial* $P_0(r)$:

$$r_1 = -3/10 \quad r_2 = 1 \quad r_3 = 1/5 \quad r_4 = -2/5 \tag{C.73}$$

and are the same as the exponents around ∞ in Table 4.3.

By substituting the ansatz (C.72) in the differential equation and employing the identity (C.69) we find the following recursion relations for the coefficients a_n of the solution $I_i(u)$:

$$\boxed{P_0(r_i + n)a_n = -\sum_{i=1}^{min\{n,8\}} a_{n-i} P_i(r_i + n - i) \qquad a_0 = 1} \tag{C.74}$$

The four series found in this way converge for $|u| < 1$ and can be evaluated numerically to arbitrary precision.

We note, at this point, that the solution corresponding to r_4 is unphysical, since it corresponds, according to Table 4.3, to the presence in the operator algebra of the theory of a composite twist field formed with a primary operator that is outside the Kac table, i.e. not present in the $\mathcal{M}(6,5)$ CFT. This suggests that the physical space of conformal blocks is actually three-dimensional, and thus, that there should be a third-order differential equation satisfied by the excited twist correlator in this setup.

One should now repeat the above computation for the solutions $J_j(u)$ around $u = 1$, since these are the ones that appear in the block expansion (4.81) of BCFT correlators. The recursion relation takes the same form as in (C.74), with different roots:

$$\lambda_1 = -1/2 \quad \lambda_2 = 9/10 \quad \lambda_3 = 23/10 \quad \lambda_4 = 23/10 + 2 \tag{C.75}$$

A slight complication appears in this case because two of the roots of the corresponding characteristic polynomial differ by an integer, that is, $r_4 = r_3 + 2$. This will lead to the truncation of the corresponding recursion relations (C.74) for r_3 because at $n = 2$, the coefficient $P_0(r_3 + 2) = 0$. A good basis of solutions in this case is $\{J_1(u), J_2(u), J_3^{(k)}(u), J_4(u)\}$, where:

$$\begin{aligned} J_i(u) &= (1-u)^{r_i} \sum_{i=0}^{\infty} a_n (1-u)^n \\ J_3^{(k)}(u) &= (1-u)^{r_3}[a_0 + a_1(1-u)] + kJ_4(u) \end{aligned} \tag{C.76}$$

where k is a free parameter and the value we choose for it should not change the final result for the physical correlator. We have chosen to set it to $k_0 = 0.04428171795178596$ and define $J_3(u) = J^{(k_0)}(u)$.

The reason for this choice becomes apparent when one looks at our solution for the fusing matrix $\mathbf{M}$:

$$\mathbf{M} = \begin{pmatrix} 0.207411 & 0.393808 & 0.152178 & 0 \\ 1.356 & -2.30281 & -0.444933 & 0 \\ 7.70383 & 71.6374 & -22.7841 & 0 \\ -8986.23 & -19156.8 & 7211.61 & 5800.8 \end{pmatrix} \tag{C.77}$$

which relates the bases of conformal blocks around $u = 1$ and $u = 0$ as:

$$J_i(u) = \sum_j M_{ij} I_j(u) \tag{C.78}$$

To obtain this solution, we have generated a linear system of equations for the unknown M_{ij} from the evaluation of the above relations at different points $\{u_i\}$ in the interval $0 < u < 1$ (where both sets of solutions converge). In this context, the parameter k_0 was tuned so that the block $J_3(u)$ does not depend on the unphysical solution $I_3(u)$ around $u = 0$. Furthermore, since the matrix elements $(M^{-1})_{i4} = 0$ can be readily checked to vanish for $i \in \{1, 2, 3\}$, we can conclude that $\{J_1(u), J_2(u), J_3(u)\}$ form the physical three-dimensional basis of conformal blocks around $u = 1$.

Appendix D

Appendix for Chapter 5

D.1 Proofs of the properties of invariant operators

In this part of the Appendix, we give the proofs for the non-trivial statements made in Sec. 5.3.1, about the properties of the operators of the form $\Phi_{[j_1,\dots,j_n]}$, $\Phi_j^{(r)}$ and $\sigma_j^{[k](r)}$ under the neutral algebra $A_n \oplus \bar{A}_n$. In particular, we say that an operator Φ is primary under $A_n \oplus \bar{A}_n$ if and only if

$$L_{m_1}^{(r_1)} \dots L_{m_p}^{(r_p)} \cdot \Phi = \bar{L}_{m_1}^{(r_1)} \dots \bar{L}_{m_p}^{(r_p)} \cdot \Phi = 0 \tag{D.1}$$

for any $(m_1, \dots, m_p)$ such that $m_1 \leq \dots \leq m_p$ and $m_1 + \dots + m_p > 0$, and $r_1 + \dots + r_p = 0$ mod n.

D.1.1 Untwisted sector

The untwisted sector contains local fields in $\mathcal{M}^{\otimes n}$ that are invariant under cyclic permutations, therefore it is spanned by fields of the form

$$\Psi = \mathcal{P}_0 \left[L_{m_1}^{(r_1)} \dots L_{m_p}^{(r_p)} \cdot \bar{L}_{\bar{m}_1}^{(\bar{r}_1)} \dots \bar{L}_{\bar{m}_{\bar{p}}}^{(\bar{r}_{\bar{p}})} \cdot (\phi_{j_1} \otimes \dots \otimes \phi_{j_n}) \right], \quad \text{with} \begin{cases} m_1 \leq \dots \leq m_p \leq 0\,, \\ \bar{m}_1 \leq \dots \leq \bar{m}_{\bar{p}} \leq 0\,. \end{cases} \tag{D.2}$$

where $\mathcal{P}_0$ is the projector onto the invariant subspace, all $m_i, \bar{m}_i$ are integers, and ϕ_{j_i} are primary fields in the mother theory. Let Π be the elementary cyclic permutation of the copies, which acts on untwisted operators as

$$\Pi \cdot (\phi_{j_1} \otimes \dots \otimes \phi_{j_{n-1}} \otimes \phi_{j_n}) \cdot \Pi^{-1} = (\phi_{j_2} \otimes \dots \otimes \phi_{j_n} \otimes \phi_{j_1})\,. \tag{D.3}$$

and let $\mathcal{P}_s$ be the projectors

$$\mathcal{P}_s[\Phi] = \frac{1}{n} \sum_{a=0}^{n-1} \omega^{-sa}\, \Pi^a \cdot \Phi \cdot \Pi^{-a}\,. \tag{D.4}$$

Since $\Pi \cdot T^{(r)}(z) \cdot \Pi^{-1} = \omega^r\, T^{(r)}(z)$, where $\omega = \exp(2i\pi/n)$, it follows that

$$\Pi \cdot L_m^{(r)} \cdot \Pi^{-1} = \omega^r\, L_m^{(r)}\,. \tag{D.5}$$

and therefore

$$L_m^{(r)} \mathcal{P}_s = \mathcal{P}_{r+s} L_m^{(r)} \tag{D.6}$$

So the field Ψ from (D.2) can be recast as

$$\Psi = L_{m_1}^{(r_1)} \dots L_{m_p}^{(r_p)} \cdot \bar{L}_{\bar{m}_1}^{(\bar{r}_1)} \dots \bar{L}_{\bar{m}_{\bar{p}}}^{(\bar{r}_{\bar{p}})} \cdot \mathcal{P}_{-r-\bar{r}}[\phi_{j_1} \otimes \dots \otimes \phi_{j_n}] \,, \tag{D.7}$$

where $r = r_1 + \dots + r_p$ and $\bar{r} = r_1 + \dots + \bar{r}_{\bar{p}}$. We now have to distinguish two cases, depending on whether $\phi_{j_1} \otimes \dots \otimes \phi_{j_n}$ is invariant or not.

Non-diagonal untwisted operators. When $\phi_{j_1} \otimes \dots \otimes \phi_{j_n}$ is not invariant under cyclic permutations, states of the form (D.2) are said to be *non-diagonal*. In particular, the most relevant field in that sector is

$$\Phi_{[j_1 \dots j_n]} \propto \mathcal{P}_0(\phi_{j_1} \otimes \dots \otimes \phi_{j_n}) \,. \tag{D.8}$$

and therefore it is necessarily primary. We now prove that any operator in the untwisted, non-diagonal sector is an $(A_n \oplus \bar{A}_n)$-descendant of some primary operator of the form $\Phi_{[j_1 \dots j_n]}$.

Let's start from a generic state of the form (D.7), that is

$$\Psi = L_{m_1}^{(r_1)} \dots L_{m_p}^{(r_p)} \cdot \bar{L}_{\bar{m}_1}^{(\bar{r}_1)} \dots \bar{L}_{\bar{m}_{\bar{p}}}^{(\bar{r}_{\bar{p}})} \cdot \mathcal{P}_{-r-\bar{r}}[\phi_{j_1} \otimes \dots \otimes \phi_{j_n}] \,, \tag{D.9}$$

where $r = r_1 + \dots + r_p$ and $\bar{r} = r_1 + \dots + \bar{r}_{\bar{p}}$. now we simply observe that

$$L_0^{(r)} \cdot \mathcal{P}_s[\phi_{j_1} \otimes \dots \otimes \phi_{j_n}] = \bar{L}_0^{(r)} \cdot \mathcal{P}_s[\phi_{j_1} \otimes \dots \otimes \phi_{j_n}] = \widehat{h}^{(r)}_{j_1 \dots j_n} \mathcal{P}_{s+r}[\phi_{j_1} \otimes \dots \otimes \phi_{j_n}] \,, \tag{D.10}$$

where

$$\widehat{h}^{(r)}_{j_1 \dots j_n} = \sum_{a=1}^{n} \omega^{ar} h_{j_a} \,. \tag{D.11}$$

The point is that in the non-diagonal sector there exists a, b such that $h_{j_a} \neq h_{j_b}$, and therefore there exists an index $q \neq 0$ such that $\widehat{h}^{(q)}_{j_1 \dots j_n} \neq 0$. Hence, for any s we have

$$\mathcal{P}_s[\phi_{j_1} \otimes \dots \otimes \phi_{j_n}] \propto L_0^{(q)} \cdot \mathcal{P}_{s-q}[\phi_{j_1} \otimes \dots \otimes \phi_{j_n}] \tag{D.12}$$

and therefore

$$\mathcal{P}_{-r-\bar{r}}[\phi_{j_1} \otimes \dots \otimes \phi_{j_n}] \propto \left(L_0^{(q)}\right)^{[[-rq^{-1}]]} \left(\bar{L}_0^{(q)}\right)^{[[-\bar{r}q^{-1}]]} \mathcal{P}_0(\phi_{j_1} \otimes \dots \otimes \phi_{j_n}) \tag{D.13}$$

Thus, we can write Ψ as $A_n \oplus \bar{A}_n$ descendant of $\Phi_{[j_1 \dots j_n]}$, namely :

$$\Psi \propto \underbrace{L_{m_1}^{(r_1)} \dots L_{m_p}^{(r_p)} \left(L_0^{(q)}\right)^{[[-rq^{-1}]]}}_{\in A_n} \cdot \underbrace{\bar{L}_{\bar{m}_1}^{(\bar{r}_1)} \dots \bar{L}_{\bar{m}_{\bar{p}}}^{(\bar{r}_{\bar{p}})} \left(\bar{L}_0^{(q)}\right)^{[[-\bar{r}q^{-1}]]}}_{\in \bar{A}_n} \Phi_{[j_1 \dots j_n]} \tag{D.14}$$

It follows that any invariant operator in the untwisted, non-diagonal sector is an $(A_n \oplus \bar{A}_n)$-descendant of some primary operator of the form $\Phi_{[j_1 \dots j_n]}$.

Diagonal untwisted operators. Let us first prove that the operators $\Phi_j^{(r)}$ are A_n primary. When $r = 0$, this follows from the fact that $\Phi_j^{(0)}$ is a highest weight-state of the full orbifold algebra. When $r \neq 0$ and $j \neq 1$, we consider

$$\Psi = L_{m_1}^{(s_1)} \dots L_{m_p}^{(s_p)} \cdot L_{-1}^{(r)} \bar{L}_{-1}^{(-r)} \cdot \Phi_j^{(0)}, \quad \text{with} \begin{cases} m_1 \leq \dots \leq m_p, \\ m = m_1 + \dots + m_p > 0, \\ s_1 + \dots + s_p = 0 \mod n. \end{cases} \tag{D.15}$$

Furthermore $m_1, \dots, m_p \in \mathbb{Z}$ because $\Phi_j^{(0)}$ is untwisted. But since $\Phi_j^{(0)}$ is a highest weight-state of the full orbifold algebra, Ψ trivially vanishes unless $m_i + \dots + m_p \leq 1$ for all i. But since $m_1 \leq \dots \leq m_p$ and $m \geq 1$, the only case to be considered is $m_p = 1$ and $m_1 = \dots = m_{p-1} = 0$. So all we need to prove is that

$$L_0^{(s_1)} \dots L_0^{(s_{p-1})} \cdot L_1^{(s_p)} L_{-1}^{(r)} \bar{L}_{-1}^{(-r)} \cdot \Phi_j^{(0)} = 0. \tag{D.16}$$

We first rewrite the *r.h.s.* using the orbifold Virasoro commutation rule

$$\left[L_1^{(r)}, L_{-1}^{(s)}\right] = 2L_0^{(r+s)} \tag{D.17}$$

yielding

$$L_0^{(s_1)} \dots L_0^{(s_{p-1})} \cdot L_1^{(s_p)} L_{-1}^{(r)} \bar{L}_{-1}^{(-r)} \cdot \Phi_j^{(0)} = 2\bar{L}_{-1}^{(-r)} \cdot L_0^{(s_1)} \dots L_0^{(s_{p-1})} \cdot L_0^{(s_p+r)} \cdot \Phi_j^{(0)}. \tag{D.18}$$

Using $L_0^{(s)} \cdot \Phi_j^{(0)} = n h_j \delta_{s0}$, we get

$$L_0^{(s_1)} \dots L_0^{(s_{p-1})} \cdot L_1^{(s_p)} L_{-1}^{(r)} \bar{L}_{-1}^{(-r)} \cdot \Phi_j^{(0)} = 2(nh_j)^p \, \delta_{s_1,0} \dots \delta_{s_{p-1},0} \cdot \delta_{s_p+r,0} \bar{L}_{-1}^{(-r)} \cdot \Phi_j^{(0)} = 0 \tag{D.19}$$

since $s_1 + \dots + s_n = 0$ and $r \neq 0$. This shows that (D.15) must vanish, and hence $\Phi_j^{(r)}$ is primary under A_n. The case $r \neq 0$ and $j = 1$ can be treated similarly: the condition on indices becomes $m_1 = \dots = m_{p-1} = 0$ and $m_p = 2$, and then the relation $L_2^{(s)} L_{-2}^{(r)} \cdot \mathbf{1} = \frac{1}{2} nc \delta_{r+s,0}$ can be used.

Let's now consider a generic state of the form (D.7) in the diagonal sector, namely

$$\Psi = \delta_{r+\bar{r},0} \, L_{m_1}^{(r_1)} \dots L_{m_p}^{(r_p)} \cdot \bar{L}_{\bar{m}_1}^{(\bar{r}_1)} \dots \bar{L}_{\bar{m}_{\bar{p}}}^{(\bar{r}_{\bar{p}})} \cdot (\phi_j \otimes \dots \otimes \phi_j), \quad \text{with} \begin{cases} m_1 \leq \dots \leq m_p \leq -1, \\ \bar{m}_1 \leq \dots \leq \bar{m}_{\bar{p}} \leq -1. \end{cases} \tag{D.20}$$

where as above $r = r_1 + \dots + r_p$ and $\bar{r} = r_1 + \dots + \bar{r}_{\bar{p}}$. If $r = \bar{r} = 0$, then Ψ is immediately an $(A_n \oplus \bar{A}_n)$-descendant of $\Phi_j^{(0)}$. If $r = -\bar{r} \neq 0$ and $j \neq 1$, we use

$$L_1^{(-r)} L_{-1}^{(r)} \cdot (\phi_j \otimes \dots \otimes \phi_j) = \bar{L}_1^{(-\bar{r})} \bar{L}_{-1}^{(\bar{r})} \cdot (\phi_j \otimes \dots \otimes \phi_j) = 2nh_j \, (\phi_j \otimes \dots \otimes \phi_j), \tag{D.21}$$

and rewrite Ψ as

$$\Psi = (2nh_j)^{-2} \left(\underbrace{L_{m_1}^{(r_1)} \dots L_{m_p}^{(r_p)} L_1^{(-r)}}_{\in A_n} \cdot \underbrace{\bar{L}_{\bar{m}_1}^{(\bar{r}_1)} \dots \bar{L}_{\bar{m}_{\bar{p}}}^{(\bar{r}_{\bar{p}})} \bar{L}_1^{(r)}}_{\in \bar{A}_n} \right) \cdot L_{-1}^{(r)} \bar{L}_{-1}^{(-r)} \cdot (\phi_j \otimes \dots \otimes \phi_j). \tag{D.22}$$

In the case $r = -\bar{r} \neq 0$ and $j = 1$, we can proceed similarly and write

$$\Psi = (nc/2)^{-2} \left(L_{m_1}^{(r_1)} \dots L_{m_p}^{(r_p)} \cdot \bar{L}_{\bar{m}_1}^{(\bar{r}_1)} \dots \bar{L}_{\bar{m}_{\bar{p}}}^{(\bar{r}_{\bar{p}})} \cdot L_2^{(-r)} \bar{L}_2^{(r)} \right) \cdot L_{-2}^{(r)} \bar{L}_{-2}^{(-r)} \cdot \mathbf{1}. \tag{D.23}$$

This shows that Ψ is an $(A_n \oplus \bar{A}_n)$-descendant of $\Phi_j^{(r)}$ or $\mathbf{1}^{(r)}$, respectively.

Twist operators. Let us prove that the operator $\sigma_j^{[k](r)}$ is primary under A_n. For $r = 0$, this is straightforward, because, by construction, the composite twist operator $\sigma_j^{[k]}$ is an OVir_n primary operator of conformal dimension h_{σ_j}. For $r \neq 0$, if $j \neq 1$ or $kr \neq 1 \mod n$, we consider

$$L_{m_1}^{(s_1)} \dots L_{m_p}^{(s_p)} \cdot L_{-[\![kr]\!]/n}^{(r)} \bar{L}_{-[\![kr]\!]/n}^{(-r)} \cdot \sigma_j^{[k]}, \quad \text{with} \begin{cases} m_1 \leq \dots \leq m_p\,, \\ m = m_1 + \dots + m_p > 0\,, \\ s_1 + \dots + s_p = 0 \mod n\,. \end{cases} \tag{D.24}$$

If this quantity is non-zero, it is an $L_0^{(0)}$ eigenvector of eigenvalue $(h_{\sigma_j} + [\![kr]\!]/n - m)$. Because of the condition $m_i \in -ks_i/n + \mathbb{Z}$, we have $m \in \mathbb{Z}$, and hence $m \geq 1$, so the eigenvalue is strictly smaller than h_{σ_j}, which is not possible within the module of $\sigma_j^{[k]}$. For $r = k^{-1}$ and $j = 1$, we consider

$$L_{m_1}^{(s_1)} \dots L_{m_p}^{(s_p)} \cdot L_{-(n+1)/n}^{(k^{-1})} \bar{L}_{-(n+1)/n}^{(-k^{-1})} \cdot \sigma_{\mathbf{1}}^{[k]}, \quad \text{with} \begin{cases} m_1 \leq \dots \leq m_p\,, \\ m = m_1 + \dots + m_p > 0\,, \\ s_1 + \dots + s_p = 0 \mod n\,. \end{cases} \tag{D.25}$$

If this quantity is non-zero, it is an $L_0^{(0)}$ eigenvector of eigenvalue $(h_{\sigma_j} - m + 1 + 1/n)$. Using a similar argument to the one in the previous case, we find that m is again a strictly positive integer: this gives a non-admissible eigenvalue, due to the null-vector relation $L_{-1/n}^{(k^{-1})} \cdot \sigma_{\mathbf{1}}^{[k]} = 0$. Hence, (D.24) and (D.25) must vanish, and thus $\sigma_j^{[k](r)}$ and $\sigma_{\mathbf{1}}^{[k](r)}$ are primary under A_n. Similar proofs hold for $\bar{A}_n$.

Let us consider a generic invariant descendant operator in the twisted sector

$$\Psi = \mathcal{P}_0 \left[L_{m_1}^{(r_1)} \dots L_{m_p}^{(r_p)} \cdot \bar{L}_{\bar{m}_1}^{(\bar{r}_1)} \dots \bar{L}_{\bar{m}_{\bar{p}}}^{(\bar{r}_{\bar{p}})} \cdot \sigma_j^{[k]} \right], \tag{D.26}$$

where $\sigma_j^{[k]}$ is a composite twist operator associated to the primary operator ϕ_j of the mother CFT. By the commutation rules of Π with the orbifold Virasoro modes, we have

$$\Psi = \delta_{r+\bar{r},0} \cdot L_{m_1}^{(r_1)} \dots L_{m_p}^{(r_p)} \cdot \bar{L}_{\bar{m}_1}^{(\bar{r}_1)} \dots \bar{L}_{\bar{m}_{\bar{p}}}^{(\bar{r}_{\bar{p}})} \cdot \sigma_j^{[k]}, \tag{D.27}$$

where $r = r_1 + \dots + r_p$ and $\bar{r} = \bar{r}_1 + \dots + \bar{r}_{\bar{p}}$. If $r = \bar{r} = 0$, then Ψ is immediately an $(A_n \oplus \bar{A}_n)$-descendant of $\sigma_j^{[k](0)} = \sigma_j^{[k]}$. For $r = -\bar{r} \neq 0$, if $j \neq 1$ or $r \neq k^{-1}$, we use

$$L_{[\![kr]\!]/n}^{(-r)} L_{-[\![kr]\!]/n}^{(r)} \cdot \sigma_j^{[k]} = \bar{L}_{[\![kr]\!]/n}^{(r)} \bar{L}_{-[\![kr]\!]/n}^{(-r)} \cdot \sigma_j^{[k]} = \frac{2[\![kr]\!] h_{\sigma_j}}{n} \sigma_j^{[k]}, \tag{D.28}$$

and rewrite Ψ as

$$\Psi = \left(\frac{n}{2[\![kr]\!] h_{\sigma_j}} \right)^2 \left(L_{m_1}^{(r_1)} \dots L_{m_p}^{(r_p)} \cdot \bar{L}_{\bar{m}_1}^{(\bar{r}_1)} \dots \bar{L}_{\bar{m}_{\bar{p}}}^{(\bar{r}_{\bar{p}})} \cdot L_{[\![kr]\!]/n}^{(-r)} \bar{L}_{[\![kr]\!]/n}^{(r)} \right) \cdot L_{-[\![kr]\!]/n}^{(r)} \bar{L}_{-[\![kr]\!]/n}^{(-r)} \cdot \sigma_j^{[k]}. \tag{D.29}$$

Similarly, if $j = 1$ and $r = k^{-1}$, we have

$$\Psi \propto \left(L_{m_1}^{(r_1)} \dots L_{m_p}^{(r_p)} \cdot \bar{L}_{\bar{m}_1}^{(\bar{r}_1)} \dots \bar{L}_{\bar{m}_{\bar{p}}}^{(\bar{r}_{\bar{p}})} \cdot L_{(n+1)/n}^{(-k^{-1})} \bar{L}_{(n+1)/n}^{(k^{-1})} \right) \cdot L_{-(n+1)/n}^{(k^{-1})} \bar{L}_{-(n+1)/n}^{(-k^{-1})} \cdot \sigma_{\mathbf{1}}^{[k]}. \tag{D.30}$$

This shows that Ψ is an $(A_n \oplus \bar{A}_n)$-descendant of $\sigma_j^{[k](r)}$ or $\sigma_{\mathbf{1}}^{[k](r)}$, respectively.

We turn to the two-point function of twist operators,

$$\langle \sigma_i^{[k](r)}(z,\bar{z})\sigma_j^{[\ell](s)}(w,\bar{w})\rangle = \langle \sigma_i^{[k](r)}|\sigma_j^{[\ell](s)}\rangle \times |z-w|^{-2h_{\sigma_i^{[k](r)}}-2h_{\sigma_j^{[\ell](s)}}} . \tag{D.31}$$

This vanishes if $i \neq j$, because the modules of ϕ_i and ϕ_j are decoupled in the mother CFT. This function also vanishes if $k+\ell \neq 0 \mod n$, by symmetry, under the cyclic permutation of the copies. For $i=j$ and $k+\ell=0$, the scalar product $\langle \sigma_j^{[k](r)}|\sigma_j^{[-k](s)}\rangle$ is easily computed using the orbifold Virasoro commutation rules, which gives

$$\langle \sigma_j^{[k](r)}|\sigma_j^{[-k](s)}\rangle = \delta_{r+s,0} . \tag{D.32}$$

D.2 Three-point functions

D.2.1 Three-point functions of twist operators

Let us first state a useful property of correlation functions, which actually derives from the orbifold Ward identity (5.64).

Property. Let $\mathcal{O}_1, \mathcal{O}_2, \mathcal{O}_3$ be three operators of the orbifold CFT, with twist charges k_1, k_2, k_3, respectively, such that $k_1 = k_2 + k_3 \mod n$. For any $r \in \mathbb{Z}_n$ and q_1, q_2, q_3 such that $q_i \in -k_i r/n + \mathbb{Z}$, and $q_1 = q_2 + q_3 + 1$, we have

$$\sum_{m=0}^{\infty} \Big[b_m \langle (L^{(r)}_{-q_1+m}\mathcal{O}_1^\dagger)\mathcal{O}_2\mathcal{O}_3\rangle - a_m \langle \mathcal{O}_1^\dagger (L^{(r)}_{q_2+m}\mathcal{O}_2)\mathcal{O}_3\rangle + e^{i\pi q_2} b_m \langle \mathcal{O}_1^\dagger \mathcal{O}_2 (L^{(r)}_{q_3+m}\mathcal{O}_3)\rangle \Big] = 0 , \tag{D.33}$$

where the coefficients a_n, b_n are given by

$$a_m = \frac{(q_3+1)q_3\dots(q_3-m+2)}{m!} , \qquad b_m = (-1)^m \frac{(q_2+1)q_2\dots(q_2-m+2)}{m!} . \tag{D.34}$$

note that, if $q_3 = -1$ (resp. $q_2 = -1$) then $a_m = \delta_{m0}$ (resp. $b_m = \delta_{m0}$). For any value of q_1, q_2, q_3, the sum in (D.33) is finite, because, for any $\mathcal{O}_i$, there exists an integer m_0 such that $L_{\pm q_i+m}\cdot\mathcal{O}_i = 0$ when $m \geq m_0$.

Proof. Consider the integral,

$$\oint dz\, (z-1)^{q_2+1} z^{q_3+1} \langle \mathcal{O}_1^\dagger(\infty) T^{(r)}(z)\mathcal{O}_2(1)\mathcal{O}_3(0)\rangle , \tag{D.35}$$

where the contour encloses the points $z=0$ and $z=1$. Since the prefactor $(z-1)^{q_2+1} z^{q_3+1}$ exactly compensates the monodromy of $T^{(r)}(z)$ around each of the $\mathcal{O}_i$'s, the integrand is single-valued, and hence the contour integral is closed. Using the Cauchy theorem, we can split the latter into a contour enclosing only $z=0$, and a contour enclosing only $z=1$. The Taylor expansions

$$(1+u)^{q_3+1} = \sum_{m=0}^{\infty} a_m u^m , \qquad (1-u)^{q_2+1} = \sum_{m=0}^{\infty} b_m u^m , \qquad \text{for } |u|<1 , \tag{D.36}$$

allow us to write the integrand for each contour as a power series in z or $(z-1)$, which in turn yields (D.33). ■

The goal of this section is to describe a recursive algorithm for the computation of OPE coefficients of the form

$$\langle \sigma_k^{\dagger(-t)}\, \sigma_i^{(r)}\, (L_{-m_1}^{(r_1)} \dots L_{-m_p}^{(r_p)} \cdot \Phi_j^{(s)}) \rangle\,, \tag{D.37}$$

where $p \geq 1$, and $m_1, \dots, m_p$ are integers, with $m_1 \geq \cdots \geq m_p \geq 1$, and $r_1 + \cdots + r_p = 0 \mod n$, in terms of the quantities

$$\langle \sigma_k\, \sigma_i\, (L_{-1}^{(u_1)} \dots L_{-1}^{(u_q)} \cdot \bar{L}_{-1}^{(\bar{u}_1)} \dots \bar{L}_{-1}^{(\bar{u}_{\bar{q}})} \cdot \Phi_j) \rangle\,, \tag{D.38}$$

where $u_1 + \cdots + u_q = -(\bar{u}_1 + \cdots + \bar{u}_{\bar{q}}) = r + s - t \mod n$.

We start with the case $r = s = t = 0$, namely

$$\langle \sigma_k^\dagger \sigma_i\, (L_{-m_1}^{(r_1)} \dots L_{-m_p}^{(r_p)} \cdot \Phi_j) \rangle\,, \tag{D.39}$$

Let us discuss the various cases, depending on the generator $L_{-m_1}^{(r_1)}$.

1. If $m_1 = 1$, then we have $m_1 = \cdots = m_p = 1$, and the correlator (D.39) is already of the form (D.38).

2. If $r_1 = 0$, then the action of $L_{-m_1}^{(0)}$ inside a correlation function is easily expressed. Using the commutator between $L_{-m_1}^{(0)}$ and a primary operator, we get

$$\langle \Phi_1 \Phi_2 (L_{-m_1}^{(0)} \cdot \mathcal{O}_3) \rangle = (m_1 h_2 - h_1 + h_3) \langle \Phi_1 \Phi_2 \mathcal{O}_3 \rangle\,, \tag{D.40}$$

where Φ_1, Φ_2 are primary, and $\mathcal{O}_3$ is any scaling operator. Here, h_1, h_2, h_3 are the conformal dimensions of $\Phi_1, \Phi_2, \mathcal{O}_3$, respectively. Hence, we have

$$\begin{aligned} &\langle \sigma_k^\dagger \sigma_i\, (L_{-m_1}^{(0)} \cdot L_{-m_2}^{(r_2)} \dots L_{-m_p}^{(r_p)} \cdot \Phi_j) \rangle \\ &\qquad = (m_1 h_{\sigma_i} - h_{\sigma_k} + h_{\Phi_j} + m')\, \langle \sigma_k^\dagger \sigma_i\, (L_{-m_2}^{(r_2)} \dots L_{-m_p}^{(r_p)} \cdot \Phi_j) \rangle\,, \end{aligned} \tag{D.41}$$

where $m' = m_2 + \cdots + m_p$. Thus, the problem of computing (D.39) with the insertion of a chain of p orbifold Virasoro generators, where the first one is of the form $L_{-m_1}^{(0)}$, has been reduced to the one with $(p-1)$ generators.

3. If $m_1 > 1$ and $r_1 \neq 0$, we shall use the linear relations (D.33) as follows.

   First, we introduce a useful definition: for any operator $\mathcal{O}$, and $p \in \mathbb{N}$, let $A_p(\mathcal{O})$ be the space of descendants defined as

$$A_p(\mathcal{O}) = \text{span}\left[L_{-l_1}^{(u_1)} \dots L_{-l_q}^{(u_q)} \cdot \mathcal{O}\,, \quad q \leq p\,, \quad l_1 \geq \cdots \geq l_q \geq 1 \} \right]. \tag{D.42}$$

   For instance, the operator $L_{-m_1}^{(r_1)} \dots L_{-m_p}^{(r_p)} \cdot \Phi_j$ in (D.39) belongs to $A_p(\Phi_j)$.

   By convention, we take $1 \leq r \leq n-1$. For any integer $m_1' \in \{2, 3, \dots, m_1\}$, if we set $q_1 = 2 - r_1/n - m_1', q_2 = 1 - r_1/n, q_3 = -m_1'$ in (D.33), we get a linear relation of the form

$$\sum_{l=0}^{m_1' + (m_2 + \cdots + m_p)} b_l\, \langle \sigma_k^\dagger \sigma_i\, (L_{-m_1'+l}^{(r_1)} \cdot L_{-m_2}^{(r_2)} \dots L_{-m_p}^{(r_p)} \cdot \Phi_j) \rangle = 0\,. \tag{D.43}$$

We rewrite this as

$$\sum_{l=2}^{m_1'} b_{m_1'-n} \langle \sigma_k^\dagger \sigma_i (L_{-l}^{(r_1)} \cdot L_{-m_2}^{(r_2)} \dots L_{-m_p}^{(r_p)} \cdot \Phi_j) \rangle = B_{m_1'} , \tag{D.44}$$

where the right-hand side

$$B_{m_1'} = - \sum_{l=-1}^{m_2+\dots+m_p} b_{m_1'+l} \langle \sigma_k^\dagger \sigma_i (L_n^{(r_1)} \cdot L_{-m_2}^{(r_2)} \dots L_{-m_p}^{(r_p)} \cdot \Phi_k) \rangle , \tag{D.45}$$

can be treated with the OVir_n commutation relations, to give a linear combination of the form

$$B_{m_1'} \in -b_{m_1'-1} \langle \sigma_k^\dagger \sigma_i (L_{-m_2}^{(r_2)} \dots L_{-m_p}^{(r_p)} \cdot L_{-1}^{(r_1)} \cdot \Phi_j) \rangle + \langle \sigma_k^\dagger \sigma_i \, A_{p-1}(\Phi_j) \rangle . \tag{D.46}$$

The relations (D.44) for $m_1' = 2, \dots, m_1$ form an invertible triangular $(m_1-1)\times(m_1-1)$ linear system for the coefficients $\langle \sigma_k^\dagger \sigma_i (L_{-l}^{(r_1)} \cdot L_{-m_2}^{(r_2)} \dots L_{-m_p}^{(r_p)} \cdot \Phi_j) \rangle$ with $l = 2, \dots, m_1$. By solving this system, on gets (D.39) in terms of the $B_{m_1'}$'s. Thus, we have reduced the computation of (D.39) to that of OPE coefficients of the form

$$\langle \sigma_k^\dagger \sigma_i (L_{-l_1}^{(u_1)} \dots L_{-l_q}^{(u_q)} \cdot \Phi_j) \rangle \quad \text{and} \quad \langle \sigma_k^\dagger \sigma_i (L_{-l_1}^{(u_1)} \dots L_{-l_q}^{(u_q)} \cdot L_{-1}^{(r_1)} \cdot \Phi_j) \rangle , \tag{D.47}$$

with $0 \le q \le p-1$.

Hence, in the three cases, the above steps define an algorithm to compute (D.39) in terms of (D.38), by recursion on p.

We now turn to OPE coefficients of the form

$$\langle \sigma_k^{\dagger(-t)} \sigma_i^{(r)} \Phi_j^{(s)} \rangle , \tag{D.48}$$

with generic values of the Fourier indices $r, s, t \in \mathbb{Z}_n$. By convention, we take $0 \le r, s, t \le n-1$, and we introduce the notations $(\bar r, \bar s, \bar t) = (n-r, n-s, n-t)$. Recall the definitions

$$\begin{aligned} \sigma_i^{(r)} &:= \text{const} \times L_{-r/n}^{(r)} \bar L_{-r/n}^{(\bar r)} \cdot \sigma_i , \\ \Phi_j^{(s)} &:= \text{const} \times L_{-1}^{(s)} \bar L_{-1}^{(\bar s)} \cdot \Phi_j , \\ \sigma_k^{\dagger(-t)} &:= \text{const} \times L_{-t/n}^{(\bar t)} \bar L_{-t/n}^{(t)} \cdot \sigma_k^\dagger , \end{aligned} \tag{D.49}$$

for non-zero r, s, t. Here, we have assumed that ϕ_i, ϕ_j, ϕ_k is different from $\mathbf{1}$, but the argument is easily adapted otherwise.

Using the Ward identity (D.33) with $q_1 = q_2 = t/n, q_3 = -1$, for the insertion of $T^{(\bar t)}(z)$ in the function $\langle (\bar L_{-t/n}^{(t)} \sigma_k^\dagger) \, \sigma_i^{(r)} \, \Phi_j^{(s)} \rangle$, we get

$$\begin{aligned} &\text{const} \times \langle \sigma_k^{\dagger(-t)} \sigma_i^{(r)} \Phi_j^{(s)} \rangle \\ &= \langle (\bar L_{-t/n}^{(t)} \sigma_k^\dagger)(L_{t/n}^{(\bar t)} \sigma_i^{(r)}) \Phi_j^{(s)} \rangle - e^{i\pi\bar r/n} \sum_{l=0}^{2} b_l \langle (\bar L_{-t/n}^{(t)} \sigma_k^\dagger) \sigma_i^{(r)} (L_{l-1}^{(\bar t)} \Phi_j^{(s)}) \rangle . \end{aligned} \tag{D.50}$$

If $t > r$, then $L_{t/n}^{(\bar t)} \sigma_i^{(r)} = 0$, and the first term on the right-hand side vanishes. If $t \le r$, using the commutation relations, we write this first term as

$$\text{const} \times \frac{t+r}{n} \langle (\bar L_{-t/n}^{(t)} \sigma_k^\dagger)(L_{(t-r)/n}^{(r-t)} \bar L_{-r/n}^{(-r)} \sigma_i) \Phi_j^{(s)} \rangle , \tag{D.51}$$

and then we use again the identity (D.33) with $q_1 = q_2 = (t-r)/n, q_3 = -1$ for the insertion of $T^{(r-t)}(z)$ in $\langle(\bar{L}^{(t)}_{-t/n}\sigma^\dagger_k)(\bar{L}^{(-r)}_{-r/n}\sigma_i)\Phi^{(s)}_j\rangle$, which yields

$$\langle(\bar{L}^{(t)}_{-t/n}\sigma^\dagger_k)(L^{(r-t)}_{(t-r)/n}\bar{L}^{(-r)}_{-r/n}\sigma_i)\Phi^{(s)}_j\rangle = \delta_{rt}h_{\sigma_k}\langle(\bar{L}^{(t)}_{-t/n}\sigma^\dagger_k)(\bar{L}^{(-r)}_{-r/n}\sigma_i)\Phi^{(s)}_j\rangle$$
$$- e^{i\pi(t-r)/n}\sum_{l=0}^{2} b'_n\langle(\bar{L}^{(t)}_{-t/n}\sigma^\dagger_k)(\bar{L}^{(-r)}_{-r/n}\sigma_i)(L^{(r-t)}_{l-1}\Phi^{(s)}_j)\rangle\,. \tag{D.52}$$

For the second term in (D.50), if $r \neq 0$, we have

$$\langle(\bar{L}^{(t)}_{-t/n}\sigma^\dagger_k)\sigma^{(r)}_i(L^{(\bar{t})}_{l-1}\Phi^{(s)}_j)\rangle = \text{const}\times\langle(\bar{L}^{(t)}_{-t/n}\sigma^\dagger_k)(L^{(r)}_{-r/n}\bar{L}^{(\bar{r})}_{-r/n}\sigma_i)(L^{(\bar{t})}_{l-1}\Phi^{(s)}_j)\rangle\,, \tag{D.53}$$

which, upon applying (D.33), yields

$$\text{const}\times\sum_{p=0}^{2-n} b''_p\langle(\bar{L}^{(t)}_{-t/n}\sigma^\dagger_k)(\bar{L}^{(\bar{r})}_{-r/n}\sigma_i)(L^{(r)}_{p-1}L^{(\bar{t})}_{l-1}\Phi^{(s)}_j)\rangle\,. \tag{D.54}$$

Hence, we have shown how to express (D.48) in the form

$$\langle\sigma^{\dagger(-t)}_k\sigma^{(r)}_i\Phi^{(s)}_j\rangle = \langle(\bar{L}^{(t)}_{-t/n}\sigma^\dagger_k)(\bar{L}^{(\bar{r})}_{-r/n}\sigma_i)(\lambda\cdot\Phi_j)\rangle\,, \tag{D.55}$$

where λ is a linear combination of generators of the form $L^{(r_1)}_{-m_1}\dots L^{(r_p)}_{-m_p}$ with $r_1 + \dots + r_p = r+s-t \mod n$. In other words, we have "pushed" the orbifold Virasoro generators entering the definition of $\sigma^{\dagger(-t)}_k$ and $\sigma^{(r)}_i$, to translate them into an action of OVir_n on $\Phi^{(s)}_j$. Proceeding similarly with the $\overline{\text{OVir}_n}$ modes, we express (D.48) as

$$\langle\sigma^{\dagger(-t)}_k\,\sigma^{(r)}_i\,\Phi^{(s)}_j\rangle = \langle\sigma^\dagger_k\,\sigma_i\,(\lambda\cdot\bar{\lambda}\cdot\Phi_j)\rangle\,, \tag{D.56}$$

where λ is the same as above, and $\bar{\lambda}$ is obtained from μ by the change $L^{(r_j)}_{-m_j}\to\bar{L}^{(-r_j)}_{-m_j}$. We can then use the algorithm described above in the case $r=s=t=0$, to express $\langle\sigma^{\dagger(-t)}_k\,\sigma^{(r)}_i\,\Phi^{(s)}_j\rangle$ in terms of (D.38). Finally, extending this line of argument for $\langle\sigma^{\dagger(-t)}_k\,\sigma^{(r)}_i\,\Phi^{(s)}_j\rangle$ to the general case of (D.39) is straightforward.

D.2.2 Calculation of a three-point function in the $\mathbb{Z}_3$ orbifold of the Yang-Lee CFT

A useful technique, which is often employed in the literature [46, 87, 109] is to *unfold* the three-point function to a mother CFT correlator defined on $\mathbb{C}$. Let us consider, as a simple example, the three-point function:

$$C^{[\mathbf{1},\phi,\phi]}_{\sigma_\phi,\sigma^\dagger_\phi} = \langle\sigma_\phi\cdot[\mathbf{1},\phi,\phi]\cdot\sigma^\dagger_\phi\rangle\,, \tag{D.57}$$

in the $\mathbb{Z}_3$ orbifold. This can be expressed as a correlator on the replicated Riemann surface Σ_3 (with Σ_3 conformally equivalent to the Riemann sphere $\mathbb{C}$):

$$C^{[\mathbf{1},\phi,\phi]}_{\sigma_\phi,\sigma^\dagger_\phi} = \sqrt{3}\,\langle\phi(\infty,\infty)\phi(1,1)\phi(e^{2\pi i},e^{2\pi i})\phi(0,0)\rangle_{\Sigma_3}\,, \tag{D.58}$$

which we map to $\mathbb{C}$, through $z\mapsto w = z^{1/3}$, to find:

$$C^{[\mathbf{1},\phi,\phi]}_{\sigma_\phi,\sigma^\dagger_\phi} = \frac{\sqrt{3}}{3^{4h_\phi}}\langle\phi(\infty,\infty)\phi(1,1)\phi(e^{2\pi i/3},e^{-2\pi i/3})\phi(0,0)\rangle_{\mathbb{C}}\,. \tag{D.59}$$

now, we use the result of [220] to express the four-point function $\langle\phi|\phi(1,1)\phi(w,\bar{w})|\phi\rangle$ in terms of hypergeometric functions:

$$\begin{aligned}&\langle\phi|\phi(1,1)\phi(w,\bar{w})|\phi\rangle\\&\quad=|w|^{4/5}|1-w|^{4/5}\left[\left|{}_2\mathrm{F}_1\left(\frac{3}{5},\frac{4}{5},\frac{6}{5}\middle|w\right)\right|^2+(C^{\phi}_{\phi\phi})^2\left|w^{-1/5}\,{}_2\mathrm{F}_1\left(\frac{3}{5},\frac{2}{5},\frac{4}{5}\middle|w\right)\right|^2\right],\end{aligned}\tag{D.60}$$

with the Yang-Lee CFT structure constant given by:

$$C^{\phi}_{\phi\phi}=\frac{i\sqrt{\frac{1}{2}(3\sqrt{5}-5)}\,\Gamma\left(\frac{1}{5}\right)^3}{10\pi\Gamma\left(\frac{3}{5}\right)}\,.\tag{D.61}$$

Thus, we find:

$$C^{[\mathbf{1},\phi,\phi]}_{\sigma_\phi,\sigma^\dagger_\phi}=-11.054494\neq 0\,.\tag{D.62}$$

D.3 Proofs for modular matrices

D.3.1 The modular matrices P_n

Let us prove some useful properties of the matrices P_n's defined in (5.118–5.119):

$$P_{m+n}=P_m\,,\tag{D.63}$$
$$P_m\cdot P_{-m^{-1}}=\mathbf{1}\,,\tag{D.64}$$
$$P_m^t=P_{m^{-1}}\,,\tag{D.65}$$
$$\overline{P}_m=P_{-m}\,,\tag{D.66}$$
$$P_m^\dagger P_m=\mathbf{1}\,,\tag{D.67}$$
$$T^{1/n}P_m\,T^{1/n}P_{1-m^{-1}}\,T^{1/n}=P_{m-1}\,,\quad\text{for } n\neq 1\mod n\,.\tag{D.68}$$

The notations $P_{-m^{-1}}, P_{m^{-1}}, P_{1-m^{-1}}$, where m^{-1} is the inverse of m in $\mathbb{Z}_n^\times$, are justified by the property (D.63), which means that P_m is actually defined for $m\in\mathbb{Z}_n^\times$.

- To prove (D.63), we remark that the integer $[[-m^{-1}]]$ is unchanged under $m\to m+n$, so we have

$$P_{m+n}=T^{-m/n-1}\cdot Q_{m+n}\cdot T^{[[-m^{-1}]]/n}\,.\tag{D.69}$$

  On the other hand, from (5.119) we have $q_{m+n}(\tau)=q_m(\tau)+1$, and hence $Q_{m+n}=T\cdot Q_n$. As a result, we get $P_{m+n}=P_m$.

- For (D.64), we use the identity $q_m[q_{[[-m^{-1}]]}(\tau)]=\tau$, which yields, for $0<m<n$:

$$P_m\cdot P_{-m^{-1}}=T^{-m/n}\cdot Q_m\cdot Q_{[[-m^{-1}]]}\cdot T^{m/n}=\mathbf{1}\,.\tag{D.70}$$

- To study the transpose P_m^t and the conjugate $\overline{P}_m$, we use the following properties of the modular group. Since $S^2=\mathbf{1}$, any element of the group can be written in the form

$$T^{p_1}\cdot S\cdot T^{p_2}\ldots S\cdot T^{p_k}\,,\tag{D.71}$$

where $p_1, \ldots, p_k \in \mathbb{Z}$. Let $t(\tau) = \tau + 1$ and $s(\tau) = -1/\tau$. Let us show, by induction on k, that the following three equations are equivalent:

$$(t^{p_1} \circ s \circ t^{p_2} \ldots s \circ t^{p_k})(\tau) = \frac{a\tau + b}{c\tau + d}\,, \tag{D.72}$$

$$(t^{p_k} \circ s \circ t^{p_{k-1}} \ldots s \circ t^{p_1})(\tau) = \frac{d\tau + b}{c\tau + a}\,, \tag{D.73}$$

$$(t^{-p_1} \circ s \circ t^{-p_2} \ldots s \circ t^{-p_k})(\tau) = \frac{-a\tau + b}{c\tau - d}\,. \tag{D.74}$$

The proof goes as follows. For $k = 2$, we have

$$t^p \circ s \circ t^q = \frac{p\tau + (pq - 1)}{\tau + q}\,, \tag{D.75}$$

and hence the equivalence is straightforward. now suppose that the above equivalence holds for some $k \geq 2$. We can write

$$(t^{p_1} \circ s \circ \ldots s \circ t^{p_{k+1}})(\tau) = \frac{a(s \circ t^{p_{k+1}})(\tau) + b}{c(s \circ t^{p_{k+1}})(\tau) + d} = \frac{b\tau + (bp_{k+1} - a)}{d\tau + (dp_{k+1} - c)}\,, \tag{D.76}$$

$$(t^{p_{k+1}} \circ s \ldots s \circ t^{p_1})(\tau) = (t^{p_{k+1}} \circ s)\left(\frac{d\tau + b}{c\tau + a}\right) = \frac{(dp_{k+1} - c)\tau + (bp_{k+1} - a)}{d\tau + b}\,, \tag{D.77}$$

$$(t^{-p_1} \circ s \circ t^{-p_2} \ldots s \circ t^{-p_{k+1}})(\tau) = \frac{-a(s \circ t^{-p_{k+1}})(\tau) + b}{c(s \circ t^{-p_{k+1}})(\tau) - d} = \frac{-b\tau + (bp_{k+1} - a)}{d\tau - (dp_{k+1} - c)}\,, \tag{D.78}$$

and thus the equivalence holds also for $k + 1$. An important consequence is that, if the matrix for (D.72) is M, then the matrices for (D.73) and (D.74) are given by M^t and $\overline{M}$ respectively.

We apply the equivalence to the matrices Q_n. Let us take $0 < m < n$ for convenience, and denote $a_m = [[-m^{-1}]]$ and $b_m = (m[[-m^{-1}]] + 1)/n$, so that

$$nb_m - ma_m = 1\,, \qquad q_m(\tau) = \frac{m\tau - b_m}{n\tau - a_m}\,. \tag{D.79}$$

Changing $m \mapsto -a_m$ gives $(a_m, b_m) \mapsto (n - m, b_m - a_m)$, whereas $m \mapsto -m$ gives $(a_m, b_m) \mapsto (n - a_m, b_m - m)$. Hence, we have

$$q_{-a_m}(\tau) = \frac{-a_m(\tau - 1) - b_m}{n(\tau - 1) + m}\,, \qquad q_{-m}(\tau) = \frac{-m(\tau - 1) - b_m}{n(\tau - 1) + a_m}\,, \tag{D.80}$$

which yields $Q_{-a_m} = Q_m^t \cdot T^{-1}$ and $Q_{-m} = \overline{Q}_m \cdot T^{-1}$, and finally

$$P_{-a_m} = T^{a_m/n} \cdot Q_m^t T^{-m/n} = P_m^t\,, \qquad P_{-m} = T^{m/n} \cdot \overline{Q}_m T^{-a_m/n} = \overline{P}_m\,. \tag{D.81}$$

- The combination of (D.64–D.66) yields the unitarity of P_m (D.67).
- For $m \neq 1 \mod n$, we define $a_m = [[-m^{-1}]]$ and $a'_m = [[-(1 + a_m)^{-1}]]$. There exist two integers b_m, b'_m such that

$$nb_m - ma_m = 1\,, \qquad nb'_m - (1 + a_m)a'_m = 1\,. \tag{D.82}$$

A simple calculation gives

$$q_m[q_{1+a_m}(\tau)] = \frac{(m-1)\tau - b''_m}{n\tau - a''_m}\,, \tag{D.83}$$

where $a''_m = nb'_m - a_m a'_m$ and $b''_m = mb'_m - b_m a'_m$, and hence $nb''_m - (m-1)a''_m = 1$. Hence, if $0 < a''_m < n$ we have $Q_m Q_{1+a_m} = Q_{m-1}$ (otherwise we can always shift a''_m by a multiple of n). This yields the identity (D.68).

For $m = 1$, we have $[[-1]] = n - 1$, and

$$q_1(\tau) = \frac{\tau - 1}{n(\tau - 1) + 1} = (s \circ t^{-n} \circ s \circ t^{-1})(\tau)\,, \tag{D.84}$$

which yields

$$P_1 = T^{-1/n} S T^{-n} S T^{-1/n}\,, \qquad P_{-1} = T^{1/n} S T^{n} S T^{1/n}\,. \tag{D.85}$$

A recursion relation for the matrices P_m

In this section, we shall reproduce and prove a recursion relation for the P_m matrices found in [253], which provides their decomposition into S and T matrices after a relatively small number of recursive steps.

The key idea is to relate P_m matrices defined at *different* n. We will first make the dependence on n of the P_m and Q_m matrices explicit through the notation:

$$P_m \to P_{m|n} \quad Q_m \to Q_{m|n} \tag{D.86}$$

We now consider the product of matrices

$$T^{n/m} S T^{m/n} P_{m|n} T^{1/(mn)} \tag{D.87}$$

We substitute in the above the definition of (5.118) in the above to find:

$$T^{n/m} S\, T^{m/n} P_{m|n} T^{1/(mn)} = T^{n/m} S\, Q_{m|n} T^{b_m/m} \tag{D.88}$$

now the S matrix is given by:

$$S = \begin{pmatrix} 0 & 1 \\ -1 & 0 \end{pmatrix} \tag{D.89}$$

while the $Q_{m|n}$ matrix is given by:

$$Q_{m|n} = \begin{pmatrix} m & -b_m \\ n & -a_m \end{pmatrix} \tag{D.90}$$

with $nb_m - ma_m = 1$. Acting from the left on the above with the S matrix, one finds:

$$S\, Q_{m|n} = \begin{pmatrix} n & -a_m \\ -m & b_m \end{pmatrix} = Q_{n|-m} \tag{D.91}$$

since $nb_m - ma_m = 1$ is equivalent to $(-m)a_m - b_m n = 1$. next, we have by the definition in (5.118) that:

$$P_{n|-m} = T^{n/m} Q_{m|n} T^{a_m/m} \tag{D.92}$$

so that we have effectively established a recursive relation:

$$\boxed{P_{m|n} = T^{-m/n} S T^{-n/m} P_{n|-m} T^{-1/(mn)}} \tag{D.93}$$

for which the recursion ends with a term $P_{0|n} = P_{0|1} \equiv S$.

Example for $n = 5$

Suppose we want to calculate the $P_{2|5}$ matrix. We use the recursion relation to find:

$$P_{2|5} = T^{-2/5} S T^{-5/2} P_{5|-2} T^{-1/10} \tag{D.94}$$

noting that $P_{5|-2} = P_{1|-2}$, and using once more the recursion relation, we find:

$$P_{1|-2} = T^{1/2} S T^2 P_{-2|1} T^{1/2} \tag{D.95}$$

But $P_{-2|1} = P_{0|1} = S$, so, one can put everything together to find:

$$P_{2|5} = T^{-2/5} S T^{-2} S T^2 S T^{2/5} \tag{D.96}$$

D.3.2 The orbifold modular $\mathcal{S}$-matrix

In this section, we will show that the solution for the orbifold $\mathcal{S}$-matrix we have found satisfies the properties (5.121)-(5.124). In our calculations, the $\mathcal{S}$ and $\mathcal{T}$ matrices (and any products made with them), are evaluated "block-by-block", in the sense that for each proof we provide here, the external indices are restricted to correspond to only one type of operator – non-diagonal (ND), diagonal(D), twisted (T). For example, checking unitarity in the D-D block means proving that:

$$(\mathcal{S}\mathcal{S}^\dagger)_{i^{(r)},j^{(s)}} = \delta_{i^{(r)},j^{(s)}} \,, \tag{D.97}$$

for generic diagonal operator labels $i^{(r)}$, $j^{(s)}$.

We will only present in this section some of the more technical demonstrations since the rest can be quickly reproduced by the interested reader through similar or simpler arguments.

Symmetry of $\mathcal{S}$

As a warm-up, let's prove the symmetry of the $\mathcal{S}$ matrix. The check is straightforward everywhere but in the TT block, where we need to employ the property (D.65) to find:

$$\mathcal{S}^t_{i^{[k](r)},j^{[\ell](s)}} = \frac{\omega^{-ks-\ell r}\,(P_{k.\ell^{-1}})_{ji}}{n} = \frac{\omega^{-ks-\ell r}\,(P_{\ell.k^{-1}})_{ij}}{n} = \mathcal{S}_{i^{[k](r)},j^{[\ell](s)}} \,. \tag{D.98}$$

Unitarity of $\mathcal{S}$

We present in this section the more involved proofs for the unitarity of $\mathcal{S}$ in the DD and TT blocks.

In the DD block. We want to check the property:

$$\sum_\alpha \mathcal{S}_{i^{(r)},\alpha} \mathcal{S}^*_{i'^{(r')},\alpha} = \delta_{(i,r),(i',r')} \,, \tag{D.99}$$

where the sum in α runs over all the invariant primary operators in the orbifold. We first consider the sum over ND operators :

$$\sum_{J=[j_1,\ldots,j_n]} \mathcal{S}_{(i,r),J} \mathcal{S}^*_{J,(i',r')} \,, \tag{D.100}$$

which, using the known form of the S-matrix elements in this sector, is:

$$\sum_J S_{i,j_1} \dots S_{i,j_n} \cdot S_{i',j_1} \dots S_{i',j_n} \,, \tag{D.101}$$

where the sum is over equivalence classes J of the n-tuples $(j_1, \cdots, j_n)$ under $\mathbb{Z}_n$, with the exception of n-tuples for which the indices are equal. This can be expressed as:

$$\sum_{J=[j_1,\dots,j_n]} = \frac{1}{n}\left(\sum_{(j_1,\cdots,j_n)} - \sum_{(j,\cdots,j)}\right), \tag{D.102}$$

where the first sum on the RHS is over all n-tuples $(j_1, \dots j_n)$. This means each j_i runs over the whole mother CFT spectrum so that the sum over the ND indices can be conveniently expressed as:

$$\sum_J \mathcal{S}_{i^{(r)},J}\mathcal{S}^*_{J,i'^{(r')}} = \frac{\delta_{i,i'}}{n} - \frac{\sum_{(j,r)} S^n_{i,j}S^n_{i',j}}{n^2} \tag{D.103}$$

On the other hand, the sum over D operators is given by:

$$\sum_{j,s} \mathcal{S}_{i^{(r)},j^{(s)}}\mathcal{S}^*_{j^{(s)},i'^{(r')}} = \frac{\sum_{j,r} S^n_{ij}S^n_{i'j}}{n^2} \tag{D.104}$$

so that we are just left with checking that the sum over T operators satisfies

$$\sum_{j,s,k} \mathcal{S}_{i^{(r)},j^{[k](s)}}\mathcal{S}^*_{j^{[k](s)},i'^{(r')}} = \frac{n\delta_{r,r'}-1}{n}\delta_{i,i'} \tag{D.105}$$

which is indeed the case.

In the TT block. We want to prove in this section that:

$$\sum_\alpha \mathcal{S}_{i^{[k](r)},\alpha}\mathcal{S}^*_{\alpha,i'^{[k']}(r')} = \delta_{i,i'}\delta_{r,r'}\delta_{k,k'} \tag{D.106}$$

where α runs once again over all invariant primary operators of the orbifold.

To start, the sum over non-diagonal entries vanishes, since the $\mathcal{S}$-matrix entries indexed by a twisted operator and a non-diagonal operator vanish. On the other hand, the sum over diagonal field entries is easily calculated to be:

$$\sum_{(j,s)} \mathcal{S}_{i^{[k](r)},(j,s)}\mathcal{S}^*_{(j,s),i'^{[k']}(r')} = \frac{1}{n^2}\sum_{(j,s)} w^{s(k-k')}S_{ij}S_{ji'} = \frac{\delta_{i,i'}\delta_{k,k'}}{n} \tag{D.107}$$

Finally, we now consider the sum over T entries:

$$\sum_{j^{[t](s)}} \mathcal{S}_{i^{[k](r)},j^{[t](s)}}\mathcal{S}^*_{j^{[t](s)},i'^{[k']}(r')} \tag{D.108}$$

We substitute our results and find:

$$\sum_{j,s,t} \mathcal{S}_{i^{[k](r)},j^{[t]s}}\,\mathcal{S}^*_{i'^{[k']}(r'),j^{[t](s)}} = \frac{1}{n^2}\sum_{j,s,t} \omega^{-s(k-k')-t(r-r')}(\mathbf{P}_{tk^{-1}})_{ij}(\mathbf{P}^\dagger_{tk'^{-1}})_{ji'} \,. \tag{D.109}$$

We now sum over s, to obtain a factor $\delta_{k^{-1},k'^{-1}} = \delta_{k,k'}$. Then, we perform the sum over j, and use the unitarity of the P_n matrices (D.67) to arrive at:

$$\sum_{j,s,t} \mathcal{S}_{i^{[k](r)},j^{[t]s}} \mathcal{S}^*_{i'^{[k']}(r'),j^{[t](s)}} = \frac{1}{n} \sum_t \omega^{-t(r-r')} \delta_{i,i'} \delta_{k,k'} \tag{D.110}$$

Finally, we sum over t and find:

$$\sum_{j,s,t} \mathcal{S}_{i^{[k](r)},j^{[t]s}} \mathcal{S}^*_{i'^{[k']}(r'),j^{[t](s)}} = \delta_{i,i'} \delta_{k,k'} \delta_{r,r'} - \frac{1}{n} \delta_{i,i'} \delta_{k,k'} \,, \tag{D.111}$$

which, added to (D.107) gives the sought after result.

The relation $(\mathcal{ST})^3 = C$

The constraint (5.124) on the modular data of the CFT is equivalent to:

$$\mathcal{STS} = \mathcal{T}^\dagger \mathcal{ST}^\dagger \tag{D.112}$$

As in the previous section, we will show that the relation above holds in the DD and TT blocks.

In the DD block. We want to check the constraint:

$$\sum_\alpha \mathcal{S}_{i^{(r)},\alpha} \mathcal{T}_\alpha \mathcal{S}_{\alpha,i'^{(r')}} = \mathcal{T}^\dagger_{i^{(r)}} \mathcal{S}_{i^{(r)},i'^{(r')}} \mathcal{T}^\dagger_{i'^{(r')}} \tag{D.113}$$

where the sum α runs over all the invariant primary operator labels.

Substituting our expressions for the $\mathcal{S}$ and $\mathcal{T}$ matrices, we find that the sum over entries labelled by untwisted operators gives:

$$\sum_{\text{untwisted } \alpha} \mathcal{S}_{i^{(r)},\alpha} \mathcal{T}_\alpha \mathcal{S}_{\alpha,i'^{(r')}} = \frac{1}{n} (STS)^n_{ii'} \tag{D.114}$$

while the sum over twisted operators vanishes. The RHS of (D.113) can also be conveniently written as:

$$\mathcal{T}^\dagger_{i^{(r)}} \mathcal{S}_{i^{(r)},i'^{(r')}} \mathcal{T}^\dagger_{i'^{(r')}} = \frac{1}{n} (TST)^n_{i,i'} \tag{D.115}$$

Since in the mother CFT the modular matrices are constrained by

$$STS = T^\dagger S T^\dagger \tag{D.116}$$

we find that the relation (5.124) is indeed satisfied in this block.

In the TT block. We want to check the constraint:

$$\sum_{\alpha \in \{D,T\}} \mathcal{S}_{i^{[k](r)},\alpha} \mathcal{T}_\alpha \mathcal{S}_{\alpha,i'^{[k']}(r')} = \mathcal{T}^\dagger_{i^{[k](r)}} \mathcal{S}_{i^{[k](r)},i'^{[k']}(r')} \mathcal{T}^\dagger_{i'^{[k']}(r')} \tag{D.117}$$

where we only need to consider the sum α running over the diagonal and twisted primary labels, since $\mathcal{S}_{i^{[k](r)},[j_1 \ldots j_n]} = 0$. The sum over diagonal operator labels on the LHS is swiftly calculated to be:

$$\sum_{j,s} \mathcal{S}_{i^{[k](r)},j^{(s)}} \mathcal{T}_{j^{(s)}} \mathcal{S}_{j^{(s)},i'^{[k']}(r')} = \frac{1}{n} (ST^n S)_{ii'} \, \delta_{k+k',0} \tag{D.118}$$

and we use (D.85) to rewrite the above as:

$$\sum_{j,s} \mathcal{S}_{i^{[k](r)},j^{(s)}} \mathcal{T}_{j^{(s)}} \mathcal{S}_{j^{(s)},i'^{[k']}(r')} = \frac{1}{n} \left(T^{-1/n} P_{-1} T^{-1/n} \right)_{ii'} \delta_{k+k',0} \tag{D.119}$$

next, we want to evaluate the sum over twisted operator labels:

$$\sum_{j,s,t} \mathcal{S}_{i^{[k](r)},j^{[t](s)}} \mathcal{T}_{j^{[t](s)}} \mathcal{S}_{j^{[t](s)},i'^{[k']}(r')} = \frac{1}{n^2} \sum_{s,t} \omega^{-t(r+r')-s(k+k'-t)} (P_{tk^{-1}} T^{1/n} P_{k't^{-1}})_{ii'} \tag{D.120}$$

We sum over s, to obtain a $\delta_{k+k',t}$ factor in the sum. If $k + k' = 0$, the expression vanishes since t runs from 1 to $n - 1$. So, we obtain:

$$\sum_{j,s,t} \mathcal{S}_{i^{[k](r)},j^{[t](s)}} \mathcal{T}_{j^{[t](s)}} \mathcal{S}_{j^{[t](s)},i'^{[k']}(r')} = \frac{(1 - \delta_{k+k',0})}{n} \omega^{-(k+k')(r+r')} (P_{(k+k')k^{-1}} T^{1/n} P_{1-k(k+k')^{-1}})_{ii'} \tag{D.121}$$

Using the relation (D.68), the sum over twist fields becomes:

$$\sum_{j,s,t} \mathcal{S}_{i^{[k](r)},j^{[t](s)}} \mathcal{T}_{j^{[t](s)}} \mathcal{S}_{j^{[t](s)},i'^{[k']}(r')} = \frac{(1 - \delta_{k+k',0})}{n} \omega^{-(k+k')(r+r')} (T^{-1/n} P_{k'k^{-1}} T^{-1/n})_{ii'} \tag{D.122}$$

so that the LHS of (D.117) is just:

$$\sum_{\alpha \in \{D,T\}} \mathcal{S}_{i^{[k](r)},\alpha} \mathcal{T}_{\alpha} \mathcal{S}_{\alpha,i'^{[k']}(r')} = \frac{1}{n} \omega^{-(k+k')(r+r')} (T^{-1/n} P_{k'k^{-1}} T^{-1/n})_{ii'} \tag{D.123}$$

Substitution of our expressions for the modular data on the RHS of (D.117) completes the proof.

Bibliography

[1] A. Einstein, B. Podolsky and N. Rosen, *"Can quantum mechanical description of physical reality be considered complete?"*, Phys. Rev. 47, 777 (1935).

[2] J. S. Bell, *"On the Problem of Hidden Variables in Quantum Mechanics"*, Rev. Mod. Phys. 38, 447 (1966).

[3] J. S. Bell, *"On the Einstein-Podolsky-Rosen paradox"*, Physics Physique Fizika 1, 195 (1964).

[4] N. D. Mermin, *"Hidden variables and the two theorems of John Bell"*, Rev. Mod. Phys. 65, 803 (1993), arxiv:1802.10119.

[5] A. Aspect, J. Dalibard and G. Roger, *"Experimental test of Bell's inequalities using time varying analyzers"*, Phys. Rev. Lett. 49, 1804 (1982).

[6] D. Deutsch and R. Jozsa, *"Rapid solution of problems by quantum computation"*, Proc. R. Soc. Lond. A 439, 553 (1992).

[7] P. W. Shor, *"Algorithms for quantum computation: discrete logarithms and factoring"*, Proc. IEEE Symp. Found. Comput. Sci. , 124 (1994).

[8] L. K. Grover, *"A Fast quantum mechanical algorithm for database search"*, quant-ph/9605043.

[9] C. H. Bennett, G. Brassard, C. Crépeau, R. Jozsa, A. Peres and W. K. Wootters, *"Teleporting an unknown quantum state via dual classical and Einstein-Podolsky-Rosen channels"*, Phys. Rev. Lett. 70, 1895 (1993).

[10] P. W. Shor, *"Scheme for reducing decoherence in quantum computer memory"*, Phys. Rev. A 52, R2493 (1995).

[11] A. Ekert and R. Jozsa, *"Quantum algorithms: Entanglement enhanced information processing"*, Phil. Trans. Roy. Soc. Lond. A 356, 1769 (1998), quant-ph/9803072.

[12] J. Yin, Y.-H. Li, S.-K. Liao, M. Yang, Y. Cao, L. Zhang, J.-G. Ren, W.-Q. Cai, W.-Y. Liu, S.-L. Li et al., *"Entanglement-based secure quantum cryptography over 1,120 kilometres"*, Nature 582, 501 (2020).

[13] G. Mussardo, *"Statistical field theory: an introduction to exactly solved models in statistical physics"*, Oxford Univ. Press (2010), New York, NY.

[14] M. Henkel, *"Conformal invariance and critical phenomena"*, Springer (1999).

[15] K. G. Wilson and J. B. Kogut, *"The Renormalization group and the epsilon expansion"*, Phys. Rept. 12, 75 (1974).

[16] L. P. Kadanoff, *"Scaling laws for Ising models near T(c)"*, Physics Physique Fizika 2, 263 (1966).

[17] Y. Nakayama, *"Scale invariance vs conformal invariance"*, Phys. Rept. 569, 1 (2015), arxiv:1302.0884.

[18] I. Jack and H. Osborn, *"Analogs for the c Theorem for Four-dimensional Renormalizable Field Theories"*, Nucl. Phys. B 343, 647 (1990).

[19] A. B. Zamolodchikov, *"Irreversibility of the Flux of the Renormalization Group in a 2D Field Theory"*, JETP Lett. 43, 730 (1986).

[20] J. Polchinski, *"Scale and Conformal Invariance in Quantum Field Theory"*, Nucl. Phys. B 303, 226 (1988).

[21] A. A. Belavin, A. M. Polyakov and A. B. Zamolodchikov, *"Infinite Conformal Symmetry in Two-Dimensional Quantum Field Theory"*, Nucl. Phys. B 241, 333 (1984).

[22] J. Zuber, *"2D-CFT's -The blossoming of the 80's"*, Talk given at conference Conformal Invariance and Harmonic Analysis.

[23] P. Di Francesco, P. Mathieu and D. Senechal, *"Conformal Field Theory"*, Springer-Verlag (1997), New York.

[24] A. Recknagel and V. Schomerus, *"Boundary Conformal Field Theory and the Worldsheet Approach to D-Branes"*, Cambridge University Press (2013).

[25] R. Blumenhagen and E. Plauschinn, *"Introduction to conformal field theory: with applications to String theory"*, Springer (2009), Berlin Heidelberg.

[26] A. B. Zamolodchikov, *"Infinite Additional Symmetries in Two-Dimensional Conformal Quantum Field Theory"*, Theor. Math. Phys. 65, 1205 (1985).

[27] P. Bouwknegt and K. Schoutens, *"W symmetry in conformal field theory"*, Phys. Rept. 223, 183 (1993), hep-th/9210010.

[28] J. L. Cardy, *"Conformal Invariance and Surface Critical Behavior"*, Nucl. Phys. B 240, 514 (1984).

[29] J. L. Cardy, *"Effect of Boundary Conditions on the Operator Content of Two-Dimensional Conformally Invariant Theories"*, Nucl. Phys. B 275, 200 (1986).

[30] J. L. Cardy and I. Peschel, *"Finite Size Dependence of the Free Energy in Two-dimensional Critical Systems"*, Nucl. Phys. B 300, 377 (1988).

[31] R. E. Behrend, P. A. Pearce, V. B. Petkova and J.-B. Zuber, *"On the classification of bulk and boundary conformal field theories"*, Phys. Lett. B 444, 163 (1998), hep-th/9809097.

[32] I. Affleck and A. W. Ludwig, *"Universal noninteger 'ground state degeneracy' in critical quantum systems"*, Phys. Rev. Lett. 67, 161 (1991).

[33] J. B. Zuber, *"Conformal field theories, Coulomb gas picture and integrable models"*, in: *"Les Houches Summer School in Theoretical Physics: Fields, Strings, Critical Phenomena"*.

[34] J. Frohlich, J. Fuchs, I. Runkel and C. Schweigert, *"Kramers-Wannier duality from conformal defects"*, Phys. Rev. Lett. 93, 070601 (2004), cond-mat/0404051.

[35] J. Frohlich, J. Fuchs, I. Runkel and C. Schweigert, *"Duality and defects in rational conformal field theory"*, Nucl. Phys. B 763, 354 (2007), hep-th/0607247.

[36] V. B. Petkova and J. B. Zuber, *"Generalized twisted partition functions"*, Phys. Lett. B 504, 157 (2001), hep-th/0011021.

[37] L. Bombelli, R. K. Koul, J. Lee and R. D. Sorkin, *"Quantum source of entropy for black holes"*, Phys. Rev. D 34, 373 (1986).

[38] M. Srednicki, *"Entropy and area"*, Phys. Rev. Lett. 71, 666 (1993), hep-th/9303048.

[39] T. Nishioka, S. Ryu and T. Takayanagi, *"Holographic Entanglement Entropy: An Overview"*, J. Phys. A 42, 504008 (2009), arxiv:0905.0932.

[40] M. Rangamani and T. Takayanagi, *"Holographic Entanglement Entropy"*, Springer (2017).

[41] A. Kitaev and J. Preskill, *"Topological entanglement entropy"*, Phys. Rev. Lett. 96, 110404 (2006), hep-th/0510092.

[42] M. Levin and X.-G. Wen, *"Detecting Topological Order in a Ground State Wave Function"*, Phys. Rev. Lett. 96, (2006), https://doi.org/10.1103/physrevlett.96.110405.

[43] M. B. Hastings, *"An area law for one-dimensional quantum systems"*, J. Stat. Mech. 0708, P08024 (2007), arxiv:0705.2024.

[44] J. Eisert, M. Cramer and M. B. Plenio, *"Area laws for the entanglement entropy - a review"*, Rev. Mod. Phys. 82, 277 (2010), arxiv:0808.3773.

[45] G. Vitagliano, A. Riera and J. I. Latorre, *"Violation of area-law scaling for the entanglement entropy in spin 1/2 chains"*, New J. Phys. 12, 113049 (2010), arxiv:1003.1292.

[46] P. Calabrese and J. L. Cardy, *"Entanglement entropy and quantum field theory"*, J. Stat. Mech. 0406, P06002 (2004), hep-th/0405152.

[47] C. G. Callan, Jr. and F. Wilczek, *"On geometric entropy"*, Phys. Lett. B 333, 55 (1994), hep-th/9401072.

[48] J. L. Cardy, *"Boundary conformal field theory"*, hep-th/0411189.

[49] S. R. White, *"Density matrix formulation for quantum renormalization groups"*, Phys. Rev. Lett. 69, 2863 (1992).

[50] U. Schollwöck, *"The density-matrix renormalization group in the age of matrix product states"*, Ann. Phys. 326, 96 (2011).

[51] B. Pirvu, G. Vidal, F. Verstraete and L. Tagliacozzo, *"Matrix product states for critical spin chains: Finite-size versus finite-entanglement scaling"*, Physical Review B 86, 075117 (2012), arxiv:1204.3934.

[52] G. Vidal, *"Class of Quantum Many-Body States That Can Be Efficiently Simulated"*, Phys. Rev. Lett. 101, 110501 (2008), quant-ph/0610099.

[53] G. Evenbly and G. Vidal, *"Quantum criticality with the multi-scale entanglement renormalization ansatz"*, Strongly correlated systems: numerical methods Chapter 4, 99 (2013).

[54] W. Donnelly, *"Decomposition of entanglement entropy in lattice gauge theory"*, Phys. Rev. D 85, 085004 (2012), arxiv:1109.0036.

[55] S. Ghosh, R. M. Soni and S. P. Trivedi, *"On The Entanglement Entropy For Gauge Theories"*, JHEP 1509, 069 (2015), arxiv:1501.02593.

[56] H. Casini, M. Huerta and J. A. Rosabal, *"Remarks on entanglement entropy for gauge fields"*, Phys. Rev. D 89, 085012 (2014), arxiv:1312.1183.

[57] I. Bengtsson and K. Zyczkowski, *"Geometry of Quantum States: An Introduction to Quantum Entanglement"*, Cambridge University Press (2007).

[58] R. Horodecki, P. Horodecki, M. Horodecki and K. Horodecki, *"Quantum entanglement"*, Rev. Mod. Phys. 81, 865 (2009), quant-ph/0702225.

[59] C. E. Shannon, *"A mathematical theory of communication"*, Bell Syst. Tech. J. 27, 379 (1948).

[60] M. J. Donald, M. Horodecki and O. Rudolph, *"The uniqueness theorem for entanglement measures"*, J. Math. Phys. 43, 4252 (2002), quant-ph/0105017.

[61] E. Chitambar, D. Leung, L. Mancinska, M. Ozols and A. Winter, *"Everything you always wanted to know about LOCC (but were afraid to ask)"*, Commun. Math. Phys. 328, 303 (2014), arxiv:1210.4583.

[62] C. H. Bennett, D. P. DiVincenzo, C. A. Fuchs, T. Mor, E. Rains, P. W. Shor and J. A. Smolin, *"Quantum nonlocality without entanglement"*, Phys. Rev. A 59, 1070 (1999), quant-ph/9804053.

[63] G. Vidal, *"Entanglement monotones"*, J. Mod. Opt. 47, 355 (2000), quant-ph/9807077.

[64] K. Horodecki, M. Horodecki, P. Horodecki and J. Oppenheim, *"Locking entanglement with a single qubit"*, Phys. Rev. Lett. 94, 200501 (2005), quant-ph/0404096.

[65] I. Peschel, *"Calculation of reduced density matrices from correlation functions"*, J. Phys. A 36, L205 (2003), cond-mat/0212631.

[66] V. Eisler and I. Peschel, *"Reduced density matrices and entanglement entropy in free lattice models"*, J. Phys. A 42, 504003 (2009), arxiv:0906.1663.

[67] M. Henkel, *"Conformal invariance and critical phenomena"*, Springer Science & Business Media (1999).

[68] M. Troyanov, *"Prescribing curvature on compact surfaces with conical singularities"*, Trans. Am. Math. Soc. 324, 793 (1991), http://www.jstor.org/stable/2001742.

[69] L. P. Kadanoff and H. Ceva, *"Determination of an Operator Algebra for the Two-Dimensional Ising Model"*, Phys. Rev. B 3, 3918 (1971).

[70] L. J. Dixon, D. Friedan, E. J. Martinec and S. H. Shenker, *"The Conformal Field Theory of Orbifolds"*, Nucl. Phys. B 282, 13 (1987).

[71] P. Calabrese, J. Cardy and E. Tonni, *"Entanglement entropy of two disjoint intervals in conformal field theory"*, J. Stat. Mech. 0911, P11001 (2009), arxiv:0905.2069.

[72] J. L. Cardy, O. A. Castro-Alvaredo and B. Doyon, *"Form factors of branch-point twist fields in quantum integrable models and entanglement entropy"*, J. Stat. Phys. 130, 129 (2008), arxiv:0706.3384.

[73] O. A. Castro-Alvaredo and B. Doyon, *"Bi-partite entanglement entropy in massive 1+1-dimensional quantum field theories"*, J. Phys. A 42, 504006 (2009), arxiv:0906.2946.

[74] B. Estienne, Y. Ikhlef and A. Morin-Duchesne, *"Finite-size corrections in critical symmetry-resolved entanglement"*, SciPost Phys. 10, 054 (2021), arxiv:2010.10515.

[75] A. Cappelli, C. Itzykson and J. B. Zuber, *"Modular Invariant Partition Functions in Two-Dimensions"*, Nucl. Phys. B 280, 445 (1987).

[76] A. Cappelli, C. Itzykson and J. B. Zuber, *"The ADE Classification of Minimal and A1(1) Conformal Invariant Theories"*, Commun. Math. Phys. 113, 1 (1987).

[77] G. W. Moore and N. Seiberg, *"Classical and Quantum Conformal Field Theory"*, Commun. Math. Phys. 123, 177 (1989).

[78] J. J. Atick, L. J. Dixon, P. A. Griffin and D. D. Nemeschansky, *"Multi-loop twist field correlation functions for ZN orbifolds"*, Nucl. Phys. B 298, 1 (1988).

[79] M. Leitner, *"The* $(2,5)$ *minimal model on genus two surfaces"*, arxiv:1801.08387.

[80] J. Henriksson, A. Kakkar and B. McPeak, *"Narain CFTs and quantum codes at higher genus"*, JHEP 2304, 011 (2023), arxiv:2205.00025.

[81] G. Felder, *"BRST Approach to Minimal Models"*, Nucl. Phys. B 317, 215 (1989), [Erratum: Nucl.Phys.B 324, 548 (1989)].

[82] H. J. Shin, *"Coulomb gas representation of minimal models on Riemann surfaces"*, Phys. Rev. D 44, 3843 (1991).

[83] O. Foda, *"Minimal models ON Riemann surfaces:the partition functions"*, Nucl. Phys. B 336, 691 (1990).

[84] V. Alba, L. Tagliacozzo and P. Calabrese, *"Entanglement entropy of two disjoint blocks in critical Ising models"*, Phys. Rev. B 81, 060411 (2010), arxiv:0910.0706.

[85] P. Calabrese, J. Cardy and E. Tonni, *"Entanglement entropy of two disjoint intervals in conformal field theory II"*, J. Stat. Mech. 1101, P01021 (2011), arxiv:1011.5482.

[86] H. Casini and M. Huerta, *"Remarks on the entanglement entropy for disconnected regions"*, JHEP 0903, 048 (2009), arxiv:0812.1773.

[87] P. Calabrese and J. Cardy, *"Entanglement entropy and conformal field theory"*, J. Phys. A 42, 504005 (2009), arxiv:0905.4013.

[88] A. Coser, L. Tagliacozzo and E. Tonni, *"On Rényi entropies of disjoint intervals in conformal field theory"*, J. Stat. Mech. 1401, P01008 (2014), arxiv:1309.2189.

[89] C. A. Agon, M. Headrick, D. L. Jafferis and S. Kasko, *"Disk entanglement entropy for a Maxwell field"*, Phys. Rev. D 89, 025018 (2014), arxiv:1310.4886.

[90] C. De Nobili, A. Coser and E. Tonni, *"Entanglement entropy and negativity of disjoint intervals in CFT: Some numerical extrapolations"*, J. Stat. Mech. 1506, P06021 (2015), arxiv:1501.04311.

[91] H.-Q. Zhou, T. Barthel, J. Fjaeretad and U. Schollwock, *"Entanglement and boundary critical phenomena"*, Phys. Rev. A 74, 050305 (2006), cond-mat/0511732.

[92] I. Affleck, N. Laflorencie and E. S. Sorensen, *"Entanglement entropy in quantum impurity systems and systems with boundaries"*, J. Phys. A 42, 504009 (2009), arxiv:0906.1809.

[93] C. Berthiere and S. N. Solodukhin, *"Boundary effects in entanglement entropy"*, Nucl. Phys. B 910, 823 (2016), arxiv:1604.07571.

[94] L. Taddia, J. Xavier, F. C. Alcaraz and G. Sierra, *"Entanglement entropies in conformal systems with boundaries"*, Phys. Rev. B 88, 075112 (2013), arxiv:1302.6222.

[95] I. Affleck, *"Conformal field theory approach to the Kondo effect"*, Acta Phys. Polon. B 26, 1869 (1995), cond-mat/9512099.

[96] N. Laflorencie, E. S. Sorensen, M.-S. Chang and I. Affleck, *"Boundary effects in the critical scaling of entanglement entropy in 1D systems"*, Phys. Rev. Lett. 96, 100603 (2006), cond-mat/0512475.

[97] S. Ryu and T. Takayanagi, *"Holographic derivation of entanglement entropy from AdS/CFT"*, Phys. Rev. Lett. 96, 181602 (2006), hep-th/0603001.

[98] S. Ryu and T. Takayanagi, *"Aspects of Holographic Entanglement Entropy"*, JHEP 0608, 045 (2006), hep-th/0605073.

[99] A. Karch and L. Randall, *"Locally localized gravity"*, JHEP 0105, 008 (2001), hep-th/0011156.

[100] T. Takayanagi, *"Holographic Dual of BCFT"*, Phys. Rev. Lett. 107, 101602 (2011), arxiv:1105.5165.

[101] M. Fujita, T. Takayanagi and E. Tonni, *"Aspects of AdS/BCFT"*, JHEP 1111, 043 (2011), arxiv:1108.5152.

[102] M. Nozaki, T. Takayanagi and T. Ugajin, *"Central Charges for BCFTs and Holography"*, JHEP 1206, 066 (2012), arxiv:1205.1573.

[103] G. Penington, *"Entanglement Wedge Reconstruction and the Information Paradox"*, JHEP 2009, 002 (2020), arxiv:1905.08255.

[104] A. Almheiri, N. Engelhardt, D. Marolf and H. Maxfield, *"The entropy of bulk quantum fields and the entanglement wedge of an evaporating black hole"*, JHEP 1912, 063 (2019), arxiv:1905.08762.

[105] A. Almheiri, R. Mahajan, J. Maldacena and Y. Zhao, *"The Page curve of Hawking radiation from semiclassical geometry"*, JHEP 2003, 149 (2020), arxiv:1908.10996.

[106] A. Almheiri, T. Hartman, J. Maldacena, E. Shaghoulian and A. Tajdini, *"Replica Wormholes and the Entropy of Hawking Radiation"*, JHEP 2005, 013 (2020), arxiv:1911.12333.

[107] G. Penington, S. H. Shenker, D. Stanford and Z. Yang, *"Replica wormholes and the black hole interior"*, JHEP 2203, 205 (2022), arxiv:1911.11977.

[108] J. L. Cardy, *"Boundary Conditions, Fusion Rules and the Verlinde Formula"*, Nucl. Phys. B 324, 581 (1989).

[109] J. Cardy and E. Tonni, *"Entanglement hamiltonians in two-dimensional conformal field theory"*, J. Stat. Mech. 1612, 123103 (2016), arxiv:1608.01283.

[110] J. Sully, M. Van Raamsdonk and D. Wakeham, *"BCFT entanglement entropy at large central charge and the black hole interior"*, JHEP 2103, 167 (2021), arxiv:2004.13088.

[111] H.-Q. Zhou, T. Barthel, J. O. Fjærestad and U. Schollwöck, *"Entanglement and boundary critical phenomena"*, Phys. Rev. A 74, 050305 (2006).

[112] D. Friedan and A. Konechny, *"On the boundary entropy of one-dimensional quantum systems at low temperature"*, Phys. Rev. Lett. 93, 030402 (2004), hep-th/0312197.

[113] H. Casini, I. Salazar Landea and G. Torroba, *"The g-theorem and quantum information theory"*, JHEP 1610, 140 (2016), arxiv:1607.00390.

[114] R. E. Behrend, P. A. Pearce, V. B. Petkova and J.-B. Zuber, *"Boundary conditions in rational conformal field theories"*, Nucl. Phys. B 570, 525 (2000), hep-th/9908036.

[115] C. Schweigert, J. Fuchs and J. Walcher, *"Conformal field theory, boundary conditions and applications to string theory"*, hep-th/0011109.

[116] F. C. Alcaraz, M. I. Berganza and G. Sierra, *"Entanglement of low-energy excitations in Conformal Field Theory"*, Phys. Rev. Lett. 106, 201601 (2011), arxiv:1101.2881.

[117] M. I. Berganza, F. C. Alcaraz and G. Sierra, *"Entanglement of excited states in critical spin chians"*, J. Stat. Mech. 1201, P01016 (2012), arxiv:1109.5673.

[118] T. Dupic, B. Estienne and Y. Ikhlef, *"Entanglement entropies of minimal models from null-vectors"*, SciPost Phys. 4, 031 (2018), arxiv:1709.09270.

[119] L. Borisov, M. B. Halpern and C. Schweigert, *"Systematic approach to cyclic orbifolds"*, Int. J. Mod. Phys. A 13, 125 (1998), hep-th/9701061.

[120] B. Estienne, Y. Ikhlef and A. Rotaru, *"Second Rényi entropy and annulus partition function for one-dimensional quantum critical systems with boundaries"*, SciPost Phys. 12, 141 (2022), arxiv:2112.01929.

[121] A. Bastianello, J. Dubail and J.-M. Stéphan, *"Entanglement entropies of inhomogeneous Luttinger liquids"*, J. Phys. A 53, 155001 (2020), arxiv:1910.09967.

[122] O. Lunin and S. D. Mathur, *"Correlation functions for M**N / S(N) orbifolds"*, Commun. Math. Phys. 219, 399 (2001), hep-th/0006196.

[123] M. Headrick, *"Entanglement Renyi entropies in holographic theories"*, Phys. Rev. D 82, 126010 (2010), arxiv:1006.0047.

[124] J. L. Cardy and D. C. Lewellen, *"Bulk and boundary operators in conformal field theory"*, Phys. Lett. B 259, 274 (1991).

[125] M. Fagotti and P. Calabrese, *"Universal parity effects in the entanglement entropy of XX chains with open boundary conditions"*, J. Stat. Mech. 1101, P01017 (2011), arxiv:1010.5796.

[126] J. C. Xavier and M. A. Rajabpour, *"Entanglement and boundary entropy in quantum spin chains with arbitrary direction of the boundary magnetic fields"*, Phys. Rev. B 101, 235127 (2020), arxiv:2003.00095.

[127] M. Fagotti and P. Calabrese, *"Entanglement entropy of two disjoint blocks in XY chains"*, J. Stat. Mech. 1004, P04016 (2010), arxiv:1003.1110.

[128] J. Dubail, J.-M. Stéphan, J. Viti and P. Calabrese, *"Conformal Field Theory for Inhomogeneous One-dimensional Quantum Systems: the Example of Non-Interacting Fermi Gases"*, SciPost Phys. 2, 002 (2017), arxiv:1606.04401.

[129] M. Mintchev and E. Tonni, *"Modular Hamiltonians for the massless Dirac field in the presence of a boundary"*, JHEP 2103, 204 (2021), arxiv:2012.00703.

[130] D. C. Lewellen, *"Sewing constraints for conformal field theories on surfaces with boundaries"*, Nucl. Phys. B 372, 654 (1992).

[131] T. Barthel, M.-C. Chung and U. Schollwöck, *"Entanglement scaling in critical two-dimensional fermionic and bosonic systems"*, Phys. Rev. A 74, 022329 (2006).

[132] S. Furukawa, V. Pasquier and J. Shiraishi, *"Mutual Information and Compactification Radius in a c=1 Critical Phase in One Dimension"*, Phys. Rev. Lett. 102, 170602 (2009), arxiv:0809.5113.

[133] L. Capizzi, P. Ruggiero and P. Calabrese, *"Symmetry resolved entanglement entropy of excited states in a CFT"*, J. Stat. Mech. 2007, 073101 (2020), arxiv:2003.04670.

[134] J. Zhang, P. Ruggiero and P. Calabrese, *"Subsystem trace distance in low-lying states of* $(1+1)$*-dimensional conformal field theories"*, JHEP 1910, 181 (2019), arxiv:1907.04332.

[135] J. Zhang, P. Ruggiero and P. Calabrese, *"Subsystem Trace Distance in Quantum Field Theory"*, Phys. Rev. Lett. 122, 141602 (2019), arxiv:1901.10993.

[136] G. B. Mbeng, A. Russomanno and G. E. Santoro, *"The quantum Ising chain for beginners"*, arxiv:2009.09208.

[137] M.-C. Chung and I. Peschel, *"Density-matrix spectra of solvable fermionic systems"*, Phys. Rev. B 64, 064412 (2001), cond-mat/0103301.

[138] F. Iglói and I. Peschel, *"On reduced density matrices for disjoint subsystems"*, EPL (Europhysics Letter 89, 40001 (2010).

[139] A. Jafarizadeh and M. A. Rajabpour, *"Entanglement entropy in quantum spin chains with broken parity number symmetry"*, SciPost Phys. 12, 195 (2022), arxiv:2109.06359.

[140] N. Ishibashi, *"The Boundary and Crosscap States in Conformal Field Theories"*, Mod. Phys. Lett. A 4, 251 (1989).

[141] I. Runkel, *"Boundary problems in conformal field theory"*.

[142] M. Oshikawa and I. Affleck, *"Boundary conformal field theory approach to the critical two-dimensional Ising model with a defect line"*, Nucl. Phys. B 495, 533 (1997), cond-mat/9612187.

[143] K. Graham, I. Runkel and G. M. T. Watts, *"Boundary renormalisation group flows of minimal models"*, in: *"24th Johns Hopkins Workshop on Nonperturbative QFT Methods and Their Applications"*, 95–113p.

[144] J. Cardy and P. Calabrese, *"Unusual Corrections to Scaling in Entanglement Entropy"*, J. Stat. Mech. 1004, P04023 (2010), arxiv:1002.4353.

[145] E. Eriksson and H. Johannesson, *"Corrections to scaling in entanglement entropy from boundary perturbations"*, J. Stat. Mech.: Theory Exp 2011, P02008 (2011).

[146] P. Calabrese, M. Campostrini, F. Essler and B. Nienhuis, *"Parity effects in the scaling of block entanglement in gapless spin chains"*, Phys. Rev. Lett. 104, 095701 (2010), arxiv:0911.4660.

[147] J. C. Xavier and F. C. Alcaraz, *"Finite-size corrections of the Entanglement Entropy of critical quantum chains"*, Phys. Rev. B 85, 024418 (2012), arxiv:1111.6577.

[148] G. Vidal, J. I. Latorre, E. Rico and A. Kitaev, *"Entanglement in quantum critical phenomena"*, Phys. Rev. Lett. 90, 227902 (2003), quant-ph/0211074.

[149] D. X. Horvath, P. Calabrese and O. A. Castro-Alvaredo, *"Branch Point Twist Field Form Factors in the sine-Gordon Model II: Composite Twist Fields and Symmetry Resolved Entanglement"*, SciPost Phys. 12, 088 (2022), arxiv:2105.13982.

[150] A. Roy and H. Saleur, *"Entanglement Entropy in the Ising Model with Topological Defects"*, Phys. Rev. Lett. 128, 090603 (2022), arxiv:2111.04534.

[151] B. Estienne, Y. Y. Ikhlef, A. Rotaru and E. Tonni, *"Entanglement entropies of an interval for the massless scalar field in the presence of a boundary"*, Journal Name XX, XXXX (Year).

[152] B. Estienne, B. Oblak and J.-M. Stéphan, *"Ergodic Edge Modes in the 4D Quantum Hall Effect"*, SciPost Phys. 11, 016 (2021), arxiv:2104.01860.

[153] T. Grava, A. P. Kels and E. Tonni, *"Entanglement of Two Disjoint Intervals in Conformal Field Theory and the 2D Coulomb Gas on a Lattice"*, Phys. Rev. Lett. 127, 141605 (2021), arxiv:2104.06994.

[154] S. Murciano, G. Di Giulio and P. Calabrese, *"Entanglement and symmetry resolution in two dimensional free quantum field theories"*, JHEP 2008, 073 (2020), arxiv:2006.09069.

[155] E. Alvarez, J. L. F. Barbon and J. Borlaf, *"T duality for open strings"*, Nucl. Phys. B 479, 218 (1996), hep-th/9603089.

[156] K. Audenaert, J. Eisert, M. Plenio and R. Werner, *"Entanglement Properties of the Harmonic Chain"*, Phys. Rev. A 66, 042327 (2002), quant-ph/0205025.

[157] A. Botero and B. Reznik, *"Spatial structures and localization of vacuum entanglement in the linear harmonic chain"*, Phys. Rev. A 70, 052329 (2004), quant-ph/0403233.

[158] M. Plenio, J. Eisert, J. Dreissig and M. Cramer, *"Entropy, entanglement, and area: analytical results for harmonic lattice systems"*, Phys. Rev. Lett. 94, 060503 (2005), quant-ph/0405142.

[159] M. Cramer, J. Eisert, M. Plenio and J. Dreissig, *"An Entanglement-area law for general bosonic harmonic lattice systems"*, Phys. Rev. A 73, 012309 (2006), quant-ph/0505092.

[160] N. Schuch, J. I. Cirac and M. M. Wolf, *"Quantum States on Harmonic Lattices"*, Commun. Math. Phys 267, 65–92 (2006).

[161] H. Casini and M. Huerta, *"Entanglement entropy in free quantum field theory"*, J. Phys. A 42, 504007 (2009), arxiv:0905.2562.

[162] C. Berthiere and W. Witczak-Krempa, *"Relating bulk to boundary entanglement"*, Phys. Rev. B 100, 235112 (2019), arxiv:1907.11249.

[163] P. Calabrese, J. Cardy and E. Tonni, *"Entanglement negativity in extended systems: A field theoretical approach"*, J. Stat. Mech. 1302, P02008 (2013), arxiv:1210.5359.

[164] H. M. Farkas and I. Kra, *"Riemann surfaces"*, Springer (1992).

[165] H. Casini, C. D. Fosco and M. Huerta, *"Entanglement and alpha entropies for a massive Dirac field in two dimensions"*, J. Stat. Mech. 0507, P07007 (2005), cond-mat/0505563.

[166] A. Bastianello, *"Rényi entanglement entropies for the compactified massless boson with open boundary conditions"*, JHEP 1910, 141 (2019), arxiv:1909.00806.

[167] C. Restuccia, *"Limit theories and continuous orbifolds"*, arxiv:1310.6857.

[168] I. Runkel and G. M. T. Watts, *"A Nonrational CFT with c = 1 as a limit of minimal models"*, JHEP 0109, 006 (2001), hep-th/0107118.

[169] S. Lievens, N. I. Stoilova and J. Van der Jeugt, *"Harmonic oscillator chains as Wigner Quantum Systems: Periodic and fixed wall boundary conditions in gl(1—n) solutions"*, J. Math. Phys. 49, 073502 (2008), arxiv:0709.0180.

[170] P. Jain, S. M. Chandran and S. Shankaranarayanan, *"Log to log-log crossover of entanglement in* (1 + 1)*− dimensional massive scalar field"*, Phys. Rev. D 103, 125008 (2021), arxiv:2103.01772.

[171] I. S. Gradshteyn and I. M. Ryzhik, *"Table of Integrals, Series, and Products"*, 7th edition, Academic Press (2007), 394p.

[172] Y. K. Yazdi, *"Zero Modes and Entanglement Entropy"*, JHEP 1704, 140 (2017), arxiv:1608.04744.

[173] B. Estienne, Y. Ikhlef and A. Rotaru, *"Rényi entropies for one-dimensional quantum systems with mixed boundary conditions"*, arxiv:2301.02124.

[174] O. A. Castro-Alvaredo and B. Doyon, *"Bi-partite entanglement entropy in massive QFT with a boundary: The Ising model"*, J. Stat. Phys. 134, 105 (2009), arxiv:0810.0219.

[175] H. Casini and M. Huerta, *"Reduced density matrix and internal dynamics for multicomponent regions"*, Class. Quant. Grav. 26, 185005 (2009), arxiv:0903.5284.

[176] F. Rottoli, S. Murciano, E. Tonni and P. Calabrese, *"Entanglement and negativity Hamiltonians for the massless Dirac field on the half line"*, J. Stat. Mech. 2301, 013103 (2023), arxiv:2210.12109.

[177] I. Peschel and V. Eisler, *"Exact results for the entanglement across defects in critical chains"*, J. Phys. A 45, 155301 (2012), arxiv:1201.4104.

[178] I. Peschel and V. Eisler, *"Exact results for the entanglement across defects in critical chains"*, J. Phys. A 45, 155301 (2012), arxiv:1201.4104.

[179] M. Gutperle and J. D. Miller, *"Entanglement entropy at CFT junctions"*, Phys. Rev. D 95, 106008 (2017), arxiv:1701.08856.

[180] M. Mintchev and E. Tonni, *"Modular Hamiltonians for the massless Dirac field in the presence of a defect"*, JHEP 2103, 205 (2021), arxiv:2012.01366.

[181] V. Fateev, A. B. Zamolodchikov and A. B. Zamolodchikov, *"Boundary Liouville field theory. 1. Boundary state and boundary two point function"*, hep-th/0001012.

[182] A. B. Zamolodchikov and A. B. Zamolodchikov, *"Liouville field theory on a pseudosphere"*, hep-th/0101152.

[183] H. Casini, M. Huerta and R. C. Myers, *"Towards a derivation of holographic entanglement entropy"*, JHEP 1105, 036 (2011), arxiv:1102.0440.

[184] A. M. Läuchli, *"Operator content of real-space entanglement spectra at conformal critical points"*, arxiv:1303.0741.

[185] R. Arias, D. Blanco, H. Casini and M. Huerta, *"Local temperatures and local terms in modular Hamiltonians"*, Phys. Rev. D 95, 065005 (2017), arxiv:1611.08517.

[186] E. Tonni, J. Rodríguez-Laguna and G. Sierra, *"Entanglement hamiltonian and entanglement contour in inhomogeneous 1D critical systems"*, J. Stat. Mech. 1804, 043105 (2018), arxiv:1712.03557.

[187] V. Alba, P. Calabrese and E. Tonni, *"Entanglement spectrum degeneracy and the Cardy formula in 1+1 dimensional conformal field theories"*, J. Phys. A 51, 024001 (2018), arxiv:1707.07532.

[188] V. Eisler and I. Peschel, *"Analytical results for the entanglement Hamiltonian of a free-fermion chain"*, J. Phys. A 50, 284003 (2017), arxiv:1703.08126.

[189] V. Eisler and I. Peschel, *"Properties of the entanglement Hamiltonian for finite free-fermion chains"*, J. Stat. Mech. 2018, 104001 (2018), arxiv:1805.00078.

[190] R. E. Arias, H. Casini, M. Huerta and D. Pontello, *"Entropy and modular Hamiltonian for a free chiral scalar in two intervals"*, Phys. Rev. D 98, 125008 (2018), arxiv:1809.00026.

[191] J. Surace, L. Tagliacozzo and E. Tonni, *"Operator content of entanglement spectra in the transverse field Ising chain after global quenches"*, Phys. Rev. B 101, 241107(R) (2020), arxiv:1909.07381.

[192] G. Di Giulio and E. Tonni, *"On entanglement hamiltonians of an interval in massless harmonic chains"*, J. Stat. Mech. 2003, 033102 (2020), arxiv:1911.07188.

[193] G. Di Giulio, R. Arias and E. Tonni, *"Entanglement hamiltonians in 1D free lattice models after a global quantum quench"*, J. Stat. Mech. 1912, 123103 (2019), arxiv:1905.01144.

[194] V. Eisler, E. Tonni and I. Peschel, *"On the continuum limit of the entanglement Hamiltonian"*, J. Stat. Mech. 1907, 073101 (2019), arxiv:1902.04474.

[195] V. Eisler, G. Di Giulio, E. Tonni and I. Peschel, *"Entanglement Hamiltonians for non-critical quantum chains"*, J. Stat. Mech. 2010, 103102 (2020), arxiv:2007.01804.

[196] V. Eisler, E. Tonni and I. Peschel, *"Local and non-local properties of the entanglement Hamiltonian for two disjoint intervals"*, J. Stat. Mech. 2208, 083101 (2022), arxiv:2204.03966.

[197] G. Vidal and R. F. Werner, *"Computable measure of entanglement"*, Phys. Rev. A 65, 032314 (2002), quant-ph/0102117.

[198] P. Calabrese, J. Cardy and E. Tonni, *"Entanglement negativity in quantum field theory"*, Phys. Rev. Lett. 109, 130502 (2012), arxiv:1206.3092.

[199] P. Calabrese, J. Cardy and E. Tonni, *"Finite temperature entanglement negativity in conformal field theory"*, J. Phys. A 48, 015006 (2015), arxiv:1408.3043.

[200] A. Coser, E. Tonni and P. Calabrese, *"Towards the entanglement negativity of two disjoint intervals for a one dimensional free fermion"*, J. Stat. Mech. 1603, 033116 (2016), arxiv:1508.00811.

[201] A. Coser, E. Tonni and P. Calabrese, *"Partial transpose of two disjoint blocks in XY spin chains"*, J. Stat. Mech. 1508, P08005 (2015), arxiv:1503.09114.

[202] V. Eisler and Z. Zimborás, *"Entanglement negativity in two-dimensional free lattice models"*, Phys. rev. B 93, 115148 (2016), arxiv:1511.08819.

[203] C. De Nobili, A. Coser and E. Tonni, *"Entanglement negativity in a two dimensional harmonic lattice: Area law and corner contributions"*, J. Stat. Mech. 1608, 083102 (2016), arxiv:1604.02609.

[204] H. Shapourian, K. Shiozaki and S. Ryu, *"Partial time-reversal transformation and entanglement negativity in fermionic systems"*, Phys. Rev. B 95, 165101 (2017), arxiv:1611.07536.

[205] N. Javerzat and E. Tonni, *"On the continuum limit of the entanglement Hamiltonian of a sphere for the free massless scalar field"*, JHEP 2202, 086 (2022), arxiv:2111.05154.

[206] V. Eisler and Z. Zimborás, *"On the partial transpose of fermionic Gaussian states"*, New J. Phys. 17, 053048 (2015), arxiv:1502.01369.

[207] L. Taddia, F. Ortolani and T. Pálmai, *"Renyi entanglement entropies of descendant states in critical systems with boundaries: conformal field theory and spin chains"*, J. Stat. Mech. 1609, 093104 (2016), arxiv:1606.02667.

[208] J. Ren, S. Zhu and X. Hao, *"Entanglement entropy in an antiferromagnetic Heisenberg spin chain with boundary impurities"*, J. Phys. B 42, 015504 (2008).

[209] J. Spalding, S.-W. Tsai and D. K. Campbell, *"Critical entanglement for the half-filled extended Hubbard model"*, Phys. Rev. B 99, 195445 (2019).

[210] R. Orus, *"A Practical Introduction to Tensor Networks: Matrix Product States and Projected Entangled Pair States"*, Annals Phys. 349, 117 (2014), arxiv:1306.2164.

[211] B. Estienne, Y. Ikhlef and A. Rotaru, *"The operator algebra of cyclic orbifolds"*, arxiv:2212.07678.

[212] M. A. Rajabpour and F. Gliozzi, *"Entanglement Entropy of Two Disjoint Intervals from Fusion Algebra of Twist Fields"*, J. Stat. Mech. 1202, P02016 (2012), arxiv:1112.1225.

[213] I. Runkel, *"Structure constants for the D series Virasoro minimal models"*, Nucl. Phys. B 579, 561 (2000), hep-th/9908046.

[214] C. Holzhey, F. Larsen and F. Wilczek, *"Geometric and renormalized entropy in conformal field theory"*, Nucl. Phys. B 424, 443 (1994), hep-th/9403108.

[215] F. Iglói and R. Juhász, *"Exact relationship between the entanglement entropies of XY and quantum Ising chains"*, Europhys. Lett. 81, 57003 (2008).

[216] Y. Zou, A. Milsted and G. Vidal, *"Conformal data and renormalization group flow in critical quantum spin chains using periodic uniform matrix product states"*, Phys. Rev. Lett. 121, 230402 (2018), arxiv:1710.05397.

[217] I. Affleck, *"Edge magnetic field in the XXZ spin-1/2 chain"*, J. Phys. A 31, 2761 (1998).

[218] A. F. Caldeira, S. Kawai and J. F. Wheater, *"Free boson formulation of boundary states in W(3) minimal models and the critical Potts model"*, JHEP 0308, 041 (2003), hep-th/0306082.

[219] D. Bianchini, O. A. Castro-Alvaredo, B. Doyon, E. Levi and F. Ravanini, *"Entanglement Entropy of Non Unitary Conformal Field Theory"*, J. Phys. A 48, 04FT01 (2015), arxiv:1405.2804.

[220] J. L. Cardy, *"Conformal Invariance and the Yang-lee Edge Singularity in Two-dimensions"*, Phys. Rev. Lett. 54, 1354 (1985).

[221] A. Recknagel, D. Roggenkamp and V. Schomerus, *"On relevant boundary perturbations of unitary minimal models"*, Nucl. Phys. B 588, 552 (2000), hep-th/0003110.

[222] F. Ares, R. Santachiara and J. Viti, *"Crossing-symmetric twist field correlators and entanglement negativity in minimal CFTs"*, JHEP 2110, 175 (2021), arxiv:2107.13925.

[223] T. Dupic, B. Estienne and Y. Ikhlef, *"The imaginary Toda field theory"*, J. Phys. A 52, 105201 (2019), arxiv:1809.05568.

[224] *"NIST Digital Library of Mathematical Functions"*, F. W. J. Olver, A. B. Olde Daalhuis, D. W. Lozier, B. I. Schneider, R. F. Boisvert, C. W. Clark, B. R. Miller, B. V. Saunders, H. S. Cohl, and M. A. McClain, eds., https://dlmf.nist.gov/.

[225] Y. Zou, *"Universal information of critical quantum spin chains from wavefunction overlap"*, Phys. Rev. B 105, 165420 (2022), arxiv:2104.00103.

[226] V. Belavin, Y. Haraoka and R. Santachiara, *"Rigid Fuchsian systems in 2-dimensional conformal field theories"*, Commun. Math. Phys. 365, 17 (2019), arxiv:1711.04361.

[227] F. Beukers, *"Gauss' Hypergeometric Function"*, Birkhäuser Basel (2007).

[228] N. Chepiga, *"Critical properties of quantum three- and four-state Potts models with boundaries polarized along the transverse field"*, SciPost Phys. Core 5, 031 (2022), arxiv:2107.08899.

[229] A. Klemm and M. G. Schmidt, *"Orbifolds by Cyclic Permutations of Tensor Product Conformal Field Theories"*, Phys. Lett. B 245, 53 (1990).

[230] C. Dong, F. Xu and N. Yu, *"S-matrix in permutation orbifolds"*, J. Algebra 606, 851 (2022).

[231] G. Höhn and S. Möller, *"Systematic Orbifold Constructions of Schellekens' Vertex Operator Algebras from Niemeier Lattices"*, arxiv:2010.00849.

[232] Y.-Z. Huang, *"Representation theory of vertex operator algebras and orbifold conformal field theory"*, Contemp. Math. 768, 221 (2021), arxiv:2004.01172.

[233] J. Cardy and C. P. Herzog, *"Universal Thermal Corrections to Single Interval Entanglement Entropy for Two Dimensional Conformal Field Theories"*, Phys. Rev. Lett. 112, 171603 (2014), arxiv:1403.0578.

[234] S. Datta and J. R. David, *"Rényi entropies of free bosons on the torus and holography"*, JHEP 1404, 081 (2014), arxiv:1311.1218.

[235] B. Chen and J.-q. Wu, *"Universal relation between thermal entropy and entanglement entropy in conformal field theories"*, Phys. Rev. D 91, 086012 (2015), arxiv:1412.0761.

[236] F. Liu and X. Liu, *"Two intervals Rényi entanglement entropy of compact free boson on torus"*, JHEP 1601, 058 (2016), arxiv:1509.08986.

[237] S. Mukhi, S. Murthy and J.-Q. Wu, *"Entanglement, Replicas, and Thetas"*, JHEP 1801, 005 (2018), arxiv:1706.09426.

[238] M. Gerbershagen, *"Monodromy methods for torus conformal blocks and entanglement entropy at large central charge"*, JHEP 2108, 143 (2021), arxiv:2101.11642.

[239] M. Caraglio and F. Gliozzi, *"Entanglement Entropy and Twist Fields"*, JHEP 0811, 076 (2008), arxiv:0808.4094.

[240] P. Calabrese, *"Entanglement entropy in conformal field theory: new results for disconnected regions"*, J. Stat. Mech. 1009, P09013 (2010).

[241] V. Alba, L. Tagliacozzo and P. Calabrese, *"Entanglement entropy of two disjoint intervals in c=1 theories"*, J. Stat. Mech. 1106, P06012 (2011), arxiv:1103.3166.

[242] O. A. Castro-Alvaredo, B. Doyon and E. Levi, *"Arguments towards a c-theorem from branch-point twist fields"*, J. Phys. A 44, 492003 (2011), arxiv:1107.4280.

[243] G. W. Moore and N. Seiberg, *"Polynomial Equations for Rational Conformal Field Theories"*, Phys. Lett. B 212, 451 (1988).

[244] G. W. Moore and N. Seiberg, *"Naturality in Conformal Field Theory"*, Nucl. Phys. B 313, 16 (1989).

[245] D. Friedan and S. H. Shenker, *"The Analytic Geometry of Two-Dimensional Conformal Field Theory"*, Nucl. Phys. B 281, 509 (1987).

[246] B. Chen and J.-q. Wu, *"Single interval Renyi entropy at low temperature"*, JHEP 1408, 032 (2014), arxiv:1405.6254.

[247] M. Kulaxizi, A. Parnachev and G. Policastro, *"Conformal Blocks and Negativity at Large Central Charge"*, JHEP 1409, 010 (2014), arxiv:1407.0324.

[248] X. Chen, W. Witczak-Krempa, T. Faulkner and E. Fradkin, *"Two-cylinder entanglement entropy under a twist"*, J. Stat. Mech. 1704, 043104 (2017), arxiv:1611.01847.

[249] Z. Li and J.-j. Zhang, *"On one-loop entanglement entropy of two short intervals from OPE of twist operators"*, JHEP 1605, 130 (2016), arxiv:1604.02779.

[250] F.-L. Lin, H. Wang and J.-j. Zhang, *"Thermality and excited state Rényi entropy in two-dimensional CFT"*, JHEP 1611, 116 (2016), arxiv:1610.01362.

[251] P. Ruggiero, E. Tonni and P. Calabrese, *"Entanglement entropy of two disjoint intervals and the recursion formula for conformal blocks"*, J. Stat. Mech. 1811, 113101 (2018), arxiv:1805.05975.

[252] P. Bantay, *"Characters and modular properties of permutation orbifolds"*, Phys. Lett. B 419, 175 (1998), hep-th/9708120.

[253] P. Bantay, *"Permutation orbifolds"*, Nucl. Phys. B 633, 365 (2002), hep-th/9910079.

[254] V. G. Kac, R. Longo and F. Xu, *"Solitons in affine and permutation orbifolds"*, Commun. Math. Phys. 253, 723 (2004), math/0312512.

[255] M. R. Gaberdiel and C. A. Keller, *"Modular differential equations and null vectors"*, JHEP 0809, 079 (2008), arxiv:0804.0489.

[256] G. Pradisi, A. Sagnotti and Y. S. Stanev, *"Planar duality in SU(2) WZW models"*, Phys. Lett. B 354, 279 (1995), hep-th/9503207.

[257] I. Runkel, *"Boundary structure constants for the A series Virasoro minimal models"*, Nucl. Phys. B 549, 563 (1999), hep-th/9811178.

[258] B. Nienhuis, *"Critical behavior of two-dimensional spin models and charge asymmetry in the Coulomb gas"*, J. Stat. Phys. 34, 731 (1984).

[259] S. Eggert and I. Affleck, *"Magnetic impurities in half integer spin Heisenberg antiferromagnetic chains"*, Phys. Rev. B 46, 10866 (1992).